PhD degree in Systems Medicine (curriculum in Molecular Oncology)
XXXIV Cycle
European School of Molecular Medicine (SEMM),
University of Milan and University of Naples “Federico II”
Settore disciplinare: MED/04

MYC-dependent transcriptional control in human lymphoma

Moysidou Eirini
Istituto Europeo di Oncologia (IEO), Milan
Matriculation n.: R12398

Tutor: Dr. Bruno Amati
Istituto Europeo di Oncologia (IEO), Milan

PhD Coordinator: Prof. Saverio Minucci

Anno accademico 2022-2023

Table of Contents

ACKNOWLEDGMENTS

During the 4 years of my PhD, I have gained invaluable experience and knowledge; I have matured both as a person and as a scientist. All these, I owe to a lot of people, whom I would like to thank here:

First and foremost, my supervisor, Dr. Bruno Amati, for giving me the opportunity to work on this project, for his guidance, help and scientific support over these 4 years. His laboratory has been a great "school" for me, teaching me science and critical thinking alike. Secondly, I would like to thank Dr. Arianna Sabò, who acted as my added co-supervisor during the first two years of my PhD. The training I received from her during those first two years followed me throughout my PhD life, as she taught me most of what I know about genomics. Of course, I am deeply indebted also to Dr. Marco Filipuzzi; his contribution was invaluable for the developing of my project, given that he did all the bioinformatic analysis presented in this thesis.

Moving on, I would like to extend my gratitude to the other members of the lab, past and present alike: Alessandro, Clarissa, Giulio, Nina, Giorgia, Francesco, Mirko and all the others, for their support and active participation in my early training in the lab. Many thanks also to: the people of IIT for providing constructive feedback on my project through our joint group meetings; my internal and external advisors, Diego Pasini and Ignacio Moreno de Alborán respectively, for their important feedback during the early stages of my PhD; Simona Ronzoni of the Flow cytometry unit, for all her help with my Flow cytometry experiments; the people from the Genomic Unit, for all the sequencing; Dr. Zuber, for sending us the MYC-AID plasmids that were the foundation of my project and Dr. Biffo, for collaborating with us on the polysome profiling experiments.

For the successful completion of a PhD, one needs not only scientific direction, but also emotional support. For this reason, I would like to deeply thank my friends from this PhD program, who have been my wonderful companions in this journey, supporting me every step of the way; my "international group": Goga, Sara, Angeli, Johannes and of course my roommate, Catiana; my "Scellerati" group: Bianca, Susi, Silvia, Giulia, Ludo, Polaz and the rest of the crew. Finally, I would like to thank my family; my parents, my two brothers and my grandfather who have been constantly surrounding me with love and positive energy, even from afar. A friend once told me that PhD is like a marathon. Looking back now, I can say it was definitely worth it, every mile of the way.

Thank you all, from the bottom of my heart!

LIST OF ABBREVIATIONS

4SU = 4-thiouridine

5-Ph-IAA = 5-Phenyl-1H-indole-3 acetic acid

AA = Amino Acid

AFF4 = ALF Transcription Elongation Factor 4

AGO2 = Argonaute RISC catalytic component 2

AID = Auxin-Inducible Degron

AKT = Protein Kinase B

ALL = Acute Lymphoblastic Lymphoma/Leukemia

AML = Acute Myeloid Leukemia

AMPK = 5' AMP-activated protein kinase

APC = Adenomatous Polyposis Coli protein

ARE = AU-rich element

ARF = ADP-ribosylation factor

ATP = Adenosine Triphosphate

AUF1 = ARE/poly(U)-binding/degradation Factor 1

BAD = BCL-2 associated agonist of cell death

BAX = BCL-2 associated X protein

BCAT1 = Branched-Chain Amino Acid Transaminase 1

BCL-XL = B-cell lymphoma- extra large

BCL-2 = B-cell lymphoma 2

BET = Bromodomain and extra-terminal domain

BFP = Blue fluorescent protein

bHLH-LZ = Basic helix-loop-helix-leucine zipper domain

BIM = BCL-2 interacting Mediator of cell death

BL = Burkitt lymphoma

bp = Base pair

BRD4 = Bromodomain-containing Protein 4

BSA = Bovine serum albumin

b-TRCP = beta-transducin repeat containing E3 ubiquitin protein ligase

CAD = Carbamoyl-Phosphate Synthetase

Cas9 = CRISPR associated protein 9

CASC11 = Cancer Susceptibility 11

CBP = CREB-binding protein

CCND1 = Cyclin D1

Cdc6 = cell division cycle 6

CDK = Cyclin dependent kinase

cDNA = Complementary DNA

Cdt1 = Chromatin licensing and DNA replication factor 1

ChIP = Chromatin Immunoprecipitation

CNBP = cellular nucleic acid-binding protein

CRISPR = Clustered regularly interspaced short palindromic repeats

CTD = Carboxyl-Terminal Domain

C-terminal = Carboxy-terminal

DEG = Differentially expressed gene

DHL = Double Hit lymphoma

DLBCL = Diffuse large B cell lymphoma

DMEM = Dulbecco's modified eagle medium

DNA = Deoxyribonucleic acid

DSB = Double-strand breaks

DSIF = DRB Sensitivity Inducing Factor

DTT = dithiothreitol

E-box = Enhancer box

EDTA = Ethylenediaminetetraacetic acid

EdU = 5-Ethynyl-2'-deoxyuridine

eIF = Eukaryotic translation initiation factor

ELAVL1 = Embryonic lethal abnormal vision like protein 1

ER = Estrogen Receptor

EZH2 = Enhancer of zeste homolog 2

FACS = Fluorescence-activated cell sorting

FBXW7 = F-Box and WD repeat domain containing 7

FC = Fold Change

FDA = Food and Drug administration

FDR = False discovery rate

FL = Follicular lymphoma

FPKM = Fragments per kilobase per million mapped reads

FSC = Forward scatter

FUCCI = Fluorescent Ubiquitination-based Cell Cycle Indicator

GB = Gene Body

GCN5 = General Control Non-repressed 5

GFP = Green Fluorescent Protein

GO = Gene Ontology

GSEA = Gene Set Enrichment Analysis

GSK-3β = Glycogen synthase kinase 3β

H2A = Histone H2A

H2AX = H2A histone family member X

HAT = Histone acetyltransferase

HBD = Hormone-binding domain

HCC = Hepatocellular Carcinoma

HCF-1 = Host Cell Factor-1

HDAC = Histone deacetylase

HIF-1a = Hypoxia-Inducible Factor 1a

HL = Hodgkin's lymphoma

hnRNPA = Heterogeneous nuclear ribonucleoprotein A

HNRPK = heterogeneous nuclear ribonucleoprotein K

IAA = Indole-3-acetic acid

Ig = Immunoglobulin

IGF2BP1 = Insulin Like Growth Factor 2 mRNA Binding Protein 1

IgH = Immunoglobulin heavy chain

iPSC = induced Pluripotent Stem Cells

JAK = Janus kinase

KEGG = Kyoto Encyclopedia of Genes and Genomes

KRAS = Kirsten rat sarcoma virus

LAST = LncRNA-assisted stabilization of transcripts

LncRNA = Long non-coding RNA

MAPK = Mitogen-activated protein kinase

MAX = MYC Associated Factor X

MB = MYC box

MCL-1 = Induced myeloid leukemia cell differentiation protein

MCM = Mini chromosome maintenance

MCT-1 = Monocarboxylic Acid Transporter 1

Mdm2 = Mouse double minute 2 homolog

MGA = MAX Dimerization Protein MGA

miRNA = MicroRNA

MIZ-1 = MYC-interacting zinc finger protein 1

MK5 = MAPK-activated protein kinase 5

MNT = MAX Network Transcriptional Repressor

mRNA = Messenger RNA

mTOR = mammalian target of rapamycin

mTORC1 = mammalian target of rapamycin complex 1

MXD1 = MAX dimerization protein 1

MYC = Myelocytomatosis oncogene

ncRNA = non-coding RNA

NHL = Non-Hodgkin's lymphoma

N-terminal = Amino-terminal

OHT = 4-hydroxytamoxifen

ORC = Origin replication complex

OxPhos = Oxidative phosphorylation

PAICS = phosphoribosyl aminoimidazole succinocarboxamide synthetase

PCR = Polymerase chain reaction

PEG = Polyethylene glycol

Phospho or p = phosphorylated

PI = Propidium Iodide

PI3K = Phosphoinositide 3-kinase

PP2A = Protein phosphatase 2A

PPAT = phosphoribosyl pyrophosphate amidotransferase

PRC2 = Polycomb repressive complex 2

PRMT5 = Protein arginine methyltransferase 5

p-TEFb = positive transcription elongation factor

PTEN = Phosphatase and tensin homolog

q-PCR = quantitative PCR

RBP = RNA binding protein

Rbp1 = Retinol binding protein 1

R-CHOP = Rituximab, cyclophosphamide, doxorubicin hydrochloride, vincristine sulfate, prednisone

RNA = Ribonucleic acid

RNAPI = RNA Polymerase I

RNAPII or RNA-PolII = RNA Polymerase II

RNAPIII = RNA Polymerase III

RNAse A = Ribonuclease A

RNMT = RNA Guanine-7-Methyltransferase

ROS = Reactive Oxygen Species

RPMI = Roswell park memorial Institute

rRNA = Ribosomal RNA

RT = Room temperature

RT-PCR = Reverse transcription PCR

S6K1 = S6 kinase 1

SAGA = Spt-Ada-Gcn5 Acetyltransferase

SD = Standard Deviation

SEC = Super elongation complex

Seq = sequencing

Ser = Serine

shRNA = short hairpin RNA

SKP2 = S-phase kinase-associated protein 2

snRNP = small nuclear ribonucleoprotein

SRF = serum response factor

SRSF1 = Serine and arginine rich splicing factor 1

STAT = Signal transducer and activator of transcription

SWI/SNF = SwItch/Sucrose Non-Fermentable

TAD = Transactivation domain

TES = Transcription ending site

Tet = tetracycline

TFEB = Transcription Factor EB

TFIIH = Transcription Factor II H

TGFβ = Transforming growth factor β

THL = Triple Hit lymphoma

Thr = Threonine

TP53 = Tumor Protein P53

TRFC = Transferrin receptor protein 1

tRNA = transfer RNA

TRRAP = Transactivation/ transformation -associated protein

TSS = Transcription starting site

TTP = tristetraprolin

UPS = ubiquitin-proteasome system degradation

USP28 = ubiquitin-specific peptidase 28

UTR = Untranslated region

UV = ultra-violet radiation

WDR5 = WD repeat-containing protein 5

WNT = Wingless-related integration site

FIGURE INDEX

SUPPLEMENTARY FIGURE INDEX

TABLE INDEX

ABSTRACT

Deregulated expression of the oncogenic transcription factor MYC is a widespread feature in cancer and is required for tumor maintenance. Despite substantial research efforts, major gaps persist in our understanding of primary MYC-dependent events in tumors. To address this issue, we inserted an in-frame cassette encoding an Auxin-inducible degron (AID) into the oncogenic *MYC* allele of three human B-cell lymphoma cell lines, thus directing expression of a conditionally degradable MYC-AID fusion protein. Treatment of the cells with Auxin caused an immediate MYC-AID drop, resulting in gradual proliferative arrest and cell death. While residual MYC-AID levels supported 3-4 residual division cycles, no long-term adaptation occurred. Hence, partial MYC inhibition may suffice to elicit potent anti-tumoral effects.

RNA-seq profiling of nascent RNA showed that MYC loss elicited rapid changes in transcriptional activity at several hundred loci in each lymphoma cell line, with a conserved core of 187 MYC-dependent genes showing immediate and persistent down-regulation (from 1 to 8 hours after treatment) followed by consistent reductions in the corresponding mature mRNAs. Other groups of genes underwent immediate gains in transcriptional activity, and yet others were activated or repressed at later times; however, none of these groups showed consistent overlaps among the different lymphoma cell lines. Hence MYC was directly required to support transcription at a discrete set of immediate MYC-dependent genes.

Since transcription factors also impact co- and post-transcriptional processes, and ultimately translation, we profiled polysome-associated RNAs following Auxin treatment. This revealed that the changes in polysome engagement closely reflected those in total RNA levels, thus providing no evidence for differential effects on translation at MYC-regulated loci.

To start addressing the mechanisms underlying MYC-dependent transcription, we established genome-wide chromatin association profiles for MYC, RNA-PolII and several histone marks. Our analyses showed that MYC-AID removal resulted in rapid losses of RNA-PolII from MYC-dependent loci. These effects were proportionate at promoters and gene bodies, suggesting a role of MYC for RNA-PolII loading at those loci.

Altogether, the above datasets shall provide us with a dynamic view of MYC-regulated transcription and of the mechanisms underlying oncogene addiction in MYC-driven Lymphoma, paving the way for the identification of new therapeutic targets.

1. INTRODUCTION

1.1. The MYC Family

1.1.1 Discovery and family members

The *c-MYC* proto-oncogene (hereafter *MYC*) encodes a transcription factor that regulates a plethora of biological functions, such as cell growth, cell cycle, proliferation, apoptosis, metabolism, etc[1]. *MYC* was among the first oncogenes discovered in the late seventies, through the observation that the avian carcinoma virus MC29 exhibited tumorigenic properties by causing myelocytomatosis in chicken. This led to the identification of *v-MYC*[2] as the tumor driver in MC29, followed by the realization that this viral oncogene originated from its cellular counterpart *c-MYC*[3-5] and that this was the same gene that was activated by translocation in human Burkitt's lymphoma[6-8]. Around the same time, Ig-MYC translocations were reported to drive B cell lymphomagenesis also in mice[9].

MYC is only one gene out of the family of three human proto-oncogenes encoding for transcription factors, with the other two being *l-MYC* (encoding for L-MYC) and *n-MYC* (encoding for N-MYC). *MYC* has the most extensive expression pattern in pre- and post-natal development, while the other two family members tend to be more tissue specific, as shown in early studies in mice[10]. *MYC* and *n-MYC* are indispensable for embryonic development, as deletion of either gene is lethal in mid-late gestation[11-14], while that is not the case for *l-MYC*[15]. Nevertheless, all three of them play important roles in physiological functions, as well as in carcinogenesis.

1.1.2 MYC Structure and Function

The three MYC-family proteins are structurally related, with several conserved sequence motifs – originally dubbed as "MYC boxes" (MB) – and functional elements, which can be described in three parts[16,17] **(Fig. 1)**: an N-terminal transactivation domain (TAD) that bears the MYC boxes MB0, MBI, MBII and can activate transcription; a central region containing a nuclear localization motif and MBIIIa, MBIIIb and MBIV; a highly conserved C-terminal domain, constituted by a bHLH-Zip dimerization and DNA-binding domain[18-20].

The DNA-binding domains of transcription factors belong to well-defined structural families[21]. In the case of bHLH-Zipper class transcription factors, such as MYC, these domains comprise of the basic, the helix-loop-helix and the Leucine-Zipper regions (**Fig. 1**); the basic region being responsible for interaction with DNA, while the HLH-Zip region is determining homo- or heterodimerization. The grand breakthrough in our understanding of MYC's function came after the discovery of MAX, its obligatory dimerization partner[22].

MAX is also a bHLH-Zip protein and its HLH-Zip region is facilitating protein-protein interactions[23]. MYC's bHLH-Zip portion of the protein remains semi-unstructured till it dimerizes with MAX[22]; the structure of said dimer is available through X-ray crystallography[23,24]**(Fig. 2)**.

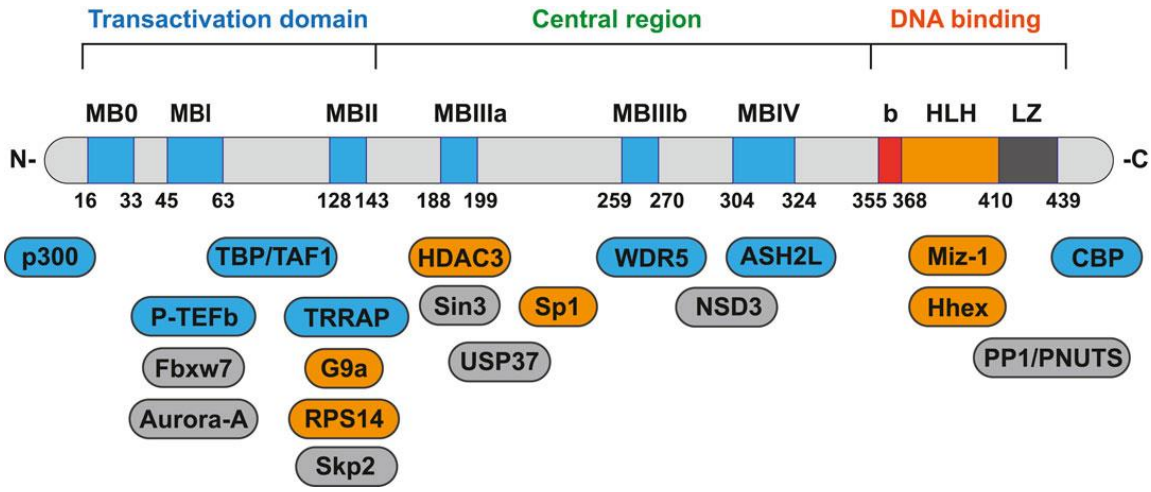

Figure 1: Schematic representation of MYC domains with their respective interactors.
Image from Zhou et al., Front. Pharmacol., 2021 (Ref. 309)

After this dimerization takes place, the MYC/MAX complex is then able to bind DNA, with a distinct preference for the E-box motif CACGTG, through which it activates transcription[1,25]. In fact, MYC's binding to chromatin and subsequently its function in transactivation and transformation is dependent on its heterodimerization with MAX[26,27]. Besides MYC/MAX dimers, MAX itself can form homodimers (unlike MYC) and most notably heterodimers, with a series of other bHLH-LZ proteins (MXD1-4, MNT or MGA): these proteins have been shown to mediate interactions with co-repressors and are thought to act as MYC antagonists[19,28,29]. That being said, they may exhibit in some cases more subtle activities that could be supporting the oncogenic action of MYC instead[30]. Beyond dimerization, the MYC and MAX bHLH-LZ domains are likely to mediate interactions with other proteins, such as MIZ-1. This interaction converts MYC from a gene activator to a repressor[31,32]

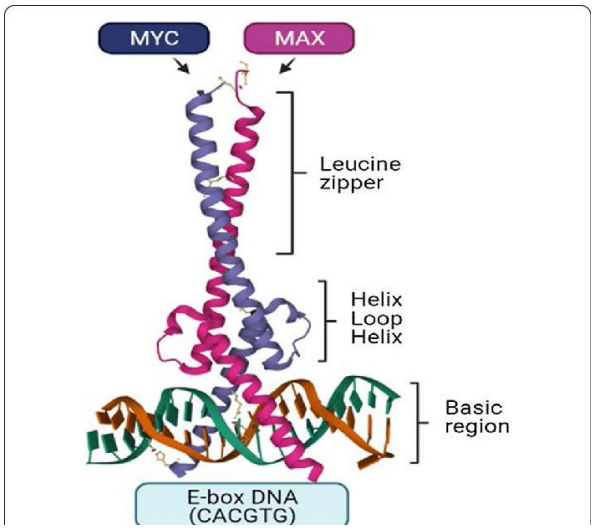

Figure 2: Crystal structure of MYC/MAX heterodimer.
MYC forms a heterodimer with its obligatory partner, MAX, in order to bind to DNA in an E-box region (CACGTG). Image from *Ahmadi et al., J Hematol Oncol, 2021* (Ref. 221).

Interestingly, MAX does not contain a TAD, so MYC is the part of the dimer

responsible for activating transcription through its own TAD. MYC's TAD itself was shown to be sufficient for transcriptional activation when fused in-frame with an heterologous DNA binding domain[33]; each of its MYC boxes is essential for a plethora of interactions that enable MYC's transcriptional activity; several of these interactions are shown in **Fig. 1** and some of them will be mentioned later.

1.1.3 Regulation of MYC

MYC as a transcription factor, holds a central position in the signaling circuitry of cells; on the one side, MYC itself is being regulated upstream by growth signaling pathways such as MAPK, Notch, mTOR and PI3K among others[1] (**Fig. 3A**). In fact, among the first observations for MYC's function were several reports that MYC levels actually correlate with cell proliferation, being characterized as an "immediate early" response gene after mitogenic stimulation[34-36]. On the other side, MYC transcribes genes involved in pivotal biological processes such as cell growth, proliferation, apoptosis, metabolism etc[1,37] (**Fig. 3B**).

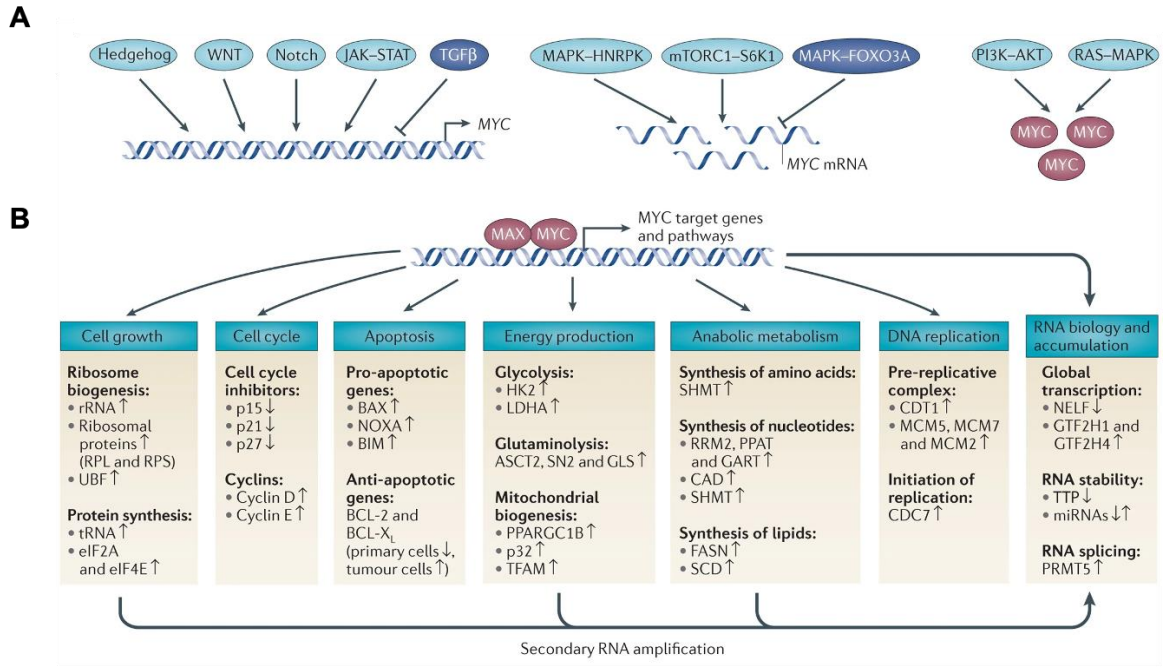

Figure 3: MYC's central position in the signaling circuitry.
(A) Some of the pathways affecting *MYC* transcription on the left, pathways affecting the MYC mRNA translation in the middle and pathways affecting MYC protein stability on the right. **(B)** Processes and pathways regulated by MYC, with a list of some of the gene products involved (This is a selected list, representing a small fraction of MYC-regulated genes). Image from *Kress et al., Nature Review Cancer, 2015* (Ref. 1).

Indeed, this central role of MYC is what endows it with oncogenic potential; given MYC's role and involvement in cell cycle, proliferation, apoptosis, metabolism etc, it becomes clear that its deregulation will lead to aberrant proliferation and therefore cancer. Hence,

it is very important for mechanisms to be in place, in order to tightly control MYC's expression and activity. This take place at multiple levels, which will be discussed below.

Transcriptional level: The first step of MYC regulation is at the gene level. MYC is directly induced by mitogenic stimuli, being categorized as an "immediate early" responsive gene to mitogens[34-36], as mentioned previously. This is explained by the fact that MYC is holding a key position downstream of a plethora of growth regulatory pathways, as exemplified in **Fig. 3A**.

More specifically, *MYC* transcription can be induced by Hedgehog[38], WNT[39], Notch[40] and JAK-STAT[41] signaling. Another important factor inducing MYC expression is the Super Elongation Complex (SEC), which was initially shown to induce several "early" response genes upon serum treatment[42], while later, several studies exhibited that *MYC* is a direct target of AFF4/SEC[43-45]. At the same time, *MYC* can be repressed by growth-inhibitory pathways such as TGFβ[46]. The tumor suppressor miR-145, which is induced through the PI-3K/Akt and p53 pathways is also suppressing *MYC* expression[47]. All in all, *MYC* is kept in a tight equilibrium between the mitogenic signaling pathways that drive its expression and growth-inhibitory pathways that suppress it. Most importantly, negative feedback loops are critical in controlling MYC levels. For example, the *MYC* promoter is regulated by MYC itself and there is a MYC mRNA repression whenever an ectopic MYC transgene is introduced into normal cells[48].

MYC mRNA level: MYC mRNA is quite unstable and has a short half-life, of about 30 minutes[49]. Several RNA binding proteins are controlling its stability, AUF1[50], ELAVL1[51], IGF2BP1[52] and AGO2[53] among them. The translation initiation factor eIF4E is responsible for its export into the cytoplasm[54], upon mitogenic signals.

Translational level: A downstream effector of mTOR, S6K1, regulates the phosphorylation of eukaryotic initiation factor eIF4B, necessary for MYC's 5' UTR region uncoiling. In that way, the mTOR/S6K1 positively affect MYC translational efficiency[55]. Meanwhile, the MAPK pathway can have a dual role **(Fig. 3A,** middle**)**. On one side, ERK-dependent phosphorylation of the heterogeneous nuclear ribonucleoprotein K (HNRPK) positively regulates MYC mRNA translation[56,57]. On the other hand, the MAPK-activated protein kinase (MK5) activates the FoxO3a transcription factor via phosphorylation. Activated FoxO3a induces the expression of miR-34b and miR34C that negatively impact MYC mRNA translation, by targeting its 3' UTR[58].

Protein level: The MYC protein has a very short half-life in normal cells[59], with its turnover mainly regulated through ubiquitin-proteasome system degradation (UPS). The

best characterized E3 ubiquitin ligase involved in MYC degradation is FBXW7. It can recognize a phospho-degron sequence that includes two phosphorylation sites: phosphorylated MYC at Ser62 and Thr58 (both sites are included in MBI)[60,61]. First comes the phosphorylation in Ser62, which is stabilizing MYC protein and for which ERK is mainly responsible[62,63]. Ser62 phosphorylation is a prerequisite for Thr58 phosphorylation[64], the latter being mediated by GSK-3β[65]. All in all, phosphorylation at both of these sites is regulated by Ras signaling[66]; the MAPK being responsible for the phosphorylation of Ser62 and the PI3K/Akt regulating negatively GSK3β[62,67]. More recent evidence show that FBXW7 requires also a Thr244 phosphorylation, for successful MYC ubiquitination[68].

FBXW7-mediated degradation is also controlled by USP28, an ubiquitin-specific protease that cleaves ubiquitin chains to antagonize the activity of ubiquitin[69]. This protease binds MYC via interaction with FBW7 and stabilizes MYC in tumor cells[70]. On the contrary, in case of UV-induced DNA damage, USP28 dissociates from FBXW7 and MYC is led for degradation instead[71]. Another FBXW7 antagonist is the F-box protein b-TRCP which binds to a phospho-recognition sequence of MYC and mediates the direct ubiquitination of its N-terminus. This in turn stabilizes the protein for cell cycle re-entry after S-phase arrest[72]. While discussing F-box proteins, SKP2 has also been shown to regulate MYC polyubiquitination and degradation, even though in a phosphorylation independent manner[73]. Seeing as ubiquitination occurs on Lysine residues, other modifications of the same residues should be able to compete with it. This was proposed for acetylation, which has also exhibited induction of MYC protein stabilization[74,75].

Last but not least, even though as mentioned, MYC's turnover is mainly regulated through ubiquitin-mediated degradation, MYC cleavage by calpains has been reported[76]; the latter occurs in the cytosol, whereas the proteasome degradation happens mainly in the nucleus. Nevertheless, calpains basically cause partial cleavage of MYC and not full degradation.

1.1.4 MYC Physiological functions

As outlined in **Fig. 3**, MYC holds a key position in the cell signaling network, as a mediator between mitogenic stimuli and downstream responses that affect pivotal cellular processes. Some of the latter will be briefly discussed below:

MYC and RNA biology: MYC is a transcription factor that regulates a plethora of target genes[1]. Besides that, it plays an even greater role in RNA biology, since its targets include genes that encode several components involved in ribosome biogenesis, mRNA processing

and translation. Ribosome biogenesis in particular is impacted by MYC at multiple levels: first, MYC facilitates RNA Polymerase I (RNAPI)-dependent transcription of ribosomal RNA (rRNA)[77-79]. Second, several of MYC's most prominent target gene products, like nucleolin, nucleoplasmin, Nop56 and others, are responsible for processing rRNA into the 18S, 5.8S and 28S components of the ribosomal subunits[80]. A recent study indicated that MYC activates the RNAPII-mediated transcription of multiple genes involved in ribosome biogenesis – among others – by interacting with Host Cell Factor-1 (HCF-1), highlighting once more the importance of specific cofactors in MYC-dependent regulatory networks[81]. Other known MYC target genes encode proteins involved in translational control[82,83],such as the eukaryotic translation factors eIF2A and eIF4E[78,84]. Lastly, MYC also facilitates tRNA transcription, via RNA Polymerase III (RNAPIII)[77-79]. In addition to these functions, MYC promotes the expression of the subunits for the transcription factor TFIIH (GTF2H1 and GTF2H4)[85].

Another mechanism by which MYC is modulating RNA abundance is by regulating genes that are in charge of stabilizing mRNA. For example, during lymphomagenesis, MYC represses the expression of the gene that codes for the RNA-binding protein tristetraprolin (TTP). This protein is responsible for the degradation of AU-rich element (ARE)-mRNAs; thus, its gene repression by MYC effectively leads to stabilization of about 16% of protein coding mRNAs[86,87]. Moreover, a plethora of MYC-regulated ncRNAs and miRNAs can also contribute to MYC's indirect altering of mRNA stabilization[88]. MYC-induced LncRNA-assisted stabilization of transcripts (LAST) is known to stimulate CCND1 expression by stabilizing its mRNA together with CNBP[89], while CASC11 promotes CCND1 transcription by stabilizing the hnRNP-K mRNA, which leads to an hnRNP-K-dependent enhanced nuclear accumulation of β-catenin[90]. Among the MYC-induced miRNAs, miR-19a/b-3p, miR-20a-5p, miR-25-3p, and miR-92a-3p prevent apoptosis by destabilizing the BIM transcript[91-93]. Similarly, miR-19a/b-3p target the PTEN, PP2A and AMPK mRNAs, which leads to a decrease in the pro-apoptotic proteins BAD, Puma, and Noxa[94-96]. Conversely, MYC-repressed miRNAs can directly target anti-apoptotic factors such as BCL2 (miR-15a/16-5p and miR-34a-5p)[97-99], BCL2L2 (miR-122-5p)[100,101] and MCL1 (miR-26b-5p and miR-29b-3p)[102,103].

Last but not least, MYC plays an important role on RNA splicing, by modulating the transcription of RNA binding proteins (RBPs) involved in alternative splicing. Such RBPs are the splicing factors serine/arginine-rich splicing factor 1 (SRSF1)[104], the heterogeneous nuclear ribonucleoprotein A1 and A2 (hnRNPA1/2)[105] and the core small nuclear ribonucleoprotein particle (snRNP) assembly genes, including the protein arginine N-

methyltransferase 5 (PRMT5)[106]. MYC's connection to the splicing machinery is such, that a recent study indicated that MYC regulates a whole network of co-expressed splicing factors in breast tumors that had overly active (and not just overexpressed) MYC; one of these splicing factor modules was even recognised as pan-cancer, occurring across 33 different tumour types[107].

MYC and DNA replication: After transcription, DNA replication is one of the key cellular processes in which MYC partakes[108,109]. Several studies have demonstrated protein-protein interactions between MYC and factors of the pre-replication complex, such as the Origin Replication Complex 1 and 2 (ORC1, ORC2)[110,111], MCM proteins[110], Cdc6[112] and Cdt1[113]. More importantly, MYC was shown in the same studies to localize in early sites of DNA replication, including at a known replication origin of *MYC* itself[110]. *Cdt1* gene has also been characterized as one of the MYC target genes[114]. Moreover, MYC interacts with Cdc7 and Cdc45, which are essential for the initiation step of DNA replication[110,115]. There is also another strong connection between MYC and DNA replication, considering that MYC is regulating the majority of the genes involved in purine and pyrimidine biosynthesis[116,117], therefore providing the necessary flux of metabolites needed for replication.

MYC and Translation: MYC's general effect on translation is well established, since as already mentioned, its transcriptional targets include genes that encode several components involved in the translational machinery. While RNAPI -dependent transcription of ribosomal RNA (rRNA)[77-79,118] is among the first ones on that list, MYC is also shown to upregulate ribosomal proteins[119], as well as other factors required for rRNA processing, ribosome assembly and nuclear export of mature ribosomal subunits into the cytoplasm[80,120]. Most importantly, MYC can regulate mRNA translation by transcribing of translation initiation factors, such as eIF4E, eIF2α, eIF4AI and eIF4GI, required for cap-dependent translation[121]. Moreover, MYC can directly promote methylation of the mRNA cap structure through RNA Guanine-7-Methyltransferase (RNMT), an indispensable modification for cap-dependent translation, since though it, the cap domain is binding to eIF4E and recruits the 40S ribosome subunit[122]. A natural consequence of the above is that MYC induces an increase in cell size. This has been observed in various contexts over the years[85,123-127], mainly due to the increased mRNA production and protein synthesis[85,123]. Another possible reason for the effect on MYC on cell mass could be due to the fact that MYC induces ribosome biogenesis[128], with the ribosomes being representatives of a cell's capacity to grow.

MYC and Cell Cycle and Growth control:

MYC has been connected to cell cycle and proliferation already from the 80's, where, as already mentioned above, several teams reported that MYC levels actually correlate with cell proliferation, characterizing it as "immediate early" response gene after mitogenic stimulation[34-36]. Further investigation of MYC's role in serum response, has confirmed in 3T9 fibroblasts that a part of the transcriptional program activated by serum is in fact MYC-dependent and enriches for genes involved directly in DNA replication and cell cycle control, but also in metabolic processes, ribosome biogenesis and RNA and protein biosynthesis among others[116], with the latter processes being just as likely to impact on cell growth and proliferation[129-131]. Moreover, it has been shown that MYC expression is sufficient to mediate cell cycle entry in quiescent cells[132], while its downregulation seems to impair cell cycle progression[133].

The aforementioned effects on cell cycle can either stem from MYC's control in the biogenesis of macromolecules or follow directly from the fact that several MYC-target genes are related to cell cycle control, like cyclin D2 and E1, Cdk4, Cdc25A and E2F1[134]. In fact, MYC overexpression has been shown to regulate the staggering amount of 37 out of 87 genes classified as belonging to the "cell cycle pathway" in the KEGG (Kyoto Encyclopedia of Genes and Genomes) category of Gene Ontology (GO), in rat fibroblasts[135]. Moreover, MYC is repressing the cyclin-dependent kinase inhibitor p21, through interaction with the initiator-binding transcription factor, MIZ-1[136]; by antagonizing several Cdk inhibitors[137], including p27[138-140], p21[136,141] and p15[31], MYC can accelerate cell proliferation rates. Recent studies have also shown that MYC can activate Cdk1, resulting in p27 phosphorylation and subsequent degradation[142].

MYC and Apoptosis: MYC has a dual role in cell fate. On the one hand, it is promoting proliferation, as discussed above. On the other hand, it can also trigger cell death, which provides a safeguard mechanism to prevent uncontrolled cell divisions upon MYC deregulation. Indeed, early studies in the field demonstrated that dual role of MYC; in the absence of survival signals, such as growth hormones or cytokines, constitutive MYC expression can induce apoptosis[143], while blockade of MYC-protein expression in T cell hybridomas was preventing the T-cell activation-induced apoptosis[144]. MYC deregulation can also lead to an increase in the ARF protein expression[145], which inhibits the Mdm2, thus stabilizing p53[146]. Activation of p53 can in turn increase Puma and Noxa levels that further downregulate the anti-apoptotic factors Bcl2 and Bcl-XL[147-149]. Along the same lines, while MYC activates the ARF-p53 apoptotic pathway in mouse embryo fibroblasts and in primary

pre-B-cell cultures, overexpression of MYC seems to select for spontaneous inactivation of said pathway during MYC-induced lymphomagenesis[150].

From the above, MYC's dual role becomes clear; its final function, whether apoptosis or proliferation depends on the equilibrium between pro- and anti- apoptotic proteins; deregulation of MYC can disrupt this balance, hence inducing apoptosis[147,151,152]. For example, it has been shown in an *Eμ-myc* mouse model of lymphomagenesis that MYC can indirectly suppress the anti-apoptotic proteins BCL2 and BCL-xL[147]. Conversely, early studies demonstrated that BCL2 has the ability to block MYC-induced apoptosis[153,154]. Lastly, there is also evidence that shows that MYC triggers apoptosis through one of the two intrinsic apoptosis "executioners", BAX; MYC induces cytochrome *c* release from the mitochondria, with subsequent activation of downstream effector caspases[155,156].

MYC and Autophagy: Autophagy is a major cellular function during which unnecessary or dysfunctional cellular components are led to the lysosome for degradation, in order for the cell to obtain energy in times of nutrient stress[157]. MYC can regulate autophagy, by antagonizing the Transcription Factor EB (TFEB)[158-160], which is a master regulator of the autophagy-lysosome pathway[161,162]. More specifically, MYC is negatively regulating autophagy by directly suppressing TFEB[160,162]. It has been shown that MYC overexpression leads to a decrease of TFEB and its target genes, as well as to lysosome biogenesis. On the contrary, inhibition of MYC activates TFEB, with concomitant increase to the autophagosomal formation and autophagic flux[160]. TFEB is also a bHLH-LZ protein, that binds an E-box motif with the same core as MYC[158]; a fact that while its biological relevance has not been fully understood yet, it has been suggested to contribute to their antagonism.

MYC and cell metabolism: As already discussed, MYC responds to mitogenic stimuli and growth signaling pathways, which will lead to downstream metabolic changes and ultimately affect various biological processes of the cells. In Drosophila, nutrient starvation reduces TOR activity, which in turn leads to lower levels of the Drosophila MYC homolog, which ultimately leads to diminished cell growth. This seems to be due to a TOR-dependent AKT phosphorylation and therefore inactivation of FOXO transcription factors. They negatively bind and regulate the Drosophila MYC homolog, in a nutrient sensing TOR-dependent way[163]. Similar results have been demonstrated also in mammals, where mTOR senses the nutrient status of cells and regulates MYC's translation accordingly[55]. Moreover, inhibition of mTOR through Amino Acid (AA) starvation, leads to promotion of MYC dephosphorylation at serine 62 and its subsequent destabilization, by AMBRA1, an autophagy scaffolding protein[164].

Apart from MYC's involvement in metabolism through mTOR/nutrient dependencies, its activity can also be regulated by hypoxia. More specifically, under hypoxia state, MYC undergoes proteolytic degradation[165,166]. Hypoxia-Inducible Factor 1a (HIF-1a), is activating the expression of MXI-1, which in turn antagonizes MYC and reduces MYC-dependent mitochondrial biogenesis[166].

MYC has also been shown to be able to mediate metabolic reprogramming upon T cell activation[131]. More specifically, it seems to be required for the activation-induced glycolysis and glutaminolysis in these cells, in order for them to meet their increased bioenergetic and biosynthetic needs for proliferation upon their activation. Indeed, MYC is known to regulate the vast majority of genes involved in glycolysis and glutaminolysis[167-169]. One of those genes codes for Monocarboxylic Acid Transporter (MCT1), which removes lactic acid, a harmful byproduct of metabolizing glucose[170]. Besides glucose metabolism, MYC is also associated with lipid synthesis, by upregulating *BCAT1* (Branched-Chain Amino Acid Transaminase 1), which in turn mediates Branched-Chain Amino Acid catabolism[171].

Nucleotide synthesis is another important metabolic process MYC is associated with, by regulating genes involved in purine and pyrimidine synthesis[116,117]. Indeed, one of the first MYC target genes to be identified was *CAD*, encoding for Carbamoyl-Phosphate Synthetase[172], which is involved in pyrimidine synthesis. Likewise, in purine synthesis, MYC positively regulates phosphoribosyl pyrophosphate amidotransferase (*PPAT*) and phosphoribosyl aminoimidazole succinocarboxamide synthetase (*PAICS*) genes[173-175].

Last but not least, MYC contributes to metabolic reprogramming of cells by promoting gene expression programs that mediate biogenesis of cell organelles like ribosomes and mitochondria[81]. Many of its target genes are encoding ribosome components such as rRNA and ribosomal proteins[118], while it also regulates the transferrin receptor TRFC, which is needed for iron uptake and therefore for proper mitochondria function[176].

1.2 MYC in cancer

1.2.1 *MYC*, a potent oncogene

As already discussed, MYC is a central regulator among many growth-regulatory pathways **(Fig. 3)**. This is exactly the reason why its tight regulation is of utmost importance for the preservation of homeostasis and is controlled at multiple levels, as discussed above. But what happens when MYC escapes its equilibrium and becomes deregulated? In short, there is uncontrollable proliferation and ultimately cancer. Indeed, either *MYC* or one of its two paralogs are found deregulated in most types of cancer[177-180] **(Fig. 4)** and a wealth of evidence over more than 3 decades has demonstrated that these genes have the potential to transform cells and promote tumorigenesis in virtually all tissues[181-185].

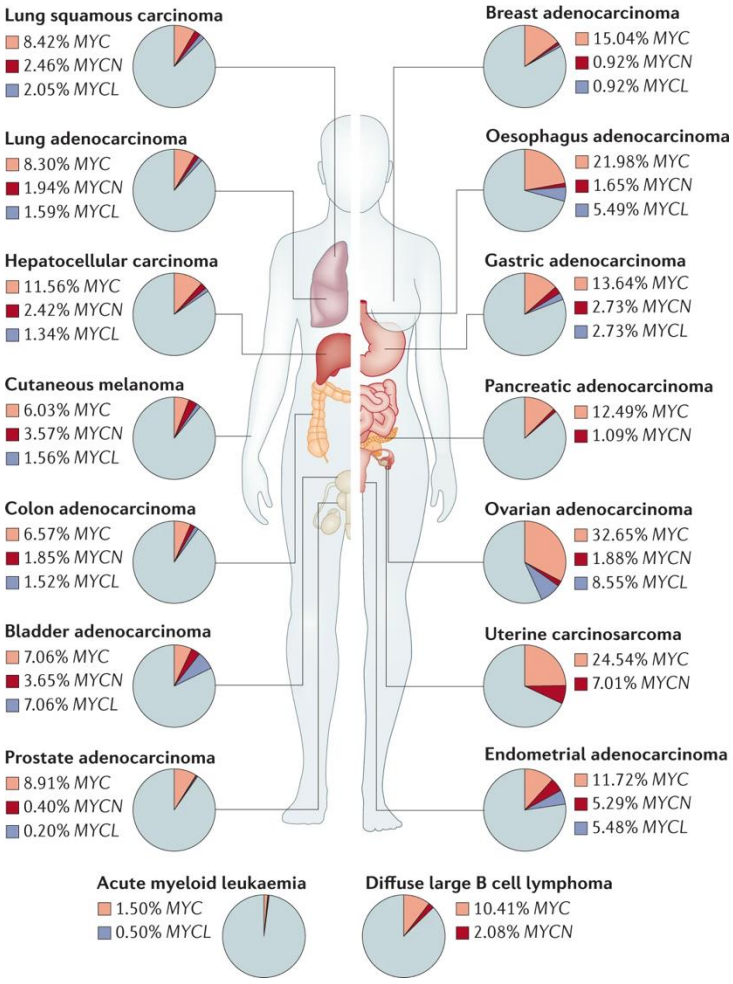

Figure 4: Gene amplification frequency of *MYC* family in various cancers. Prevalence of genetic alterations leading to amplification of *MYC*, *MYCN* and *MYCL* across 16 different types of cancers, as taken from The Cancer Genome Atlas. Image from *Dhanasekaran et al., Nature reviews Clinical Oncology, 2022* (Ref. 179).

Remarkably, MYC not only promotes uncontrolled cell proliferation, but has the potential to promote the acquisition of other fundamental cancer hallmarks, such as genomic instability, self-renewal, metabolic reprogramming, invasiveness, angiogenesis or immune evasion[29,179] **(Fig. 5)**. Due to the ubiquitous association of deregulated MYC expression in cancer, it has been proposed that this feature may qualify as a molecular cancer hallmark of its own[182].

While describing in detail how MYC affects each cancer hallmark would be beyond the scope of this introduction, genomic instability will be briefly discussed. Deregulated expression of *MYC* can result in genomic instability[186], possibly due to its ability to override cell cycle checkpoints and induce uncontrollable DNA replication and cell division[187]. Therefore, its overexpression leads to replication stress[188]. Indeed, MYC overexpression has been previously correlated to an increase in the formation of γ-H2AX foci in normal human fibroblasts, which is a marker of Double-Strand Breaks (DSBs) and consequently of genomic instability[189]. MYC has been previously held accountable for DSB formation due to its ability to increase Reactive Oxygen Species (ROS)[190], even though other studies have demonstrated that MYC can actually induce DSBs independently of the accumulation of ROS[191]. Regardless of these, MYC has also been shown to actually repress the DSB repair process[189,192,193].

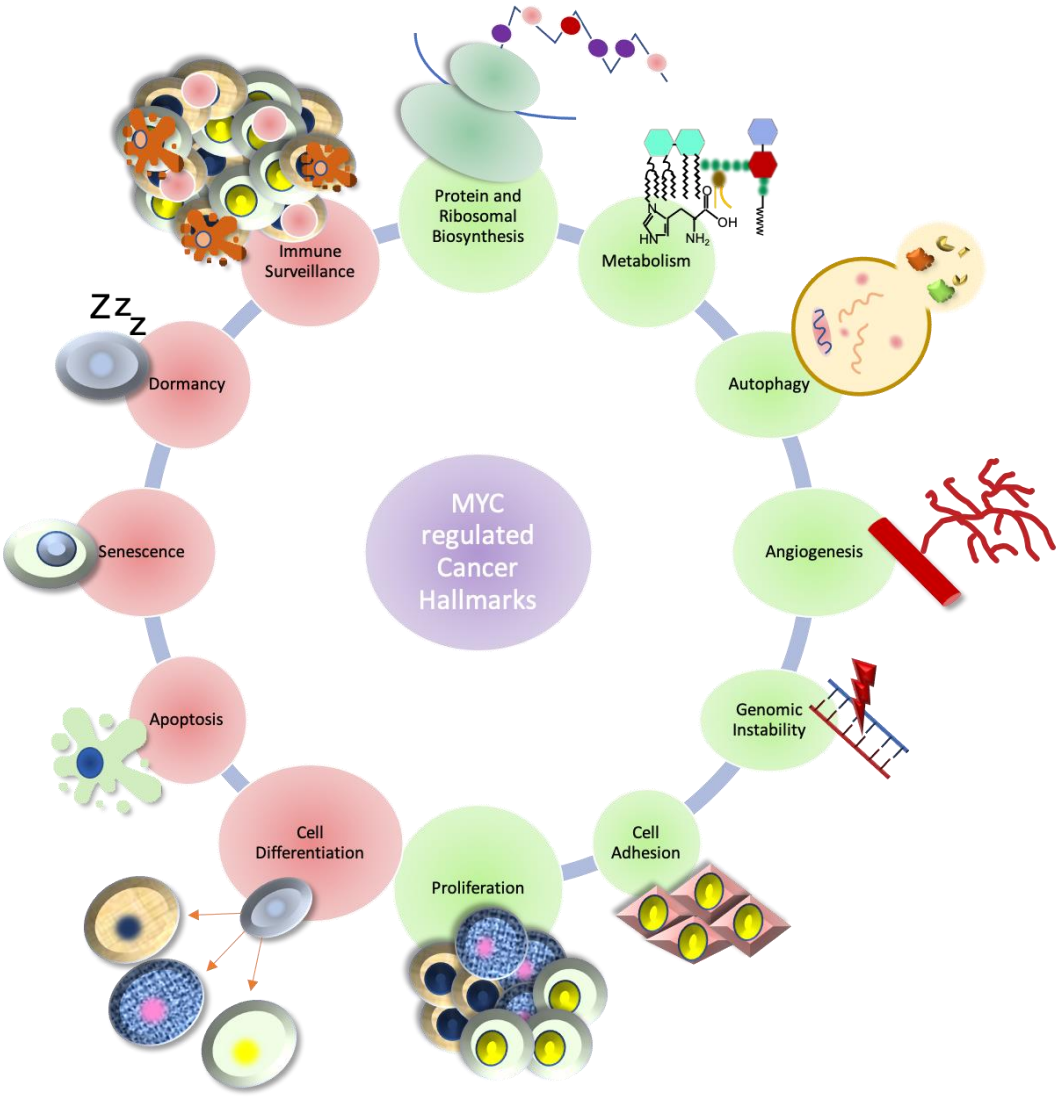

Figure 5: *MYC*, regulating cancer hallmarks.
MYC induces cell growth and survival, promoting tumorigenesis (green area). *MYC* also promotes cancer by blocking pathways related to differentiation and apoptosis (red area).

MYC's potency as an oncogene became clear already by early studies in the field, where its expression was able to drive B cell lymphomagenesis in mice[9,194], as well as in humans[6]. Soon followed other studies connecting MYC deregulation with various cancer types in humans[195,196]. Conversely, inactivation of MYC in transgenic mouse models has been linked with proliferative arrest and tumor regression[197-200]. Similar results were noted also after MYC inhibition with a synthetic MYC inhibitor called Omomyc, which exhibited significant tumour regression in various contexts[201,202]. However, MYC deregulation alone is not sufficient or essential for tumour initiation since the tumorigenic functions of oncogenic MYC are restrained by many physiological mechanisms. It can only cause transformation in specific cell lines that are already "primed" for it, by having acquired other oncogenic events[198,203].

Unlike other known oncogenes, *MYC* is not mutated in its coding sequence; instead, in the majority of cases, its oncogenic potential rises by mechanisms that deregulate (and usually over activate) its expression. As a matter of fact, its deregulation can be mediated by alterations in the genomic, transcriptional and post-translational level, summarized in **Fig. 6**.

Genomic alterations: *MYC* gene amplification is one of the most commonly observed types of MYC deregulation in malignancies and was first identified in human leukemia cells in the 80's[204], with the discovery of amplifications of MYCN[205] and MYCL[206] coming soon after. Another type of *MYC* genomic alteration is *MYC* translocations, that are usually found in B or T cell leukemias and lymphomas[207]. More specifically, in Burkitt's B-cell lymphomas, the trademark oncogenic event is translocations between a portion of MYC-carrying chromosome 8 and chromosome 14 or, less frequently, chromosomes 2 and 22, all of the latter carrying immunoglobulin gene regulatory elements[6]. Translocation events are quite frequent, also in other types of B-cell lymphomas, such as in diffuse large B-cell lymphoma, multiple myeloma, or progressed follicular B-cell lymphoma and chronic lymphocytic leukemia, all characterized by aggressive clinical courses and poor prognosis[208,209].

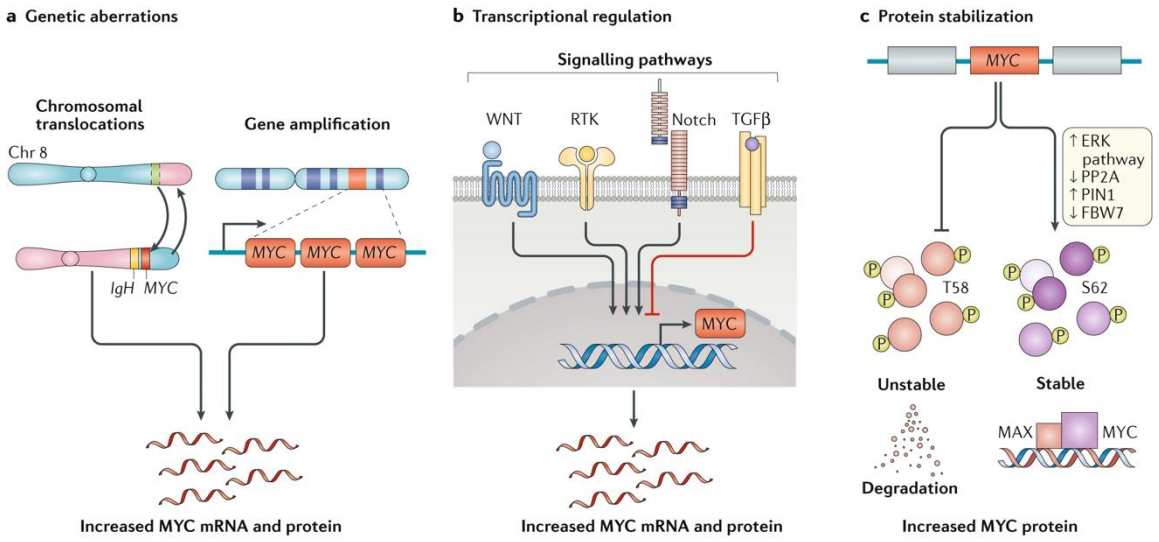

Figure 6: Main mechanisms of *MYC* deregulation in cancer.
A) Increased *MYC expression due to* genomic alterations. **B)** *MYC* expression is influenced by aberrant upstream mitogenic signal or loss of tumour supressing molecules. **C)** Mechanisms that lead to increased MYC protein stability. Image by *Dhanasekaran et al., Nature reviews Clinical Oncology, 2022* (Ref. 179).

Transcriptional alterations: Since *MYC* is being regulated by a plethora of growth regulatory pathways (see **Fig. 3**), its aberrant expression can be triggered by abnormal activity of upstream regulators, such as WNT[210], NOTCH[211] or STAT3[41]. Besides deregulation of upstream oncogenes, loss of tumor suppressors such as APC[39] or TGFβ[212] can also lead to MYC overexpression and ultimately to cancer.

Post-translational alterations: The last mechanism of MYC deregulation is involving mutations in factors that are involved in procedures such as MYC degradation, which will ultimately increase MYC's protein stability (summarized in **Fig. 6C**). As mentioned previously, MYC levels are being tightly regulated, with its phosphorylation on Ser62 and Thr58 having a central role in its proteasome-dependent degradation. Indeed, tumours with high levels of pSer62 and low levels of pThr58 are common[64]. Increased pSer62 is known to stabilize MYC protein and it is usually the result of abnormalities in upstream mitogenic pathways, such as the MAPK pathway[64,66]. Besides Ras-dependent induction of pSer62, mutations that result in low levels of the Ser/Thr phosphatase PP2A can also increase the stability of MYC protein[213]. Most importantly, there are also mutations that affect the Thr58 residue and therefore its ability to phosphorylate, leading to accumulation of pSer62 instead, stabilizing MYC levels further[214]. Moreover, FBXW7, the E3-ligase mainly responsible for MYC's proteasome dependent degradation, can be found inactivated during cancer, which leads to elevated MYC levels[215].

Regardless of the mechanism mediating *MYC* deregulated expression, the main point to be enunciated again here, is the fact that it has been shown in various contexts that

inactivation or inhibition of MYC results in tumour regression[197-199,201,202,216]. Indeed, it is a quite common phenomenon for cancer cells to show dependency on some oncogenes, which means that they need the sustained deregulated expression of this particular oncogene in order to survive, whereas the said oncogene's downregulation results in cell differentiation or apoptosis. This phenomenon is called "oncogene addiction"[217] and it is very frequently observed for *MYC*[197-199,201,202,216,218], indicating that MYC -and presumably a subset of its target genes- are required for tumor maintenance. Finally, besides the *MYC* overexpression in the majority of cancers and the addiction phenomenon in a plethora of them, it is noteworthy to mention that deregulated *MYC* expression is the actual first mutational event that drives several lymphoid cancers. For example, in Burkitt's Lymphoma, the driving event is the translocation of one *MYC* allele from chromosome 8 under the IgH locus of chromosome 14, which leads to constitutive *MYC* expression and therefore cancer[219]. Those types of cancer also exhibit *MYC* addiction.

1.2.2 MYC-driven Lymphomas

MYC is an important proto-oncogene, that is found deregulated in the majority of malignancies[1]. However, its deregulation is of more importance in some cancers than others; given its crucial role in B-cell clonal expansion and differentiation, it is no surprise that MYC aberrations are among the driving mutations in several hematological cancers, with various lymphoma subtypes holding a central position in that list[220,221].

Lymphomas constitute a group of malignant lymphocyte neoplasms with more than 90 subtypes. They are divided in a broader classification as non-Hodgkin or Hodgkin lymphoma. Hodgkin lymphoma (HL) is an uncommon neoplasm with occurrence mainly in young adults. HL is generally characterized by rare malignant cells (large multinucleated cells derived from B lymphocytes, known as Hodgkin and Reed–Sternberg cells); its most characteristic trademark is that those malignant cells are usually present in a microenvironment rich in immune effector cells. Most fortuitously, they have a high cure rate, being quite sensitive to radiation therapy, even in cases where the patients already are at an advanced metastatic spread stage[222].

On the other hand, non- Hodgkin Lymphomas (NHLs) consist of an heterogenous group of lymphoproliferative malignancies that are much less predictable than HLs. Among the most frequently observed NHL subtypes are the Diffuse Large B-cell Lymphoma (DLBCL), comprising a 30% of the cases and Follicular Lymphoma (FL) with a 20% occurrence. All of the other NHL subtypes have a frequency of less than 10% of the total cases[223].

MYC rearrangements are among the most common causes of MYC deregulation in hematologic malignancies. In fact, it is a recurring genetic abnormality in several aggressive B-cell lymphomas, among which are included Burkitt Lymphomas (BLs), DLBCLs, unclassifiable lymphomas with features between BL and DLBCL, rare de novo Acute Lymphoblastic Lymphoma/Leukemia (ALL), transformed Follicular lymphoma and plasmablastic lymphoma[220,224]. While MYC's part in the development of all the aforementioned malignancies is undoubtedly major, there are some distinctions regarding MYC's role in these tumors, which is likely reflecting on whether MYC deregulation consists a primary or a secondary event during the progression of the disease. For this reason, the presence of a *MYC* rearrangement in these diseases is of utmost diagnostic and prognostic importance[225], since it is usually linked with aggressive clinical behavior[226].

As mentioned, DLBCLs are the most common of lymphoma cases. Translocation of *MYC* can occur in this type of lymphoma, being observed in a 5-10% of the cases and it is indicative of poor clinical outcome[224]; this could be attributed also to the fact that in a large proportion of these cases, MYC rearrangements also co- occur with translocations of BCL2 and/or BCL6, giving rise to the more aggressive double- or triple- hit lymphomas (DHLs and THLs respectively)[219]. However, the DHLs and THLs do not originate only from DLBCLs, but they have also been observed in follicular lymphomas and B- cell lymphoblastic leukemias/lymphomas. While the most frequent rearrangements observed in DHLs is *MYC*/*BCL2*, there is also a small subset with *MYC*/*BCL6* instead[224,227].

Most importantly, translocation of *MYC* is the driving mutation for Burkitt lymphoma; its occurrence reaching 95% of the cases. The t(8:14)/*MYC-IGH* is the main genetic hallmark of BLs, being observed in 70-80%[228], with less common variations being t(2:8)/KAPPA-MYC and t(8;22)/MYC-LAMBDA[224]. While the juxtaposition of one of the *MYC* alleles under the promoter of immunoglobulin genes leads to constitutive *MYC* expression and therefore to malignancy, the non-translocated allele is silenced, or expressed at very low levels[229,230]. Since in non-transformed B-cells, MYC overexpression causes apoptosis via a p53-dependent pathway, in some occasions neoplastic BL cells harbor also TP53 tumor suppressor gene mutations[231].

1.3 MYC and Transcription

1.3.1 MYC, a selective transcriptional regulator

As already highlighted, MYC is a pleiotropic transcription factor with a key position in the growth regulatory circuitry, moderating the transcription of genes involved in cell cycle, proliferation, apoptosis, metabolism etc (**Fig. 3**). Its transcriptional activity has been studied diligently for many years, especially during the past decade, where the advances in next generation sequencing techniques has enabled access to enormous gene expression datasets, coupled with DNA-binding profiles[85,232-237].

Despite the vast amount of data available, profiling MYC-dependent transcriptional changes is complicated by a number of confounding issues. To begin with, MYC exhibits promiscuous DNA-binding profiles with a general inclination towards regions with active regulatory elements (i. e. promoters and enhancers). Indeed, MYC-binding is mainly associated with regions enriched for active chromatin elements, such as CpG islands, histone H3 lysine 4 methylation (H3K4me3, H3K4me1) and histone H3 lysine 27 acetylation (H3K27ac), or even the basal transcription machinery (mainly for RNAPII)[85,232,238,239]. As a matter of fact, upon its over expression, MYC can be detected virtually on all of these regions -a phenomenon called "invasion"[85,232,233,237].

The second issue is that as expected, overexpression of MYC will eventually lead to increased levels of total RNA[85,232,233,237], since MYC is affecting target genes that are involved in processes that feed back on global RNA synthesis and therefore general transcriptional changes happen as a secondary effect. This phenomenon, termed RNA amplification, together with the invasion mentioned previously, gave rise to the "general amplification" model of MYC, which supports that MYC can bind to every active chromatin element and this invasion will functionally lead to transcription of all of those loci, giving rise to the general RNA amplification previously documented.

Important work in our lab[85,234,240] and others[235,237], along with careful interpretation of the evidence presented in the "general amplification" model studies[232,233], leads to the conclusion that the one unifying model to interpret MYC transcriptional activity is the one describing MYC as a selective transcriptional regulator, meaning that it only regulates specific target genes, whether positively or negatively, a conclusion that has been discussed in several publications of our lab[1,25,240,241]. In fact, a very recent study[242] compared MYC-dependent gene regulation across data sets acquired from genetically engineered mouse models for T-cell acute lymphoblastic lymphoma[197], B-cell lymphoma[9], lung

adenocarcinoma[243], hepatocellular carcinoma[244] and renal cell carcinoma[245] and showed that even though the MYC-induced transcriptional changes are mainly tissue- and lineage-specific, there were common patterns such as the upregulation of embryonic stem cell gene programs and the downregulation of tissue-of-origin gene programs, which converges with a dedifferentiation phenotype. Importantly, across all five types of cancer, a common feature was deregulation of ribosome biogenesis genes, which are among MYC's most noted gene targets[118].

The main reasons for supporting MYC's function as a selective transcriptional regulator are the following: Firstly, previous work in our lab has exhibited that MYC expression does not always correlate with increased total RNA content, but does so only when there is a proliferative or metabolic switch in cell state afoot[85]. In the same study, overexpression of MYC in already proliferating fibroblasts did induce invasion of the majority of active promoters and enhancers, but this did not correlate with RNA amplification; the gene sets affected rapidly (either activated or repressed) were specific and distinct. Most importantly, in a more recent study from our lab, it became clear that even though MYC invasion to all active promoters is a fact, the majority of those interactions represent non-specific DNA-binding events, which do not lead to productive gene regulation[240]. Another reason, albeit technical, regards the normalization of the RNA-seq datasets[1]. More specifically, the studies of "general amplification" model were proposing the measurement of RNA levels per cell equivalent (instead of comparing them to housekeeping genes or average expression as per norm for this kind of studies), in order to avoid scoring genes that were less induced compared to average as "repressed". Nevertheless, since MYC is selectively regulating distinct gene sets, the proper way to normalize this type of data would be to normalize them both on cell equivalent and on average expression, in order to be able to discriminate between primary and secondary events.

All in all, MYC is a selective transcriptional regulator with specific gene targets, the unravelling and mapping of which is very important, in order to i) better our understanding of the mechanistics of MYC regulation and to ii) discover new therapeutic vulnerabilities among MYC effectors, since MYC itself is quite hard to target in disease (see section **1.4**).

1.3.2 Chromatin recognition, binding and regulatory chromatin modifications

The first step for MYC's regulatory activity is the chromatin recognition and binding. As previously mentioned, MYC requires heterodimerization with its obligatory partner MAX, in order to bind to chromatin with preferential tendency towards the E-box motif CACGTG[246] or variants thereof[246-248], in order to exert its transcriptional activity[1,25]. Most

importantly, MYC heterodimerization with MAX is not only required for binding E-boxes, but also “non consensus” sites[249].

MYC associates with active chromatin regions, such as CpG islands, regions bearing active histone modifications (H3K4me3, H3K4me1 and H3K27ac), basal transcriptional machinery presence and also DNAseI-hypersensitive sites (regions with chromatin accessibility)[239,250,251]. Indeed, in eukaryotes chromatin organization is such, that the DNA is wrapped around nucleosomes, which results in a tightly packaged chromatin structure, that transcription factors cannot bind. MYC itself, has not been recorded binding compacted, heterochromatic regions, even in the presence of E-boxes[85,239,250]. In fact, in a study about induced pluripotent stem cell (iPSC) reprogramming, MYC was shown to cooperate with Oct4, Sox2 and Klf4 (the 4 Yamanaka factors needed for iPSC generation[252]), but it required prior Klf4 activity in order to access closed chromatin[251]. Moreover, MYC seems to prefer promoters where RNAPII is already bound to[85,232,239,253], even if it has also been documented to enhance RNAPII loading to its target promoters[253].

From the above it becomes clear that MYC target gene recognition and binding requires the important regulatory step of chromatin remodelling and opening, which includes histone acetylation and ATP-dependent remodelling[109,152] (**Fig.7**). As a matter of fact, MYC is recruiting histone acetyltransferases (HATs) or HAT-associated proteins, such as TRAPP, GCN5, Tip60, HBO1 or CBP/p300 which are acetylating histone lysine residues, activating chromatin[74,75,253-256]. More specifically, MYC, through the MBII, is interacting with TRRAP (transactivation/transformation-associated protein)[257], which is an integral subunit of two distinct classes of HAT complexes GCN5/SAGA and TIP60/NuA4[255]; this correlates with its ability to promote histone acetylation at target promoters. Moreover, MYC also interacts with INI1, a core component of the chromatin remodelling complex SWI/SNF which is needed for MYC transactivation[258,259].

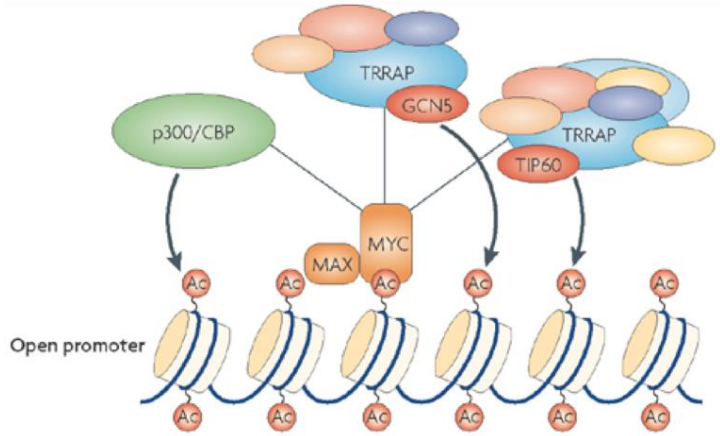

Figure 7: Chromatin remodelling by MYC.
MYC-MAX dimer recruits acetyltransferases, which modify chromatin in an open and active state. Image was adapted from *Cole and Cowling, Nature reviews Molecular Cell Biology, 2008* (Ref. 109).

Most noteworthy, MYC is also known to interact with Bromodomain Protein 4 (BRD4), a chromatin-binding protein with both HAT and kinase activities[260,261]. More precisely, BRD4

can phosphorylate MYC at Thr58, which will lead to MYC's ubiquitination and subsequent proteasome degradation[260]. On the other hand, it can also regulate chromatin remodelling by acetylating H3K122, which will eventually lead to eviction of the nucleosomes and subsequent accessibility of chromatin to the transcriptional machinery[262]. Several studies have shown BRD4 localizing with MYC on chromatin[263,264]. Another MYC interactor that affects the epigenome, is the G9 histone methyltransferase. This interaction is mediated by the MBII domain of MYC and has been proposed to mediate MYC's repressive activity[265].

In general, MYC has been implied in changing chromatin architecture several times[216,253,266]. There are studies that exhibit global changes in chromatin organization, such as decreases in H3 and H4 acetylation and increases in H3K9me3 (all of these changes being indicative of inactive chromatin), upon N-MYC or c-MYC downmodulation. This effect was noticed in various cell models, such as in Burkitt's lymphoma P493-6 cells or mouse osteosarcoma, hepatocellular carcinoma and T-cell acute lymphoblastic leukemia (ALL)[216,266], with the global effect being attributed to MYC's regulation of *GCN5*[266]. Besides association with HATs and HAT-activity proteins, MYC is also interacting with HDACs[267,268], which gives it an extra layer of control as an epigenetic regulator. Besides recruiting HDAC3 through MBIIIa interaction[267,268], it also has been shown to upregulate HDAC2 in various contexts and cancer types[269,270], a feature that together with MYC-dependent upregulation of HATs and GCN5 raises some questions over the specificity of the effect[271]. In addition to this, N-MYC has been shown to majorly decrease active histone marks in the genome, such as H3K9ac and H3K4 methylation[272], which further confirms once more that MYC has the ability to induce opening of the chromatin.

On the other hand, studies from our lab show that MYC is required for histone hyperacetylation and transcriptional activation of its specific target loci instead, upon mitogenic stimulation of rodent fibroblasts[273]. Consistently with this, it has also been demonstrated by our lab that there is an important correlation between MYC and histone modifications, mainly on high-affinity sites (namely at MYC-target gene promoters)[239,253]. In more detail, there is a simple combinatorial organization of histone marks, with specific groups gathering on specific promoters; chromatin bearing high H3 K4/K79 methylation and H3 acetylation[239], which marks "euchromatic islands" and is largely associated with pre-engaged basal transcription machinery[274], is indispensable for recognition of any target site by MYC, whether this is a canonical E-box or another sequence[275]. Following this, Martinato and colleagues[253] showed that MYC does indeed induce acetylation on several lysine residues of H3 and H4, but most of these acetylation events where in fact enriched

for MYC's target promoters, with only H3K14ac showing increase also in non-target promoters. This was in accordance with the notion of MYC recruiting and cooperating with HATs or HAT-associated proteins[74,75,253-256] that was previously mentioned. In the same study, they also exhibited that MYC has no effect on H3K4 methylation, since this modification precedes MYC binding on chromatin[239]. Of note, they also established a specific connection between MYC and the histone variant H2A.Z. In fact, it was shown that MYC induction was increasing H2A.Z incorporation on target sites, while no such effect was recorded for non-target promoters[253].

From all the above mentioned, there are three main points to be summarised: One is that MYC requires an open and poised chromatin context in order to bind to the promoters and transcriptionally regulate its target genes; E-boxes outside of such context are not significantly bound. The second one is that upon MYC-binding, further chromatin modifications are induced and this is an important mechanism contributing to the fine-tuning of gene expression in response to extra-cellular stimuli. However, the whole of MYC-regulated chromatin modifications on its target loci needs to be further explored. Lastly, even if MYC is binding practically all active promoters and enhancers upon its overexpression, this binding still does not go out of sequence context; it just becomes less selective, in the sense that it will bind also to lower affinity variant sites[85,232,240]. The point to be stressed here again is that not all the chromatin binding events during MYC "invasion" to promoters are productive. Instead, the majority belongs to non-specific DNA binding, which is important for engagement unto genomic regulatory regions, but the real informative factor for MYC's transcriptional activation is the sequence recognition[240].

1.3.3 MYC and RNAPII Interplay

RNA Polymerase II (RNAPII) is a holoenzyme that catalyzes the transcription of protein coding genes and a lot of non-coding RNA genes. Its large subunit, Rbp1, contains the Carboxyl-Terminal Domain (CTD), which is highly conserved and composed of repeats of the heptapeptide sequence Y_1-S_2-P_3-T_4-S_5-P_6-S_7. While all of those residues can be modified in various ways, the two best studied and most important modifications for RNAPII transcriptional function are the phosphorylation in Ser2 and Ser5[276]. The TFIIH-associated kinase CDK7 is usually responsible for the RNAPII phosphorylation at Ser5 and this is a form of RNAPII mainly found at the 5' end of the genes[277,278]; CDK9 on the other hand, a core subunit of p-TEFb (positive transcription elongation factor), is responsible for RNAPII phosphorylation of Ser2, which is an RNAPII form gradually accumulating as RNAPII progresses, with higher levels towards the 3' end of the gene[277,278]. Given this, the

prevalent model regarding RNAPII says that it is recruited to promoters in a hypo-phosphorylated CTD form; subsequently, the CTD becomes phosphorylated in Ser5 during initiation of transcription, naming the RNAPII phosphor-Ser5 as the "initiating" RNAPII form. Finally, the CTD starts becoming phosphorylated on Ser2 during productive elongation, naming the RNAPII phosphor-Ser2 form as the "elongating" RNAPII[279].

The procedure of transcription involves three major steps; initiation, elongation, and termination[280]. During the first step of initiation, transcription factors are recruiting RNAPII and several cofactors to their target genes. Afterwards, RNAPII is producing a short transcript of around 20-50 base pairs (bp) downstream of Transcription Starting Site (TSS), till transcriptional pause factors induce its pausing. Subsequently, the elongation factor P-TEFb needs to be recruited to RNAPII; As previously mentioned, one of P-TEFb's core subunits, Cdk9, is responsible for phosphorylation of Serine 2 of the Rbp1 CTD of RNAPII. Phosphorylation of both RNAPII and of the pausing factors results in productive transcriptional elongation. The last step of transcription is transcriptional termination, which is stimulated by recognition of polyadenylation sites by RNAPII-associated factors during elongation.

MYC is a transcription factor heavily involved with RNAPII function. Early studies in the field have shown that MYC is mainly influencing the RNAPII elongation step. More specifically, studies on the *CAD* gene, a gene among the first ones to be discovered as a MYC target gene, have shown that RNAPII was constitutively bound to the *CAD* promoter, while full-length of mRNA or RNAPII at the end of the gene were noticed only in S phase, which was coinciding with MYC occupancy. Furthermore, the E-box sites at the *CAD* promoter were dispensable for RNA Pol II recruitment, which led to the conclusion that for this gene, MYC binding was required for the step of transcription elongation, but not for the initiation[281]. In fact, in a follow up study of the same team, they showed that the effect on CAD transcription elongation was due to MYC's recruitment of P-TEFb to the promoter[282]; actually, MYC binding to the *CAD* promoter seemed to not be needed for transcriptional activation when P-TEFb was directly recruited to the promoter. More recent studies further confirmed that MYC can interact with the P-TEFb subunits Cyclin T1 and CDK9[283-285]. Of course, CDK9 is needed for phosphorylation of RNAPII at Ser2, a fact that establishes a link between MYC and transcriptional elongation. Another link that needs to be noted is that MYC can also interact with the elongation factor DSIF and more specifically with one of its subunits, SPT5. MYC recruits SPT5 to RNAPII and therefore enhances

productive transcription, since SPT5 and by extension MYC, is required for fast and processive transcription[286].

Since phosphorylation of RNAPII to Ser2 by P-TEFb is required in order for the paused RNAPII to be released and proceed to elongation, it has been suggested that MYC's regulatory role in the transcriptional activity of RNAPII lies in the step of pause-release and not the RNAPII recruitment, unlike other transcription factors[285,287]. More specifically, it has been shown that inhibition of MYC led to lower levels of RNAPII phospho-Ser2 levels, while there was no significant difference noted for the levels of RNAPII phospho-Ser5, which led the authors to propose that MYC was not having an effect on the initiation step; instead, without MYC, RNAPII could not be released into productive elongation. They reported the same effect also for total RNAPII, where MYC inhibition led to decreased occupancy of RNAPII in transcribed regions, while its levels seemed unaffected at the promoters of MYC bound genes. However, the decreased RNAPII occupancy effect they noticed in transcribed regions upon MYC inhibition was milder than the one they got after treatment with the CDK9 inhibitor flavopiridol, which is a true inducer of RNAPII pausing[285]; this indicates that MYC's main role in RNAPII regulation may in fact not be in the pause-release step.

Indeed, previous work from our lab has shown that MYC's primary function in transcription regulation is the loading of RNAPII[234]. This study computed the variations of RNAPII throughout the genes upon MYC overexpression. Modelling of RNAPII across four different features, namely flux at the promoter, pause-release rate, elongation rate and release rate from Transcription Ending Site (TES), showed the following key features: Firstly, consistently with the pause-release studies[285], MYC activation resulted in increased levels of pause-release phenomena at activated promoters. However, these changes were associated with sudden and more prominent changes in RNAPII loading, suggesting that in fact, MYC is promotes both RNAPII loading and pause-release. Secondly, RNAPII flux at promoters was in accordance with the MYC share (MYC binding), while the other 3 features seemed to be significantly less relevant. Most importantly, the opposite effects were noted for MYC-repressed genes, where there was an important decrease of RNAPII at the promoters, primarily due to low loading; the latter was concluded because levels of RNAPII pause-release went down accordingly to the promoter RNAPII levels[234].

Lastly, there has been a recent study that connects MYC with transcription termination too[288]. In brief, an interaction between MYC and Protein Arginine Methyltransferase 5 (PRMT5) was uncovered; PRMT5 catalyzes symmetrical dimethylation of RNAPII at the arginine residue R1810 (R1810me2s), a modification necessary for proper transcriptional

termination and splicing of transcripts. While MYC overexpression led to an increase of said modification, MYC inhibition with shRNA or Omomyc expression led to restraint of that effect. More importantly, MYC inhibition also exhibited decreased levels of RNAPII phosphor-Ser2, confirming once more the role of MYC in elongation. However, Omomyc induction also caused an increase in total RNAPII, both at promoters and at the end of MYC-bound genes, with the researchers suggesting that RNAPII accumulation at the promoters is due to Omomyc's ability to decrease pause-release, while the accumulation at the TES could be explained by the impaired RNAPII R1810 symmetrical dimethylation, which has been previously shown to affect transcription termination and could lead to RNAPII accumulation at termination regions of active genes[289].

1.3.4 MYC-dependent repression

Most of the information already mentioned for MYC's transcriptional regulation regarded mainly its function as a transcriptional activator. However, MYC is a selective transcriptional regulator and while it upregulates the vast majority of its target genes, it also exerts suppressive transcriptional effects in a smaller portion of them[85,234,235,237].

In truth, mechanisms of MYC-mediated transcriptional repression are less understood than the ones of activation, but many studies indicate that MYC's direct suppressive function stems by interactions with various cofactors, the most well studied one being MIZ-1[237,290,291]. MYC target gene repression via MIZ1 is spanning along a wide range of genes, including cell cycle inhibitors, cell adhesion molecules and tumor suppressive miRNAs[16] and it is crucial for several biological activities of MYC, such as apoptosis, cell cycle progression, self-renewal and cell adhesion[1].

For example, some of the most known MYC-repressed genes are encoding CDK inhibitors, such as p15, p16, p21 and p27[31,136,141,292,293]. Repression of these genes leads to accelerated cell cycle and growth promotion. In fact, TGF-β, which was previously mentioned to suppress MYC-dependent growth induction[46], does so by positively regulating p15, leading to cell cycle arrest; this is not happening upon MYC deregulation[294], where MYC/MIZ-1 mediates p15 induction and promotes cell growth and proliferation instead. Another example of MYC/MIZ-1 suppression that affects cell cycle and proliferation regards the suppression of genes regulating the circadian clock. More specifically, it was shown that upon overexpression of MYC in U2OS cells, MYC formed a repressive complex with MIZ-1, targeting the circadian clock genes *BMAL1*, *CLOCK* and *NPAS2*[295].

Another well-defined MYC repressed gene is the one encoding for integrin β1, a very important factor for cell adhesion between stem cells and their niche. Suppression of integrin β1 by MYC leads to subsequent differentiation of the stem cells and exhaustion of the stem cell pool[296]. Besides this, MYC/MIZ-1 interaction can also suppress transcription factors such as the serum response factor (SRF). In mammary epithelial cells, overexpression of MYC leads to the repression of SRF-regulated genes, an effect that contributes to MYC-induced apoptosis[291].

Interaction with MIZ-1 is not the only way for MYC to exert repressive activity. Another, more indirect way of MYC suppression, relies on MYC inducing the expression of EZH2, a member of the Polycomb Repressive Complex 2 (PRC2), by directly suppressing miR26a, a miRNA negatively regulating EZH2 and therefore Polycomb-mediated transcriptional repression[297,298]. Finally, MYC can also indirectly repress transcription by recruiting HDACs to chromatin; subsequent histone deacetylation leads to nucleosome compaction and inaccessibility of chromatin, which impedes transcription[267].

1.4 Targeting MYC for cancer therapy

From everything discussed so far, it is clear that MYC has an important role, not only in tumor initiation, but also in maintenance[182]. This of course implies that MYC is an ideal candidate for pharmacological inhibition as an anti-tumoral therapy. Despite major research efforts in the field, MYC was generally considered to be "undruggable" up till recently, with very few successful inhibitors in clinical trials. There are several reasons why MYC targeting has posed such a challenge over the years. First of all, MYC's structure is lacking the binding pocket necessary for pharmacological interaction. Secondly, as a transcription factor, it is mainly localizing in the nucleus, so any potential inhibitory compound would need to be able to penetrate the nuclear membrane in order to disrupt MYC. Another possible reason is that MYC, together with MYCN and MYCL could be functionally redundant between them, so any potential inhibitor should be able to target all of them at the same time. All the various reasons that have hindered the development of viable MYC inhibitors over the years have been reviewed and addressed elsewhere[299-303].

Despite the fact that no specific MYC inhibitor has reached the clinic yet, significant efforts in the field are continuing, towards two main directions: Interference of MYC's production or its function.

There have been several approaches towards inhibiting *MYC* transcription. One of them is by using small molecule ligands that stabilize the G-quadruplexes, that tend to form in guanine-rich regions, such as the *MYC* promoter, thus repressing transcription. One of those ligands was thought to be a specific binder of *MYC* G-quadruplex and had reached clinical trial level, but then was shown to also disrupt nucleolin bound to G-quadruplexes in ribosomal DNA and therefore suppression of *MYC* could be due to off target effects[304,305].

Other attempts for direct MYC inhibition revolve around the use of antisense oligonucleotides and siRNAs. Several antisense oligonucleotides were shown to inhibit *MYC* expression in vitro, either directly[306] or indirectly (e.g by preventing ribosomal assembly and therefore *MYC* mRNA translation)[307]. Some of them reached clinical trials but never reached the clinic. The same thing stands for some shRNAs[308] approaches, where their development stopped, due to not optimal pharmacokinetics.

On the other hand, indirect inhibition of MYC's transcription seems to be more promising so far[309]. *MYC* expression is regulated by multiple factors, with the bromodomain proteins being among them. In fact, their pharmacological inhibition causes downregulation of MYC and its target genes[310,311]. For example, targeting of BRD4 -which was previously demonstrated to induce MYC transcription[312]- with JQ1, a selective small-molecule inhibitor, caused cell cycle arrest and cellular senescence in three murine models of multiple myeloma[311]. Significant antitumor activity upon BET-bromodomain inhibition was also reported in xenograft models of Burkitt's lymphoma and acute myeloid leukemia[310], as well as in three neuroblastoma models[313]. Nevertheless, there is a drawback in this approach and it lies with the fact that bromodomain proteins control a plethora of other genes[235,314], which renders the effect non-specific to MYC. Moreover, in case of BRD4 inhibitors, this strategy is limited to cases where BRD4 is the predominant regulator of *MYC* transcription, and may be ineffective in a subset of tumors with *MYC* gene amplification or protein stabilization[315].

Another indirect way of targeting MYC is through inhibition of CDK9, the catalytic subunit of p-TEFb, which is associated with BRD4 and is one of the major components of the MYC transcription regulatory complex[285,316]. Suppression of CDK9 has exhibited ablation of MYC and MYC-dependent transcriptional programs, accompanied by tumor regression in MYC-driven hepatocellular carcinoma and B cell lymphomas[317,318].

MYC transcription is also dependent on CDK7 activity. Indeed, the CDK7 inhibitor THZ1 has shown anti-proliferative efficacy in various cancer models, including pre-clinical models of small cell lung cancer with high MYC expression[319]. CDK7 inhibition was proven fruitful

also in neuroblastoma cells and a mouse model of high-risk neuroblastoma, where THZ1 selectively disrupted the transcription of amplified MYCN, resulting in significant global repression of MYCN-dependent transcriptional amplification and tumor regression, without toxicity[320]. Other models where TZH1 treatment was successful include i) hepatocellular carcinoma with high MYC expression, where THZ1 treatment significantly impaired tumor growth[321] and ii) patient-derived xenografts models of ovarian cancer patients, where THZ1 causes significant tumor growth inhibition and downregulation of *MYC* expression[322].

Provided that MYC is regulated also by the PI3K-AKT-mTOR signalling (**Fig. 3**), inhibition of mTOR has exhibited a decrease of MYC mRNA translation in lymphomas and multiple myelomas[323]. This is due to lack of mTOR-dependent 4EBP1 phosphorylation, allowing 4EBP1 to negatively regulate the translation initiation factor eIF4E and therefore MYC translation[324]. Similarly, inhibitors for translation initiation factors such as eIF4A, also have been shown to reduce MYC mRNA translation, along with exhibiting tumour regression in mouse models of colorectal cancer [325].

Besides targeting MYC's production, another main strategy for MYC inhibition is to interfere with its function. Since MYC needs to dimerize with its obligatory partner MAX, in order to enforce its transcriptional activity, the disruption of MYC-MAX interaction seems a very promising therapeutic target. Numerous small molecule inhibitors have been developed in order to inhibit MYC/MAX dimerization or DNA binding, or alternatively stabilize the monomeric form of MAX, although their therapeutic utility has so far been limited by poor bioavailability, rapid metabolism, inadequate target site penetration and unclear off-target activities[326,327]. Nevertheless, during the last years some progress has been made, with the identification of compounds that show ameliorated in vivo properties[328]. Other newly discovered compounds show promising results in MYC-driven cancer cell lines, by disrupting the MYC/MAX heterodimerization and also potentially unstabilizing the MYC protein, leading to recess of proliferation[329]. It remains to be seen if the same efficacy will be achieved also in vivo. However, another recently developed small molecule inhibitor of MYC/MAX dimerization, MYCMI-6, has shown very promising results both in vitro and in vivo, in neuroblastoma xenografted mice, where tumor regression and induction of apoptosis were documented[330]. Lastly, there are also compounds that allow MYC/MAX dimerization, but are blocking its binding to DNA, therefore successfully inhibiting MYC's transcriptional activity. In fact, one of them, KSI-3716 was shown to induce

apoptosis in promyelotic leukemia cells and also to inhibit tumor growth in bladder cancer xenografted mice[331,332].

Even though progress in the field of MYC inhibition is continuous, there is still no inhibitory compound clinically available. Nevertheless, a successful development in the field comes in the shape of Omomyc, a dominant negative *MYC* mutant, that is currently in clinical trials[299]. Basically, Omomyc is a MYC mutant, that retains the MYC dimerization domain, but bears four mutations in the leucine zipper region. This allows it the ability to homodimerize, whereas the wild type MYC cannot[333]. These dimers can bind to DNA with low affinity, resulting in a dominant negative form of MYC, which impairs MYC's transcriptional activities by preventing its binding to E-boxes[202,333]. Omomyc can selectively bind not only to MYC, but also N-MYC, MAX and MIZ-1, without interacting with other bHLH proteins. Even though it also interacts with MIZ-1, it retains the MIZ-1 dependent repression function[334].Of note, Omomyc induces apoptosis, while reducing cell proliferation, especially in MYC over-expressing cells[335]. Most importantly, any toxic effects noticed, were minor and reversible[301], while it has been efficient in various preclinical mouse models, including KRas-driven lung cancer[201], pancreatic β-cell insulinomas[336], gliomas[337] and skin papillomatosis[338]. However, despite its encouraging results in all these models, till recently, the Omomyc mini-protein has been considered to be therapeutically unviable, being overly bulky and unfit for intracellular delivery, which kept it classified as a proof of concept for MYC inhibition. Nevertheless, a new, purified version of the mini-protein was proven to have intrinsic cell-penetrating properties, enabling its direct delivery in vivo and rendering Omomyc fit for clinical trials[20,339].

Lastly, there is another popular approach for targeting MYC indirectly, taking advantage of "synthetic lethality", which is defined as the emergence of a deleterious phenotype after perturbation of two genes in combination, whereas none of the two genes individually could have caused said phenotype[340]. This approach is frequently exploited in cancer, in order to study how particular oncogenic mutations may sensitize tumor cells to those therapies targeting synthetic-lethal factors, in order to avoid severe toxic effects on normal tissues. In the case of MYC, this approach is very important, mainly because the plethora of its cofactors and interactors could be synthetic lethal in MYC-addicted tumours, thus providing a therapeutic vulnerability.

As an example, MYC is known to regulate the cell cycle, by interacting with a number of Cyclin-Dependent Kinases (CDKs) and CDK-inhibitory proteins[177,341]; this interaction has been exploited pharmacologically and indeed, several studies show that pharmacological

inhibition or genetic ablation of certain CDKs can impair the growth of cells with deregulated MYC activity[342,343]. Most importantly, some CDK inhibitors have also reached the clinical trial level, being effective in vivo against aggressive MYC-driven B-cell lymphoma[317] or multiple myeloma[344], causing downregulation of the anti-apoptotic factor MCL1.

Other quite prominent examples of MYC synthetic lethality stem from MYC's implication in apoptosis. Since a plethora of cancers exhibit deregulated expression of the BCL-2 family (pro- apoptotic and pro-survival proteins), the connection between them and MYC is investigated. Venetoclax, an FDA approved selective BCL2 inhibitor is used for several haematological malignancies[345]. In MYC-driven diffuse large B cell lymphomas (DLBCLs), the combination of Venetoclax with R-CHOP (the first line chemo treatment for several non Hodgkin lymphomas) recently showed potential for improved efficacy over the monotreatment of R-CHOP[346]. Furthermore, inhibition of mitochondrial translation by the antibiotic Tigecycline, synergizes in vitro with Venetoclax in killing human cells of "double hit lymphoma" (DHL) – a subtype of DLBCL characterized by overexpression of *MYC* and *BCL2*, due to chromosomal rearrangements of both– and revealed strong antitumor effect in xenografted mice[347]. Moreover, in MYC-driven lymphomas that are also characterized by high BCL2 expression, such as DHL or "double expressor lymphomas" (high co-expression of MYC and BCL2 without underlying chromosomal rearrangement), venetoclax synergizes with BET inhibitors leading to a reduction in tumour burden and increased survival of xenograft-bearing mice[348]. As with BCL-2, high levels of the anti-apoptotic protein MCL-1 are also common among diverse cancer types and its overexpression coupled with high expression of MYC can accelerate lymphomagenesis. Indeed, genetic ablation of *MCL-1* in *Eμ-MYC* transgenic mice or blockade of MCL-1 in myeloma cells, has showed delayed MYC-driven lymphomagenesis and increased cell death respectively, indicating MCL-1 as critical for MYC-driven tumorigenesis[344,349].

Of course, seeing that MYC's main function is transcription, there are several interactions there that could be exploited. For example, one of the most important MYC interactors is WDR5, which is recruiting MYC on chromatin[350,351]. Indeed, disruption of the MYC-WDR5 interaction in vitro is suppressing cell growth in neuroblastoma cells[352], while also inducing tumor regression in vivo[350]. Other transcriptional cofactors of MYC that are valid candidates for MYC targeting are the HATs P300/CBP and GCN5. In fact, both of them have been shown to downregulate *MYC* expression upon their inhibition[353,354]. Of note, GCN5 is overexpressed in Burkitt's lymphoma and its inhibition is downregulating MYC target

genes, inducing reduction of viability and proliferation in vitro[355]. Lastly, other MYC interactors, such as HDACs have exhibited promising features as therapeutic targets in MYC-driven cancers[356-358].

Of course, MYC is also key regulator of metabolism. Work in our lab and others has shown that MYC-overexpressing cells exhibit enhanced dependency on mitochondrial activities, such as transcription, translation and Oxidative Phosphorylation (OxPhos)[359-361]. Disruption of these processes sensitizes MYC-driven lymphomas to apoptosis, providing therapeutic synergy with inhibitors of anti-apoptotic BCL2 proteins (BH3-mimetics)[347,360].

All in all, the road to MYC inhibition has been long and windy, with MYC still largely being thought as "undruggable". However, during the last decade, the field's efforts have started paying off, with various small molecule inhibitors for MYC or for its upstream regulators/cofactors/interactors showing encouraging results in MYC-addicted malignancies, proving that MYC inhibition is indeed a worthy holy grail for cancer.

1.5 Cellular models to study MYC effects

MYC has been in the center of scientific focus for more than forty years now. Huge efforts in the field have given us a lot of in vivo and in vitro models in which to study MYC effects at physiological levels or deregulated ones (whether up- or down-regulated). Here we will mention some of the most historic cellular models, along with some used for the purposes of this thesis.

1.5.1 MYC super- activation: The MycER^{TM} model

Intracellular proteins can be converted to become hormone-dependent by fusing their coding sequence with the hormone binding domain (HBD) of steroid receptors. This approach has been successfully used to generate conditional forms of various proteins, including transcription factors and kinases[362]. The idea behind this approach, is that since most cell types do not express endogenous estrogen receptor (ER), the HBD can be used as an heterologous regulatory domain. Indeed, one of the proteins successfully fused to the ER is MYC. While the initial version of MycER was allowing conditional MYC activation[363,364], there were two major drawbacks in the system; one was that ER possesses an inherent ligand-dependent transactivation activity, which contributes to the total transcriptional activity of the fusion protein. The second was about culture media and serum containing phenol red (a weak ER agonist) and estrogens respectively; both of those characteristics contributed to the system's leakiness[365]. Luckily, the solution to these problems came by introduction of a mutant form of murine ER that cannot bind oestrogen; instead, the fitting

ligand is the synthetic steroid 4- hydroxy-tamoxifen (OHT), which lacks the inherent transactivation function[366]. This led to the model as we know it today (**Fig. 8**); MycER^{TM}, a switchable form of the c-MYC protein that is sequestered in the cytoplasm and only upon OHT treatment it can move in the nucleus, leading to MYC overactivation. Since then, this model has been extensively used in a plethora of studies[85,367-370] (and was briefly used also here for the purposes of this thesis) as a tool for investigation of MYC's biological function in both cultured cells and most importantly transgenic animals[365].

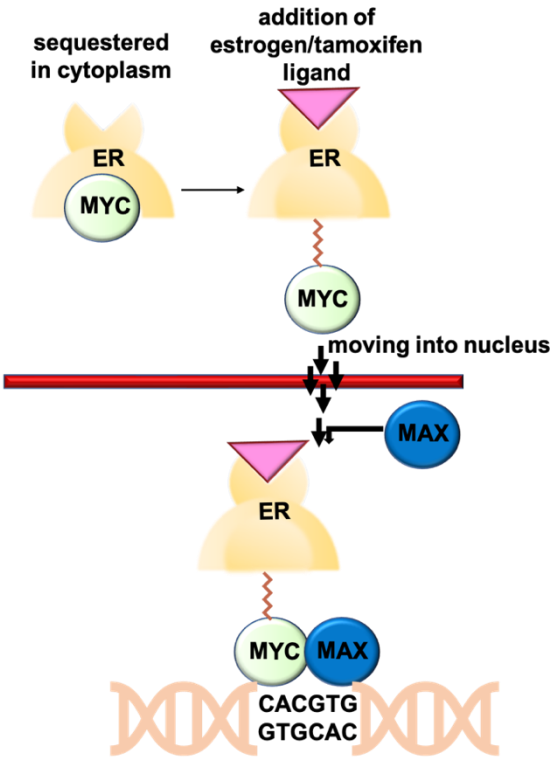

Figure 8: Schematic representation of MycER^{TM} model.

1.5.2 MYC down-regulation

Since MYC has a very important role in several biological processes such as proliferation, cell cycle, apoptosis etc[1] and its deregulation leads to cancer, it stands to logic that it poses an appealing target for cancer therapy. Nevertheless, as already discussed, MYC is largely considered to be "undruggable"[299], therefore models that downmodulate MYC are highly appealing, in order to get insights on how cells react to MYC inhibition. Since genetic perturbations leading to knockouts of *c-MYC* and *N-MYC* are embryonic lethal in mice[11,12], the most popular approaches by which MYC inhibition can be achieved are revolving around conditional knockout or knockdown systems, such as Cre-mediated recombination[13,350,371-373], tetracycline dependent Tet-on/off systems[85,127,232,374-377], or inducible degron systems[235]. Here we will mention some of the key in vitro cellular models:

P493-6 human B-cell lymphoma model: Tet on/off models are quite popular, because they allow comparison between high versus low levels of the protein of interest. Indeed, the P493-6 cells with a MYC Tet-repressible system have been extensively used in the literature as a model for manipulating MYC[85,127,232,374,376,377]. Basically, these cells bear a conditional tetracycline-regulatable *MYC* construct; in the absence of tetracycline, *MYC* is expressed in high levels (MYC-high), comparable to those of Burkitt lymphoma lines, which till recently made these cells the cell line of choice for modelling MYC functions in human lymphoma. Upon tetracycline treatment, the construct is not expressed and therefore the

cells switch to the 'MYC-low" state. While this constitutes a tractable model and a vast amount of data on MYC regulation in lymphomas have been gathered with it, it does not reproduce the exact biological features of MYC-associated lymphoma and it also might be slightly unfavourable for acute MYC elimination and careful kinetic studies, since it takes several hours for MYC to shut down to satisfactory levels.

Cre-inducible *MYC* knockout: Another alternative to study MYC inhibition is inducible gene ablation, which has been favoured in various models and has also been applied successfully in vivo[371-373]. A good example of an inducible MYC knockout in vitro was used in a recent study[350], where the authors took advantage of CRISPR-facilitated homologous recombination in order to introduce CRE-ER inducible recoded versions of *MYC* exon 3 in their cells (**Fig. 9**).

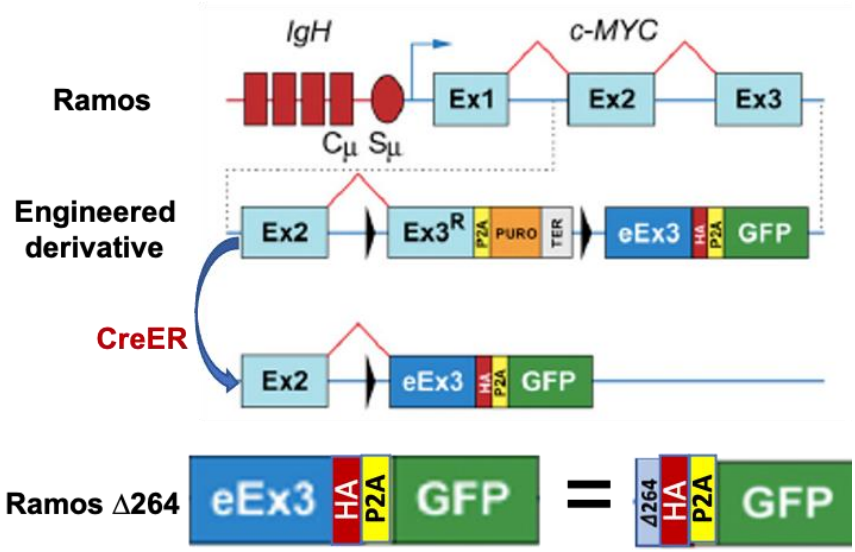

Figure 9: Schematic representation of *MYC* switchable knockout model.
Image was modified from *Thomas et al., Proc Natl Acad Sci U S A, 2019* (Ref. 350)

More specifically, they used a Burkitt's lymphoma cell line, Ramos, which bears the t(8:14)/*MYC-IGH* and they engineered them to express the Cre recombinase linked to the estrogen receptor binding domain. Subsequently they inserted a recoded *MYC* exon 3 (containing a cassette with a truncated at residue 264 (Δ264) version of exon 3 and a GFP marker). In the unswitched state, Ramos *Δ*264 express a wild-type MYC protein and puromycin resistance. Upon CreER activation through OHT treatment, the allele is switched to express the exchanged Exon3 (eEx3), encoding a modified form of MYC, followed by GFP. This leads to the production of a truncated, inactive form of MYC (*Δ*264), resulting in complete loss of function. This is a valuable model for profiling MYC-dependent changes in human Burkitt lymphoma (briefly used also for the purposes of this thesis), with its main disadvantage being that it needs a lot of hours for the exon switch to take place, which renders it unsuitable for acute MYC downmodulation kinetics studies.

Conditional MYC degradation: Last but not least, a very appealing choice for acute studies on the effects of proteins is taking advantage of degron systems that allow conditional degradation of the protein of interest. The main advantage of these types of

models lies with the fact that acting directly on the protein is of course a faster way of its downmodulation that trying to induce changes at the genetic level first.

One such model, developed in the last decade or so, is the Auxin -inducible degron system[378]. This model is exploiting a plant system where the plant hormone auxin is able to induce rapid degradation of some transcriptional repressors through the SCF E3 ligase pathway. The key point here is that even if eukaryotes share this protein degradation pathway with plants, they are unaffected by auxin. Therefore, it is possible for one to insert the Auxin Inducible Degron (AID) system in non-plant cells, in order to target a protein of interest for degradation upon auxin treatment. In brief, an AID-tag is introduced to the coding sequence of the protein of interest. Then the cells are infected with the auxin-binding receptor Tir1; treatment with auxin (IAA) will lead to polyubiquitylation and swift proteasome degradation of the AID-tagged protein (**Fig. 10**). The advantages of this approach are that the degradation of the protein is i) inducible and reversible, ii) highly effective and most importantly, iii) rapid. The latter in particular, is what renders this system an ideal tool for the assessment of immediate effects of the protein of interest; rapid protein degradation allows careful, kinetic studies to take place before accumulated secondary effects can confound the results.

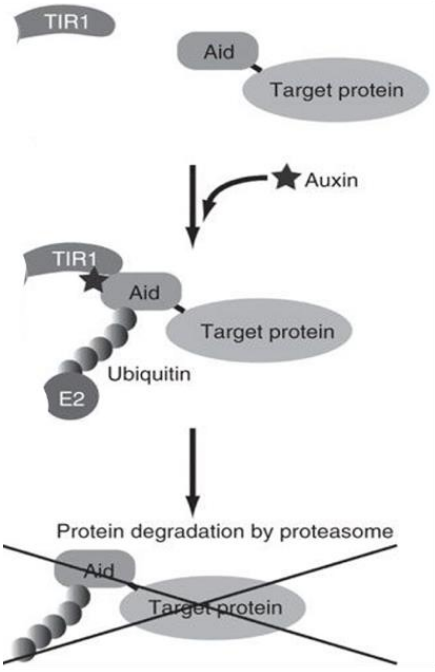

Figure 10: Schematic representation of Auxin Inducible Degron System (AID). Image was adapted from *Nishimura et al., Nature Methods, 2009* (Ref. 378)

Indeed, a recent study used this approach in order to dissect direct MYC and BRD4 effects on transcription. Rapid and efficient degradation of these proteins in the Chronic Myelogenous Leukemia cell line K562, allowed them to report that MYC acts as a selective transcriptional activator, while BRD4 had a general effect on RNAPII transcription[235]. Whereas this study used a first generation AID degron (which we are also using for the purposes of this thesis), a more evolved version of the system, called AID2, is now available[379]. While the two systems seem to be quite comparable in terms of time and effectiveness of degradation, the AID2 can also be introduced in animals, a very interesting feature that should allow comparison between the effects of a protein of interest in vitro and in vivo.

1.6 Aim of the project

MYC-driven malignancies generally show oncogene addiction, but the primary MYC-dependent events involved in tumor maintenance remain to be fully understood. Indeed, profiling MYC-dependent transcriptional changes in tumor cells is complicated by a number of confounding issues such as MYC's promiscuous DNA-binding profiles and the induction of RNA amplification as a secondary effect upon MYC overexpression. Thus, discriminating between direct and indirect effects becomes of utmost importance in the field. Therefore, the goal of my project is the identification of primary MYC-dependent transcriptional programs and mechanisms in MYC-driven lymphoma, based on the controlled, rapid inactivation of MYC and short-term profiling of the consequent regulatory changes. This profiling entails following changes both at the chromatin and transcriptional level, in order to gain an integrated mechanistic view on MYC-regulated transcription and the molecular underpinnings of oncogenic addiction in MYC-driven lymphoma; this in turn should provide important mechanistic and biological insights towards possible therapeutic interventions.

2. MATERIALS AND METHODS

2.1 Cell lines

2.1.1 Construction of the MYC-AID lymphoma cell lines

The human B-cell Lymphoma cell lines Ramos, Raji and SU-DHL-6 were grown in RPMI 1640 with stable Glutamine, supplemented with 10% Fetal Bovine Serum (South American origin), 1% Penicillin-Streptomycin and 1% Sodium Pyruvate (NaP). For the construction of the MYC-AID derivatives, we followed the procedure described by Muhar et al. for the K562 cell line[235]: parental cells were electroporated with 1μg each of px458-sgMYC.C2 and pX458-MYC-AID. For electroporation, two pulses of 1000 volts, with pulse width 50 ms each, were performed with a Neon® Transfection System, and successfully electroporated cells were then selected with blasticidin 8μg/ml. For the SU-DHL-6 line, immunoblot analysis of the blasticidin-resistant bulk population revealed expression of both MYC and MYC-AID: we thus derived single-cell clones by limiting dilution and screened for those expressing solely MYC-AID, prior to introduction of Tir1. For Ramos and Raji, only MYC-AID was detectable in the blasticidin-resistant pools, allowing us to proceed directly to the next step. The three lines were then infected with the Tir1-expressing vector pRRL-SFFV-OsTir1_3xMyc-tag-T2A-eBFP2, followed by sorting of BFP+ cells with a BD FACSMelody™ cell sorter and derivation of single-cell clones, either by direct plating of single cells in a 96-well plate during sorting, or by limiting dilution of the bulk BFP+ population. The clones were subsequently screened by Western blotting, and those expressing only MYC-AID (as distinguished by its size) and showing effective degradation of the protein upon Indole-3-acetic acid (IAA) (Catalog# I5148, Sigma-Aldrich) treatment were chosen for further characterization. All of the above plasmids were a gift from Johannes Zuber.

For derivation of the MYC-AID FUCCI lymphoma cells, the MYC-AID lines were infected with the FUCCI(CA)2 vector[380] and subsequently selected for FUCCI positivity (mCherry, mVenus or both) with a BD FACSMelody™ cell sorter.

All of the above cell lines were grown in suspension and passaged by dilution in fresh medium every second day, at concentrations of 400.000-500.000 cells/mL. All cells were kept in incubators with stable conditions of 37 °C and 5% CO2.

2.1.2 Other cell lines used in this study

The switchable MYC knockout line Ramos 1E9 (a gift from William Tansey)[350] was cultured in the same medium as the MYC-AID lines, complemented with 50μg/ml Hygromycin and 200ng/ml Puromycin. For Cre-ERT2 activation and induction of the switch

(**Fig. 19**), 4-hydroxytamoxifen (OHT) 200nM was added to the growth medium for 16 hours, before sorting the cells for GFP fluorescence. The aforementioned duration of the OHT treatment was chosen through a GFP competition trial time-course (10, 16, 20, 24h), as an early enough time-point with a good proportion of GFP expressing cells. From the step of Cre-ER activation onward, puromycin was omitted from the medium.

The mouse 3T9 fibroblasts expressing MycER^{TM} (**Fig. 28D-F, S13**) were described previously[85] and were grown in DMEM medium supplemented with 10% serum, 1% penicillin/streptomycin and 2mM L-Gln. These cells were passaged by trypsinization (Trypsin-EDTA 1x in PBS, Euroclone Spa) and kept in subconfluent, exponential growth prior to the experiments. For MycER^{TM} activation, the cells were treated for 4 hours with 400nM OHT.

2.2 Transfection and Spin infection of B cells with lentiviral Tir-1 and FUCCI(CA)2 vectors

Packaging HEK-293T cells were co-transfected with 10μg of DNA of the vector of interest (whether Tir-1 or FUCCI(CA)2), 5μg of DNA of pMD2.G plasmid (#12259, Addgene) for VSV-G envelope expression and 5μg DNA of pCMV delta R8.2 plasmid (#12263, Addgene) for Pol and Gag packaging protein expression. The Lipofectamine™ 3000 transfection reagents (L3000001, ThermoFisher) were used according to the manufacturer's protocol. Viral supernatants were harvested 48h post transfection, cleared of cellular debris by filtration through a 0.45μm PES filter (VWR) and either used fresh (for Tir-1), or after concentrating them with PolyEthylene Glycol (PEG) (for FUCCI(CA)2, 100x concentrated virus), they were stored at -80°C. For concentrating the viral supernatants with PEG (stock solution: 120gr of PEG, 2,7 gr NaCl, 200 ml H2O): 10ml of PEG were mixed well together with 40ml of viral supernatant; the mix was stored overnight at +4C. The next day, the mix was centrifuged for 1h at 1500g +4C. The resulting pellet was resuspended in cold PBS (concentrating 100x: 10μl of PBS for every 1ml of fresh virus).

For spin infection, all B-cell lines were seeded on 6-well plates, centrifuged at 1500RPM at Room Temperature (RT) for 5 minutes, in order for them to attach on the plates. Viral supernatants were supplemented with 2μg/ml polybrene (Merck Millipore) and added onto the cells. Cells were subsequently spun with the virus, at 2500 RPM for 1hour at RT. The cells remained in the viral supernatant for several hours before a fresh medium replacement. In the case of FUCCI(CA)2 vector, 2 rounds of spin infection were used.

2.3 Phenotypic analysis of cells by Flow Cytometry

Measurement of viability was performed by adding a final concentration of 0,4 μg/ml of Propidium iodide (PI) to the cultures and detecting PI positive cells by flow cytometry analysis. To evaluate apoptosis through caspase activity, cells were incubated 30 minutes at 37°C with the CaspGLOW™ Active Caspase Staining Kit (Catalog# K190-25, Biovision), prior to flow cytometry analysis, according to the manufacturer's instructions.

For cell cycle analysis, S-phase cells were marked by a 20 minute pulse of EdU (10 μM) and labeled either with the BaseClick EdU-Click 647 Cell proliferation kit (Catalog# BCK-EDU647, Sigma-Aldrich) or, for multiple stainings, the Click-iT™ Plus EdU Alexa Fluor™ 647 Flow Cytometry Assay Kit (C10634, ThermoFisher) according to the manufacturer's instructions.

For Base Click EdU-Click 647, cells were fixed in PBS with 4% formaldehyde for 15 minutes at RT, washed and permeabilized in 90% methanol; ice-cold methanol was added to the cells drop-wise under agitation and cells were left on ice for 30 minutes after that. Samples were then either stored at -20°C for several days, or used directly for staining. For staining, after 2 washes of 3% BSA in PBS, the click-it reaction master mix was added to the cells for 30 minutes RT in the dark, containing dH2O, the reaction buffer, the catalyst solution, the azide dye and the buffer additive.

For Click-iT™ Plus EdU Alexa Fluor™ 647, cells were fixed in Click-iT™ fixative supplemented with 4% paraformaldehyde, for 15 minutes at RT. After washing with 1% BSA in PBS, the cells were permeabilized with a Click-iT™ fixative saponin-based perm-and-wash reagent 1X for 15 minutes, washed with the same reagent before adding the click-it master mix, followed by incubation for 30 minutes in the dark at RT; the click-it master mix contains PBS, a copper protectant, the picolyl azide fluorescent dye and the reaction buffer additive. The difference of this kit lies with the copper protectant, which protects the samples against the quenching of fluorescence that copper induces in click reactions; this feature allows for multiplexing applications, thus providing a better option for simultaneous EdU and γ-H2AX staining.

For both EdU staining protocols, DNA content was assessed by addition of 2.5 μg/ml Propidium Iodide (PI) and 250 μg/ml RNAse A overnight, prior to flow cytometer acquisition.

For measurement of γ-H2AX levels, cells were incubated again after the Click-iT™ Plus EdU reaction in the saponin-based perm-and-wash 1X reagent for 15 minutes. Subsequent

washes with this reagent followed, before adding an FITC-conjugated anti-phospho-Histone H2A.X (Ser139) mAb (clone JBW301, Merck-Millipore) at a final concentration of 3μg/mL for 1,5 hours in the dark, at RT. After incubation, cells were washed twice in perm/wash buffer 1X and resuspended in PBS with PI and RNAse A overnight. After this, cells are ready for flow cytometric acquisition.

For the monitoring of cell divisions by dye dilution, we used the CellTrace™ Far Red Cell Proliferation Kit (Catalog# C34564, ThermoFisher). The cells were stained at day 0 by incubation with 1 μM CellTrace Far Red (for 20 minutes at 37°C), washed in PBS, resuspended in fresh medium, and replaced in the incubator for continued culture and daily sampling for flow cytometric acquisition.

For flow cytometric measurement of MYC levels, cells were fixed in PBS with 4% formaldehyde for 15 minutes at RT, washed and permeabilized in 90% methanol; ice-cold methanol was added to the cells drop-wise under agitation and cells were left on ice for 30 minutes after that. Samples were then either stored at -20°C for several days, or used directly for staining. For staining: After 2 washes with PBS cells were resuspended in 100 μl incubation buffer (0,5% BSA in PBS) supplemented with the anti c-MYC/N-MYC rabbit mAb D3n8f (13987, Cell Signaling, 1:100 dilution), incubated for 1 hour at RT, washed 2x in incubation buffer, and finally incubated as above with an anti-Rabbit Alexa 647 fluorochrome-conjugated secondary antibody (30 minutes in the dark, at RT), washed again (3X) and resuspended in PBS, for acquisition with the MACSQuant® Analyzer 10 Flow Cytometer (Miltenyi Biotec). For the acquisition of FUCCI data (**Fig. 18, S6, S7**), samples were acquired with a BD FACSCelesta™ Flow Cytometer. Flo data were then analyzed with BD FlowJo™ Software. All plots were created with the GraphPad Software.

2.4 Western Blotting

Protein extraction was carried out by resuspending $3x10^6$ cells in Lysis buffer (300mM NaCl, 1% NP-40, 50mM Tris-HCl pH8.0, 1mM EDTA, 0,1% SDS, 0,5% Na-deoxycholate) supplemented with fresh protease and phosphatase inhibitors (Complete™ Mini Protease Inhibitor Cocktail #11836153001, and PhosSTOP™ EASYpack, #04906837001, Roche-Merck). Cell lysates were then sonicated for 10 seconds, cleared by centrifugation at 13000 rpm for 15 minutes at 4°C and quantified by Bradford assay (#5000006, Bio-Rad Protein Assay). Upon quantification and addition of 1/4 volume of 4X Laemmli-DTT buffer (0,4M Tris-HCl pH 6.8, 4% SDS, 20% glycerol, 0.08% bromophenol blue and freshly added DTT 1:20), lysates were boiled (5 minutes at 95°C), electrophoresed on handmade 10%

polyacrylamide gels and transferred to a nitrocellulose membrane with a Trans-Blot® Turbo Transfer apparatus, Bio-Rad (30 minutes, 25 V, 1 A). Membranes were then washed in TBS-T (10mM Tris-HCl, 100mM NaCl, 0.1% Tween at pH7.4) and blocked with 5% milk in TBS-T for 30 minutes, incubated overnight at 4°C, or for 2 hours RT with the specific primary antibodies, washed three times for 5 minutes with TBS-T and then incubated at room temperature for 1 hour with the corresponding secondary antibodies. After subsequent washes in TBS-T, imaging was performed with the enhanced chemiluminescence (ECL) detection kit (Bio-Rad, Hercules, CA, USA) followed by analysis with ChemiDoc XRS+ imaging system and Image Lab Software (Bio-Rad). The primary antibodies used in this study were the following: MYC (Y69, ab32072, Abcam), Vinculin (V9264, Sigma).

2.5 RT-qPCR

Total RNA was extracted by using the Quick-RNA™ MiniPrep RNA extraction kit (#R1054, Zymo Research) following manufacturer's protocol. cDNA was produced using the reverse transcriptase ImPromII™ Reverse Transcription System (#A3800, Promega). 10ng of cDNA were used for Real-time RT-PCR reactions with Applied Biosystems™ Fast SYBR™ Green Master Mix (#4385612 Applied Biosystems™) and the primers that are shown in Table 1.

	Species	Amplicon	Forward Sequence	Reverse Sequence
Expression	mouse	Reep6	GTGCAATGTCATCGGATTTG	TTGCCCGCGTAGTAGAAAG
		Rrp9	AGAGACCGCACAGGAAAAGA	ACTTCTGCAACCTGCCTCTC
		ST6galnac4	TGGTCTACGGGATGGTCA	CTGCTCATGCAAACGGTACAT

Table 1: List of Primers used for RT-PCR

2.6 Chromatin Immunoprecipitation

ChIP was performed as previously described [85]. Ramos cells (typically ~100 million) were resuspended in PBS (20 ml) and fixed by addition of formaldehyde to a final concentration of 1%, and incubation for for 10 min at RT. Fixation was stopped by addition of glycine to a final concentration of 0.125 M. Cells were washed in PBS, resuspended in 6 ml SDS buffer (50 mM Tris pH 8.1, 0.5% SDS, 100 mM NaCl, 5 mM EDTA, phosphatase and protease inhibitors) and stored at −80°C before further processing for ChIP as previously described[273]. Upon thawing, cells were pelleted down at 2000 RPM, RT for 10 minutes and resuspended in 4ml (volume for ~100 million cells) of ice-cold IP buffer (1 vol. SDS buffer, 0,5 vol. Triton Dilution Buffer [100mM Tris-HCl ph 8.6, 100mM NaCl, 5mM EDTA, 5% Triton X-100], Protease and phosphatase inhibitors). Samples were then sonicated to an average length of 500-250 base pairs, using a Branson sonifier at 30% sonication power for several

(4-9) 30-second sonication cycles. Chromatin fractionation was checked at this point by removing 50 μl of lysates after each round of sonication, de-crosslinking it with addition of 100 μl of2% SDS in TE for 3-4 hours at 65 °C, and extracting the DNA with a Qiagen PCR purification kit. DNA was then loaded on a 1,5% agarose gel, together with appropriate DNA markers in order to assess the size of the DNA fragments. If the size was larger than intended, we added extra sonication rounds and checked the fractionation levels again. When satisfied with the DNA fractionation, we adjusted the volume of the samples with IP buffer to reach ~1ml per immunoprecipitation (~50μg of DNA per IP sample, or ~10-15μg/IP for abundant targets, e. g histone modifications). Before proceeding to pre-clearing of the lysates, Protein A beads (Cytiva, #GEH17078001) were blocked as follows: Beads were incubated in TE 1x with 0,5mg/ml tRNA (Sigma) and 0,5mg/ml BSA for 1h at +4C on a rotating wheel. Following centrifugation and removal of the supernatant, beads were washed in TE+BSA 0,5mg/ml and resuspended 50% slurry in TE+BSA 0,5mg/ml. For pre-clearing of the lysates, 25μl of blocked Protein A beads were added per ml of lysate, with subsequent incubation for 1 hour at 4°C on a rotating wheel, followed by the discarding of the beads by microcentrifugation (10 minutes, 3000 RPM). At this point, the chromatin was quantified by Nanodrop and subsequently spiked with 5% mouse chromatin (acquired from NIH-3T3 cells and processed in the same way as described here for the ChIP samples). Next, a volume equal to 5% of the lysate used for each IP was taken and stored at 4°C to be used later as the total “input” control. Primary antibodies were then added to the lysates (10μg/IP or 4μg/IP for abundant targets), followed by overnight incubation at 4°C on a rotating wheel. The next day, lysates were centrifuged for 20 minutes at full speed, and the supernatants transferred to clean Eppendorf tubes pre-loaded with 40μl of Blocked protein A beads followed by incubation for 3 hours at 4°C on a rotating wheel. The beads were centrifuged for 1 minute at 4000 RPM, washed 3 times in Mixed Micelle Washing Buffer (150mM NaCl, 20mM Tris-HCl pH 8.1, 5mM EDTA, 5,2% w/v sucrose, 1% Triton X-100, 0,2% SDS), twice in Buffer 500 (0,1% deoxycholic acid, 1mM EDTA, 50mM HEPES, 500mM NaCl, 1% Triton X-100), twice in LiCl/detergent solution Buffer (0,5% deoxycholic acid, 1mM EDTA, 250mM LiCl, 0,5% NP-40, 10mM Tris-HCl pH 8) and once more in TE, before final resuspension in 200μl TE with 2% SDS and overnight incubation at 65°C for decrosslinking. Finally, the beads were discarded by centrifugation and the supernatants moved to clean Eppendorf tubes, followed by DNA purification on Qiaquick columns (Qiagen).

For ChIP-sequencing, DNA was eluted in 60µl of nuclease-free H2O and quantified using Qubit™ dsDNA HS Assay kits (Invitrogen). 1.5–2 ng of ChIP DNA was end-repaired, A-tailed, ligated to the sequencing adapters, amplified with 17 PCR cycles, size selected (200–300 bp) according to the TruSeq ChIP Sample Prep Kit (Illumina) instructions. ChIP-Seq libraries were then run on the Agilent 2100 Bioanalyser (Agilent Technologies) for quantification and quality control and were subsequently used for Paired-End sequencing on a Novaseq 6000 Illumina sequencer.

2.7 Antibodies

The antibodies used in this thesis are listed in Table 2.

Antibody	Company	Host	Application	Dilution/ µg used
MYC (Y69)	Abcam (ab32072)	Rabbit	WB	1:2000
Vinculin	Sigma-Aldrich (V9264)	Mouse	WB	1:5000
c-MYC/N-MYC (Dn38F)	Cell Signaling (13987)	Rabbit	Flow Cytometry	1:100
IgG XP® Isotype Control (DA1E)	Cell Signaling (3900S)	Rabbit	Flow Cytometry	1:100
Anti-phospho-Histone H2A.X (Ser139), clone JBW301, FITC conjugate	Merck-Millipore (16-202-A)	Mouse	Flow Cytometry	3µg/mL
c-MYC (N-262) X	Santa Cruz (Sc-764)	Rabbit	ChIP	10µg/IP
MAX	Bethyl (A302-866A)	Rabbit	ChIP	10µg/IP
IgG	Santa Cruz (Sc-2027)	Rabbit	ChIP	10µg/IP or 4µg/IP
Rpb1 NTD (D8L4Y) (RNAPII)	Cell Signaling (14958S)	Rabbit	ChiP	10µg/IP
H3K4me3	Active Motif (#39159)	Rabbit	ChIP	4µg/IP
H3K4me1	Abcam (ab8895)	Rabbit	ChIP	4µg/IP
H3k27ac	Abcam (ab4729)	Rabbit	ChIP	4µg/IP

Table 2: Primary antibodies used for WB, Flow Cytometry or ChIP experiments.

2.8 4-SU metabolic labelling for sequencing

For each time-point of the time-course, ~12 million cells were removed from the main culture and exposed to a 10-minute pulse of 300 μM 4-thiouridine (4SU Sigma, #T4509) that was added directly to the culture medium at 37°C; incorporation of 4SU was then stopped by transferring of the cells on ice and washing with cold PBS. Cells were then pelleted and stored at -80°C. For RNA purification with the miRNeasy Mini kit (Qiagen), the pellets were thawed and resuspended in 700 μl QIAzol lysis reagent, homogenized with a syringe and left at RT for 5 minutes. 140 μl of chloroform were then added, samples mixed vigorously for 15 seconds and left for 3 minutes to incubate at RT, before centrifuging for 15 minutes (12000g at 4°C). The upper acqueous phase was transferred to a new Eppendorf, mixed with 1.5 volume of 100% EtOH, loaded on miRNeasy Mini spin columns and centrifuged at max speed for 1 minute at RT. A DNAse digestion step was performed on column, with incubation of the DNAseI for 15 minutes at RT, as per manufacturer's instructions. After two washes with RPE buffer, total RNA was eluted in 50 μl DEPC-treated H_2O.

The purified total RNA was then biotinylated: 30-50 μg of RNA were adjusted to a final volume of 100 μl, mixed with 100 μl of 2.5x biotin labelling buffer (25mM Tris-HCl pH 7.4, 2.5mM EDTA, DEPC-treated H2O) complemented with 50 μl of Biotin-HPDP/DMF (stock concentration 1mg/ml) and incubated at RT for 2 hours under the chemical hood.

The next step was the removal of unbound biotin-HPDP, using high density MaXtract tubes (Qiagen). First, the columns were spun at 16000g for 2 minutes for equilibration. Then an equal volume of chloroform/isoamylalcohol 24:1 (250 μl) was added to the biotinylated samples and the whole mixture was loaded on the MaXtract tubes. The phases were mixed thoroughly by repeated inversion of the tubes and tubes were finally centrifuged at 16000g for 5 minutes at 4°C. The upper, RNA-containing phase was transferred to new tubes and a volume of 5M NaCl equivalent to the 1/10 of the sample volume was added to the mix. The samples were then supplemented with an equal volume (~240 μl) of isopropanol and centrifuged at full speed for 30 minutes at 4°C for precipitation of the RNA. The supernatants were was and replaced by an equal volume of 75% ethanol. Following centrifugation at full speed for 10 minutes at 4°C, the ethanol was discarded and the pellets dried at RT. Finally, the pellets were resuspended in 100 μl of RNase-free H2O.

For purification of 4SU labeled RNA, Dynabeads MyOne Streptavidin T1 (Invitrogen) were washed in Dynabeads washing solution A (100mM NaOH, 50mM NaCl, 10 ml H2O) and B

(100mM NaCl, 10ml H2O) and then resuspended in 2x Dynabeads washing buffer (2M NaCl, 10mM Tris-HCl pH 7.5, 1mM EDTA, 0.1% Tween20 and 50ml H2O). Subsequently, an equal volume of beads was added to the biotinylated RNA and the mix was incubated for 15 minutes in RT under rotation. Then the beads were separated from the liquid with a tabletop magnet for 2-3 minutes and washed 3 times with Dynabeads washing buffer 1X. For elution of labeled RNA, beads were resuspended in 100μl of 10mM EDTA in 95% formamide and incubated for 10 minutes at 65°C. Then beads were separated with the magnet, resuspended in the same supernatant and separated again, collecting the supernatant for extraction of 4SU-labeled RNA. The 100 μl of RNA collected from the previous step were mixed with 700 μl of QIAzol and RNA purified on a miRNeasy Micro Qiagen kit, most suitable for recovery of very small quantities of RNA. Finally, the 4SU-labeled, purified RNA was eluted in 14 μl of RNase-free H2O and quantified with a Qubit™ RNA HS Assay kit (Invitrogen) as per manufacturer's instructions. RNA quality was assessed using the Agilent 2100 Bioanalyzer (Agilent Technologies) before proceeding with library preparation with a TruSeq Total Stranded RNA Kit (Illumina) and Paired-End sequencing on a Novaseq 6000 Illumina sequencer.

2.9 Total RNA-seq

Total RNA was purified onto Quick-RNA columns (Zymo, R1054) and treated on-column with DNaseI (Zymo, R1504). RNA quality was assessed using the Agilent 2100 Bioanalyzer (Agilent Technologies), before proceeding with library preparation with a TruSeq Total Stranded RNA Kit (Illumina) and Paired-End sequencing on a Novaseq 6000 Illumina sequencer.

2.10 Polysome Profiling

Polysome profiles were generated as previously described[381]. Cycloheximide 100μg/ml was added to the cells 10 minutes before harvesting and lysis. ~20 million cells were lysed for 30 minutes on ice in 500 μl of Lysis buffer (50mM Tris HCl pH 7.5, 100mM NaCl, 30mM MgCl2, 0.1% NP-40, 100μg/ml cycloheximide, 40U/ml RNasin, Proteases inhibitor cocktail). An equal amount (ca. 8μg) of RNA from each lysate, as calculated by Optical Density measurement, was loaded on a sucrose gradient (15-50%) and centrifuged in a SW41Ti Beckman rotor (39,000 rpm for 3:30 hours at +4C). Absorbance at 254 nm was recorded by a UV-Biologic LP software for the generation of profiles, while fractions (11-12 in total) were being collected. For RNA extraction, proteinase K and SDS were added to the collected 1ml fractions (final concentration 100μg/mL and 1% respectively) followed by incubation

at 37C for 1 hour, Phenol/chloroform extraction, isopropanol precipitation (overnight at -80C) and resuspension of the RNA pellets in 30µl RNAse free water.

After RNA extraction, the fractions were pooled into three categories, one containing the light mRNA components (fractions 1-5), one containing the monosomes and light polysomes (fractions 6-8) and one containing the heavy polysomes (9-11/12). The total RNA used for comparison was reconstituted by adding equal volumes of RNA from each fraction. RNA quality was assessed using the Agilent 2100 Bioanalyzer (Agilent Technologies) before proceeding with library preparation with a TruSeq Total Stranded RNA Kit (Illumina) and Paired-End sequencing on a Novaseq 6000 Illumina sequencer.

2.11 Computational analysis

2.11.1 RNA-seq and data analysis for polysome profiling

Pair-end sequencing of the samples was performed on the Illumina NovaSeq platform. RNA-Seq NGS reads were aligned to the mm10 mouse or hg19 human reference genome using the TopHat aligner (version 2.0.8) with default parameters[382]. Read counts were associated to each gene (based on UCSC-derived mm10 or hg19 GTF gene annotations), using the featureCounts software (http://bioinf.wehi.edu.au/featureCounts/) setting the options -T 2 -p -P[383]. Absolute gene expression was defined determining reads per kilobase per million mapped reads (RPKM). DESeq2 was used to analyze RNA-seq data, as genes with q value < 0.05[384].

2.11.2 4SU labeled and Total RNA-seq data analysis

Pair-end sequencing of the samples was performed on the Illumina NovaSeq platform. RNA-Seq NGS reads were aligned to the mm10 mouse or hg19 human reference genome using the STAR aligner[385] (version 2.7.3a) with default parameters[382]. Read counts were associated to each gene (based on UCSC-derived mm10 or hg19 GTF gene annotations), using the featureCounts software (http://bioinf.wehi.edu.au/featureCounts/) setting the options -T 2 -p -P[383]. Absolute gene expression was defined determining fragments per kilobase per million mapped reads (FPKM). DESeq2 was used to analyze RNA-seq data, as genes with q value < 0.05[384].

2.12 ChIP-seq data analysis

The HTS-flow pipeline was used to align the ChIP-seq reads to the hg19 human (ChIP-seq signal) or mm10 mouse (Spike-in signal) reference genome using the STAR aligner (version 2.7.3a) through the BWA aligner using default settings[386]. The MACS software[387] was then used for peak calling, using a cut-off parameter q value<1e-5. To compute the signal from

ChIP-seq data in a region of interest, the read counts found inside that genomic region were spike-in normalized using the following formula:

Norm ChIP-seq signal = (ChIP-seq signal / Spike-in signal) x (Spike-in input / ChIP-seq input)

Promoters were defined as the region centered on the TSS ±1.5 Kbp, TES regions as the ones centered on the TES ±1.5 Kbp. A promoter was considered bound if a peak from ChIP-seq data was overlapping by at least 1bp. Distal regions were defined as all regions not belonging to a promoter region.

Bioconductor and compEpiTools packages[388,389] were used for statistical analyses. Metagene's profile analysis was performed with ChroKit tool (https://github.com/ocroci/ChroKit).

2.13 Gene Set Enrichment Analysis (GSEA) and Gene Ontology Analysis (GO)

Differentially Expressed Genes (DEGs) derived from RNA-seq analysis were subject to Gene Set Enrichment Analysis (GSEA)[390,391] using the Molecular Signatures Database (MSigDB)[390,392,393] of annotated gene sets (https://www.gsea-msigdb.org/gsea/msigdb/human/annotate.jsp), which allows an enrichment analysis based on hypergeometric distribution followed by FDR correction. As output, a hierarchical graph summarizing the top enriched biological processes is created, based on the negative logarithm of the q value (see **Fig. S12E, S13E**). Gene ontology (GO) analyses were performed using the clusterProfiler[394,395] package using enrichGO and enrichr functions with gene sets from MSigDB.

3. RESULTS

3.1 Engineering of MYC-AID lymphoma cell lines

In order to profile immediate MYC-dependent transcriptional effects in MYC-driven cancer, we should need a model that allows rapid elimination of the MYC protein in cells. Towards this aim, we took advantage of the Auxin-inducible degron (AID), a model that relies on the plant hormone auxin, which binds to the Tir1 ubiquitin ligase, triggering rapid poly-ubiquitination and proteasome-dependent degradation of AID-containing proteins[378]. We used CRISPR/Cas9 technology to engineer three human lymphoma cell lines, two from Burkitt's (Ramos and Raji) and one from MYC/BCL2 double-hit lymphoma (SU-DHL-6), by inserting the AID coding sequence at the 3' end of the translocated MYC allele (**Fig. 11A**). The cells were electroporated with two plasmids: one containing a DNA cassette encoding the AID moiety and blasticidin resistance flanked by MYC-homology arms (**Fig. S1A**) and the other expressing the hSpCas9 originating from S. pyogenes, together with specifically designed sgRNAs (**Fig. S1B**), as previously described in the leukemic cell line K562[235]. Following blasticidin selection and control by immunoblotting for expression of MYC-AID (without w.t. MYC), recombinant cells were infected with a lentiviral vector expressing Tir1 and BFP (**Fig. S1C**), followed by derivation of BFP+ single-cell clones that showed rapid and efficient degradation of MYC-AID upon auxin treatment (IAA, **Fig. 11B**). Notably, flow-cytometric staining with MYC antibodies showed that MYC-AID levels dropped to a minimum by 1 hour and remained stable upon prolonged incubation with IAA (up to 6-8 days: **Fig. 11C**), as also confirmed by immunoblotting (**Fig. S2**); quantification of the MYC staining following subtraction of the IgG control signal showed that the residual signal in IAA-treated cells ranged between ca. 11 and 30% of untreated controls (% values in **Fig. 11C**).

3.2. Phenotypic characterization of MYC-AID lymphoma cell lines

3.2.1 MYC-AID degradation leads to protracted proliferative arrest and cell death

Given the role of MYC in cell growth, proliferation and apoptosis[16,37,197,396-398], we investigated these parameters in our Ramos, Raji and SU-DHL-6 lines over a week of continuous treatment with 100μM IAA. Albeit with slight differences in kinetics, all MYC-AID lines eventually stopped proliferating from day 2-4 (**Fig. 12A**) concomitant with a reduction in S-phase cells (**Fig. 12B**) and, ca. 2 days later, increased cell death (**Fig. 12C, D**). Ramos seemed to be the cell line with the latest response, while the other two reacted faster to MYC down-regulation. Of note, the SU-DHL-6 and Raji lines showed a transient

restoration of S-phase cells at Day 4 (**Fig. 12B**): the basis for this phenomenon remains unclear at this stage, and requires further investigation, but it was fully replicable in another independent triplicate experiment. Finally, as expected, IAA had no effect on the parental lines, neither on MYC levels (**Fig. 13A**), nor on cell proliferation and death (**Fig. 13B, C**).

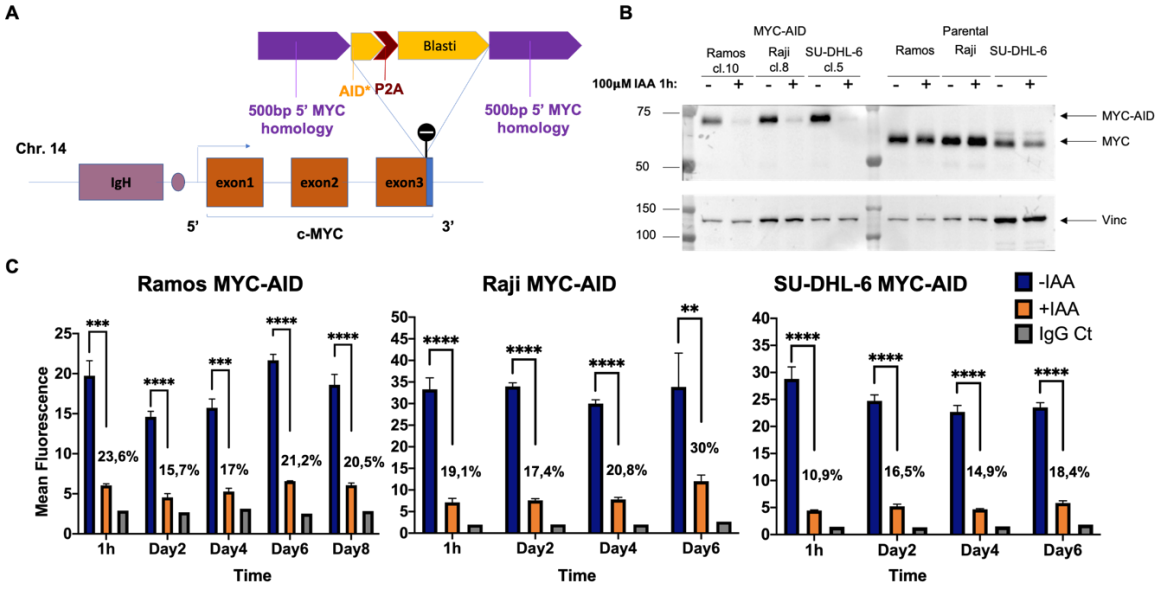

Figure 11: Tagging *MYC* with an auxin-inducible degron (AID) in lymphoma cell lines.
Auxin (IAA) binds to the Tir1 E3 ubiquitin ligase, resulting in ubiquitylation and proteasome degradation of the AID-tagged protein. **(A)** Schematic representation of the in-frame AID cassette inserted at the 3' end of the translocated MYC allele in three human Lymphoma cell lines (Ramos, Raji and SU-DHL-6). Part of the initial steps for constructing the MYC-AID cell lines were achieved with technical assistance by A. Verrecchia in our group. **(B)** MYC protein levels were assessed by immunoblotting in the indicated MYC-AID clones (left), compared with the parental lymphoma cell lines (right), before and 1h after addition of 100 µM IAA. **(C)** MYC-AID protein levels in cells treated with IAA for the indicated periods of time, as assessed by intracellular MYC staining and flow cytometry. Error bars represent Standard Deviation. Statistical analysis by T test (* P≤0.05, **P≤0.01, *** P≤0.001, **** P≤0.0001), n=3 biological replicates. The percentage values indicate the residual MYC signal in IAA-treated cells relative to untreated controls, following subtraction of the experimental background measured with an IgG Isotype control Antibody (IgG).

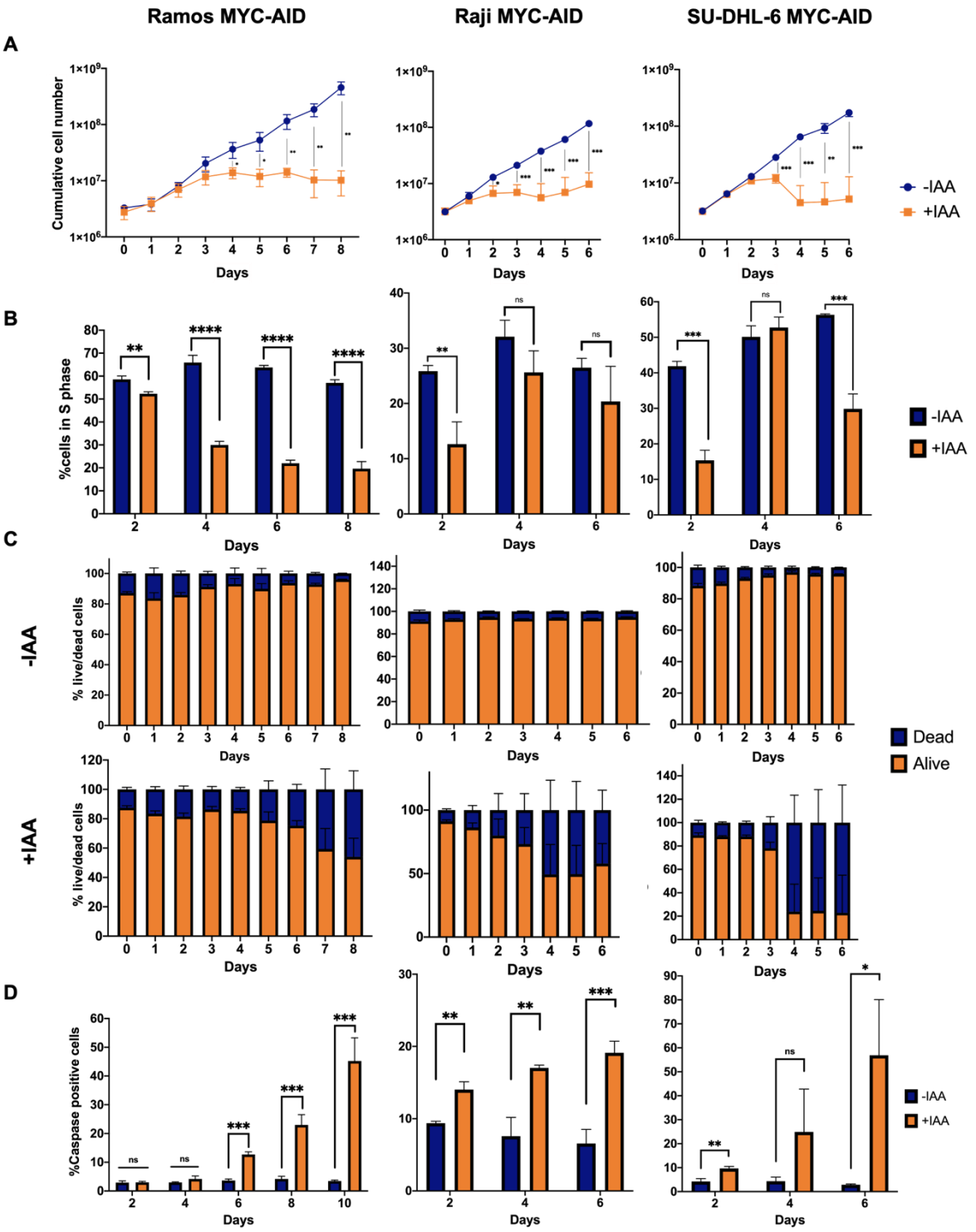

Figure 12: Proliferation, Cell Cycle and Cell Death in MYC depleted cells.
Cultures of the indicated cell lines were passaged with Auxin (+IAA: 100 µM) or without it (-IAA) and followed for the indicated time-points (Days). **(A)** Cumulative live-cell numbers: dead cells were scored by Propidium Iodide (PI) staining and excluded from the cell counts. **(B)** Percentages of S-phase cells, as assessed after a 20 minute pulse of EdU incorporation (10 µM). The EdU profiles of one representative replicate per cell line are shown **in Fig. S4A**. **(C)** Live/dead-cell percentages, determined as in (A). **(D)** Percentages of apoptotic cells, as assayed by flow cytometric staining for active caspases. All data represent the means and SD (T test) from 3 biological replicates; *P≤0.05, **P≤0.01, *** P≤0.001, **** P≤0.0001.

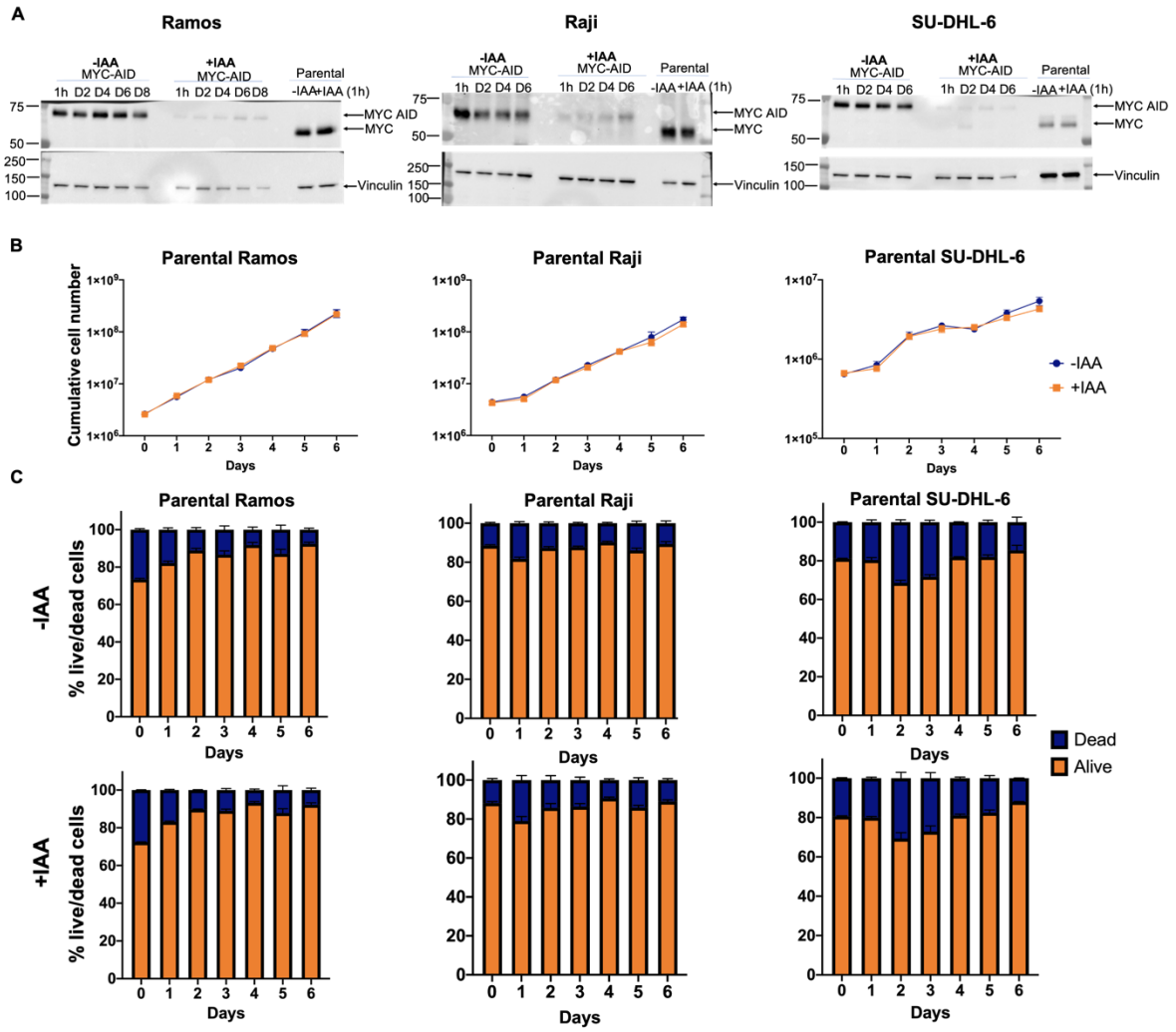

Figure 13: Effects of IAA on the parental cell lines.
Parallel cultures of the indicated cell lines were passaged with Auxin (+IAA: 100 µM) or without it (-IAA), at the indicated time-points (Days). **(A)** MYC-AID and MYC protein levels, as assessed by immunoblotting. Vinculin was used as loading control. **(B)** Cumulative live-cell numbers and (**C**) live/dead-cell percentages for the parental cell lines (as shown in for the MYC-AID lines in Fig. 12A and 12C, respectively). The data represent the means and SD (T test) from 3 biological replicates.

Direct counting of cell divisions with CellTrace labeling and dye-dilution analysis[399] revealed that IAA-treated cells kept dividing until day 3, in all three lines, with doubling rates comparable to those of untreated cells (**Fig. 14A**). While dye dilution in treated cultures persisted at later time-points, this was lower than in untreated controls and might be attributable to reduction in cell mass, as assessed by the Forward Scatter parameter in flow cytometry (**Fig. 14B**). Most noteworthy, some experiments with Raji and SU-DHL-6 showed evidence for a cell subpopulation that persisted dividing at the latest time-point in IAA-treated cultures (e.g. Raji in **Fig. 14A, S3A** highlighted with red asterisks), which might also correlate with an increase in cell size (**Fig. 14B**).

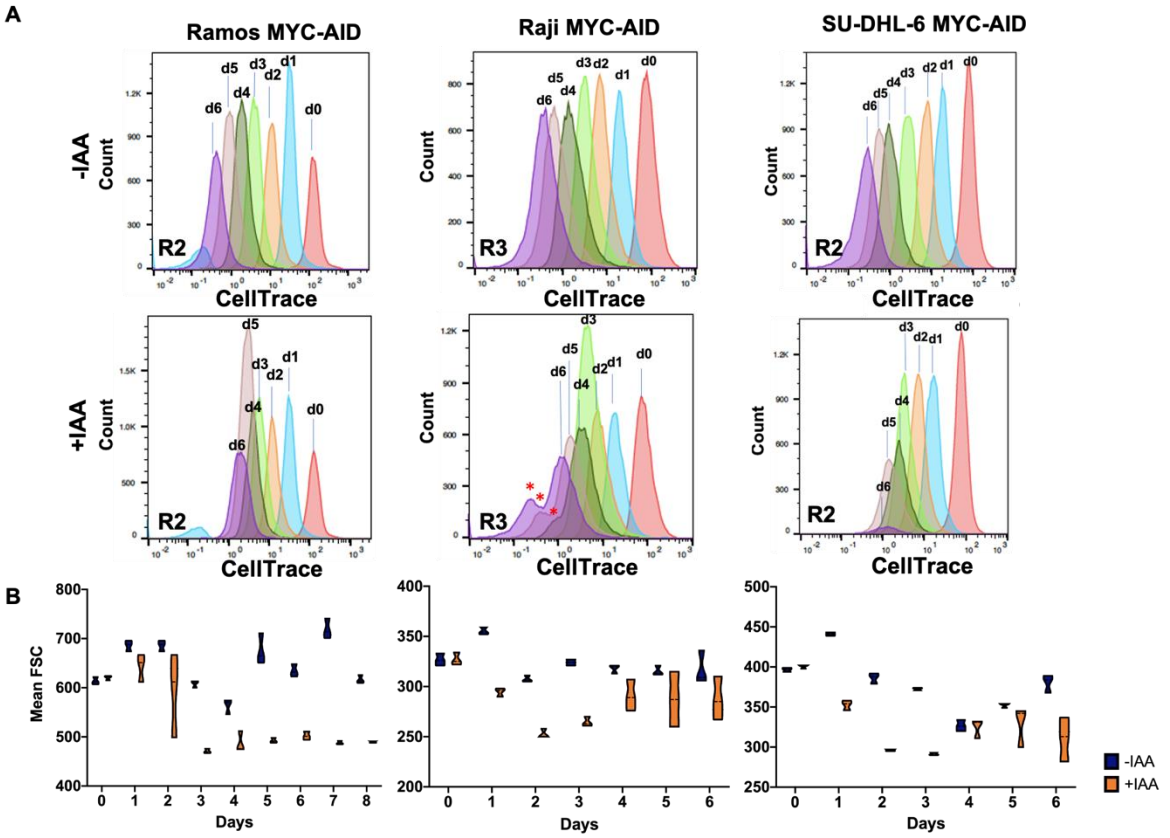

Figure 14: Counting of Cell Divisions in MYC-AID cells.
Parallel cultures of the indicated cell lines were passaged with Auxin (+IAA: 100 µM) or without it (-IAA), at the indicated time-points (Days). Live cells were stained for 20 minutes on day 0 with 1 µM CellTrace™ Far Red. **(A)** Dye dilution in the MYC-AID cell lines as monitored by daily flow-cytometric measurement (d0-d6). A representative experiment out of 3 is shown for each cell line, while the other 2 experiments are shown in **Fig. S3**. The red asterisks point to the escaping subpopulations and the respective replicate identifier is indicated on the graph. **(B)** Mean FSC values in the same cultures as in (A). n=3

Careful examination of the MYC-staining flow cytometry data showed that the increase in MYC levels for Raji at the later time-point (d6, **Fig. 11C**) was accompanied by the rise of a second cell population, with MYC levels comparable to those in untreated cells (**Fig. S3B** highlighted with red asterisks); the same effect, albeit milder, was noticed for some of the SU-DHL-6 replicates (**Fig. S3B**), suggesting that late-dividers are cells that escaped MYC-AID degradation. Most importantly, such late dividers never occurred in the Ramos MYC-AID line, and only stochastically in Raji and SU-DHL-6. We conclude that while showing occasional outgrowth of escapers – which are of course under strong positive selective pressure – none of the in IAA treated cultures showed adaptation to grow with low MYC levels.

3.2.1.1 MYC-dependent cell cycle changes and arrest

Close examination of EdU incorporation profiles revealed that, albeit with some differences in kinetics, our three MYC-AID cell lines showed an accumulation of cells in G1 that paralleled the decrease in S-phase cells in IAA-treated cultures (**Fig. 15A-B**), while G2/M levels did not follow a unifying trend (**Fig. 15C**). Of note, in the Ramos MYC-AID line, IAA treatment led to an increase in cells with intermediate DNA content but no incorporation of EdU, which we hereby refer to as "faulty S-phase" (**Fig. 15D, S4A**). This observation was a first indication towards the notion that MYC depletion could impact cell cycle progression. This phenomenon, however, was less apparent for the other two cell lines, reaching significance only at day 6. In the same experiment, the S-phase fraction in Ramos appeared to undergo a general drop of mean EdU fluorescence (**Fig. S4B**), accompanied by the rise of a small population of "high EdU incorporating" cells (**Fig. S4A**, highlighted with red asterisks). These observations were not confirmed in the other two cell lines (**Fig. S4A, B**) and the S-phase SU-DHL-6 cells showed no particular change in the mean EdU fluorescence after IAA treatment (**Fig. S4B**). However, Raji in particular exhibited the opposite effect of Ramos for the mean EdU fluorescence (**Fig. S4B**); this increase upon MYC ablation was attributed to a technical staining issue, which is apparent in the Raji EdU profiles (**Fig. S4A**).

Nevertheless, the results in Ramos together with the unexplained transient restoration of S-phase cells in day 4 of IAA treatment for Raji and SU-DHL-6, pointed to a faulty S-phase progression, prompting us to investigate the possible presence of genotoxic stress. Toward this aim, we repeated the same EdU- and PI-staining experiment, with the addition of phosphorylated H2AX (γ-H2AX) staining in order to define the cycle-phase most affected by MYC-associated genotoxic stress[188,189,191,192,400].

The EdU incorporation profiles in the new experiment (**Fig. 16**) confirmed our previous observations (**Fig. 15**): reduction in S phase accompanied with a G1/G0 arrest (**Fig. 16A, B**), and lack of a consistent/reproducible trend in G2/M (**Fig. 16C**). Once again, we observed the gradual accumulation of faulty, EdU-negative S-phase cells in Ramos (**Fig. 16D**), and the reduction in the mean EdU Fluorescence for Ramos accompanied by the late emergence of a small population of "higher EdU incorporating" cells (**Fig. S5**). While the SU-DHL-6 cells behaved as in the previous experiment for the mean EdU fluorescence, Raji on the other hand exhibited a general drop in mean EdU fluorescence upon IAA treatment (**Fig. S5B**). Also, SU-DHL-6 and – albeit less markedly – Raji showed again the peculiar rebounce of S phase cells at day 4 (**Fig. 16B**).

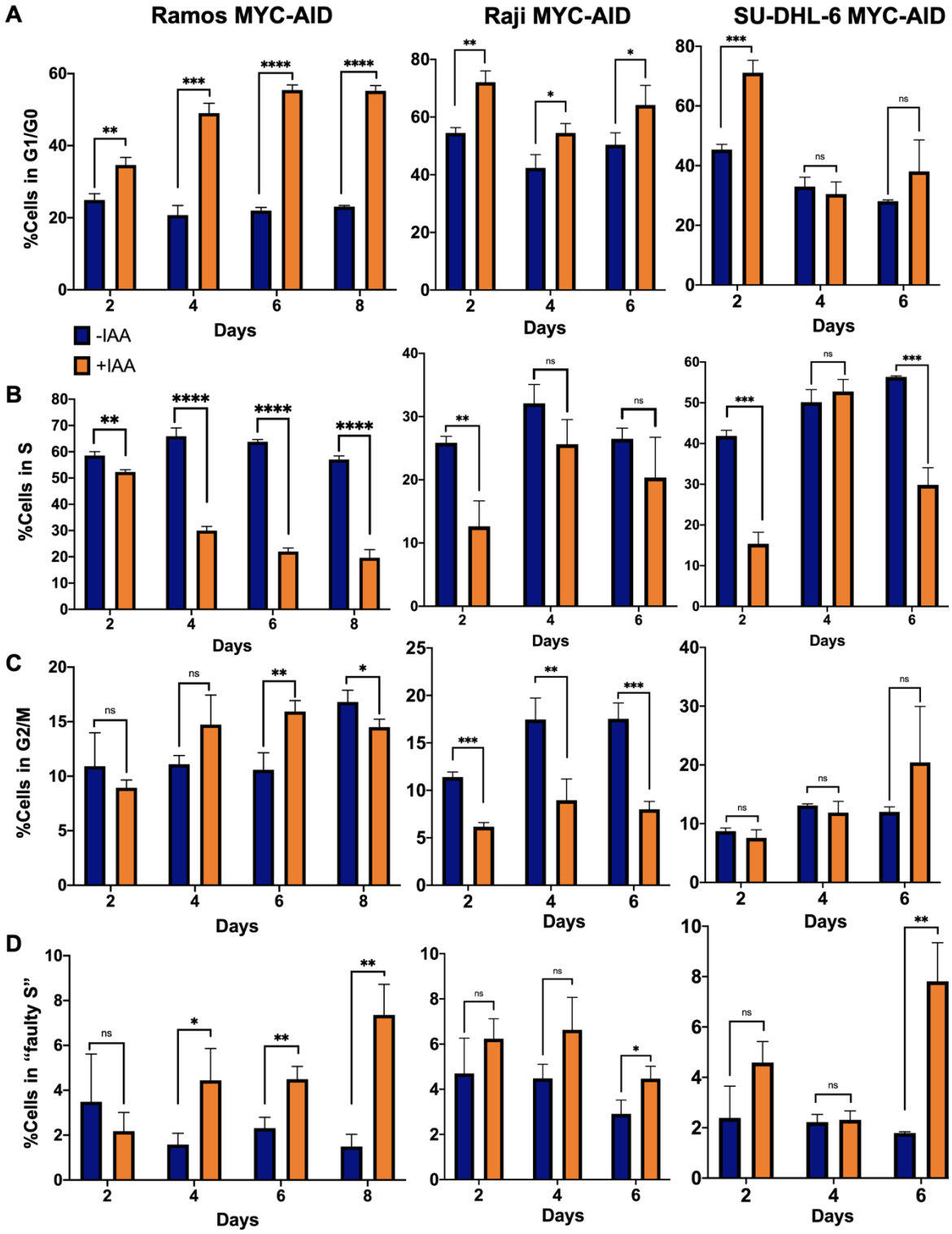

Figure 15: Percentages of cells in the various cell cycle phases.
Parallel cultures of the indicated cell lines were passaged with Auxin (+IAA: 100 µM) or without it (-IAA). At the indicated time-points (Days), cells were subject to a 20-minute pulse of EdU incorporation (10 µM) and processed for 2D-Flow cytometric analysis with EdU and PI staining. Percentages of cells in **(A)** G1/G0, **(B)** S, **(C)** G2/M and **(D)** "Faulty S" (see text and **Fig. S4A**). The data originate from the same experiment as **Fig. 12**: for the sake of clarity, the same panel B is shown in both figures. All data represent the means and SD (T test) from 3 biological replicates; *P≤0.05, **P≤0.01, *** P≤0.001, **** P≤0.0001.

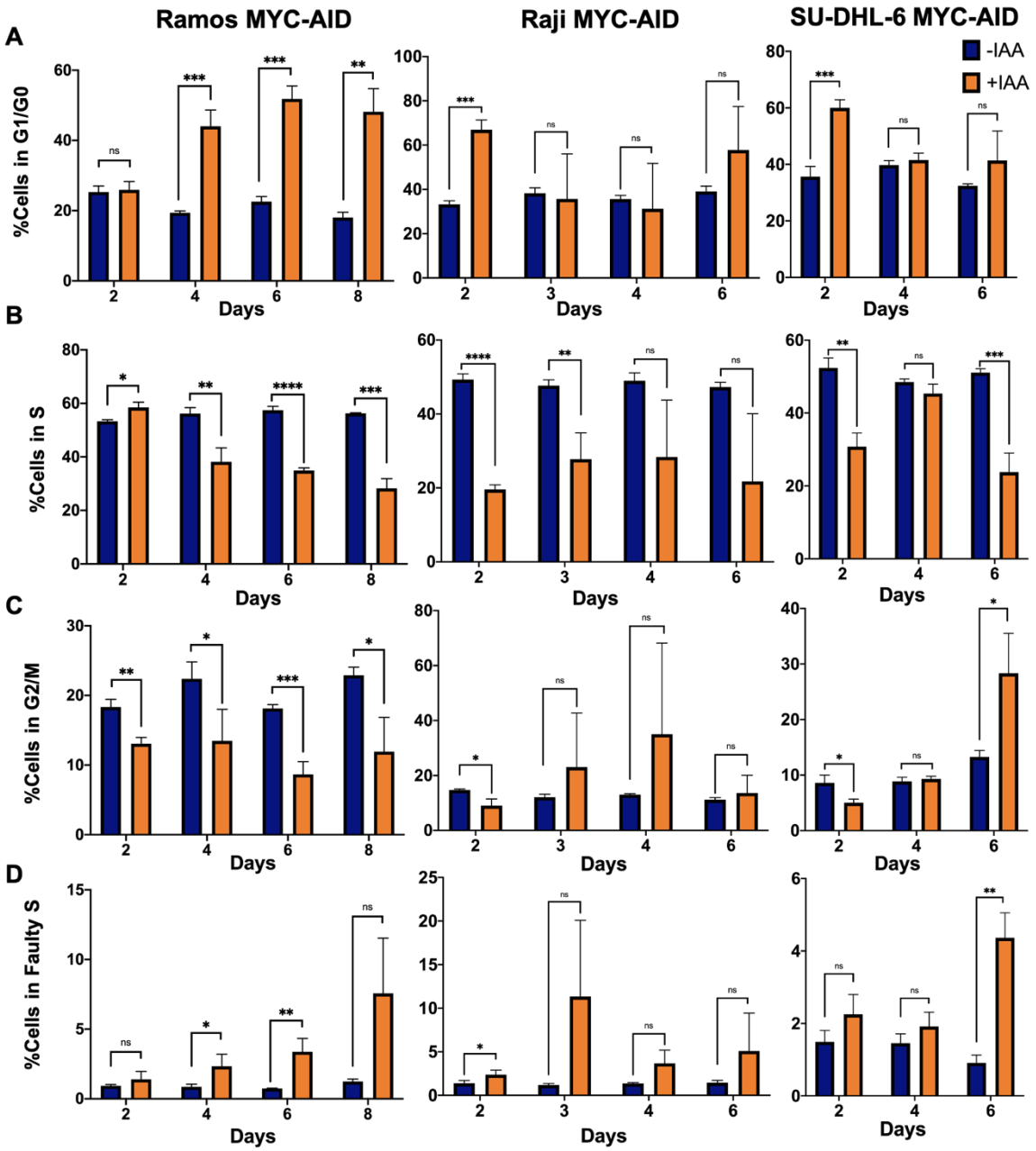

Figure 16: Percentages of cells in each cell cycle phase for the EdU/γ-H2AX experiment.
Same as **Fig. 15** from a separate experiment (with slightly different time-points for Raji), also used for γ-H2ax staining. The corresponding EdU profiles of one representative replicate per cell line are shown **in Fig. S5A** and the γ-H2ax data shown in **Fig. 17**. Cell lines and time-course are indicated on the graphs. All data represent the means and SD (T test) from 3 biological replicates; *P≤0.05, **P≤0.01, *** P≤0.001, **** P≤0.0001.

While prone to substantial experimental variation, γ-H2AX staining indicated a tendency towards a gradual increase in total γ-H2AX levels in all three cell lines, in particular at late time-points, pointing to an accumulation of genotoxic stress (**Fig. 17A**). However, a definitive interpretation of those data is complicated by a number of confounding issues. First, untreated Ramos cells showed peculiarly elevated γ-H2AX levels, which decreased over the time course (**Fig. 17A**); while this might be attributed to some culture-associated stress, it is perplexing to see higher γ-H2AX in the untreated, rather than the treated

cultures. Second, the level of variation between replicates, in particular for Raji, resulted in sizeable standard deviation error bars, blurring the significance of the observed effects.

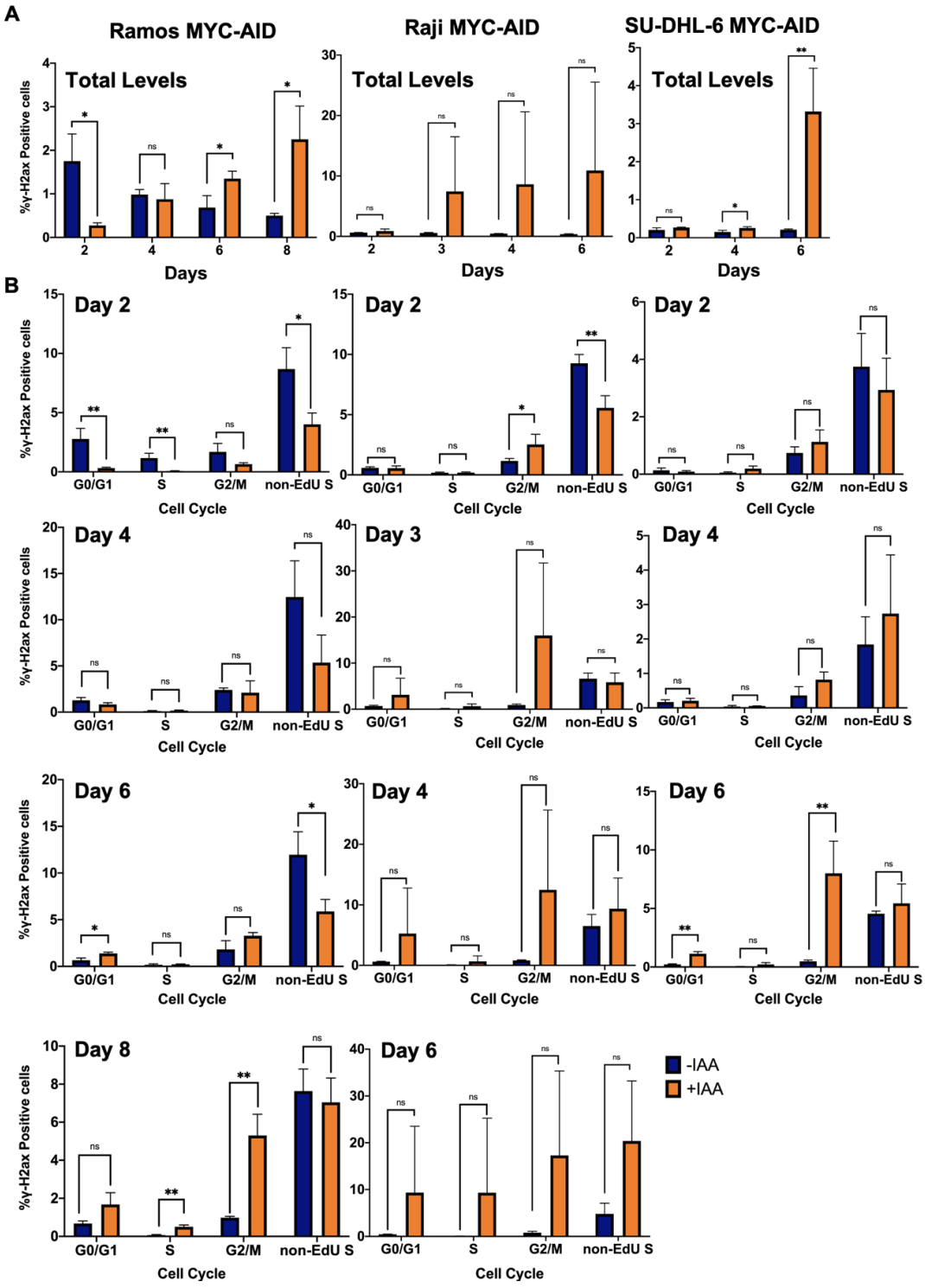

Figure 17: Cell cycle and γ-H2AX distribution.
Parallel cultures of the indicated cell lines were passaged with Auxin (+IAA: 100 µM) or without it (-IAA). At the indicated time-points (Days) cells were co-stained for EdU incorporation (data in **Fig. 16** and **Fig. S5**) and γ-H2AX. **(A)** Total levels of γ-H2AX across the time-course as indicated. **(B)** Percentages of γ-H2AX positive cells within each cell cycle fraction at the different time-points, as indicated. All data represent the means and SD (T test) from 3 biological replicates; *P≤0.05, **P≤0.01, *** P≤0.001, **** P≤0.0001.

Notwithstanding the above limitations, most of the γ-H2AX positive cells in all samples were accounted for by the faulty, EdU-negative S-phase (**Fig. 17B**); these cells should be having by definition a problematic S phase and, consistent with this notion, showed elevated γ-H2AX levels in both IAA-treated and control cultures in all cell lines and time-points. Moreover, the difference in the percentages of cells in this "Faulty S" between treated and non-treated cultures was similar in both experiments (**Fig. 15D** and **16D**), pointing to an increase of cells with problematic S phase upon MYC degradation in all three cell lines. Of note, in SU-DHL-6 and Raji, there was a transient decrease of cells in "Faulty S" for Day 4 in the treated cultures, concomitant with the aforementioned transient restoration of normal S-phase cells. Lastly, besides the "faulty S", all 3 IAA-treated cell lines showed substantial increases of γ-H2AX levels in the G2/M phase (**Fig. 17B**), suggesting that cells could be entering Mitosis without having repaired the pre-existing DNA damage. Most importantly, these are all conclusions based on preliminary data that will require further clarification.

At this point, it must be stressed that analysis of EdU/PI data is often quite complex, as exhibited in the raw data of **Fig. S4A** and **S5A**. In particular, the existence of intermediate DNA content non-EdU cells, makes the distinction between the latter, G1 and G2/M cells difficult based on DNA content alone, and is somewhat subject to the observer's eye. For these reasons, we decided to assess the phenotype of IAA-treated cells with an alternative approach, by introducing a Fluorescent Ubiquitination-based Cell Cycle Indicator (FUCCI) system in our MYC-AID cell lines.

Progression through the cell cycle is controlled by ubiquitin-mediated proteolysis of key regulatory factors[401]. This feature was exploited to develop an assay, commonly referred to as the FUCCI system[402], allowing colorimetric, live-cell and real-time analysis of cell cycle transitions. The assay takes advantage of the cell-cycle dependent proteolysis of chromatin licensing and DNA replication factor 1 (Cdt1) and of its inhibitor Geminin by the E3 ubiquitin-ligase complexes APC^{Cdh1} and SCF^{Skp2}, respectively[401,403-406]. These proteins oscillate inversely, with Cdt1 levels being maximal during G1, and Geminin levels during S and G2/M[403,405,406]. Therefore, fusing Cdt1 and Geminin to distinct fluorescent proteins in live cells provides probes that allow discriminating between G1 and S-G2/M in real-time[402]. While the original system allowed sharp discrimination between G1 and S, it did not do so for the transition between S and G2/M; since then, new probes were developed that allow clear discrimination between G1, S and G2. One such example is provided by FUCCI(CA)2[380], which we used for our experiments: this version still has the APC^{Cdh1}-sensitive Geminin-

based probe but entails a re-engineered version of the original Cdt1-based sensor, which responds to S-phase specific $CUL4^{Ddb1}$-mediated ubiquitylation. In short, FUCCI(CA)2 gives off a triple colouration that sharply distinguishes between G1, S and G2, with a $CUL4^{Dbd1}$-sensitive hCdt1-based probe marking G1 with mCherry (red), an APC^{Cdh1}-sensitive hGem-based probe marking S phase with mVenus (green) and the combinatorial colour of the two (yellow) marking G2/M (**Fig. 18A**). We thus infected our MYC-AID cell lines with the FUCCI(CA)2 vector, which co-expresses the two reporter proteins[380].

Of note here, the initial flow-cytometric screens of our MYC-AID clones had made us aware that Raji MYC-AID and SU-DHL-6 MYC-AID retained a small percentage of cells negative for BFP (data not shown), the marker used for expression of the auxin binding receptor Tir1 (**Fig. S1C**; see section **3.1**): these small BFP/Tir1 negative subpopulations (ca 5% or less) were most likely the reason for the occasional rise of escapers after a prolonged IAA (**Fig. 14A** and **S3**; section **3.2**). The presence of these BFP-negative cells was confirmed in both non-infected and FUCCI-infected cells prior to sorting (**Fig. S6A, B**, blue cells circled in red). Surprisingly, after infection with the FUCCI vector, Raji MYC-AID cultures reached ca. 50% BFP positivity (**Fig S6B**, middle) indicative of a significant loss of BFP/Tir1 cells; this phenomenon remains unexplained and was not noticed in the two other cell lines (**Fig. S6B**). Nevertheless, as will become clear below, this subset of BFP/Tir1-negative cells provided a valuable internal negative control in our Raji MYC-AID FUCCI cultures.

After infection with the FUCCI(CA)2 vector, we proceeded to sort FUCCI-positive cells (based on double positivity for mCherry and mVenus). The resulting FUCCI MYC-AID cultures were treated with IAA and followed over time-courses of 7-10 days (**Fig. 18B**). In all three cell lines, IAA induced decreases in the percentages of S-phase cells and, for Ramos and SU-DHL-6, also of G2/M cells. In all cases, this was accompanied by variable, yet proportionate increases in the fraction of G1/G0 cells, consistent with cell cycle arrest. Most importantly, the peculiar recovery of S phase at Day 4 in IAA-treated SU-DHL-6 cultures (**Fig. 15B** and 1**6B**) was also apparent with the FUCCI system (**Fig.18B**, red arrow).

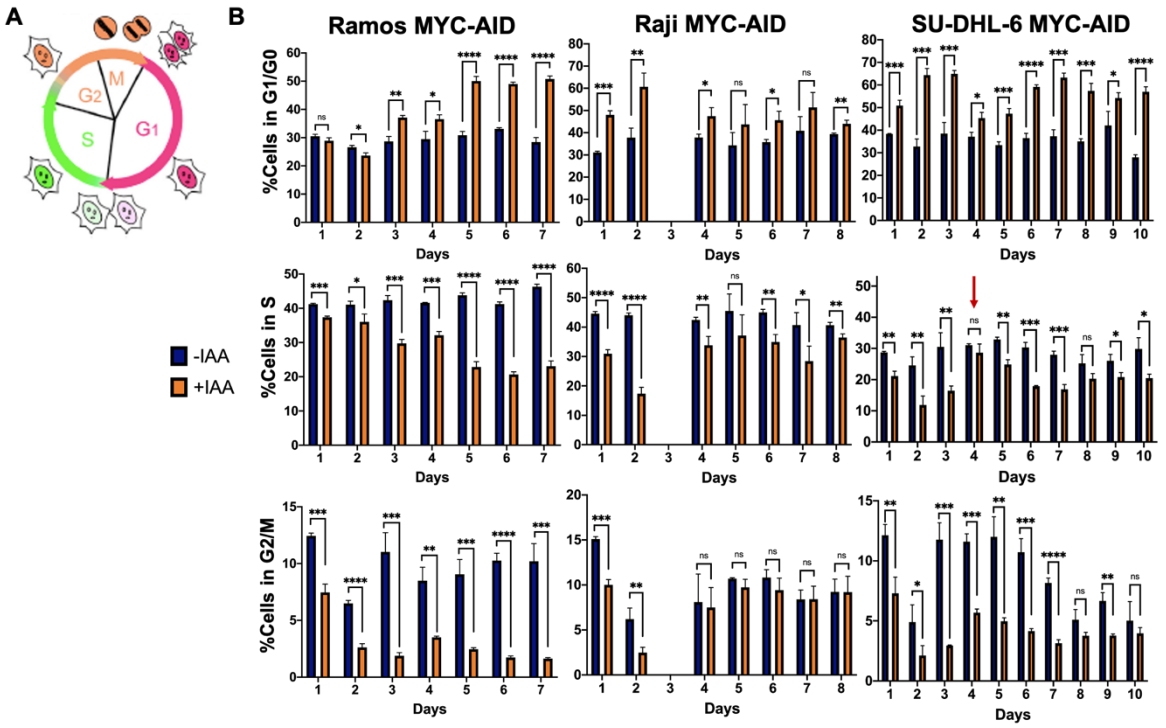

Figure 18: Cell Cycle monitoring with the FUCCI system upon MYC-AID degradation.
(A) Schematic representation of the FUCCI(CA)2 system. Image was adapted from *Sakaue-Sawano, Mol Cell,* 2017 (Ref.[380]). **(B)** Parallel cultures of the indicated cell lines were passaged with Auxin (+IAA: 100 µM) or without it (-IAA). At the indicated time-points (Days), live cells were subject to flow cytometric acquisition and analysis. Percentages of cells in each cell cycle phase as indicated; G1/G0 on top, S in the middle and G2/M on bottom side. The data represent the means and SD (T test) from 3 biological replicates; *P≤0.05, **P≤0.01, *** P≤0.001, **** P≤0.0001.

As mentioned above, ~50% of the Raji FUCCI cells in our cultures had seemingly lost BFP/Tir1 and thus, in principle, the capacity for IAA-triggered MYC-AID degradation. We used this to our advantage, producing separate analysis of the Flow Cytometric data in BFP-negative cells as a negative control. As expected, IAA treatment had no effect on the BFP-negative subset, which exhibited patterns identical to those of untreated BFP-positive cultures (**Fig. S7A)**. Since the BFP-negative cells in our cultures should be under strong selective pressure upon IAA treatment, we proceeded with profiling the proportion of BFP positive/negative cells in all three cell lines throughout their respective time-courses. While this proportion remained steady over time for untreated cultures, IAA treatment lad to the expected increase in BFP-negative subpopulations (**Fig. S7B**): this was the most apparent in Raji, in line with the larger initial size of this escaper subset in those cultures (**Fig. S6B**, circled in red). The Ramos line, where there was a minuscule percentage of BFP-negative cells to begin with, remained almost completely BFP positive for the whole duration of the time-course (**Fig. S7B**, top), while minor fractions of escapers became apparent in SU-DHL-6 only at late time-points (**Fig. S7B**, bottom).

To summarise the part of MYC-dependent cell cycle changes, the loss of MYC shows clear effect on cell cycle distributions in all three cell lines; albeit with some differences in kinetics, it causes a loss of S-phase cells with a concomitant arrest in G1. While the FUCCI system consolidated our previous EdU-based observations, some aspects of these observations remain to be further investigated. More importantly, the general conclusion of the whole section **3.2.1**, is that all three cell lines (with differences in kinetics) eventually encounter cell cycle arrest, stopping of proliferation and apoptosis upon MYC withdrawal, these effects are not immediate; despite the absence of MYC, the cells seem to retain a protracted proliferative capacity for 2-3 days.

3.2.2 Comparing MYC-AID degradation and genetic ablation of MYC

Albeit transitory, the maintenance of proliferative capacity upon MYC-AID loss was unexpected, prompting us to address whether full genetic ablation of MYC would yield the same effect. Toward this aim, we took advantage of the engineered cell line Ramos-Δ264, allowing conditional, CreER-mediated replacement of *MYC* exon 3 by a mutant cassette, resulting in a truncated, inactive version of the protein (MYC Δ264) and concomitant expression of GFP[350] (**Fig. 19A**). Following activation of CreER by treatment with 4-OHT, the cells were sorted based on GFP fluorescence and then followed with the CellTrace assay: while non-recombined GFP- cells maintained daily divisions over the full time-course (d1-d6), recombined GFP+ cells divided only once (between d0 and d1) followed by immediate, full proliferative arrest (**Fig. 19B**) and progressive cell death (**Fig. 19C**). Flow-cytometric MYC staining confirmed full loss of the protein in recombined Ramos-Δ264 cells, with staining levels comparable to those of a negative IgG control (**Fig. 19D**, top). Instead, IAA-treated MYC-AID cells expressed residual levels of the protein, clearly detectable above experimental background (**Fig. 19D**, bottom).

Altogether, the above data reveal a key difference between the genetic ablation of MYC, which caused immediate growth arrest, and post-translational targeting of the protein, in which this arrest was protracted. While IAA caused virtually immediate degradation of MYC-AID, the residual protein levels that persisted in this model (consistent with continuous biosynthesis and degradation) allowed ca. 3 residual division cycles; yet, those cells eventually lost biomass, withdrew from the cell cycle, and died. Most importantly the residual MYC-AID protein did not appear to support an adaptive recovery of these cultures: while some cultures (in particularly Raji) contained a fraction of late-dividing cells, those

were due to the selection of escapers. These observations imply that MYC-translocated lymphomas show continuous dependence upon elevated MYC proteins levels.

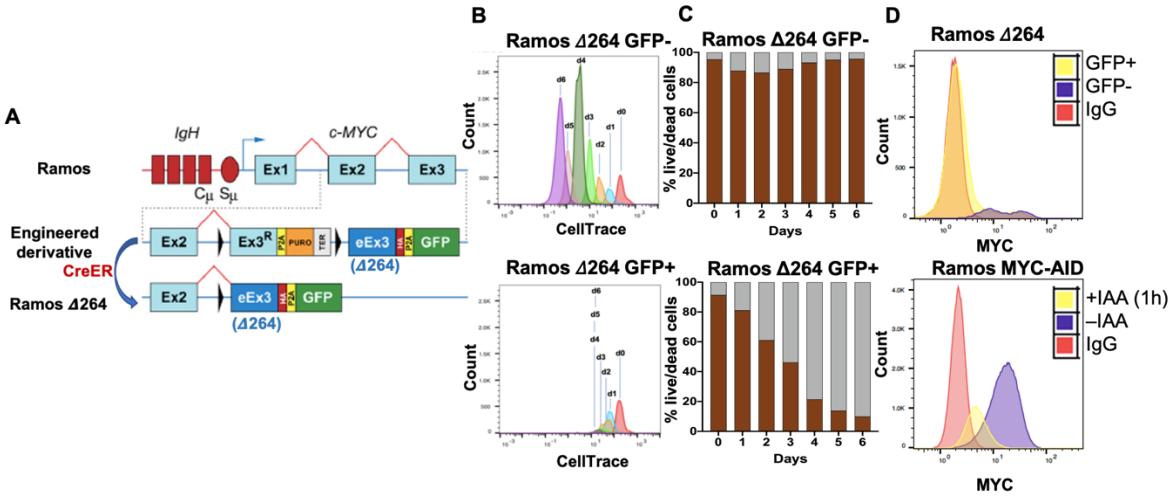

Figure 19: Conditional *MYC* knockout vs. MYC-AID in the Ramos Burkitt Lymphoma cell line.
(A) Structure of the MYC locus in the parental Ramos cells line and in the engineered Δ264 derivative. Image was adapted from *Thomas et al., Mol Cell, Proc Natl Acad Sci U S A, 2019* (Ref.[350]). Cells were a gift from the Tansey lab. In the unswitched state, Ramos Δ264 express the wild-type MYC protein and puromycin resistance. Upon CreER activation through OHT treatment, the allele is switched to express the exchanged Exon3 (eEx3), encoding a modified form of MYC, followed by GFP. This leads to the production of a truncated, inactive form of MYC (Δ264), resulting in complete loss of function. Prior to the measurements shown in **(B-D)**, GFP fluorescence was used to sort switched (GFP+) and unswitched (GFP–) cells, which were then cultured in the absence of OHT and followed over time. **(B)** Monitoring of cell division with CellTrace™ Far Red. **(C)** Percentage of dead (PI positive) versus live (PI negative) cells. **(D)** Comparison of MYC protein levels by staining for flow cytometric analysis in the Ramos-Δ264 and Ramos MYC-AID models, either with or without treatment, as indicated. In either model MYC staining was performed at the earliest available time-point (immediately post-sorting for Δ264; after 1h of IAA treatment for MYC-AID); as negative controls, untreated cells were stained with an IgG Isotype Antibody.

3.3 Transcriptional dynamics in MYC-AID cells

3.3.1 Kinetics of mRNA synthesis and accumulation

Taking advantage of our MYC-AID lines, we sought to profile the immediate changes in RNA synthesis caused by MYC inactivation. Untreated and IAA-treated cells (1, 2, 4 and 8 hours) were used for RNA-seq profiling of total and newly synthesized RNA, the latter based on metabolic labeling with a 10 min pulse of 4-thiouridine (4SU), as previously done in our own[85,234] and other studies[235,407]. We then used DESeq2[384] to call for differentially expressed genes (DEGs) at each IAA time-point, relative to untreated cells (0h). To determine the optimal conditions for DEG calling in 4SU-seq data, we initially applied lax criteria (padj <0.05 with no thresholds for mRNA levels or fold-change) and tested the effects of introducing fold-change thresholds ($|\log_2 FC| > 0.5$ or >1; **Fig. 20A** and **S8A, B**). As previously reported in K562 cells [235], MYC-AID degradation led to the suppression of RNA synthesis at hundreds of loci within 1h (e. g. 280 to 1100 in Ramos: **Fig. 20A**, left), with increasing numbers over time (**Fig. 20A** and **S8A**). Up-regulated loci were less abundant,

consistent with the notion that MYC predominantly acts as a transcriptional activator[85,234,235].

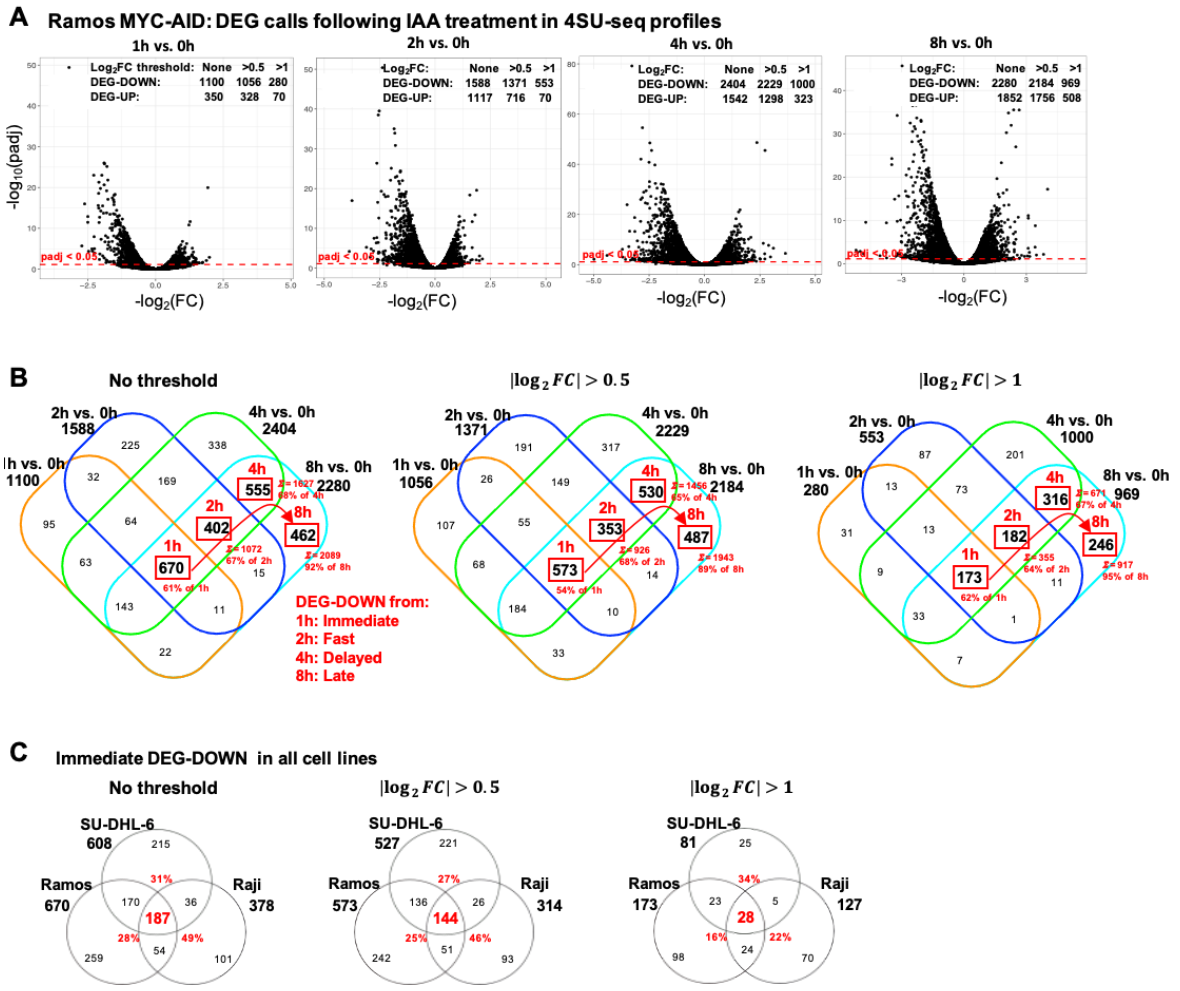

Figure 20: Temporal dynamics of IAA-induced transcriptional changes in Ramos MYC-AID cells.
Ramos, Raji and SU-DHL-6 MYC-AID cells treated with IAA 100 µM for a time-course of 0, 1, 2, 4 and 8 hours were pulsed with 300 µM 4SU for 10 minutes and processed for purification and sequencing of nascent 4SU-labeled RNA (4SU-seq). The data shown here are from 4SU-seq in Ramos and are reproduced in **Fig. S8** for Raji and SU-DHL-6. **(A)** Volcano plots showing the changes in RNA synthesis (4SU-labeled RNA) upon IAA treatment at the indicated time-points relative to untreated cells. Red dashed line represents padj=0.05 and genes above it are considered as differentially expressed (DEGs). The numbers of differentially expressed genes (DEG-DOWN and -UP) called with different log_2FC thresholds are indicated within each plot. **(B)** Overlaps among the DEG-DOWN genes called in Ramos at the different time points with the indicated log2FC thresholds. Numbers in red squares represent the temporally defined gene lists: Immediate, DEG from 1h onwards; Fast, DEG from 2hrs onwards; Delayed, DEG from 4hrs onwards; Late, DEG from 8hrs. The cumulative percentages represented by these gene lists at the corresponding time-point are indicated in red. **(C)** Overlaps of the Immediate DEG-DOWN genes among the three cell lines, with the indicated log_2FC thresholds. The numbers of common genes and their percentage within each cell line are highlighted in red.

To dissect the temporal dynamics of transcriptional changes, we examined the overlaps between the down-regulated mRNAs called at different time-points of IAA treatment in each MYC-AID cell line (**Fig. 20B and S8B**). Most noteworthy, a majority of the DEG-down loci called at 1 hour showed a coherent pattern of reduced RNA synthesis, being called also at the subsequent time-points (e. g. 670 loci in Ramos, or 61%: **Fig. 20B**, left): we hereby refer to this group as the **Immediate MYC-dependent genes**. Following the same logic,

other numerically predominant groups showed coherent suppression from 2h (**Fast**), 4h (**Delayed**) or only at 8h (**Late**): when cumulated, these groups constituted the majority of the DEGs called at each time-point, reaching up to 90% and higher (**Fig. 20B and S8B**). While the total numbers in each group dropped when applying a threshold of $|\log_2 FC| > 1$], their relative abundances remained largely unaffected. Finally, when comparing the Immediate MYC-dependent genes called in each of the three cell lines, maximal levels of overlap were obtained without applying a $\log_2 FC$ threshold (**Fig. 20C**). Altogether, these observations confirm the validity of calling for DEGs with no $\log_2 FC$ threshold: while more prone to experimental noise, applying this condition to the profiles obtained in 3 distinct lymphoma cell lines (with n=3 biological replicates for each line) allowed maximal recovery of immediate MYC-dependent genes.

Additional insight was provided by confronting the distributions of the four temporally defined groups among the three lymphoma cell lines in both 4SU-seq (**Fig. 21A, B**) and total RNA-seq profiles (**Fig. 21C, D**). In 4SU-seq, the substantial overlap seen among Immediate MYC-dependent genes (**Fig. 21A**, top) was essentially lost for the subsequent DEG-down groups (Fast, Delayed, Late). Moreover, unlike the DEG-DOWN, Immediate DEG-UP genes showed no substantial overlap between the three cell lines (**Fig. 21B**, top). Altogether, these data imply that direct MYC-dependent mechanisms common to all cell lines are required to support transcription at a core set of MYC-dependent genes.

Relative to 4SU-seq, total RNA-seq profiles showed lower numbers of Immediate MYC-dependent mRNAs (**Fig. 21C**, top; compare with **Fig. 21A**) but the numbers of down-regulated mRNAs steadily increased at later time-points (**Fig. 21C**), with a similar trend for up-regulated mRNAs (**Fig. 21D**). Most noteworthy, while 13-32% of the Immediate MYC-dependent genes, as defined by 4SU-seq, showed the same classification in total RNA-seq, larger proportions scored among the subsequent temporal groups (**Fig. 22A**): altogether, 79-89% of the Immediate MYC-dependent genes were accounted for in one of the four down-regulated total mRNA groups. Similarly, while immediate DEG-UP genes mapped by 4SU-seq were less abundant, most scored amongst up-regulated mRNAs (58-92%, **Fig. 22B**). These data have two important implications: first, at the technical level, they confirm the good concordance between our 4SU- and total RNA-seq datasets; second, and as expected, they imply that immediate transcriptional changes were followed by consistent, but kinetically variable changes in mRNA levels.

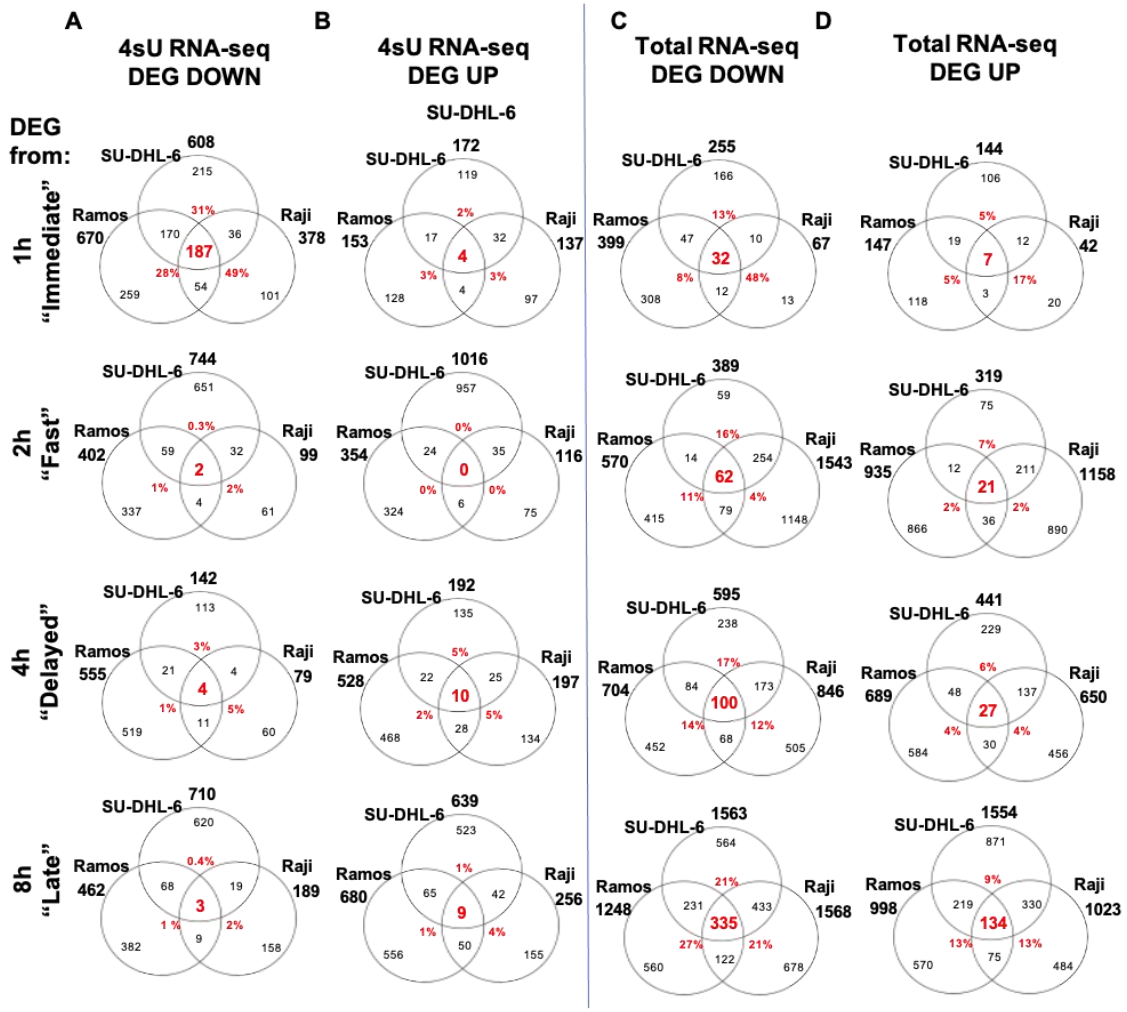

Figure 21: Overlap of the temporally defined genes lists among the three MYC-AID cell lines .
Ramos, Raji and SU-DHL-6 MYC-AID cells treated with IAA 100 µM for a time-course of 0, 1, 2, 4 and 8 hours and were either pulsed with 4SU for 4SU RNA-seq as described in Fig. 10, or collected directly for purification and bulk RNA-seq. The temporally defined lists of DEG-DOWN and DEG-UP genes (Immediate, Fast, Delayed, Late) were determined in each dataset as defined in Fig. 10B for 4SU-seq DEG-DOWN genes. The Venn diagrams show the overlaps among the three cell lines, for each gene list (indicated on the left) as determined by 4SU-seq (**A, B**) or total RNA-seq (**C, D**) for either DEG-DOWN (**A, C**) or DEG-UP genes (**B, D**). For each cell line, the percentage of genes common to all cell lines is highlighted in red.

Of note, a reciprocal comparison revealed that lower and somewhat variable proportions (8-43%) of the late down-regulated mRNAs were accounted-for among the four temporal groups by 4SU-seq (**Fig. 22C**), with slightly higher overlaps for up-regulated mRNAs (20-46%, **Fig. 22D**). We surmise that the loss of direct MYC-dependent gene products may impact on larger numbers of mRNAs at the post-transcriptional levels, accounting for their differential loss/accumulation at late time-points (**Fig. 21C-D**). Such secondary effects may occur at multiple levels, including RNA modifications, processing or translation, ultimately converging on turnover[107,408]. Most importantly here our data highlight the immediacy and selective nature of MYC's action, emphasizing the need for time-controlled, kinetic analysis of transcriptional profiles[85,234].

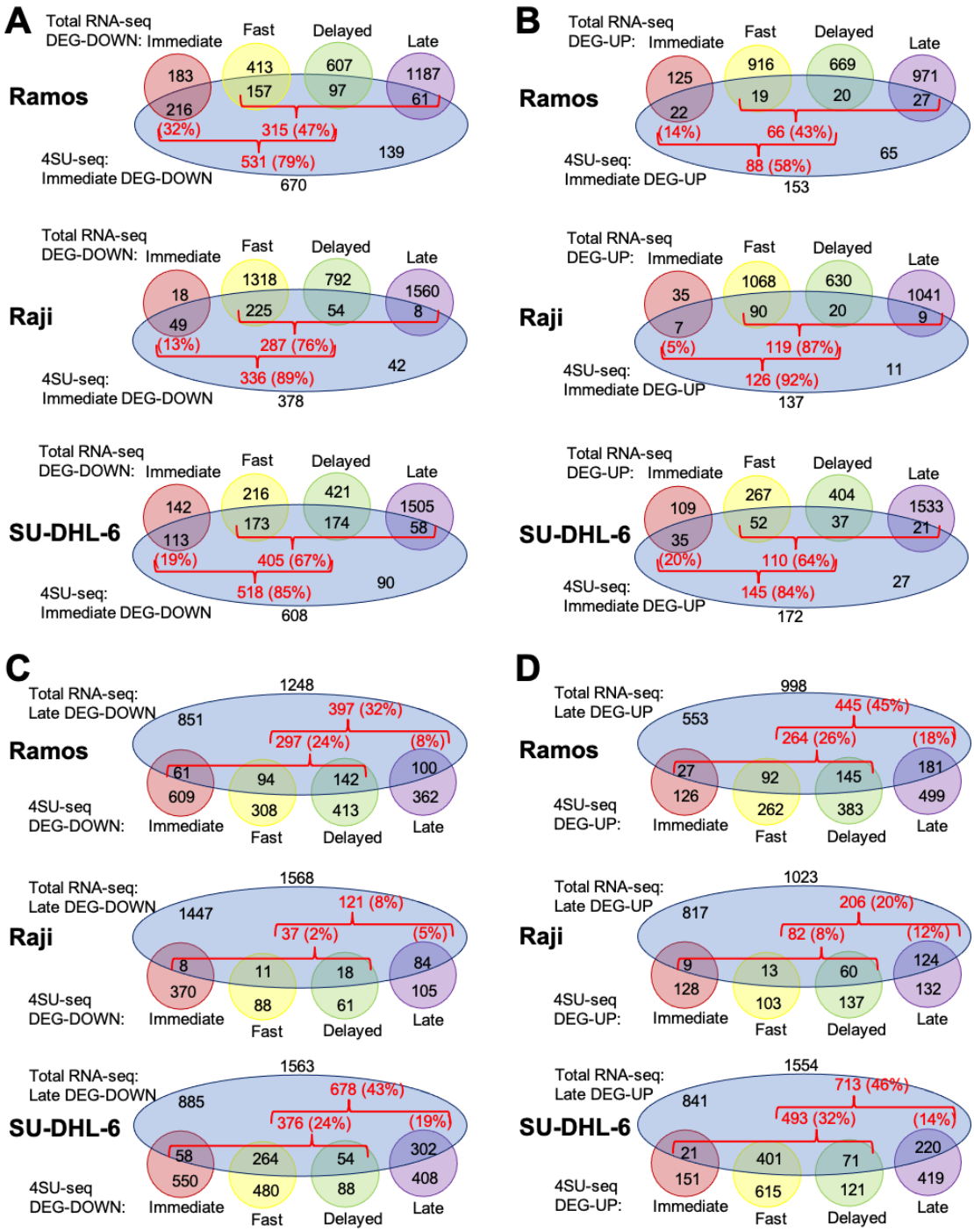

Figure 22: Temporal overlaps between differentially expressed genes determined by 4SU- and total- RNA-seq.
The groups of DEGs shown in Fig. 21 were used to address the overlap between 4SU-seq and total RNA-seq profiles in each cell line. (**A**) Venn diagrams representing the overlap between the Immediate DEG-DOWN group defined by 4SU-seq and the Immediate, Fast, Delayed and Late DEG-DOWN groups from total RNA-seq, as indicated. The cumulative numbers of overlapping genes and their percentages within the reference Immediate DEG-DOWN group. **(B)** As in (A), for DEG-UP genes. **(C, D)** as in (A) and (B) taking the Late DEG-DOWN and -UP genes as reference groups, respectively.

Gene Ontology analysis provided further indication for the rapid down-regulation of MYC-dependent gene programs upon IAA treatment, with *MYC TARGETS V1* and *V2* as the top enriched Hallmarks in the Immediate DEG-down group called by 4SU-seq in our three cell lines, and less consistently in the subsequent groups (**Fig. 23A**). Reciprocally, by total RNA-seq, those MYC-associated hallmark signatures were most consistently enriched – albeit at variable levels – in the later groups (**Fig. 23B**), in line with the aforementioned lag between transcriptional shutdown and mRNA decay. The same analysis was performed with our core group of common 187 Immediate MYC-dependent genes (**Fig. 20C**, left), yielding once again strongest enrichment of the MYC V1 and V2 hallmarks (**Fig. 24A**). Most noteworthy here, this group also showed substantial overlaps with MYC-target gene lists determined in other studies[235,242] (**Fig. 24B**).

Unlike DEG-DOWN, GO analysis on 4SU-seq-defined DEG-UP genes yielded no consistently enriched Hallmark among the three cell lines, neither for the Immediate, nor for the subsequent groups (**Fig. S9A**). While the Fast DEG-UP group (up from 2h) in total RNA-seq showed common enrichment of some Hallmarks (**Fig. 23B**: Mitotic Spindle, G2/M checkpoint, E2F targets, PI3K AKT MTOR signaling), the same or closely related Hallmarks were also detected in some of the DEG-DOWN groups (**Fig. 23B**): the significance of these pathways to the phenotypic responses of our MYC-AID cells remains to be addressed.

Altogether, at the current level of resolution, the Immediate MYC-dependent genes identified in our profiles enrich for known MYC-regulated genes. Further computational analysis will address what other functional categories and/or regulatory pathways may be consistently deregulated following MYC-AID degradation.

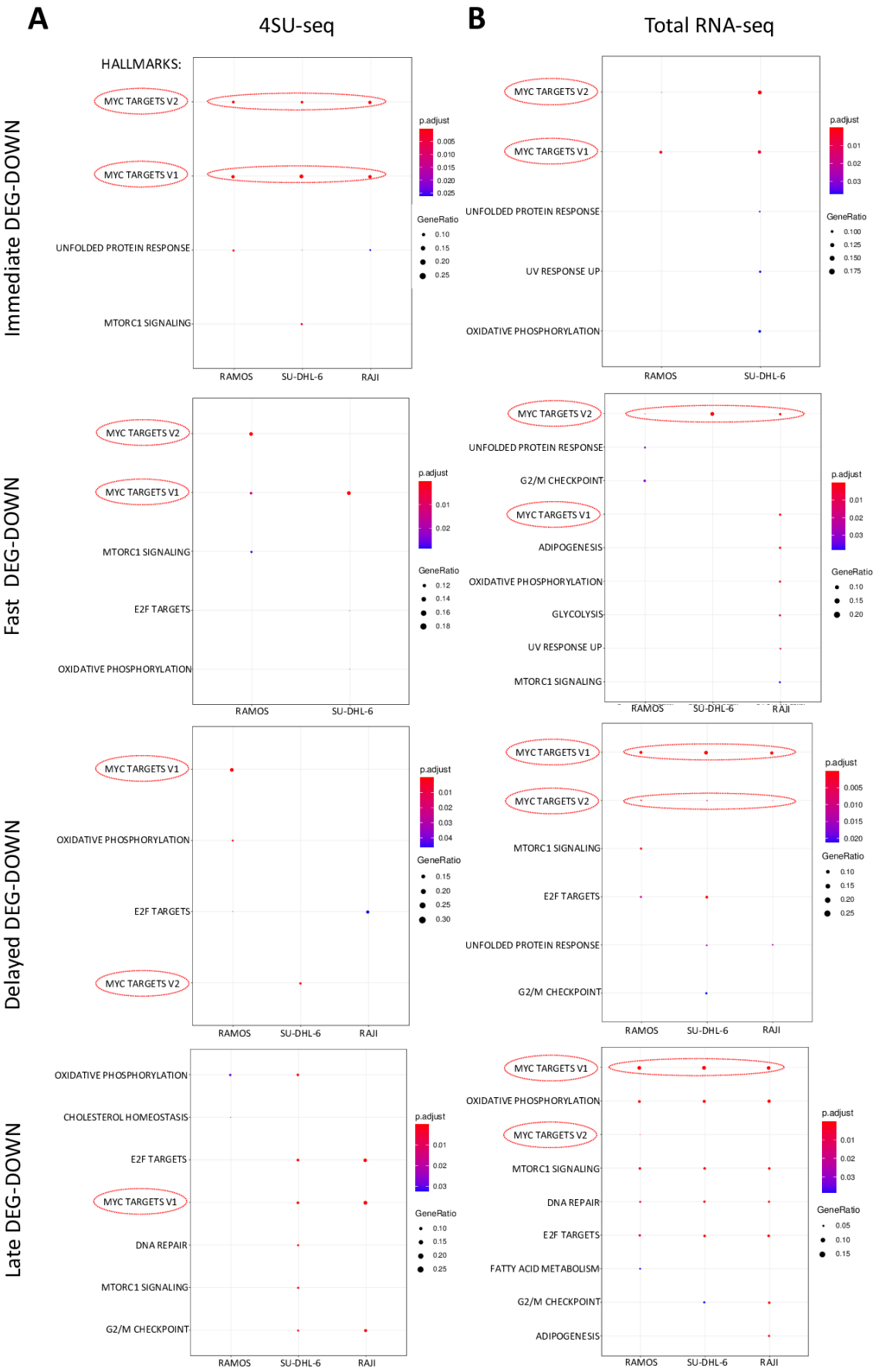

Figure 23: Gene Ontology Analysis on DEG-DOWN gene lists from 4SU- and Total RNA-seq for the three cell lines.
Gene ontologies (GO) for hallmark gene sets using the indicated DEG-DOWN lists (Immediate, Fast, Delayed, Late) acquired by **(A)** 4SU-seq and **(B)** Total-seq in the three MYC-AID cell lines. "p.adj" is the P-value adjusted using the Benjamini-Hochberg procedure, "Gene ratio" is the percentage of total DEGs in the given GO term (only input genes with at least one GO term annotation were included in the calculation). Circled in red are the MYC TARGETS V1 and V2 sets, as well as the instances where they occur simultaneously in all the three cell lines

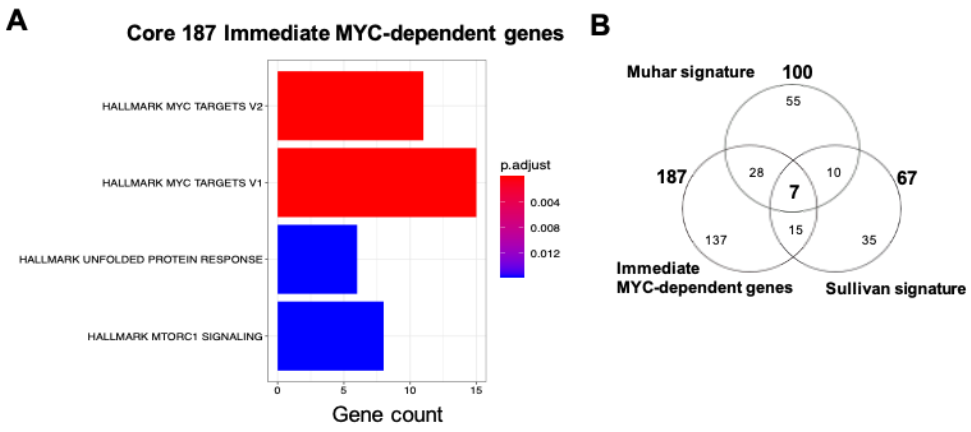

Figure 24: Immediate MYC-dependent genes enrich for known MYC targets.
The core 187 Immediate MYC-dependent genes common to our three MYC-AID cell lines (**Fig. 20C** and **21A**) were used for **(A)** Gene ontology (GO) analysis using hallmark gene sets ("p.adj" and "Gene count" are defined as **Fig. 23**) and **(B)** determine their overlap with MYC-target gene lists from other studies[235,242].

3.3.2 ChIP-seq profiling: MYC and RNA-Polymerase II dynamics

We used ChIP-seq to profile the distribution of MYC and RNA-PolII across the genome in Ramos MYC-AID cells, treated or not with IAA for 1h. Focusing on annotated genes showed that, as previously reported[85,234,240], MYC was associated with active promoters, as defined by the presence of RNA Polymerase II (RNAPII) and active histone marks (H3K4me3, H3K27ac), while inactive loci lacking these features remained unbound (**Fig. 25A** and data not shown). Likewise, distal MYC-binding sites showed distinctive features of active enhancers (RNAPII, H3K4me1 and H3K27ac) (**Fig. 25B** and data not shown). This widespread association of MYC with active regulatory elements, sometimes termed "invasion" has been documented in multiple studies[1,85,232,233,237]; most importantly, this effect reflects general chromatin accessibility and non-specific DNA-binding, does not depend on E-box recognition by MYC, and cannot be systematically associated with functional regulatory interactions[240].

We then addressed the changes in MYC and RNA-PolII binding at the promoters of down-regulated loci (i. e. DEG-down by 4SU-seq at 1h), with an expression-matched set of non-regulated genes as control (NO-DEG; **Fig. S10A**). As expected, MYC was detected on the promoter region in both sets of genes, with stronger binding at MYC-dependent loci[234,240] and a general drop upon IAA treatment (**Fig. 26A, C, D**). RNA-PolII was preferentially lost from the down-regulated loci, with proportionate drops in the various gene regions (TSS, Gene Body, TES) (**Fig. 26B, D, E**). In line with these observations, direct comparison of the variations **at MYC-bound promoters** following IAA treatment showed that down-regulated loci underwent the highest drop in MYC binding, accompanied by selective loss of RNA-PolII

(**Fig. 27A**). Of note, albeit less extensive, a fraction of the non-regulated (NO-DEG) promoters also showed reductions in RNA-PolII (**Fig. 26E** left, **Fig. 27A**). At the time of writing, we suspect that the latter effect might be due to cross-contamination of the NO-DEG group used in our analysis with DEG-DOWN loci, owing to the fact that these groups were defined by padj >0.05 and <0.05 respectively, without any threshold on log2FC values. This will be addressed in further analyses.

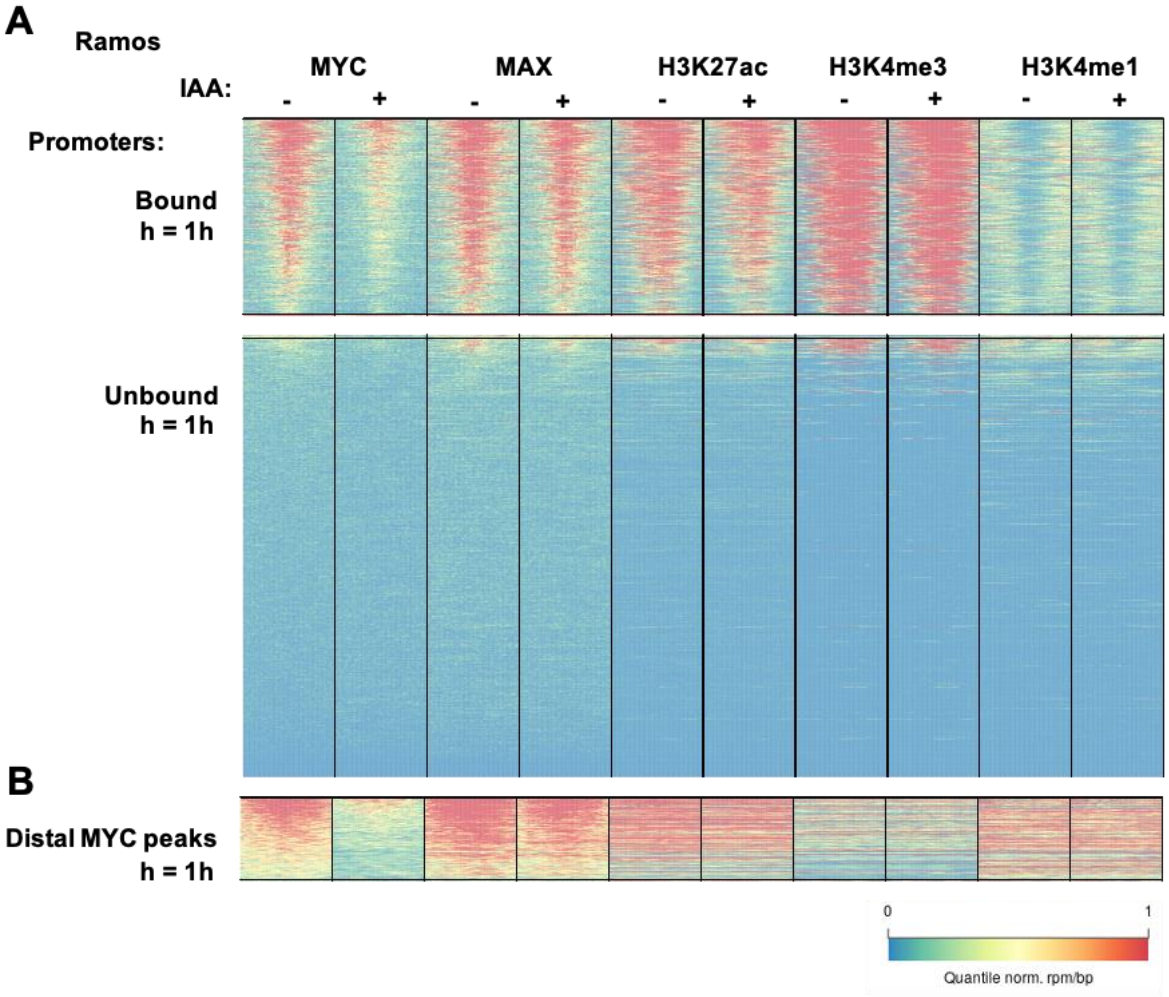

Figure 25: Impact of IAA treatment on genome-wide MYC-AID binding profiles.
Ramos MYC-AID cells were treated with IAA (1h) and profiled by ChIP-seq with antibodies against MYC, MAX or the indicated histone marks. The heatmaps represent spike-in normalized ChIP-seq intensities in **(A)** MYC-bound (top) and unbound (bottom) promoters and (**B**) distal MYC-binding sites. Peak calling (see Methods) was used to distribute annotated promoters among the two categories, as well as to map distal binding sites. Each row represents a genomic site out of a subsample of 2000 regions, with 545 bound, 1224 unbound promoters and 231 distal peaks, ranked according to MYC enrichment in untreated cells. The total counts on the same elements in the genome are of 19174, 38666 and 6374, respectively. Promoter regions span a 3 kb-wide genomic interval centered on the TSS, while distal regions interval depends on the width of the MYC peak.

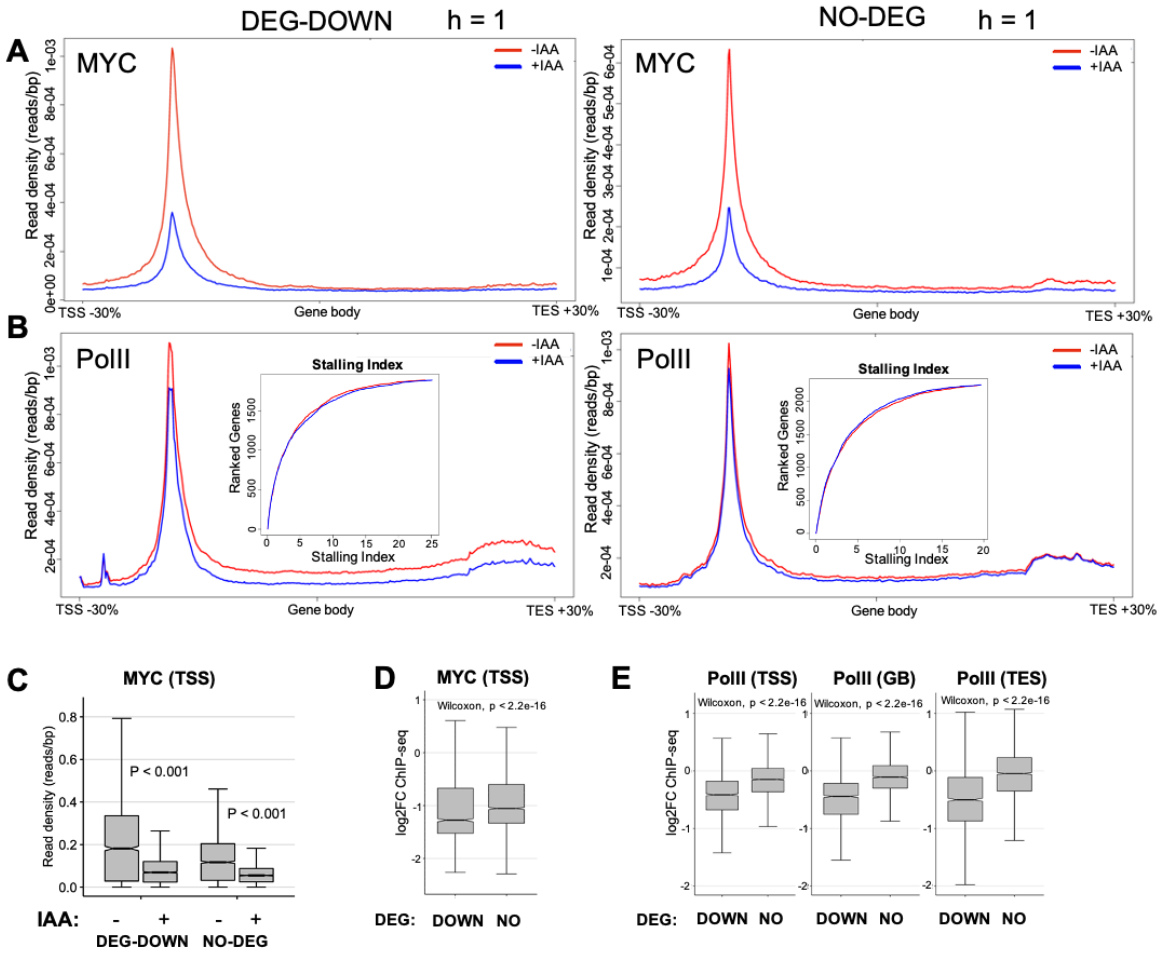

Figure 26: Impact of IAA treatment on MYC-PolII dynamics.
Metagene representations of **(A)** MYC and **(B)** total RNA-PolII ChIP-seq profiles in Ramos MYC-AID cells, with (+IAA; 1h) and without auxin treatment (-IAA, red line), on two distinct gene populations: left, DEG-DOWN genes (as defined by 4SU-seq at 1h); right, a set of expression-matched non-regulated control genes (NO-DEG; see Fig. S10). For the metagene profiles, each gene, plus a neighboring region of ±30% of transcript size, was split in 500 bins and the number of reads falling in each bin was evaluated. The insets show cumulative distribution plots of RNA-PolII stalling indexes, defined as the ratio of the total PolII reads on the TSS divided by those in the corresponding gene body**.** Box-whisker plots were used to report **(C)** the cumulative densities of MYC ChIP-seq reads and **(D)** their variation upon IAA treatment (expressed as log2FC treated/untreated) in the promoter regions (TSS) of DEG-DOWN and NO-DEG genes, as indicated. **(E)** Same as (D) for RNA-PolII ChIP-seq reads in promoters (TSS), gene bodies (GB) or termination sites (TES). Statistical analysis was performed with either paired samples (C) or unpaired two-samples Wilcoxon test (D, E).

The above observations are consistent with a series of prior reports. First, in all datasets in which combined RNA expression and DNA-binding data were available, gene activation by MYC – as opposed to repression – correlated with the strongest gain in MYC binding to promoters[234,235,237,409], mirroring both the stronger association of MYC-AID at DEG-DOWN loci (**Fig. 26C**) and the higher magnitude of its loss upon IAA treatment (**Fig. 26D, Fig. 27A-E**). Second, while MYC has the potential to regulate pause-release[285,287,410], our previous data showed that it is rate-limiting for RNA-PolII loading at activated loci[234], consistent with the proportional losses of RNA-PolII from the TSS and Body of MYC-dependent genes upon MYC-AID degradation, as also corroborated by the unaltered distributions of stalling indices following IAA treatment (**Fig. 26B**).

Finally, up-regulated loci showed the same general loss of MYC binding (**Fig. S11A, C**). On those genes, IAA treatment was followed by increases RNA-PolII levels in the gene-body and termination region, as expected, but without apparent increases in loading at promoters (**Fig. S11A, C, Fig. 27A**), suggesting that MYC loss may favor pause-release or processivity at those loci, through mechanisms that remain to be investigated.

3.3.3 MYC-dependent changes in histone modifications: preliminary data.

Besides MYC and RNA-PolII, our initial ChIP-seq profiles included MAX, H3K27ac, H3K4me3 and H3K4me1 (**Fig. 25**). Hence, as done for RNA-PolII (**Fig. 27A**), we compared the IAA-induced changes in MYC and each of these features at MYC-bound promoters (**Fig. 27B-E**). From this preliminary analysis, MAX showed a general decrease in binding, albeit not as strong as – nor fully proportional to that of MYC (**Fig. 27B**). This may be consistent with the notion that MAX can dimerize and bind DNA with alternative bHLH-LZ partners, such as MXD1-4, MNT of MGA[28,29]: whether any of those alternative MAX dimers contribute to differential gene regulation upon MYC loss remains to be addressed.

Most remarkably, while H3K4me3 remained relatively stable following MYC loss (**Fig. 27C**), this was not true for H3K27ac, which dropped not only from MYC-dependent genes (DEG-DOWN) but also – albeit less markedly – from non-regulated promoters (**Fig. 27D**). Hence, as a preliminary conclusion, MYC may impact on H3K27ac at two levels, one associated with gene activation (underlying the strongest loss H3K27ac upon at MYC-dependent genes after IAA treatment) and the other not: the mechanistic basis for these effects remains to be addressed, in particular if considering the role of sequence recognition in transcriptional activation by MYC[240].

H3K4me1 was not significantly regulated at promoters but showed a slightly wider spread of log2FC values (**Fig. 27E**), in contrast with the more uniformly stable state of H3K4me3 (**Fig. 27C**). However, H3K4me1 levels were low at promoters and the highest at distal sites (**Fig. 25**), consistent with the enrichment of this mark at enhancers[411,412]. Hence, it will be more relevant to address whether variations in H3K4me1 may eventually underlie a regulatory role of MYC at enhancers. Indeed, while an effect of MYC on enhancer activity has been proposed[413,414], this was based largely on correlative data and remains to be formally established.

Finally, we have recently established ChIP-seq profiles for a series of other features, including H4K5ac, H4K12ac, H3K14ac, H3K18ac, H3k36me3, H3K79me2 and will address which of these may be functionally associated with MYC-dependent transcription.

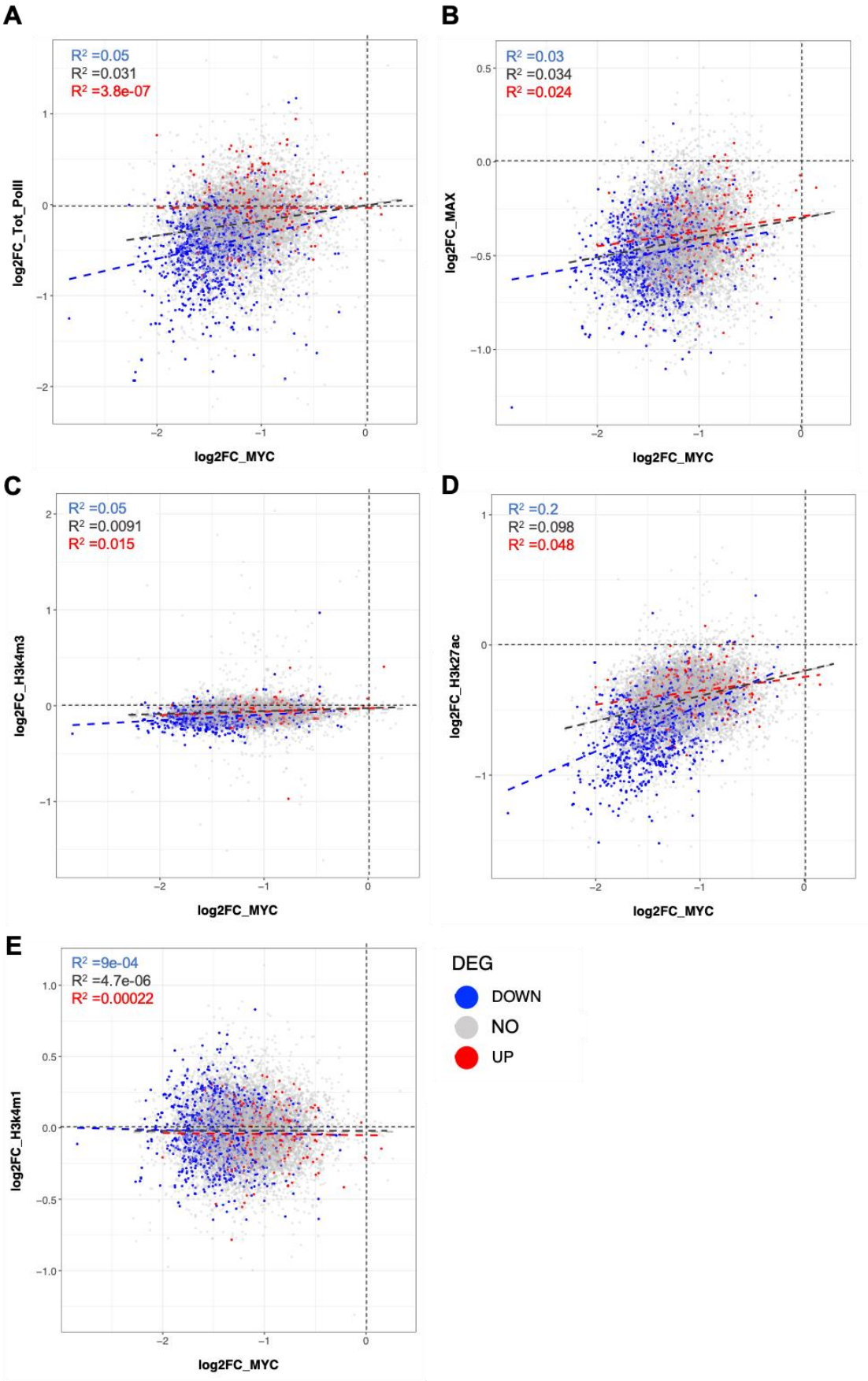

Figure 27: Variations of RNA-PolII, MAX and histone marks relative to MYC at promoters.
Ramos MYC-AID cells were analyses by ChIP-seq as described in Fig. 25. The dot plots illustrate the log2FC distribution of each feature against that or MYC. **(A)** RNA-PolII, **(B)** MAX, **(C)** H3K4me3, **(D)** H3K27ac and **(E)** H3K4me1. Each dot represents an individual MYC-bound promoter. Promoters belonging genes previously identified as DEG-DOWN by 4SU-seq (1h) are colored in blue, DEG-UP in red, and NO-DEG in grey. Linear regression and R^2 are computed separately for each group, as indicated.

3.4 MYC and Translation

Beyond transcription per se, MYC is well positioned to control additional layers of the gene expression program, by regulatory cross-talk with RNA-PolII, and in particular with its C-Terminal Domain (CTD). The CTD consists of multiple copies of the consensus repeat YSPTSPS in which posttranslational modifications, in particular phosphorylation of Serines 5 and 2 by the kinase complexes TFIIH and P-TEFb, modulate a large number of protein-protein interactions: these, in turn, coordinate the different phases of the transcription cycle with co- and post-transcriptional processes such as mRNA capping, splicing, export and translation[415,416]. By recruiting TFIIH[417] and P-TEFb[282], among others, MYC can modulate these processes at its target loci[282,408,418,419]. Through these mechanisms, MYC is likely to impact on co- and post-transcriptional processes, which in turn would be expected to impact a common ultimate endpoint: mRNA translation. We thus decided to profile the changes in either total or polysome-associated mRNAs – as a proxy of translation[420] – upon MYC-AID degradation in Ramos cells.

To generate translational profiles, we collected cell lysates from three biological replicates after 4 hours of IAA treatment. Degradation of MYC-AID in the samples was confirmed by Western Blot (**Fig. S12A**). Cell lysates were fractionated on sucrose gradients, allowing to separate free, monosome and polysome-associated mRNAs, the latter sedimenting in the heavier fractions of the gradient. Following collection of all fractions, UV absorption profiles were generated to determine RNA contents (**Fig. 28A, Fig. S12B**). RNA recovered from the various fractions was then pooled in three main categories: free mRNA was collected from the lighter soluble fractions, monosomes from the medium weight fractions, and polysomes from the heavier fractions, as indicated (**Fig. 28A, Fig. S12B**). Two RNA populations were subjected to RNA-seq analysis: Polysome-associated RNA, extracted from the pooled polysomal fractions, and total RNA, reconstituted from all the fractions.

The differential representation of mRNAs upon MYC-AID degradation was determined by DEG calling in either total or polysome-associated RNA. Remarkably, MYC-induced changes in those two RNA populations were largely correlated (**Fig. 28B**). In line with this feature, most of the mRNAs called as differentially expressed in the polysome-associated RNA population were included among the DEGs called in total RNA (**Fig. 28C, Fig. S12C**). Hence, at this level of resolution, the data provided no evidence for a differential impact of MYC-AID degradation on the translation of its target mRNAs.

As an important note here, our polysome fractionations were performed early-on in the project, before the aforementioned 4SU- and RNA-seq profiles (section **3.3**). With hindsight, some caution is required regarding the polysome profiles, as comparing the reconstituted total RNA from the polysome fractions with our bulk RNA-seq profiles yielded a very poor overlap (**Fig. S12D**), with a much wider range of Fold Changes in the bulk RNA-seq. Hence, our pooled total fractions may have lost something out of the overall expression profiles. This notwithstanding, Gene Set Enrichment Analysis (GSEA) confirmed that the DEGs called in our polysome profiles as down-regulated had *MYC TARGETS V1* and *V2* gene sets amongst the top enriched Hallmark categories (**Fig. S12E**, top, circled in red), while the rest of the Hallmark categories (**Fig. S12E**, top) had a very good overlap with our bulk-RNA-seq DEG-DOWN GO categories (**Fig. 23**) (MTORC1 signaling, unfolded protein response, G2/M checkpoint, UV response UP, E2F targets etc). In addition to this, they were enriching for known MYC-regulated processes, such as ribosome biogenesis and RNA processing (**Fig. S12E**, bottom).

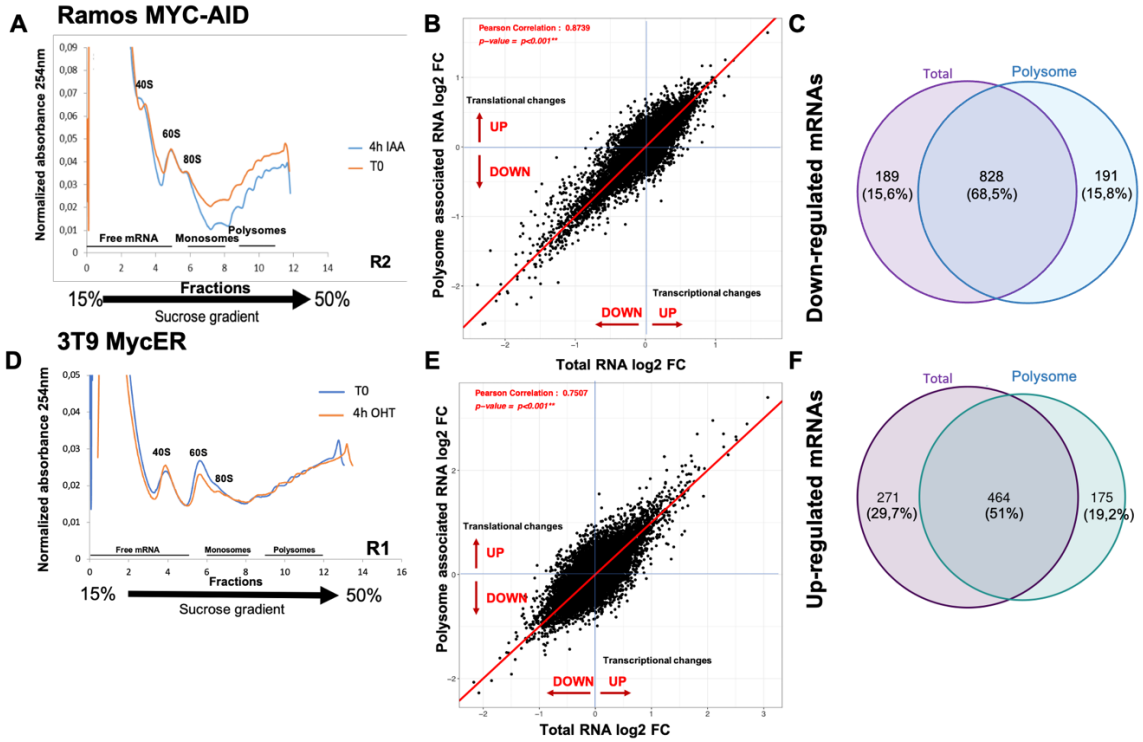

Figure 28: Close correlation between differential RNA expression and translation upon MYC alterations.
Ramos MYC-AID cells treated or not with IAA 100 µM for 4 hours were used for a comparison of Polysome-associated and total RNA-seq profiles. (**A**) UV absorption profile of fractions of cytoplasmic lysates after sedimentation in a 15%-50% sucrose gradient gel for one representative sample out of 3 (the other two replicate profiles are shown in **Fig. S13B**). The 40S, 60S, 80S and polysome fractions are indicated above the curves, and the pooled RNA fractions at the bottom. **(B)** Comparison of the fold-changes (log2FC) of each mRNA determined by total (X-axis) and polysome-associated RNA-seq (Y-axis). **(C)** Overlap between the RNA populations called as DEG-DOWN in the total and polysome-associated profiles. DEGs were computed using DESeq2, with p-adj < 0.05 (n=3 biological replicates). **(D-F)** as (**A-C**) for 3T9 MycER fibroblasts, following 4h of OHT 400 nM treatment. **(F)** Overlap between the RNA populations called as DEG-UP in the total and polysome-associated profiles. Note that MYC-activated genes are computed as down- and up-regulated in the MYC-AID and MycER models, respectively.

Complementary to the loss-of-function scenario provided by the MYC-AID model, we addressed the effects of the opposite intervention, i.e. the ectopic super-activation of MYC above endogenous levels in non-transformed cells. Toward this aim, we used 3T9 fibroblasts expressing an OHT-activated MycER chimera[366], previously used to profile MYC-dependent transcription in our group[85,234]. Triplicate samples were collected, known MYC-induced mRNAs controlled by RT-PCR (**Fig. S13A**), and polysome profiles generated (**Fig. 28D, Fig. S13B**). As above, fractions were pooled into three categories, and the polysome and total RNA populations analyzed by RNA-seq. Once again, we observed a close correlation between the two populations following 4 hours of MycER activation (**Fig. 18E**) and a close overlap among DEGs (**Fig. 28F, Fig. S13C**). Most importantly, in this instance, we observed a good overlap between the DEGs called in our reconstituted total RNA and our previously published bulk RNA-seq data from the same cells[85] (**Fig. S13D**). In accordance with this, Gene Set Enrichment analysis confirmed that MYC-dependent gene expression programs were up-regulated, with the DEG-UPs called in our polysome profiles enriching for *MYC TARGETS V1* and *V2* (**Fig. S13E**, top, circled in red) and for known MYC-regulated processes, mirroring the findings of down-regulated biological processes categories in the Ramos polysome profiling experiment (**Fig. S13E**, bottom).

Overall, acute loss- and gain-of-function, as achieved with MYC-AID and MycER respectively, showed that the changes elicited by MYC at the transcriptional level were rapidly and proportionally forwarded unto polysomes.

3.5 Targeting MYC in combination with BH3-mimetics

MYC promotes cell proliferation[37], but it can also sensitize pre-cancerous cells to undergo apoptosis[144] by changing the equilibrium of pro- and anti-apoptotic factors[154,421]. The key regulators of the intrinsic apoptosis pathway are the BCL-2 family proteins, divided in pro-apoptotic (BAD, BIM, BID, PUMA and Noxa among others) and anti-apoptotic; the latter including BCL-2, BCL-X_L, BCL-W, BFL1 and MCL-1[422]. BCL2 and MYC are known to be synergizing in lymphomagenesis for many decades[154,423], with MYC/BCL2 Double-Hit Lymphomas exhibiting poor prognosis[219]. This is attributable to the ability of BCL2 to block the proapoptotic activity of MYC while leaving its proliferative potential intact[349].

It has been previously demonstrated that MYC synthetic-lethal interactors can kill lymphoma cells synergistically with BCL2-family inhibitors (BH3-mimetics)[347,360]. Pharmacological compounds such as tigecycline, an antibiotic inhibiting mitochondrial translation[424], or IACS, a mitochondrial electron transport chain (ETC) complex 1 inhibitor[425]

both exhibit synergistic effects with Venetoclax, a selective BCL2 inhibitor, in DHL cells[347,360]. Following the same pattern, IACS and MCL-1 inhibition cooperate in killing Ramos cells, that do not bear an activating translocation for *BCL2*, but overexpress the anti-apoptotic protein MCL-1 instead[360].

Given MYC's dual role in proliferation versus apoptosis, as well as the aforementioned synergy between MYC's synthetic-lethal interactors and BH3-mimetics, we initiated a series of preliminary experiments in order to define whether these compounds could provide the same cooperative effects with direct MYC inhibition. We thus treated our three lymphoma cell lines with various concentrations of BH3-mimetics, alone or in combination with IAA, following the cells for 72 hours. On the SU-DHL-6 Double-Hit Lymphoma cell line, we tested the MCL-1 inhibitor S63845 and the BCL2 inhibitor ABT-199 (Venetoclax). For the Burkitt lymphoma lines Ramos and Raji, we tested only the MCL-1 inhibitor, since they overexpress MCL-1 but not BCL2, which makes them resistant to Venetoclax[347,426-428]. Interestingly, we observed different effects in each cell line.

Consistent with our previous results (**Fig. 12A**), treatment of Ramos with IAA alone did not induce a significant decrease in proliferation within the 72 hours of observation (**Fig. 29A**). The MCL-1 inhibitor S63845 caused a dose-dependent suppression of proliferation, with clear killing effects at the highest concentrations (**Fig. 29A, B**). Most noteworthy, the combination of IAA with S63845 appeared to rescue cells from the toxic effects of the MCL-1 inhibitor (**Fig. 29A**), as also confirmed by the decrease of cell death observed in these samples (**Fig. 29B**). Hence, in Ramos, MYC contributes to S63845-induced cell death, consistent with the notion that MCL-1 is required to suppress MYC-induced apoptosis.

Surprisingly, this effect was not observed in our other Burkitt Lymphoma cell line, Raji. More specifically, none of the S63845 concentrations used for Raji gave significant effects in cell proliferation; neither a low drug concentration set (10, 25, 50nM, **Fig. 30** on the left) nor a higher one (100, 150, 200nM, **Fig. 30** on the right) were notably efficient, so much so, that the differences incurred in cell proliferation by the drug could only be discernible using a log2 Y axis instead of a log10 (**Fig. 30A**). This notwithstanding, it seemed like MCL-1 inhibition alone was affecting cell proliferation accordingly with the drug concentration (**Fig. 30A**), a conclusion supported also by the cell death percentages (**Fig. 30B**). While IAA alone also did not cause significant changes in proliferation or cell death (**Fig. 30**), the effect of the combination of the two drugs seemed to be quite similar to the effect of MCL-1 inhibition alone, in all concentrations tried (**Fig. 30B**).

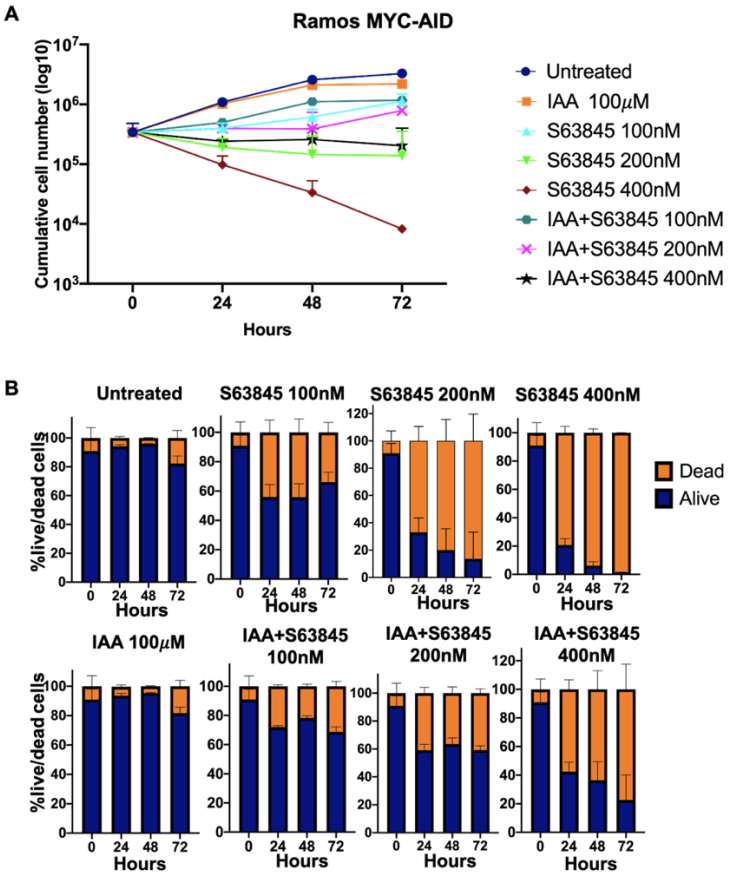

Figure 29: Effect of combinatorial MYC+MCL-1 inhibition in Ramos cells.
(A) Cumulative live-cell numbers and **(B)** live/dead-cell percentages based on PI staining and Flow cytometric Analysis for Ramos MYC-AID after treatment with various concentrations of the MCL-1 inhibitor S63845 (100, 200, 400 nM), alone or together with 100μM IAA at the indicated time-points (Hours). Dead cells were scored by Propidium Iodide (PI) staining and excluded from the cell counts. The data represent the means and SD (T test) from 3 biological replicates.

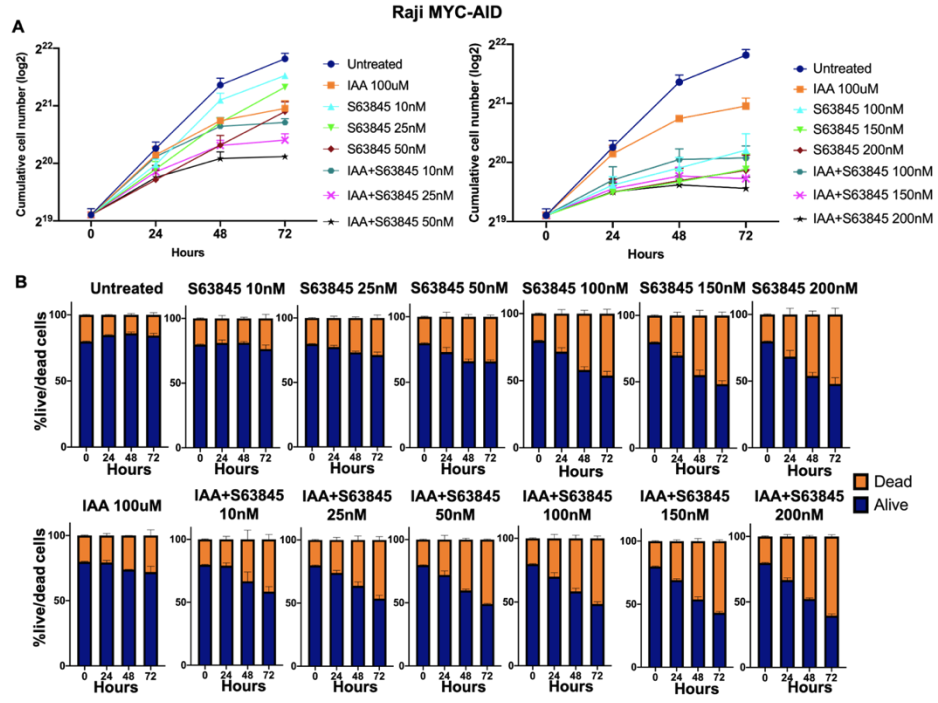

Figure 30: Effect of combinatorial MYC+MCL-1 inhibition in Raji cells.
(A) Cumulative live-cell numbers and **(B)** live/dead-cell percentages based on PI staining and Flow cytometric Analysis for Raji MYC-AID cells, treated as defined in **Fig. 29**. In (**A**) the graphs are divided between the lower (left) and higher concentrations of S63845.

Lastly, in SU-DHL-6 we tried the MCL-1 or the BCL-2 inhibitors, alone or in combination with MYC inhibition. The results indicated that neither MCL-1 inhibition nor Venetoclax are inducing any significant decrease in cell proliferation, with mild effects comparable to those of IAA alone (**Fig. 31A, B**). This moderate outcome was also concomitant with the levels of cell death (**Fig. 31C, D**) and was also in line with what was previously observed in the lab[347,360]. However, there was a clear cooperative effect between MYC inhibition and the two BH3-mimetics used, at the levels of both cell proliferation (**Fig. 31A, B**) and death (**Fig. 31C, D**), the most pronounced effect being seen with S63845 (**Fig. 31A, C**). Hence, the outcome of combining MYC inhibition with BH3-mimetic compounds was highly context-dependent, with opposite effects in different lymphoma cell lines.

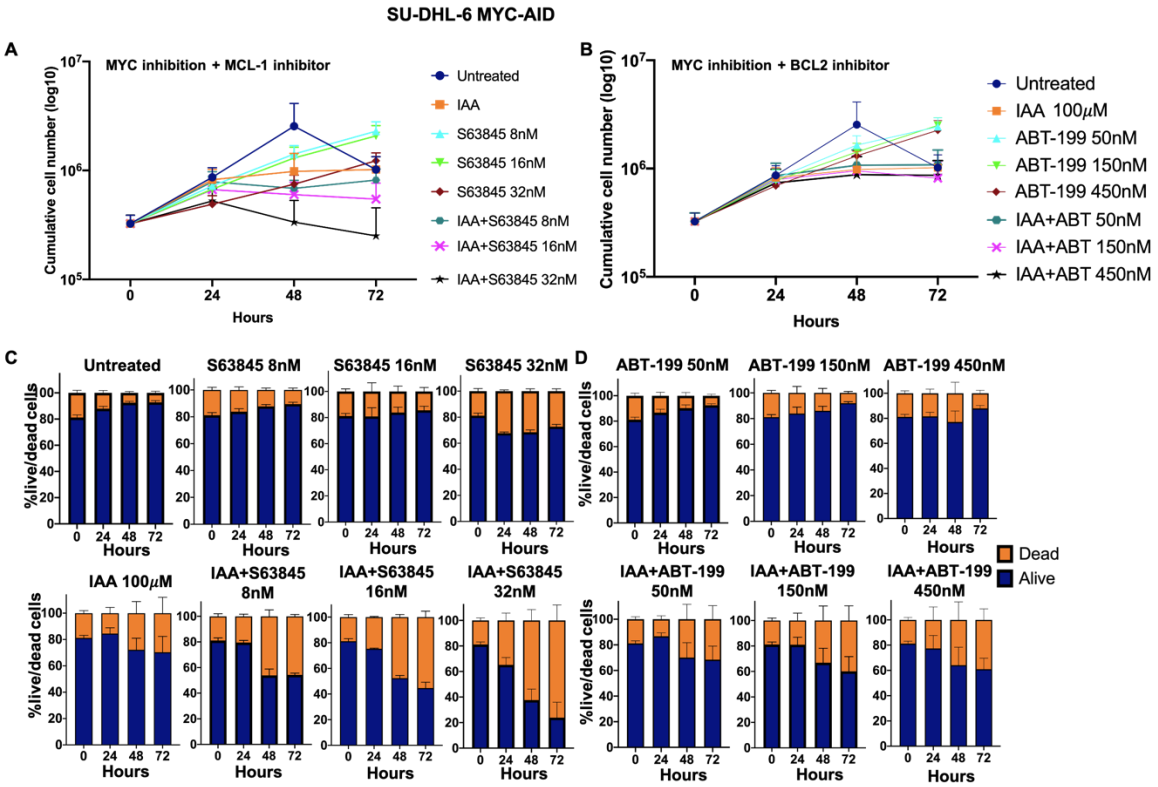

Figure 31: Effect of combinatorial MYC+BCL2 inhibition in DHL cells (SU-DHL-6).
(A, B) Cumulative live-cell numbers and **(C, D)** live/dead-cell percentages, based on PI staining and Flow cytometric Analysis for SU-DHL-6 MYC-AID after treatment with various concentrations of **(A, C)** the MCL-1 inhibitor S63845 (8, 16, 32 nM) or **(B, D)** the BCL2 inhibitor ABT-199 (Venetoclax, 50, 150, 450 nM) alone or together with IAA 100μM, at the indicated time-points (Hours). Dead cells were scored by Propidium Iodide (PI) staining and excluded from the cell counts. The data represent the means and SD (T test) from 3 biological replicates.

4. DISCUSSION

4.1 Targeting MYC in human lymphoma

The *MYC* proto-oncogene and its product, the MYC transcription factor, are a general driving force in cancer. In normal cells, MYC is induced by mitogenic stimuli and orchestrates pivotal gene expression programs that promote cell growth and proliferation[16,85,184,429]. Indeed, it is this central position in the cell's regulatory circuitry which endows MYC with high oncogenic potential, as its deregulated expression enforces the same cellular responses in an uncontrolled manner, most likely through aberrant activation of MYC target genes, including both physiological and tumor-specific targets[1,184,429].

MYC's important role in tumor initiation, progression and maintenance[29,182] would imply that it is a perfect candidate for therapeutic inhibition. Indeed, it is quite common for MYC overexpressing tumors to develop MYC addiction, a phenomenon confirmed by cessation of proliferation and tumor regression upon MYC's inactivation or inhibition[197-199,201,202,216,218]. However, direct therapeutical inhibition of MYC was quite challenging so far, with very few inhibitors reaching the clinical trials level[299-303]. This is mainly owing to MYC's structure lacking the binding pocket necessary for pharmacological interaction, as well as MYC's nuclear localization, which means that any potential inhibitory compound needs to be able to penetrate this compartment in order to disrupt it[299-303]. While the efforts towards MYC inhibition are continuing and various promising approaches are emerging[299,302,430,431], it becomes clear that gaining a better understanding of MYC's direct transcriptional programs, especially in MYC-addicted malignancies, could provide valuable input in the search of therapeutic vulnerabilities in MYC-driven cancer.

Despite substantial research efforts in the field, many gaps still persist in our understanding of MYC-dependent transcriptional changes, especially in a tumor context. Profiling MYC-dependent transcriptional changes in tumor cells is complicated by a number of confounding issues. First, MYC shows promiscuous DNA-binding profiles with a general inclination towards active regulatory elements (i. e. promoters or enhancers) and, when expressed at high levels, becomes detectable on virtually all of these regions - a phenomenon termed as "invasion"[85,232,233,237]. However, recent work in our laboratory showed that most of those interactions represent non-specific DNA-binding events, which do not lead to productive gene regulation[240]. In line with this finding, even when over-expressed, MYC regulates select sets of genes, and acute removal of MYC in tumor cells causes variations in only a few hundred mRNAs[85,130,234,235,237,375,409]. Moreover, many of the changes observed

in tumor cells (including general increase in transcriptional activity) occur as secondary consequences of MYC activity[1,241]. Hence, identification of primary MYC-dependent events will require a controlled, rapid inactivation of MYC, followed by short-term profiling of the consequent regulatory changes.

For all the aforementioned reasons, here we undertook the mapping of MYC-dependent events in three human, MYC-driven lymphoma cell lines, including two Burkitt (Ramos, Raji) and one Double-Hit Lymphoma line (SU-DHL-6). Toward this aim, we targeted the translocated *MYC* allele present in those cells with an in-frame cassette, encoding an Auxin-inducible degron (AID)[378], thus converting MYC into the conditionally degraded MYC-AID fusion protein, as previously described in AML cells[235]. We then proceeded to phenotypic characterization of these cell lines, before addressing our main question; elucidating the integrated immediate effects of MYC-AID degradation on chromatin, transcription and RNA maturation.

The AID system is a powerful tool that should allow careful kinetic studies upon protein degradation of various substrates, reaching full degradative potential within minutes[235,378,432], as opposed to other, more time-consuming approaches such as RNAi or genetic ablation. Indeed, here, it granted us all the prerequisites for the aims of this project. It allowed us conditional, efficient and above all, rapid degradation of MYC, enabling us to discriminate between direct and secondary effects on chromatin and transcription. This notwithstanding, as exhibited in **Fig. 11C, 13A, 19D** and **S2**, the degradation achieved in our cells is efficient, but it is not full; residual MYC-AID protein levels persist, consistent with the continuous rates of biosynthesis and degradation. In an effort to better optimize this, A. Verrecchia in our lab compared the MYC-AID degradation between the AID system and an evolved version, known as AID2, based on the expression of the mutant Tir1 variant (F47G) and its activation with lower concentrations of the Auxin analog 5-Ph-IAA[379]. AID2 has been recently reported to counteract some of the previous system's drawbacks, such as a small steady state leakiness or the requirement of relatively high doses of Auxin (IAA), allowing sharper and faster protein degradation[379,433]. However, the comparison between the two systems did not give us reason to believe that AID2 outdid AID in the context of this thesis, as MYC-AID degradation levels and kinetics were very similar for the two systems (data not shown). Most importantly, the IAA concentration used for AID, while admittedly much higher than that of 5-Ph-IAA with the AID2 system, did not show any signs of cell toxicity when used on the parental cell lines (**Fig. 13**). Nevertheless, one of the advantages of the AID2 system is that it can be inserted in mice, whereas this is not possible

for AID[379]. This is a feature that may be exploitable in the future, to extend the applications of conditional MYC-AID targeting to mouse tumor models.

4.2 Protracted proliferative capacity upon MYC depletion

Having achieved conditional MYC-AID degradation in three MYC-driven human lymphoma cell lines, Ramos, Raji and SU-DHL-6, we proceeded to characterize the phenotypic effects of MYC withdrawal. While in all three cell lines (with some differences in kinetics) we report cell cycle arrest, cessation of cell proliferation, decrease in cell mass and finally cell death by apoptosis (**Fig. 12** and **14**), as was expected given the well-established role of MYC in all these processes[1,37,429], there are several aspects to be considered here.

First of all, the effects of MYC depletion were not implemented as fast as we expected, with IAA-treated cells maintaining proliferative capacity for ~3 division rounds before finally stopping (**Fig. 14**), and cell death following later (especially in the case of Ramos) (**Fig. 12**). Our data comparing MYC-AID degradation with genetic ablation (**Fig. 19**) allowed us to conclude that, low residual MYC-AID levels were enough to sustain their proliferation for a few residual cycles. It is obvious, however, that the residual MYC-AID levels cannot properly sustain these cells; if it were so, the cells would be expected to adjust to the new, low MYC levels and survive indefinitely, which was not what we observed. While the basis of this phenomenon is currently unclear, it might hypothetically be related to the findings of an earlier study, which illustrated MYC's role as a division timer in T and B lymphocytes[434]. Their main finding, relative to our results, was that higher initial levels of MYC upon lymphocyte stimulation were translated into more divisions, with division halting after MYC levels dropped below a certain threshold. Ramos, Raji and SU-DHL-6, owing to their translocated *MYC* allele, have very high MYC levels[435], which based on the above premises, could be driving the few extra divisions before proliferative arrest. However, this theory loses credit if one looks closer to the initial MYC AID levels among the three cell lines (**Fig. 11C** and data not shown), Ramos seem to have slightly lower levels of MYC to begin with, even though it is the cell line that survives the most after MYC withdrawal (**Fig. 12**). This would lean towards supporting a scenario where Raji and SU-DHL-6 are reacting faster and more intensely to MYC degradation because they have higher levels of MYC, therefore being more "MYC-addicted" than Ramos. However, given that the data presented in Fig.11C were produced separately per each cell line, a direct comparison between the MYC levels of the 3 cell lines is not allowed.

Most importantly here, MYC's effects are known to vary according to tissue specificity and tumor context[242,431]. While all of our three cell lines are human MYC-driven B-cell lymphomas, so tissue specificity and tumor context should be largely overlapping, these are still different tumors, with i) possibly slightly different levels of MYC and ii) different additional mutations. On these premises, it will be interesting to inquire in our transcriptional datasets, what are the unique MYC-driven transcriptional programs in any of these cell lines, alongside their common signatures.

As demonstrated in **Fig. 19**, *MYC* genetic ablation yielded strikingly different results relative to MYC-AID degradation in Ramos cells. There was immediate cessation of cell division and cell death started much earlier upon *MYC* knockout, as opposed to the protracted proliferation seen in MYC-AID cells. Most importantly, we observe a clear difference in residual MYC protein levels upon MYC-AID degradation or induction of *MYC* knockout (**Fig. 19D**): it is this difference that led us to the conclusion that the extended survival and proliferative capacity of the MYC-AID cells upon MYC depletion is due to the persistence of the low, residual MYC-AID levels in the system. However, as already mentioned, for the purposes of this study, we are in need of a model that allows rapid and homogeneous down-regulation of MYC in whole cell populations, which was not the case with the knockout model (data not shown). Most noteworthy here, the residual MYC-AID levels represent a more faithful model of the partial inhibition that will most likely be achieve with any compound that may effectively inhibit MYC for therapeutic purposes.

All the above features define MYC-AID as a most adequate model for the pharmacological inhibition of MYC in lymphoma, with both (i.) immediate on-target degradation and (ii.) sustained residual activity of the driving oncoprotein (in this instance, MYC-AID). Concomitantly, based on its immediate and homogenous degradation across the whole cell population, MYC-AID also provides the best tool so far to address the direct consequences of MYC inhibition and unravel primary MYC-dependent events in cancer cells.

4.3 Effects of MYC downmodulation on cell cycle and size

MYC's role in cell cycle and growth are well-established[37,137,181]. In accordance with it, we report both cell size reduction and cell cycle arrest upon MYC depletion. Cell size reduction in combination with the protractive proliferative effect that we have noted, would suggest that a possible scenario for these cells' extended survival could be an increase in autophagy levels. If this was the case, increased autophagy could give the cells some extra spur to

survive under stress for a small period of time[436]. This scenario would also be in accordance with a purported negative effect of MYC on autophagy, in particular through the suppression of TFEB[160,162]. On these premises, we monitored the levels of the autophagic marker LC3[437] throughout our MYC-degradation time-courses (days 2-6/8) by immunoblotting (data not shown) but, at this level of resolution, did not obtain evidence for a significant impact of MYC-AID degradation on autophagy. Most likely, the loss of cell mass observed upon MYC-AID degradation may follow from MYC's role in ribosome biogenesis[82]. Indeed, apart from ribosome biogenesis being among the most enriched Biological Process gene sets upon 4 hours of both MYC up-modulation and down-modulation during our polysome profiling Gene Set Enrichment Analysis (**Fig. S12E, S13E** bottom), we also noted a decrease in the total levels of ribosomal protein S6 by immunoblotting in all the three cell lines, already from day2 of MYC down-modulation (data not shown). This suggests that indeed, there is a decrease in ribosomes that may underlie the loss of cell mass.

As far as cell cycle is concerned, there were a number of puzzling effects in our results. Firstly, it was quite unexpected that Ramos should be actively cycling up to 4 days after MYC depletion (**Fig. 15, 16 ,18**). Given MYC's pervasive impact on cell cycle control[137], we were expecting the arrest to happen earlier, as was the case for the other two cell lines. Nevertheless, as soon as cell cycle arrest started in Ramos, the percentages of S-phase cells were gradually decreasing, with cells never seemingly recovering their ability to re-enter cell cycle (**Fig. 15,16**). A different, somewhat paradoxical effect was observed in the two other cell lines, with a transient restoration of S-phase cells after four days without MYC: while partial on Raji, this effect was quantitative in SU-DHL-6 cells, and fully replicable (**Fig. 15, 16, 18**). Most noteworthy, this restoration of S phase cells was accompanied in both cell lines (most prominently in SU-DHL-6) with concomitant decrease in the percentages of non-EdU incorporating intermediate DNA-content cells (namely "faulty S" cells) (**Fig. 15, 16**). While these results imply that SU-DHL-6 and Raji could have the ability to transiently exit the cell cycle in order to fix possible DNA damage, before re-entering it at day 4, it becomes clear that they cannot sustain that capacity, giving in to cell cycle arrest soon after (**Fig. 15, 16, 18**). In an effort to determine a connection between this phenomenon and DNA damage, we have profiled cell cycle changes together with the genotoxic stress marker γ-H2AX, but our results on the latter remain preliminary and prone to substantial experimental variation (**Fig. 17**), rendering a definitive interpretation and integration with cell cycle effects hindered; the role of possible MYC-induced DNA damage remains to be

further investigated. Lastly, no matter the cause for this transient restoration of S-phase cells, it became clear that Ramos cells cannot replicate this effect at all (**Fig. 15, 16, 18**). These variations in cell cycle kinetics, bring once more to the front the need to decipher carefully the MYC-dependent programs in each separate cell line; this should provide some insight as to e. g. which unique cell cycle-related programs enable SU-DHL-6 cells to transiently recover their cell cycle activities.

4.4 MYC-dependent transcriptional programs in human MYC-driven lymphomas

The main aim of this thesis pertained to the dynamic profiling of MYC-dependent transcription and the dissection of associated mechanisms following acute down-regulation of MYC in B-cell lymphomas. This aim was based on the hypothesis that the action of MYC at its target promoters results in a multi-layered modulation of chromatin-based regulatory processes: deciphering and integrating these mechanisms with the transcriptional output should not only shed light into the determinants of MYC-regulated transcription, but should also point to new therapeutic vulnerabilities in MYC-driven cancers.

Having phenotypically characterized our MYC-AID lymphoma cell lines, we used them to generate profiles of total and nascent (4SU-labeled) RNA-seq profiles along a time-course of 1, 2, 4 and 8 hours upon MYC degradation. Analysis following the calling for differentially expressed genes (DEGs) at each IAA time-point relative to untreated cells (0h), confirmed previous observations in our lab and others[85,234,235,237]: MYC functions as a specific transcriptional regulator, as it affected the expression of only few hundreds of loci within the first 1 hour of MYC shutdown **(Fig. 20A, S8A)**. A majority of the affected loci were downregulated (DEG-DOWN) after MYC depletion, in accordance with the concept that MYC's primary function is that of a transcriptional activator[85,234,235]. Most noteworthy here, while a sizeable number of genes showed increased RNA synthesis by 4SU-seq at 1h (DEG-UP), these were less consistent among cell lines (see below).

In order to better our understanding on the temporal dynamics governing the transcriptional changes we observed, we compared the overlaps between all the DEG-DOWN genes that we called in each time-point separately. An important feature that came to our attention by doing that, was that there were substantially-sized groups of genes that became downregulated already from 1h hour of MYC shutdown, staying consistently downregulated throughout the rest of the time-course. (**Fig. 20B, S8B**) We therefore termed these gene groups as "Immediate" MYC-dependent genes. Similarly, sizeable gene

groups showed coherent suppression from 2h, 4h or 8h of MYC shutdown, which we refer to as “Fast”, “Delayed” and “Late” respectively (**Fig. 20B, S8B**). Following the same reasoning, we defined these groups also for DEG-UP.

Further insight was provided by analyzing the overlaps between the aforementioned DEG-DOWN and DEG-UP groups over time in the three lymphoma cell lines (**Fig. 20C or 21A, B)**. In 4SU-seq data in particular the only transcriptional groups that showed significant overlap were the Immediate DEG-DOWN (down-regulated from 1 hour), with 187 genes common to all cell lines, while the subsequent DEG-DOWN groups, as well as all DEG-UP groups, were largely unique to each cell line (**Fig. 20C or 21A, B)**. We surmise that the main, direct MYC-dependent transcriptional changes common to all cell lines had all occurred within 1 hour, and resulted in the down-regulation of a common core of MYC-dependent genes. We surmise that despite MYC’s varying effects from cell line to cell line, this common transcriptional core may be the primary driver of MYC-dependent responses. This notion is substantiated further in **Fig. 24B**, showing that our common Immediate MYC-dependent genes are overlapping at a ratio of ~1/3 with MYC-dependent signatures previously published in Acute Myeloid Leukemia cell lines[235] or from the integrated study of 5 different MYC-driven mouse tumor models[242].

Unlike 4SU-seq, total RNA-seq data showed increasing numbers of deregulated genes over time, both up and down, with consistent overlaps across all cell lines (**Fig. 21C, D?)**. Hence, the immediate impact of MYC degradation on core MYC-dependent genes may trigger a series of conserved secondary effects, which most likely account for the subsequent changes in mRNA populations. These data highlight the relevance of kinetic analyses in interpreting gene expression profiles.

Preliminary Gene Ontology (GO) analysis provided further indication for the rapid down-regulation of MYC-dependent gene programs upon IAA treatment, with *MYC TARGETS V1* and *V2* as the top enriched Hallmarks in the Immediate DEG-down group called by 4SU-seq in our three cell lines. Most noteworthy, these two gene sets seemed to lose enrichment in the subsequent 4SU-defined groups of Fast, Delayed and Late, which means that the genes associated with the *MYC TARGETS V1* and *V2* sets became downregulated already from 1 hour and consistently stayed down for the rest of the time-points (**Fig. 23A**).

While this GO analysis is still preliminary, some recurrent Hallmark categories have surfaced among our 4 DEG-DOWN introduced categories (Immediate, Early, Delayed and Late) (**Fig. 23**), among which mTORC1 signaling and E2F targets. MYC has been known to induce transcription of several E2F family members, such as E2F1, E2F2 and E2F3[66,438-440].

Therefore, it stands to logic that downmodulation of MYC could lead to downmodulation of these E2F transcription factors and subsequently of their targets. In line with this speculation, E2F targets in DEG-DOWN Hallmark GO analysis start emerging more consistently in the 4SU Late gene group (**Fig. 23A**, bottom left) and from the Delayed onwards in the Total; this indicates that it could be a secondary effect. However, speculating about mTORC1 is slightly more complicated. The mTOR Complex 1 (mTORC1) is located upstream of MYC in the cellular circuitry and it is known to positively regulate *MYC*'s mRNA translation[55,441]. At this level of resolution, we cannot say for certain why it is enriched in our gene sets, however, a plausible reasoning could be that since the mTORC1 Hallmark gene set comprises by genes downstream of mTORC1, it is highly possible that it involves also several MYC targets.

Nevertheless, it is worth mentioning that both E2F targets and mTORC1 were enriched also in the GO analysis for the 4SU and Total DEG-UPs (**Fig. S9**). The biological meaning of this remains to be fully addressed with further analysis. As a matter of fact, it is in our immediate plans to implement our datasets with Ingenuity Pathway Analysis for Upstream Regulator, as previously done in the lab[360], in order to better dissect the pathways affected by MYC depletion and define towards which direction they were affected.

4.5 MYC and RNA-Polymerase II interplay

In parallel with RNA profiling, we used Chromatin Immunoprecipitation sequencing (ChIP-seq) to profile MYC and total RNA-PolII in Ramos cells after 1 hour of MYC-AID inactivation, allowing us to determine the extent of MYC binding to genomic regulatory elements and address its mechanistic impact on transcriptional activity. In this setting, we analysed three groups of genes (DEG DOWN, DEG UP, no DEG) as determined by Ramos 4SU-seq 1 hour, on which we addressed the distribution of MYC, total RNA-PolII and active chromatin histone marks (H3K27ac, H3K4me1, H3K4me3).

As previously known from the literature, MYC is strictly associated with active chromatin regions; CpG islands, regions bearing active histone modifications (H3K4me3, H3K4me1 and H3K27ac), as well as the basal transcriptional machinery (RNA Pol II)[239]. Our results recapitulated that, with MYC found on (i.) active promoters, as assessed by the presence of RNA Polymerase II (RNAPII), H3K4me3 and H3K27ac) (**Fig. 25A**) and (ii.) active enhancers, as assessed by distal binding in loci exhibiting RNAPII, H3K4me1 and H3K27ac (**Fig. 25B**). While "invasion" of active regulatory chromatin by MYC was previously documented[1,85,232,233,237], it needs to be outlined that the majority of these MYC/chromatin

interactions do not represent actual E-box sequence recognition by MYC and therefore do not lead to productive transcription[240]; a notion supported also by the only few hundreds of DEGs we reported from 4SU-nascent RNA-seq after 1hour of MYC shutdown (**Fig. 20A**, left).

As expected upon IAA treatment, the majority of MYC was lost from chromatin, at both MYC-regulated (DEG-DOWN or UP) and non-regulated genes (NO-DEGs) (**Fig. 26A**). At DEG-DOWN loci, this loss of MYC was accompanied by a concerted and proportionate loss of Pol II in the TSS, Gene body and TES, which was also reflected in the lack of major variations in stalling index (**Fig. 26B**, left). While we observed a slight loss of Pol II also from the NO-DEG promoters (**Fig. 26E** left, **Fig. 27A**) this remains to be analysed in better detail, as it might possibly be due to cross-contamination between the DEG-DOWN and NO-DEG groups used in our analysis, given the lax criteria (without a log2FC threshold) used to define these groups. Hence, we will redefine these gene groups and proceed with further analysis to determine whether or not the loss of Pol II from a fraction of NO-DEG promoters is a real effect.

An important feature to be mentioned here is that while the MYC-dependent DEG-DOWN genes showed proportionate loss of Pol II from promoter, gene body and TES (**Fig. 26B**), we did not see the equivalent changes at MYC-repressed genes (DEG-UP in our context) (**Fig. S11B**). More specifically, while there was a gain of Pol II in the gene body and TES regions, we did not note any significant gain in Pol II binding in promoters. This was unexpected and suggests that MYC might be favoring pause-release, rather than loading in those loci: the mechanisms of this effect remain to be disentangled. While MYC has indeed been implicated in RNA Pol II loading[285], this affect was deemed to be relevant for MYC-activated genes. Moreover, prior observations[234], along with our own results on the Pol II stalling index in the DEG-DOWNs (**Fig. 26B**) suggest that MYC's primary role regarding Pol II should be loading and not pause-release. Hence, whether MYC acts to suppress pause-release at repressed loci, and does so directly or indirectly, remains to be clarified.

4.6 MYC-induced histone modifications

The first step for MYC's regulatory activity is the chromatin recognition and binding. However, as mentioned above, it requires an open and poised chromatin context in order to bind to the promoters. While it can bind at pre-existing open chromatin, it was also shown to be required for histone hyperacetylation and transcriptional activation of its specific target loci[273]. Along the same lines, an important correlation between MYC and

histone modifications at MYC-target gene promoters has been reported[239,253]; there is a simple combinatorial organization of histone marks, with specific groups of histone marks gathering on specific promoters. For example chromatin bearing high H3 K4/K79 methylation and H3 acetylation[239], which marks "euchromatic islands" is largely associated with pre-engaged basal transcription machinery[274] and is indispensable for recognition of any target site by MYC[275]. Following this, previous work from our lab showed that MYC induces acetylation on several lysine residues of H3 and H4; most of these acetylation events where enriched specifically on MYC's target promoters[253], consistent with the idea that MYC is recruiting and cooperating with HATs or HAT-associated proteins, such as TRAPP, GCN5, Tip60, HBO1 or CBP/p300[74,75,253-256]. As a matter of fact, in this study, H3k27ac was not one of the MYC-induced acetylations, with its levels being almost the same between MYC-target and non-target promoters; this indicates that this particular modification is not a direct effect of MYC, thus explaining its loss not only from MYC-dependent genes (DEG-DOWN), but also from non-regulated promoters (**Fig. 27D**). Moreover, MYC has no known effect on H3K4 methylation, which precedes MYC binding on chromatin[239]; this is also in accordance with our own results, for both H3K4me1 and H3K4me3 (**Fig. 27C, E**). Finally, previous work from our lab has shown that MYC induction increases the histone variant H2A.Z incorporation on target sites, while no such effect was recorded for non-target promoters[253].

Based on the above premises, and since the aforementioned studies of our lab were based on ChIP-qPCR, but were not extended genome-wide[239,253], we have initiated a series of ChIP-seq profiles for various histone modifications and variants, in order to define MYC-induced changes in the chromatin regulatory landscape, in Ramos MYC-AID cells following 1 hour of IAA treatment. The targets we have chosen are H3K27ac, H3K4me1, H3K4me3 (**Fig. 27**), followed by H4K5ac, H4K12ac, H3K14ac, H3K18ac, H3K36me3, H3K79me2, H2A and H2A.Z. The analysis of these datasets is ongoing.

4.7 Beyond transcription? Translational profiling of MYC-regulated mRNAs.

In this study, we also took advantage of our Ramos MYC-AID cell line in order to inquire whether or not MYC could impact the translation efficiency of its target loci. To this end, undertook Polysome profiling and subsequent sequencing of Polysome associated RNA and Total RNA, following 4 hours of IAA treatment. The time-point of 4 hours was selected based on the premises that it should be late enough to enable visualization of MYC-dependent changes in translation, but at the same time early enough to maximize direct

cis-acting effects, as opposed to secondary alterations in translational activity. What we observed was that whatever transcriptional changes were elicited by MYC-degradation were rapidly and proportionally reflected on polysomes (**Fig. 28B**). In a complementary approach, we used the same procedure following conditional super-activation of MYC in 3T9 MycER fibroblasts, with an identical outcome (**Fig. 28E**). Altogether, these data provide little evidence for any differential impact of MYC on the translation of its target mRNAs.

The above notwithstanding, several studies reported the identification of genes with differential translational efficiency upon MYC modulation. Comparison between Ribo-seq and total RNA-seq profiles in U2OS cells upon 36 hours of MYC activation revealed a large correlation between transcription and translation, as reported here, but also led to the identification few MYC target genes, both repressed and activated, that exhibited differential translational efficiency, on top of changes in mRNA levels[442]. Along the same lines, MYC overexpression together with KRAS activation in a murine model of Hepatocellular Carcinoma (HCC) led to very few statistically significant differences in mRNA levels, as compared to KRAs alone, while impacting translational efficiency (both up and down) at a distinct subset of transcripts[443]. Reciprocally, following 24 hours of MYC downmodulation in the human B-cell line P493-6, a majority of transcripts showed changes in translation in accordance with their changes in mRNA abundance, but a subset of transcripts was identified for which translation was disproportionally affected by MYC[377].

While the aforementioned studies were consistent with a potential effect of MYC on the translation of its target loci, they did not allow to discriminate between cis-acting mechanisms deriving from the action of MYC on promoters, and trans-acting effects such as the modulation of translation-regulatory factors. Indeed, the relatively late time-points used in all of these studies would have left ample margin for secondary changes. In our Polysome Profiling experiment (**Fig. S12E, S13E**), GSEA analysis showed enrichment for various processes impacting on the general translational machinery (ribosome biogenesis, ribosomal subunits biogenesis, RRNA metabolic processing, tRNA processing, etc.), suggesting that longer time-points might indeed have led to a prevalence of indirect effects.

4.8 Combinatorial effects between MYC inhibition and BH3-mimetics

Given the dual role of MYC in proliferation[37] versus apoptosis[144], as well as the documented synergy between MYC synthetic-lethal interactors and BCL2-family inhibitors[347,360], we decided to take advantage of our MYC-AID cell lines in order to inquire

whether MYC inhibition might provide similar synergistic effects with BH3-mimetics. For the two Burkitt lines, we tried only MCL-1 inhibition, since they are overexpressing MCL-1, but not BCL-2, which makes them resistant to BCL-2 inhibition[347,426-428]. For SU-DHL-6, we tried both. Surprisingly, our data showed that this combinatorial strategy yielded different results for each cell line (**Fig. 29, 30, 31**). In Ramos, inhibition of MCL-1 with S63845 alone induced a dose-dependent suppression of proliferation, with concomitant effects on cell death. Upon combination with MYC inhibition, cells were partially rescued from the killing effects of S63845 (**Fig. 29**). Thus, in this cell line, MYC seems to be contributing to the cell death caused by MCL-1 inhibition, in accordance with MCL-1's role in suppressing MYC-induced apoptosis. In Raji cells, instead, combining S63845 with IAA did not bring upon any significant differences in proliferation or cell death, with the combined effect resembling that of S63845 alone. This was especially true for the higher S63845 concentrations used, while there was a slight additive effect between IAA and the lower S63845 concentrations at late time-points (**Fig. 30**). Finally, in SU-DHL-6 cells, combinatorial treatment of IAA together with either S63845 or Venetoclax caused synergistic killing (**Fig. 31**), with the most pronounced effect being in combination with S63845.

While still preliminary, the above data indicate that MYC's dual role in the balance of proliferation versus apoptosis can lead to different results, even among cell lines of the same tumor type. Since the outcome of combining MYC inhibition with BH3-mimetic compounds seems to be highly context-dependent, further investigation will be needed in to gain a better understanding of the mechanisms underlying the effects in each cell line: this should hopefully allow to derive general principles, which in turn may point to new therapeutic opportunities in these MYC-driven malignancies.

4.9 Future perspectives

As already mentioned in this Discussion, our immediate plans include a careful analysis and re-definition of our MYC-regulated gene groups, especially for ChIP-seq analysis, implementation of Upstream regulator analysis, ChIP-seq on histone modifications and variants. Besides those, we are also thinking ahead towards two major directions:

First, as previously mentioned, therapeutically targeting MYC has been quite challenging. This notwithstanding, the field is advancing fast and a number of candidate inhibitors have been described[444]. One of the main problems with most of the purported MYC-inhibitory agents is that their mode of action remains generally unclear, with substantial potential for the predominance of off-target effects. Until now, the field was lacking adequate

biomarkers for the selective inhibition of MYC, precluding rigorous validation and characterization of candidate MYC-inhibitory molecules. In this regard, an important leap forward may be provided by our MYC-AID lymphoma cell lines, as these represent a unique model for rapid, specific and selective MYC inhibition by pharmacological means (IAA). In particular, we are planning to use our MYC-dependent chromatin and transcriptional profiles as a direct benchmark against which to confront the effects of candidate MYC-inhibitory compounds. This benchmarking strategy should first be tested as a proof-of-principle. Toward this aim, we will use what is as yet the best characterized MYC-inhibitory agent, namely the cell-permeable peptide Omomyc[335,339].

Second, since MYC is a difficult target for direct inhibition, a good alternative strategy is investigating MYC interactors or co-factors that might prove to be therapeutic vulnerabilities in MYC addicted tumors. Towards this aim, we are planning to set up a series of ChIP-seq, in order to characterize MYC interactors and co-factors. Part of the candidates will be decided among a list of novel MYC interactors previously identified in the lab by Chromatin Proteomics (ChroP) in the tet-MYC B-cell line P493-6. This analysis will also be extended to some of the known MYC cofactors, like WDR5[351], the Tip60/NuA4 complex and other histone acetyl-transferases[253,256,273], TFIIH[417], P-TEFb[282], or topoisomerases[445], in order to address their roles in MYC-dependent gene regulation.

To conclude, we have undertaken the profiling of MYC-dependent transcriptional changes and associated changes in chromatin dynamics in a MYC-driven tumor context. We have identified a common core of Immediate MYC-target genes across three different human lymphoma cell lines and gathered preliminary results on MYC/Pol II/chromatin crosstalk. While several parts of this work are still ongoing, the combination of our nascent and Total RNA-seq, together with our ChIP-seq profiles upon MYC-degradation shall provide a dynamic, integrated view of MYC-regulated transcription and of the mechanisms underlying oncogene addiction in MYC-driven Lymphoma.

5. REFERENCES

1 Kress, T. R., Sabo, A. & Amati, B. MYC: connecting selective transcriptional control to global RNA production. *Nat Rev Cancer* **15**, 593-607 (2015). https://doi.org/10.1038/nrc3984

2 Sheiness, D. & Bishop, J. M. DNA and RNA from uninfected vertebrate cells contain nucleotide sequences related to the putative transforming gene of avian myelocytomatosis virus. *J Virol* **31**, 514-521 (1979). https://doi.org/10.1128/JVI.31.2.514-521.1979

3 Hayward, W. S., Neel, B. G. & Astrin, S. M. Activation of a cellular onc gene by promoter insertion in ALV-induced lymphoid leukosis. *Nature* **290**, 475-480 (1981). https://doi.org/10.1038/290475a0

4 Vennstrom, B., Sheiness, D., Zabielski, J. & Bishop, J. M. Isolation and characterization of c-myc, a cellular homolog of the oncogene (v-myc) of avian myelocytomatosis virus strain 29. *J Virol* **42**, 773-779 (1982). https://doi.org/10.1128/JVI.42.3.773-779.1982

5 Roussel, M. *et al.* Three new types of viral oncogene of cellular origin specific for haematopoietic cell transformation. *Nature* **281**, 452-455 (1979). https://doi.org/10.1038/281452a0

6 Dalla-Favera, R. *et al.* Human c-myc onc gene is located on the region of chromosome 8 that is translocated in Burkitt lymphoma cells. *Proc Natl Acad Sci U S A* **79**, 7824-7827 (1982). https://doi.org/10.1073/pnas.79.24.7824

7 Dalla-Favera, R., Martinotti, S., Gallo, R. C., Erikson, J. & Croce, C. M. Translocation and rearrangements of the c-myc oncogene locus in human undifferentiated B-cell lymphomas. *Science* **219**, 963-967 (1983). https://doi.org/10.1126/science.6401867

8 Mitchell, K. F. *et al.* The effect of translocations on the cellular myc gene in Burkitt lymphomas. *J Cell Physiol Suppl* **3**, 171-177 (1984). https://doi.org/10.1002/jcp.1041210420

9 Adams, J. M. *et al.* The c-myc oncogene driven by immunoglobulin enhancers induces lymphoid malignancy in transgenic mice. *Nature* **318**, 533-538 (1985). https://doi.org/10.1038/318533a0

10 Zimmerman, K. A. *et al.* Differential expression of myc family genes during murine development. *Nature* **319**, 780-783 (1986). https://doi.org/10.1038/319780a0

11 Charron, J. *et al.* Embryonic lethality in mice homozygous for a targeted disruption of the N-myc gene. *Genes Dev* **6**, 2248-2257 (1992). https://doi.org/10.1101/gad.6.12a.2248

12 Davis, A. C., Wims, M., Spotts, G. D., Hann, S. R. & Bradley, A. A null c-myc mutation causes lethality before 10.5 days of gestation in homozygotes and reduced fertility in heterozygous female mice. *Genes Dev* **7**, 671-682 (1993). https://doi.org/10.1101/gad.7.4.671

13 de Alboran, I. M. *et al.* Analysis of C-MYC function in normal cells via conditional gene-targeted mutation. *Immunity* **14**, 45-55 (2001). https://doi.org/10.1016/s1074-7613(01)00088-7

14 Trumpp, A. *et al.* c-Myc regulates mammalian body size by controlling cell number but not cell size. *Nature* **414**, 768-773 (2001). https://doi.org/10.1038/414768a

15 Hatton, K. S. *et al.* Expression and activity of L-Myc in normal mouse development. *Mol Cell Biol* **16**, 1794-1804 (1996). https://doi.org/10.1128/MCB.16.4.1794

16 Tansey, W. P. Mammalian MYC Proteins and Cancer. *New Journal of Science* **2014**, 757534 (2014). https://doi.org/10.1155/2014/757534

17 Stone, J. *et al.* Definition of regions in human c-myc that are involved in transformation and nuclear localization. *Mol Cell Biol* **7**, 1697-1709 (1987). https://doi.org/10.1128/mcb.7.5.1697-1709.1987

18 Murre, C., McCaw, P. S. & Baltimore, D. A new DNA binding and dimerization motif in immunoglobulin enhancer binding, daughterless, MyoD, and myc proteins. *Cell* **56**, 777-783 (1989). https://doi.org/10.1016/0092-8674(89)90682-x

19 Conacci-Sorrell, M., McFerrin, L. & Eisenman, R. N. An overview of MYC and its interactome. *Cold Spring Harb Perspect Med* **4**, a014357 (2014). https://doi.org/10.1101/cshperspect.a014357

20 Beaulieu, M. E., Castillo, F. & Soucek, L. Structural and Biophysical Insights into the Function of the Intrinsically Disordered Myc Oncoprotein. *Cells* **9** (2020). https://doi.org/10.3390/cells9041038

21 Lambert, S. A. *et al.* The Human Transcription Factors. *Cell* **175**, 598-599 (2018). https://doi.org/10.1016/j.cell.2018.09.045

22 Blackwood, E. M. & Eisenman, R. N. Max: a helix-loop-helix zipper protein that forms a sequence-specific DNA-binding complex with Myc. *Science* **251**, 1211-1217 (1991). https://doi.org/10.1126/science.2006410

23 Luscher, B. & Larsson, L. G. The basic region/helix-loop-helix/leucine zipper domain of Myc proto-oncoproteins: function and regulation. *Oncogene* **18**, 2955-2966 (1999). https://doi.org/10.1038/sj.onc.1202750

24 Nair, S. K. & Burley, S. K. X-ray structures of Myc-Max and Mad-Max recognizing DNA. Molecular bases of regulation by proto-oncogenic transcription factors. *Cell* **112**, 193-205 (2003). https://doi.org/10.1016/s0092-8674(02)01284-9

25 Sabò, A. & Amati, B. Genome recognition by MYC. *Cold Spring Harb Perspect Med* **4** (2014). https://doi.org/10.1101/cshperspect.a014191

26 Amati, B. *et al.* Transcriptional activation by the human c-Myc oncoprotein in yeast requires interaction with Max. *Nature* **359**, 423-426 (1992). https://doi.org/10.1038/359423a0

27 Amati, B., Littlewood, T. D., Evan, G. I. & Land, H. The c-Myc protein induces cell cycle progression and apoptosis through dimerization with Max. *EMBO J* **12**, 5083-5087 (1993). https://doi.org/10.1002/j.1460-2075.1993.tb06202.x

28 Diolaiti, D., McFerrin, L., Carroll, P. A. & Eisenman, R. N. Functional interactions among members of the MAX and MLX transcriptional network during oncogenesis. *Biochim Biophys Acta* **1849**, 484-500 (2015). https://doi.org/10.1016/j.bbagrm.2014.05.016

29 Carroll, P. A., Freie, B. W., Mathsyaraja, H. & Eisenman, R. N. The MYC transcription factor network: balancing metabolism, proliferation and oncogenesis. *Front Med* **12**, 412-425 (2018). https://doi.org/10.1007/s11684-018-0650-z

30 Nguyen, H. V. *et al.* Development and survival of MYC-driven lymphomas require the MYC antagonist MNT to curb MYC-induced apoptosis. *Blood* **135**, 1019-1031 (2020). https://doi.org/10.1182/blood.2019003014

31 Staller, P. *et al.* Repression of p15INK4b expression by Myc through association with Miz-1. *Nat Cell Biol* **3**, 392-399 (2001). https://doi.org/10.1038/35070076

32 Wiese, K. E. *et al.* The role of MIZ-1 in MYC-dependent tumorigenesis. *Cold Spring Harb Perspect Med* **3**, a014290 (2013). https://doi.org/10.1101/cshperspect.a014290

33 Kato, G. J., Barrett, J., Villa-Garcia, M. & Dang, C. V. An amino-terminal c-myc domain required for neoplastic transformation activates transcription. *Mol Cell Biol* **10**, 5914-5920 (1990). https://doi.org/10.1128/mcb.10.11.5914-5920.1990

34 Kelly, K., Cochran, B. H., Stiles, C. D. & Leder, P. Cell-specific regulation of the c-myc gene by lymphocyte mitogens and platelet-derived growth factor. *Cell* **35**, 603-610 (1983). https://doi.org/10.1016/0092-8674(83)90092-2

35 Dean, M. *et al.* Regulation of c-myc transcription and mRNA abundance by serum growth factors and cell contact. *J Biol Chem* **261**, 9161-9166 (1986).

36 Reed, J. C., Alpers, J. D., Nowell, P. C. & Hoover, R. G. Sequential expression of protooncogenes during lectin-stimulated mitogenesis of normal human lymphocytes.

Proc Natl Acad Sci U S A **83**, 3982-3986 (1986). https://doi.org/10.1073/pnas.83.11.3982
37 Dang, C. V. c-Myc target genes involved in cell growth, apoptosis, and metabolism. *Mol Cell Biol* **19**, 1-11 (1999). https://doi.org/10.1128/MCB.19.1.1
38 Sicklick, J. K. *et al.* Dysregulation of the Hedgehog pathway in human hepatocarcinogenesis. *Carcinogenesis* **27**, 748-757 (2006). https://doi.org/10.1093/carcin/bgi292
39 He, T. C. *et al.* Identification of c-MYC as a target of the APC pathway. *Science* **281**, 1509-1512 (1998). https://doi.org/10.1126/science.281.5382.1509
40 Palomero, T. *et al.* NOTCH1 directly regulates c-MYC and activates a feed-forward-loop transcriptional network promoting leukemic cell growth. *Proc Natl Acad Sci U S A* **103**, 18261-18266 (2006). https://doi.org/10.1073/pnas.0606108103
41 Kiuchi, N. *et al.* STAT3 is required for the gp130-mediated full activation of the c-myc gene. *J Exp Med* **189**, 63-73 (1999). https://doi.org/10.1084/jem.189.1.63
42 Lin, C. *et al.* Dynamic transcriptional events in embryonic stem cells mediated by the super elongation complex (SEC). *Genes Dev* **25**, 1486-1498 (2011). https://doi.org/10.1101/gad.2059211
43 Erb, M. A. *et al.* Transcription control by the ENL YEATS domain in acute leukaemia. *Nature* **543**, 270-274 (2017). https://doi.org/10.1038/nature21688
44 Luo, Z. *et al.* The super elongation complex family of RNA polymerase II elongation factors: gene target specificity and transcriptional output. *Mol Cell Biol* **32**, 2608-2617 (2012). https://doi.org/10.1128/MCB.00182-12
45 Wan, L. *et al.* ENL links histone acetylation to oncogenic gene expression in acute myeloid leukaemia. *Nature* **543**, 265-269 (2017). https://doi.org/10.1038/nature21687
46 Frederick, J. P., Liberati, N. T., Waddell, D. S., Shi, Y. & Wang, X. F. Transforming growth factor beta-mediated transcriptional repression of c-myc is dependent on direct binding of Smad3 to a novel repressive Smad binding element. *Mol Cell Biol* **24**, 2546-2559 (2004). https://doi.org/10.1128/MCB.24.6.2546-2559.2004
47 Sachdeva, M. *et al.* p53 represses c-Myc through induction of the tumor suppressor miR-145. *Proc Natl Acad Sci U S A* **106**, 3207-3212 (2009). https://doi.org/10.1073/pnas.0808042106
48 Penn, L. J., Brooks, M. W., Laufer, E. M. & Land, H. Negative autoregulation of c-myc transcription. *EMBO J* **9**, 1113-1121 (1990). https://doi.org/10.1002/j.1460-2075.1990.tb08217.x
49 Dani, C. *et al.* Extreme instability of myc mRNA in normal and transformed human cells. *Proc Natl Acad Sci U S A* **81**, 7046-7050 (1984). https://doi.org/10.1073/pnas.81.22.7046
50 Liao, B., Hu, Y. & Brewer, G. Competitive binding of AUF1 and TIAR to MYC mRNA controls its translation. *Nat Struct Mol Biol* **14**, 511-518 (2007). https://doi.org/10.1038/nsmb1249
51 Keene, J. D. RNA regulons: coordination of post-transcriptional events. *Nat Rev Genet* **8**, 533-543 (2007). https://doi.org/10.1038/nrg2111
52 Weidensdorfer, D. *et al.* Control of c-myc mRNA stability by IGF2BP1-associated cytoplasmic RNPs. *RNA* **15**, 104-115 (2009). https://doi.org/10.1261/rna.1175909
53 Zhang, K. *et al.* AGO2 Mediates MYC mRNA Stability in Hepatocellular Carcinoma. *Mol Cancer Res* **18**, 612-622 (2020). https://doi.org/10.1158/1541-7786.MCR-19-0805
54 Culjkovic, B., Topisirovic, I., Skrabanek, L., Ruiz-Gutierrez, M. & Borden, K. L. eIF4E is a central node of an RNA regulon that governs cellular proliferation. *J Cell Biol* **175**, 415-426 (2006). https://doi.org/10.1083/jcb.200607020
55 Csibi, A. *et al.* The mTORC1/S6K1 pathway regulates glutamine metabolism through the eIF4B-dependent control of c-Myc translation. *Curr Biol* **24**, 2274-2280 (2014). https://doi.org/10.1016/j.cub.2014.08.007
56 Evans, J. R. *et al.* Members of the poly (rC) binding protein family stimulate the activity of the c-myc internal ribosome entry segment in vitro and in vivo. *Oncogene* **22**, 8012-8020 (2003). https://doi.org/10.1038/sj.onc.1206645
57 Notari, M. *et al.* A MAPK/HNRPK pathway controls BCR/ABL oncogenic potential by regulating MYC mRNA translation. *Blood* **107**, 2507-2516 (2006). https://doi.org/10.1182/blood-2005-09-3732
58 Kress, T. R. *et al.* The MK5/PRAK kinase and Myc form a negative feedback loop that is disrupted during colorectal tumorigenesis. *Mol Cell* **41**, 445-457 (2011). https://doi.org/10.1016/j.molcel.2011.01.023
59 Hann, S. R. & Eisenman, R. N. Proteins encoded by the human c-myc oncogene: differential expression in neoplastic cells. *Mol Cell Biol* **4**, 2486-2497 (1984). https://doi.org/10.1128/mcb.4.11.2486-2497.1984
60 Farrell, A. S. & Sears, R. C. MYC degradation. *Cold Spring Harb Perspect Med* **4** (2014). https://doi.org/10.1101/cshperspect.a014365
61 Welcker, M. *et al.* The Fbw7 tumor suppressor regulates glycogen synthase kinase 3 phosphorylation-dependent c-Myc protein degradation. *Proc Natl Acad Sci U S A* **101**, 9085-9090 (2004). https://doi.org/10.1073/pnas.0402770101
62 Sears, R. C. The life cycle of C-myc: from synthesis to degradation. *Cell Cycle* **3**, 1133-1137 (2004).
63 Bachireddy, P., Bendapudi, P. K. & Felsher, D. W. Getting at MYC through RAS. *Clin Cancer Res* **11**, 4278-4281 (2005). https://doi.org/10.1158/1078-0432.CCR-05-0534
64 Sears, R. *et al.* Multiple Ras-dependent phosphorylation pathways regulate Myc protein stability. *Genes Dev* **14**, 2501-2514 (2000). https://doi.org/10.1101/gad.836800
65 Gregory, M. A., Qi, Y. & Hann, S. R. Phosphorylation by glycogen synthase kinase-3 controls c-myc proteolysis and subnuclear localization. *J Biol Chem* **278**, 51606-51612 (2003). https://doi.org/10.1074/jbc.M310722200
66 Sears, R., Leone, G., DeGregori, J. & Nevins, J. R. Ras enhances Myc protein stability. *Mol Cell* **3**, 169-179 (1999). https://doi.org/10.1016/s1097-2765(00)80308-1
67 Tsai, W. B. *et al.* Activation of Ras/PI3K/ERK pathway induces c-Myc stabilization to upregulate argininosuccinate synthetase, leading to arginine deiminase resistance in melanoma cells. *Cancer Res* **72**, 2622-2633 (2012). https://doi.org/10.1158/0008-5472.CAN-11-3605
68 Welcker, M. *et al.* Two diphosphorylated degrons control c-Myc degradation by the Fbw7 tumor suppressor. *Sci Adv* **8**, eabl7872 (2022). https://doi.org/10.1126/sciadv.abl7872
69 Nijman, S. M. *et al.* A genomic and functional inventory of deubiquitinating enzymes. *Cell* **123**, 773-786 (2005). https://doi.org/10.1016/j.cell.2005.11.007
70 Popov, N. *et al.* The ubiquitin-specific protease USP28 is required for MYC stability. *Nat Cell Biol* **9**, 765-774 (2007). https://doi.org/10.1038/ncb1601
71 Popov, N., Herold, S., Llamazares, M., Schulein, C. & Eilers, M. Fbw7 and Usp28 regulate myc protein stability in response to DNA damage. *Cell Cycle* **6**, 2327-2331 (2007). https://doi.org/10.4161/cc.6.19.4804
72 Popov, N., Schulein, C., Jaenicke, L. A. & Eilers, M. Ubiquitylation of the amino terminus of Myc by SCF(beta-TrCP) antagonizes SCF(Fbw7)-mediated turnover. *Nat Cell Biol* **12**, 973-981 (2010). https://doi.org/10.1038/ncb2104
73 Kim, S. Y., Herbst, A., Tworkowski, K. A., Salghetti, S. E. & Tansey, W. P. Skp2 regulates Myc protein stability and activity. *Mol Cell* **11**, 1177-1188 (2003). https://doi.org/10.1016/s1097-2765(03)00173-4
74 Faiola, F. *et al.* Dual regulation of c-Myc by p300 via acetylation-dependent control of Myc protein turnover and coactivation of Myc-induced transcription. *Mol Cell Biol* **25**, 10220-10234 (2005). https://doi.org/10.1128/MCB.25.23.10220-10234.2005
75 Vervoorts, J. *et al.* Stimulation of c-MYC transcriptional activity and acetylation by recruitment of the cofactor CBP. *EMBO Rep* **4**, 484-490 (2003). https://doi.org/10.1038/sj.embor.embor821
76 Small, G. W., Chou, T. Y., Dang, C. V. & Orlowski, R. Z. Evidence for involvement of calpain in c-Myc proteolysis in

vivo. *Arch Biochem Biophys* **400**, 151-161 (2002). https://doi.org/10.1016/S0003-9861(02)00005-X
77 Oskarsson, T. & Trumpp, A. The Myc trilogy: lord of RNA polymerases. *Nat Cell Biol* **7**, 215-217 (2005). https://doi.org/10.1038/ncb0305-215
78 Gomez-Roman, N. *et al.* Activation by c-Myc of transcription by RNA polymerases I, II and III. *Biochem Soc Symp*, 141-154 (2006). https://doi.org/10.1042/bss0730141
79 Campbell, K. J. & White, R. J. MYC regulation of cell growth through control of transcription by RNA polymerases I and III. *Cold Spring Harb Perspect Med* **4** (2014). https://doi.org/10.1101/cshperspect.a018408
80 Schlosser, I. *et al.* A role for c-Myc in the regulation of ribosomal RNA processing. *Nucleic Acids Res* **31**, 6148-6156 (2003). https://doi.org/10.1093/nar/gkg794
81 Popay, T. M. *et al.* MYC regulates ribosome biogenesis and mitochondrial gene expression programs through its interaction with host cell factor-1. *Elife* **10** (2021). https://doi.org/10.7554/eLife.60191
82 van Riggelen, J., Yetil, A. & Felsher, D. W. MYC as a regulator of ribosome biogenesis and protein synthesis. *Nat Rev Cancer* **10**, 301-309 (2010). https://doi.org/10.1038/nrc2819
83 Lin, C. J., Cencic, R., Mills, J. R., Robert, F. & Pelletier, J. c-Myc and eIF4F are components of a feedforward loop that links transcription and translation. *Cancer Res* **68**, 5326-5334 (2008). https://doi.org/10.1158/0008-5472.CAN-07-5876
84 Rosenwald, I. B., Rhoads, D. B., Callanan, L. D., Isselbacher, K. J. & Schmidt, E. V. Increased expression of eukaryotic translation initiation factors eIF-4E and eIF-2 alpha in response to growth induction by c-myc. *Proc Natl Acad Sci U S A* **90**, 6175-6178 (1993). https://doi.org/10.1073/pnas.90.13.6175
85 Sabo, A. *et al.* Selective transcriptional regulation by Myc in cellular growth control and lymphomagenesis. *Nature* **511**, 488-492 (2014). https://doi.org/10.1038/nature13537
86 Rounbehler, R. J. *et al.* Tristetraprolin impairs myc-induced lymphoma and abolishes the malignant state. *Cell* **150**, 563-574 (2012). https://doi.org/10.1016/j.cell.2012.06.033
87 Mukherjee, N. *et al.* Global target mRNA specification and regulation by the RNA-binding protein ZFP36. *Genome Biol* **15**, R12 (2014). https://doi.org/10.1186/gb-2014-15-1-r12
88 Swier, L., Dzikiewicz-Krawczyk, A., Winkle, M., van den Berg, A. & Kluiver, J. Intricate crosstalk between MYC and non-coding RNAs regulates hallmarks of cancer. *Mol Oncol* **13**, 26-45 (2019). https://doi.org/10.1002/1878-0261.12409
89 Cao, L., Zhang, P., Li, J. & Wu, M. LAST, a c-Myc-inducible long noncoding RNA, cooperates with CNBP to promote CCND1 mRNA stability in human cells. *Elife* **6** (2017). https://doi.org/10.7554/eLife.30433
90 Zhang, Z. *et al.* Long non-coding RNA CASC11 interacts with hnRNP-K and activates the WNT/beta-catenin pathway to promote growth and metastasis in colorectal cancer. *Cancer Lett* **376**, 62-73 (2016). https://doi.org/10.1016/j.canlet.2016.03.022
91 Mogilyansky, E. & Rigoutsos, I. The miR-17/92 cluster: a comprehensive update on its genomics, genetics, functions and increasingly important and numerous roles in health and disease. *Cell Death Differ* **20**, 1603-1614 (2013). https://doi.org/10.1038/cdd.2013.125
92 Petrocca, F., Vecchione, A. & Croce, C. M. Emerging role of miR-106b-25/miR-17-92 clusters in the control of transforming growth factor beta signaling. *Cancer Res* **68**, 8191-8194 (2008). https://doi.org/10.1158/0008-5472.CAN-08-1768
93 Xiao, C. *et al.* Lymphoproliferative disease and autoimmunity in mice with increased miR-17-92 expression in lymphocytes. *Nat Immunol* **9**, 405-414 (2008). https://doi.org/10.1038/ni1575
94 Mavrakis, K. J. *et al.* Genome-wide RNA-mediated interference screen identifies miR-19 targets in Notch-induced T-cell acute lymphoblastic leukaemia. *Nat Cell Biol* **12**, 372-379 (2010). https://doi.org/10.1038/ncb2037
95 Mu, P. *et al.* Genetic dissection of the miR-17~92 cluster of microRNAs in Myc-induced B-cell lymphomas. *Genes Dev* **23**, 2806-2811 (2009). https://doi.org/10.1101/gad.1872909
96 Olive, V. *et al.* miR-19 is a key oncogenic component of mir-17-92. *Genes Dev* **23**, 2839-2849 (2009). https://doi.org/10.1101/gad.1861409
97 Bommer, G. T. *et al.* p53-mediated activation of miRNA34 candidate tumor-suppressor genes. *Curr Biol* **17**, 1298-1307 (2007). https://doi.org/10.1016/j.cub.2007.06.068
98 Bonci, D. *et al.* The miR-15a-miR-16-1 cluster controls prostate cancer by targeting multiple oncogenic activities. *Nat Med* **14**, 1271-1277 (2008). https://doi.org/10.1038/nm.1880
99 Cimmino, A. *et al.* miR-15 and miR-16 induce apoptosis by targeting BCL2. *Proc Natl Acad Sci U S A* **102**, 13944-13949 (2005). https://doi.org/10.1073/pnas.0506654102
100 Lin, C. J., Gong, H. Y., Tseng, H. C., Wang, W. L. & Wu, J. L. miR-122 targets an anti-apoptotic gene, Bcl-w, in human hepatocellular carcinoma cell lines. *Biochem Biophys Res Commun* **375**, 315-320 (2008). https://doi.org/10.1016/j.bbrc.2008.07.154
101 Wang, B. *et al.* Reciprocal regulation of microRNA-122 and c-Myc in hepatocellular cancer: role of E2F1 and transcription factor dimerization partner 2. *Hepatology* **59**, 555-566 (2014). https://doi.org/10.1002/hep.26712
102 Jiang, C., Long, J., Liu, B., Xie, X. & Kuang, M. Mcl-1 Is a Novel Target of miR-26b That Is Associated with the Apoptosis Induced by TRAIL in HCC Cells. *Biomed Res Int* **2015**, 572738 (2015). https://doi.org/10.1155/2015/572738
103 Mott, J. L., Kobayashi, S., Bronk, S. F. & Gores, G. J. mir-29 regulates Mcl-1 protein expression and apoptosis. *Oncogene* **26**, 6133-6140 (2007). https://doi.org/10.1038/sj.onc.1210436
104 Das, S., Anczukow, O., Akerman, M. & Krainer, A. R. Oncogenic splicing factor SRSF1 is a critical transcriptional target of MYC. *Cell Rep* **1**, 110-117 (2012). https://doi.org/10.1016/j.celrep.2011.12.001
105 David, C. J., Chen, M., Assanah, M., Canoll, P. & Manley, J. L. HnRNP proteins controlled by c-Myc deregulate pyruvate kinase mRNA splicing in cancer. *Nature* **463**, 364-368 (2010). https://doi.org/10.1038/nature08697
106 Koh, C. M. *et al.* MYC regulates the core pre-mRNA splicing machinery as an essential step in lymphomagenesis. *Nature* **523**, 96-100 (2015). https://doi.org/10.1038/nature14351
107 Urbanski, L. *et al.* MYC regulates a pan-cancer network of co-expressed oncogenic splicing factors. *Cell Rep* **41**, 111704 (2022). https://doi.org/10.1016/j.celrep.2022.111704
108 Dominguez-Sola, D. & Gautier, J. MYC and the control of DNA replication. *Cold Spring Harb Perspect Med* **4** (2014). https://doi.org/10.1101/cshperspect.a014423
109 Cole, M. D. & Cowling, V. H. Transcription-independent functions of MYC: regulation of translation and DNA replication. *Nat Rev Mol Cell Biol* **9**, 810-815 (2008). https://doi.org/10.1038/nrm2467
110 Dominguez-Sola, D. *et al.* Non-transcriptional control of DNA replication by c-Myc. *Nature* **448**, 445-451 (2007). https://doi.org/10.1038/nature05953
111 Takayama, M. A., Taira, T., Tamai, K., Iguchi-Ariga, S. M. & Ariga, H. ORC1 interacts with c-Myc to inhibit E-box-dependent transcription by abrogating c-Myc-SNF5/INI1 interaction. *Genes Cells* **5**, 481-490 (2000). https://doi.org/10.1046/j.1365-2443.2000.00338.x
112 Takayama, M., Taira, T., Iguchi-Ariga, S. M. & Ariga, H. CDC6 interacts with c-Myc to inhibit E-box-dependent transcription by abrogating c-Myc/Max complex. *FEBS Lett* **477**, 43-48 (2000). https://doi.org/10.1016/s0014-5793(00)01756-7
113 Dominguez-Sola, D. *et al.* The proto-oncogene MYC is required for selection in the germinal center and cyclic reentry. *Nat Immunol* **13**, 1083-1091 (2012). https://doi.org/10.1038/ni.2428

114 Valovka, T. *et al.* Transcriptional control of DNA replication licensing by Myc. *Sci Rep* **3**, 3444 (2013). https://doi.org/10.1038/srep03444

115 Kwan, K. Y., Shen, J. & Corey, D. P. C-MYC transcriptionally amplifies SOX2 target genes to regulate self-renewal in multipotent otic progenitor cells. *Stem Cell Reports* **4**, 47-60 (2015). https://doi.org/10.1016/j.stemcr.2014.11.001

116 Perna, D. *et al.* Genome-wide mapping of Myc binding and gene regulation in serum-stimulated fibroblasts. *Oncogene* **31**, 1695-1709 (2012). https://doi.org/10.1038/onc.2011.359

117 Liu, Y. C. *et al.* Global regulation of nucleotide biosynthetic genes by c-Myc. *PLoS One* **3**, e2722 (2008). https://doi.org/10.1371/journal.pone.0002722

118 Grandori, C. *et al.* c-Myc binds to human ribosomal DNA and stimulates transcription of rRNA genes by RNA polymerase I. *Nat Cell Biol* **7**, 311-318 (2005). https://doi.org/10.1038/ncb1224

119 Kim, S., Li, Q., Dang, C. V. & Lee, L. A. Induction of ribosomal genes and hepatocyte hypertrophy by adenovirus-mediated expression of c-Myc in vivo. *Proc Natl Acad Sci U S A* **97**, 11198-11202 (2000). https://doi.org/10.1073/pnas.200372597

120 Zeller, K. I. *et al.* Characterization of nucleophosmin (B23) as a Myc target by scanning chromatin immunoprecipitation. *J Biol Chem* **276**, 48285-48291 (2001). https://doi.org/10.1074/jbc.M108506200

121 Schmidt, E. V. The role of c-myc in regulation of translation initiation. *Oncogene* **23**, 3217-3221 (2004). https://doi.org/10.1038/sj.onc.1207548

122 Cole, M. D. & Cowling, V. H. Specific regulation of mRNA cap methylation by the c-Myc and E2F1 transcription factors. *Oncogene* **28**, 1169-1175 (2009). https://doi.org/10.1038/onc.2008.463

123 Iritani, B. M. & Eisenman, R. N. c-Myc enhances protein synthesis and cell size during B lymphocyte development. *Proc Natl Acad Sci U S A* **96**, 13180-13185 (1999). https://doi.org/10.1073/pnas.96.23.13180

124 Piedra, M. E., Delgado, M. D., Ros, M. A. & Leon, J. c-Myc overexpression increases cell size and impairs cartilage differentiation during chick limb development. *Cell Growth Differ* **13**, 185-193 (2002).

125 Baena, E. *et al.* c-Myc regulates cell size and ploidy but is not essential for postnatal proliferation in liver. *Proc Natl Acad Sci U S A* **102**, 7286-7291 (2005). https://doi.org/10.1073/pnas.0409260102

126 Kieffer-Kwon, K. R. *et al.* Myc Regulates Chromatin Decompaction and Nuclear Architecture during B Cell Activation. *Mol Cell* **67**, 566-578 e510 (2017). https://doi.org/10.1016/j.molcel.2017.07.013

127 Schuhmacher, M. *et al.* Control of cell growth by c-Myc in the absence of cell division. *Curr Biol* **9**, 1255-1258 (1999). https://doi.org/10.1016/s0960-9822(99)80507-7

128 Mori, T. *et al.* c-Myc overexpression increases ribosome biogenesis and protein synthesis independent of mTORC1 activation in mouse skeletal muscle. *Am J Physiol Endocrinol Metab* **321**, E551-E559 (2021). https://doi.org/10.1152/ajpendo.00164.2021

129 Marchingo, J. M., Sinclair, L. V., Howden, A. J. & Cantrell, D. A. Quantitative analysis of how Myc controls T cell proteomes and metabolic pathways during T cell activation. *Elife* **9** (2020). https://doi.org/10.7554/eLife.53725

130 Tesi, A. *et al.* An early Myc-dependent transcriptional program orchestrates cell growth during B-cell activation. *EMBO Rep* **20**, e47987 (2019). https://doi.org/10.15252/embr.201947987

131 Wang, R. *et al.* The transcription factor Myc controls metabolic reprogramming upon T lymphocyte activation. *Immunity* **35**, 871-882 (2011). https://doi.org/10.1016/j.immuni.2011.09.021

132 Armelin, H. A. *et al.* Functional role for c-myc in mitogenic response to platelet-derived growth factor. *Nature* **310**, 655-660 (1984). https://doi.org/10.1038/310655a0

133 Heikkila, R. *et al.* A c-myc antisense oligodeoxynucleotide inhibits entry into S phase but not progress from G0 to G1. *Nature* **328**, 445-449 (1987). https://doi.org/10.1038/328445a0

134 Lutz, W., Leon, J. & Eilers, M. Contributions of Myc to tumorigenesis. *Biochim Biophys Acta* **1602**, 61-71 (2002). https://doi.org/10.1016/s0304-419x(02)00036-7

135 Yap, C. S., Peterson, A. L., Castellani, G., Sedivy, J. M. & Neretti, N. Kinetic profiling of the c-Myc transcriptome and bioinformatic analysis of repressed gene promoters. *Cell Cycle* **10**, 2184-2196 (2011). https://doi.org/10.4161/cc.10.13.16249

136 Wu, S. *et al.* Myc represses differentiation-induced p21CIP1 expression via Miz-1-dependent interaction with the p21 core promoter. *Oncogene* **22**, 351-360 (2003). https://doi.org/10.1038/sj.onc.1206145

137 Bretones, G., Delgado, M. D. & Leon, J. Myc and cell cycle control. *Biochim Biophys Acta* **1849**, 506-516 (2015). https://doi.org/10.1016/j.bbagrm.2014.03.013

138 Acosta, J. C. *et al.* Myc inhibits p27-induced erythroid differentiation of leukemia cells by repressing erythroid master genes without reversing p27-mediated cell cycle arrest. *Mol Cell Biol* **28**, 7286-7295 (2008). https://doi.org/10.1128/MCB.00752-08

139 Vlach, J., Hennecke, S., Alevizopoulos, K., Conti, D. & Amati, B. Growth arrest by the cyclin-dependent kinase inhibitor p27Kip1 is abrogated by c-Myc. *EMBO J* **15**, 6595-6604 (1996).

140 Perez-Roger, I., Solomon, D. L., Sewing, A. & Land, H. Myc activation of cyclin E/Cdk2 kinase involves induction of cyclin E gene transcription and inhibition of p27(Kip1) binding to newly formed complexes. *Oncogene* **14**, 2373-2381 (1997). https://doi.org/10.1038/sj.onc.1201197

141 Gartel, A. L. *et al.* Myc represses the p21(WAF1/CIP1) promoter and interacts with Sp1/Sp3. *Proc Natl Acad Sci U S A* **98**, 4510-4515 (2001). https://doi.org/10.1073/pnas.081074898

142 Garcia-Gutierrez, L. *et al.* Myc stimulates cell cycle progression through the activation of Cdk1 and phosphorylation of p27. *Sci Rep* **9**, 18693 (2019). https://doi.org/10.1038/s41598-019-54917-1

143 Evan, G. I. *et al.* Induction of apoptosis in fibroblasts by c-myc protein. *Cell* **69**, 119-128 (1992). https://doi.org/10.1016/0092-8674(92)90123-t

144 Shi, Y. *et al.* Role for c-myc in activation-induced apoptotic cell death in T cell hybridomas. *Science* **257**, 212-214 (1992). https://doi.org/10.1126/science.1378649

145 Zindy, F. *et al.* Myc signaling via the ARF tumor suppressor regulates p53-dependent apoptosis and immortalization. *Genes Dev* **12**, 2424-2433 (1998). https://doi.org/10.1101/gad.12.15.2424

146 Weber, J. D., Taylor, L. J., Roussel, M. F., Sherr, C. J. & Bar-Sagi, D. Nucleolar Arf sequesters Mdm2 and activates p53. *Nat Cell Biol* **1**, 20-26 (1999). https://doi.org/10.1038/8991

147 Eischen, C. M., Woo, D., Roussel, M. F. & Cleveland, J. L. Apoptosis triggered by Myc-induced suppression of Bcl-X(L) or Bcl-2 is bypassed during lymphomagenesis. *Mol Cell Biol* **21**, 5063-5070 (2001). https://doi.org/10.1128/MCB.21.15.5063-5070.2001

148 Maclean, K. H., Keller, U. B., Rodriguez-Galindo, C., Nilsson, J. A. & Cleveland, J. L. c-Myc augments gamma irradiation-induced apoptosis by suppressing Bcl-XL. *Mol Cell Biol* **23**, 7256-7270 (2003). https://doi.org/10.1128/MCB.23.20.7256-7270.2003

149 Oda, E. *et al.* Noxa, a BH3-only member of the Bcl-2 family and candidate mediator of p53-induced apoptosis. *Science* **288**, 1053-1058 (2000). https://doi.org/10.1126/science.288.5468.1053

150 Eischen, C. M., Weber, J. D., Roussel, M. F., Sherr, C. J. & Cleveland, J. L. Disruption of the ARF-Mdm2-p53 tumor suppressor pathway in Myc-induced lymphomagenesis. *Genes Dev* **13**, 2658-2669 (1999). https://doi.org/10.1101/gad.13.20.2658

151 Mitchell, K. O. *et al.* Bax is a transcriptional target and mediator of c-myc-induced apoptosis. *Cancer Res* **60**, 6318-6325 (2000).

152 Oster, S. K., Ho, C. S., Soucie, E. L. & Penn, L. Z. The myc oncogene: MarvelouslY Complex. *Adv Cancer Res* **84**, 81-154 (2002). https://doi.org/10.1016/s0065-230x(02)84004-0

153 Bissonnette, R. P., Echeverri, F., Mahboubi, A. & Green, D. R. Apoptotic cell death induced by c-myc is inhibited by bcl-2. *Nature* **359**, 552-554 (1992). https://doi.org/10.1038/359552a0

154 Fanidi, A., Harrington, E. A. & Evan, G. I. Cooperative interaction between c-myc and bcl-2 proto-oncogenes. *Nature* **359**, 554-556 (1992). https://doi.org/10.1038/359554a0

155 Dansen, T. B., Whitfield, J., Rostker, F., Brown-Swigart, L. & Evan, G. I. Specific requirement for Bax, not Bak, in Myc-induced apoptosis and tumor suppression in vivo. *J Biol Chem* **281**, 10890-10895 (2006). https://doi.org/10.1074/jbc.M513655200

156 Juin, P. *et al.* c-Myc functionally cooperates with Bax to induce apoptosis. *Mol Cell Biol* **22**, 6158-6169 (2002). https://doi.org/10.1128/MCB.22.17.6158-6169.2002

157 Glick, D., Barth, S. & Macleod, K. F. Autophagy: cellular and molecular mechanisms. *J Pathol* **221**, 3-12 (2010). https://doi.org/10.1002/path.2697

158 Annunziata, I. *et al.* MYC competes with MiT/TFE in regulating lysosomal biogenesis and autophagy through an epigenetic rheostat. *Nat Commun* **10**, 3623 (2019). https://doi.org/10.1038/s41467-019-11568-0

159 Garcia-Prat, L. *et al.* TFEB-mediated endolysosomal activity controls human hematopoietic stem cell fate. *Cell Stem Cell* **28**, 1838-1850 e1810 (2021). https://doi.org/10.1016/j.stem.2021.07.003

160 Yun, S. *et al.* TFEB links MYC signaling to epigenetic control of myeloid differentiation and acute myeloid leukemia. *Blood Cancer Discov* **2**, 162-185 (2021). https://doi.org/10.1158/2643-3230.BCD-20-0029

161 Napolitano, G. & Ballabio, A. TFEB at a glance. *J Cell Sci* **129**, 2475-2481 (2016). https://doi.org/10.1242/jcs.146365

162 Fernandez, M. R. *et al.* Disrupting the MYC-TFEB Circuit Impairs Amino Acid Homeostasis and Provokes Metabolic Anergy. *Cancer Res* **82**, 1234-1250 (2022). https://doi.org/10.1158/0008-5472.CAN-21-1168

163 Teleman, A. A., Hietakangas, V., Sayadian, A. C. & Cohen, S. M. Nutritional control of protein biosynthetic capacity by insulin via Myc in Drosophila. *Cell Metab* **7**, 21-32 (2008). https://doi.org/10.1016/j.cmet.2007.11.010

164 Cianfanelli, V. *et al.* AMBRA1 links autophagy to cell proliferation and tumorigenesis by promoting c-Myc dephosphorylation and degradation. *Nat Cell Biol* **17**, 706 (2015). https://doi.org/10.1038/ncb3171

165 Okuyama, H., Endo, H., Akashika, T., Kato, K. & Inoue, M. Downregulation of c-MYC protein levels contributes to cancer cell survival under dual deficiency of oxygen and glucose. *Cancer Res* **70**, 10213-10223 (2010). https://doi.org/10.1158/0008-5472.CAN-10-2720

166 Zhang, H. *et al.* HIF-1 inhibits mitochondrial biogenesis and cellular respiration in VHL-deficient renal cell carcinoma by repression of C-MYC activity. *Cancer Cell* **11**, 407-420 (2007). https://doi.org/10.1016/j.ccr.2007.04.001

167 Gao, P. *et al.* c-Myc suppression of miR-23a/b enhances mitochondrial glutaminase expression and glutamine metabolism. *Nature* **458**, 762-765 (2009). https://doi.org/10.1038/nature07823

168 Wise, D. R. *et al.* Myc regulates a transcriptional program that stimulates mitochondrial glutaminolysis and leads to glutamine addiction. *Proc Natl Acad Sci U S A* **105**, 18782-18787 (2008). https://doi.org/10.1073/pnas.0810199105

169 Hu, S. *et al.* 13C-pyruvate imaging reveals alterations in glycolysis that precede c-Myc-induced tumor formation and regression. *Cell Metab* **14**, 131-142 (2011). https://doi.org/10.1016/j.cmet.2011.04.012

170 Doherty, J. R. *et al.* Blocking lactate export by inhibiting the Myc target MCT1 Disables glycolysis and glutathione synthesis. *Cancer Res* **74**, 908-920 (2014). https://doi.org/10.1158/0008-5472.CAN-13-2034

171 McCalley, S. *et al.* Metabolic analysis reveals evidence for branched chain amino acid catabolism crosstalk and the potential for improved treatment of organic acidurias. *Mol Genet Metab* **128**, 57-61 (2019). https://doi.org/10.1016/j.ymgme.2019.05.008

172 Miltenberger, R. J., Sukow, K. A. & Farnham, P. J. An E-box-mediated increase in cad transcription at the G1/S-phase boundary is suppressed by inhibitory c-Myc mutants. *Mol Cell Biol* **15**, 2527-2535 (1995). https://doi.org/10.1128/MCB.15.5.2527

173 Wang, X. *et al.* Purine synthesis promotes maintenance of brain tumor initiating cells in glioma. *Nat Neurosci* **20**, 661-673 (2017). https://doi.org/10.1038/nn.4537

174 Barfeld, S. J. *et al.* Myc-dependent purine biosynthesis affects nucleolar stress and therapy response in prostate cancer. *Oncotarget* **6**, 12587-12602 (2015). https://doi.org/10.18632/oncotarget.3494

175 Agarwal, S. *et al.* PAICS, a Purine Nucleotide Metabolic Enzyme, is Involved in Tumor Growth and the Metastasis of Colorectal Cancer. *Cancers (Basel)* **12** (2020). https://doi.org/10.3390/cancers12040772

176 O'Donnell, K. A. *et al.* Activation of transferrin receptor 1 by c-Myc enhances cellular proliferation and tumorigenesis. *Mol Cell Biol* **26**, 2373-2386 (2006). https://doi.org/10.1128/MCB.26.6.2373-2386.2006

177 Dang, C. V. MYC on the path to cancer. *Cell* **149**, 22-35 (2012). https://doi.org/10.1016/j.cell.2012.03.003

178 Kalkat, M. *et al.* MYC Deregulation in Primary Human Cancers. *Genes (Basel)* **8** (2017). https://doi.org/10.3390/genes8060151

179 Dhanasekaran, R. *et al.* The MYC oncogene - the grand orchestrator of cancer growth and immune evasion. *Nat Rev Clin Oncol* **19**, 23-36 (2022). https://doi.org/10.1038/s41571-021-00549-2

180 Schaub, F. X. *et al.* Pan-cancer Alterations of the MYC Oncogene and Its Proximal Network across the Cancer Genome Atlas. *Cell Syst* **6**, 282-300 e282 (2018). https://doi.org/10.1016/j.cels.2018.03.003

181 Dang, C. V. MYC, metabolism, cell growth, and tumorigenesis. *Cold Spring Harb Perspect Med* **3** (2013). https://doi.org/10.1101/cshperspect.a014217

182 Gabay, M., Li, Y. & Felsher, D. W. MYC activation is a hallmark of cancer initiation and maintenance. *Cold Spring Harb Perspect Med* **4** (2014). https://doi.org/10.1101/cshperspect.a014241

183 Cowling, V. H., D'Cruz, C. M., Chodosh, L. A. & Cole, M. D. c-Myc transforms human mammary epithelial cells through repression of the Wnt inhibitors DKK1 and SFRP1. *Mol Cell Biol* **27**, 5135-5146 (2007). https://doi.org/10.1128/MCB.02282-06

184 Meyer, N. & Penn, L. Z. Reflecting on 25 years with MYC. *Nat Rev Cancer* **8**, 976-990 (2008). https://doi.org/10.1038/nrc2231

185 Adhikary, S. & Eilers, M. Transcriptional regulation and transformation by Myc proteins. *Nat Rev Mol Cell Biol* **6**, 635-645 (2005). https://doi.org/10.1038/nrm1703

186 Kuzyk, A. & Mai, S. c-MYC-induced genomic instability. *Cold Spring Harb Perspect Med* **4**, a014373 (2014). https://doi.org/10.1101/cshperspect.a014373

187 Felsher, D. W. & Bishop, J. M. Transient excess of MYC activity can elicit genomic instability and tumorigenesis. *Proc Natl Acad Sci U S A* **96**, 3940-3944 (1999). https://doi.org/10.1073/pnas.96.7.3940

188 Campaner, S. & Amati, B. Two sides of the Myc-induced DNA damage response: from tumor suppression to tumor maintenance. *Cell Div* **7**, 6 (2012). https://doi.org/10.1186/1747-1028-7-6

189 Karlsson, A. *et al.* Defective double-strand DNA break repair and chromosomal translocations by MYC overexpression. *Proc Natl Acad Sci U S A* **100**, 9974-9979 (2003). https://doi.org/10.1073/pnas.1732638100

190 Vafa, O. *et al.* c-Myc can induce DNA damage, increase reactive oxygen species, and mitigate p53 function: a mechanism for oncogene-induced genetic instability. *Mol*

Cell **9**, 1031-1044 (2002). https://doi.org/10.1016/s1097-2765(02)00520-8
191 Ray, S. *et al.* MYC can induce DNA breaks in vivo and in vitro independent of reactive oxygen species. *Cancer Res* **66**, 6598-6605 (2006). https://doi.org/10.1158/0008-5472.CAN-05-3115
192 Li, Z. *et al.* c-Myc suppression of DNA double-strand break repair. *Neoplasia* **14**, 1190-1202 (2012). https://doi.org/10.1593/neo.121258
193 Ambrosio, S. *et al.* MYC impairs resolution of site-specific DNA double-strand breaks repair. *Mutat Res* **774**, 6-13 (2015). https://doi.org/10.1016/j.mrfmmm.2015.02.005
194 Leder, A., Pattengale, P. K., Kuo, A., Stewart, T. A. & Leder, P. Consequences of widespread deregulation of the c-myc gene in transgenic mice: multiple neoplasms and normal development. *Cell* **45**, 485-495 (1986). https://doi.org/10.1016/0092-8674(86)90280-1
195 Gurel, B. *et al.* Nuclear MYC protein overexpression is an early alteration in human prostate carcinogenesis. *Mod Pathol* **21**, 1156-1167 (2008). https://doi.org/10.1038/modpathol.2008.111
196 Stock, C., Kager, L., Fink, F. M., Gadner, H. & Ambros, P. F. Chromosomal regions involved in the pathogenesis of osteosarcomas. *Genes Chromosomes Cancer* **28**, 329-336 (2000). https://doi.org/10.1002/1098-2264(200007)28:3<329::aid-gcc11>3.0.co;2-f
197 Felsher, D. W. & Bishop, J. M. Reversible tumorigenesis by MYC in hematopoietic lineages. *Mol Cell* **4**, 199-207 (1999). https://doi.org/10.1016/s1097-2765(00)80367-6
198 Li, Y., Casey, S. C. & Felsher, D. W. Inactivation of MYC reverses tumorigenesis. *J Intern Med* **276**, 52-60 (2014). https://doi.org/10.1111/joim.12237
199 Lourenco, C. *et al.* Modelling the MYC-driven normal-to-tumour switch in breast cancer. *Dis Model Mech* **12** (2019). https://doi.org/10.1242/dmm.038083
200 Arvanitis, C. & Felsher, D. W. Conditional transgenic models define how MYC initiates and maintains tumorigenesis. *Semin Cancer Biol* **16**, 313-317 (2006). https://doi.org/10.1016/j.semcancer.2006.07.012
201 Soucek, L. *et al.* Inhibition of Myc family proteins eradicates KRas-driven lung cancer in mice. *Genes Dev* **27**, 504-513 (2013). https://doi.org/10.1101/gad.205542.112
202 Jung, L. A. *et al.* OmoMYC blunts promoter invasion by oncogenic MYC to inhibit gene expression characteristic of MYC-dependent tumors. *Oncogene* **36**, 1911-1924 (2017). https://doi.org/10.1038/onc.2016.354
203 Spencer, C. A. & Groudine, M. Control of c-myc regulation in normal and neoplastic cells. *Adv Cancer Res* **56**, 1-48 (1991). https://doi.org/10.1016/s0065-230x(08)60476-5
204 Collins, S. & Groudine, M. Amplification of endogenous myc-related DNA sequences in a human myeloid leukaemia cell line. *Nature* **298**, 679-681 (1982). https://doi.org/10.1038/298679a0
205 Schwab, M. *et al.* Amplified DNA with limited homology to myc cellular oncogene is shared by human neuroblastoma cell lines and a neuroblastoma tumour. *Nature* **305**, 245-248 (1983). https://doi.org/10.1038/305245a0
206 Nau, M. M. *et al.* L-myc, a new myc-related gene amplified and expressed in human small cell lung cancer. *Nature* **318**, 69-73 (1985). https://doi.org/10.1038/318069a0
207 Boxer, L. M. & Dang, C. V. Translocations involving c-myc and c-myc function. *Oncogene* **20**, 5595-5610 (2001). https://doi.org/10.1038/sj.onc.1204595
208 Pasqualucci, L. & Dalla-Favera, R. Genetics of diffuse large B-cell lymphoma. *Blood* **131**, 2307-2319 (2018). https://doi.org/10.1182/blood-2017-11-764332
209 Bisso, A., Sabo, A. & Amati, B. MYC in Germinal Center-derived lymphomas: Mechanisms and therapeutic opportunities. *Immunol Rev* **288**, 178-197 (2019). https://doi.org/10.1111/imr.12734
210 Bahrami, A. *et al.* Therapeutic Potential of Targeting Wnt/beta-Catenin Pathway in Treatment of Colorectal Cancer: Rational and Progress. *J Cell Biochem* **118**, 1979-1983 (2017). https://doi.org/10.1002/jcb.25903
211 Weng, A. P. *et al.* c-Myc is an important direct target of Notch1 in T-cell acute lymphoblastic leukemia/lymphoma. *Genes Dev* **20**, 2096-2109 (2006). https://doi.org/10.1101/gad.1450406
212 Yagi, K. *et al.* c-myc is a downstream target of the Smad pathway. *J Biol Chem* **277**, 854-861 (2002). https://doi.org/10.1074/jbc.M104170200
213 Arnold, H. K. & Sears, R. C. Protein phosphatase 2A regulatory subunit B56alpha associates with c-myc and negatively regulates c-myc accumulation. *Mol Cell Biol* **26**, 2832-2844 (2006). https://doi.org/10.1128/MCB.26.7.2832-2844.2006
214 Wang, X. *et al.* Phosphorylation regulates c-Myc's oncogenic activity in the mammary gland. *Cancer Res* **71**, 925-936 (2011). https://doi.org/10.1158/0008-5472.CAN-10-1032
215 Reavie, L. *et al.* Regulation of c-Myc ubiquitination controls chronic myelogenous leukemia initiation and progression. *Cancer Cell* **23**, 362-375 (2013). https://doi.org/10.1016/j.ccr.2013.01.025
216 Wu, C. H. *et al.* Cellular senescence is an important mechanism of tumor regression upon c-Myc inactivation. *Proc Natl Acad Sci U S A* **104**, 13028-13033 (2007). https://doi.org/10.1073/pnas.0701953104
217 Weinstein, I. B. Cancer. Addiction to oncogenes--the Achilles heal of cancer. *Science* **297**, 63-64 (2002). https://doi.org/10.1126/science.1073096
218 Jain, M. *et al.* Sustained loss of a neoplastic phenotype by brief inactivation of MYC. *Science* **297**, 102-104 (2002). https://doi.org/10.1126/science.1071489
219 Rosenquist, R., Bea, S., Du, M. Q., Nadel, B. & Pan-Hammarstrom, Q. Genetic landscape and deregulated pathways in B-cell lymphoid malignancies. *J Intern Med* **282**, 371-394 (2017). https://doi.org/10.1111/joim.12633
220 Cai, Q., Medeiros, L. J., Xu, X. & Young, K. H. MYC-driven aggressive B-cell lymphomas: biology, entity, differential diagnosis and clinical management. *Oncotarget* **6**, 38591-38616 (2015). https://doi.org/10.18632/oncotarget.5774
221 Ahmadi, S. E., Rahimi, S., Zarandi, B., Chegeni, R. & Safa, M. MYC: a multipurpose oncogene with prognostic and therapeutic implications in blood malignancies. *J Hematol Oncol* **14**, 121 (2021). https://doi.org/10.1186/s13045-021-01111-4
222 Connors, J. M. *et al.* Hodgkin lymphoma. *Nat Rev Dis Primers* **6**, 61 (2020). https://doi.org/10.1038/s41572-020-0189-6
223 Ekstrom-Smedby, K. Epidemiology and etiology of non-Hodgkin lymphoma--a review. *Acta Oncol* **45**, 258-271 (2006). https://doi.org/10.1080/02841860500531682
224 Ott, G., Rosenwald, A. & Campo, E. Understanding MYC-driven aggressive B-cell lymphomas: pathogenesis and classification. *Blood* **122**, 3884-3891 (2013). https://doi.org/10.1182/blood-2013-05-498329
225 Slack, G. W. & Gascoyne, R. D. MYC and aggressive B-cell lymphomas. *Adv Anat Pathol* **18**, 219-228 (2011). https://doi.org/10.1097/PAP.0b013e3182169948
226 Johnson, N. A. *et al.* Lymphomas with concurrent BCL2 and MYC translocations: the critical factors associated with survival. *Blood* **114**, 2273-2279 (2009). https://doi.org/10.1182/blood-2009-03-212191
227 Pasqualucci, L. *et al.* Analysis of the coding genome of diffuse large B-cell lymphoma. *Nat Genet* **43**, 830-837 (2011). https://doi.org/10.1038/ng.892
228 Molyneux, E. M. *et al.* Burkitt's lymphoma. *Lancet* **379**, 1234-1244 (2012). https://doi.org/10.1016/S0140-6736(11)61177-X
229 Eick, D. & Bornkamm, G. W. Expression of normal and translocated c-myc alleles in Burkitt's lymphoma cells: evidence for different regulation. *EMBO J* **8**, 1965-1972 (1989). https://doi.org/10.1002/j.1460-2075.1989.tb03602.x
230 Bemark, M. & Neuberger, M. S. The c-MYC allele that is translocated into the IgH locus undergoes constitutive hypermutation in a Burkitt's lymphoma line. *Oncogene* **19**, 3404-3410 (2000). https://doi.org/10.1038/sj.onc.1203686

231 Giulino-Roth, L. *et al.* Targeted genomic sequencing of pediatric Burkitt lymphoma identifies recurrent alterations in antiapoptotic and chromatin-remodeling genes. *Blood* **120**, 5181-5184 (2012). https://doi.org/10.1182/blood-2012-06-437624

232 Lin, C. Y. *et al.* Transcriptional amplification in tumor cells with elevated c-Myc. *Cell* **151**, 56-67 (2012). https://doi.org/10.1016/j.cell.2012.08.026

233 Nie, Z. *et al.* c-Myc is a universal amplifier of expressed genes in lymphocytes and embryonic stem cells. *Cell* **151**, 68-79 (2012). https://doi.org/10.1016/j.cell.2012.08.033

234 de Pretis, S. *et al.* Integrative analysis of RNA polymerase II and transcriptional dynamics upon MYC activation. *Genome Res* **27**, 1658-1664 (2017). https://doi.org/10.1101/gr.226035.117

235 Muhar, M. *et al.* SLAM-seq defines direct gene-regulatory functions of the BRD4-MYC axis. *Science* **360**, 800-805 (2018). https://doi.org/10.1126/science.aao2793

236 Patange, S. *et al.* MYC amplifies gene expression through global changes in transcription factor dynamics. *Cell Rep* **38**, 110292 (2022). https://doi.org/10.1016/j.celrep.2021.110292

237 Walz, S. *et al.* Activation and repression by oncogenic MYC shape tumour-specific gene expression profiles. *Nature* **511**, 483-487 (2014). https://doi.org/10.1038/nature13473

238 Fernandez, P. C. *et al.* Genomic targets of the human c-Myc protein. *Genes Dev* **17**, 1115-1129 (2003). https://doi.org/10.1101/gad.1067003

239 Guccione, E. *et al.* Myc-binding-site recognition in the human genome is determined by chromatin context. *Nat Cell Biol* **8**, 764-770 (2006). https://doi.org/10.1038/ncb1434

240 Pellanda, P. *et al.* Integrated requirement of non-specific and sequence-specific DNA binding in Myc-driven transcription. *EMBO J* **40**, e105464 (2021). https://doi.org/10.15252/embj.2020105464

241 Sabo, A. & Amati, B. BRD4 and MYC-clarifying regulatory specificity. *Science* **360**, 713-714 (2018). https://doi.org/10.1126/science.aat6664

242 Sullivan, D. K. *et al.* MYC oncogene elicits tumorigenesis associated with embryonic, ribosomal biogenesis, and tissue-lineage dedifferentiation gene expression changes. *Oncogene* **41**, 4960-4970 (2022). https://doi.org/10.1038/s41388-022-02458-9

243 Tran, P. T. *et al.* Combined Inactivation of MYC and K-Ras oncogenes reverses tumorigenesis in lung adenocarcinomas and lymphomas. *PLoS One* **3**, e2125 (2008). https://doi.org/10.1371/journal.pone.0002125

244 Shachaf, C. M. *et al.* MYC inactivation uncovers pluripotent differentiation and tumour dormancy in hepatocellular cancer. *Nature* **431**, 1112-1117 (2004). https://doi.org/10.1038/nature03043

245 Shroff, E. H. *et al.* MYC oncogene overexpression drives renal cell carcinoma in a mouse model through glutamine metabolism. *Proc Natl Acad Sci U S A* **112**, 6539-6544 (2015). https://doi.org/10.1073/pnas.1507228112

246 Blackwell, T. K., Kretzner, L., Blackwood, E. M., Eisenman, R. N. & Weintraub, H. Sequence-specific DNA binding by the c-Myc protein. *Science* **250**, 1149-1151 (1990). https://doi.org/10.1126/science.2251503

247 Blackwell, T. K. *et al.* Binding of myc proteins to canonical and noncanonical DNA sequences. *Mol Cell Biol* **13**, 5216-5224 (1993). https://doi.org/10.1128/mcb.13.9.5216-5224.1993

248 Solomon, D. L., Amati, B. & Land, H. Distinct DNA binding preferences for the c-Myc/Max and Max/Max dimers. *Nucleic Acids Res* **21**, 5372-5376 (1993). https://doi.org/10.1093/nar/21.23.5372

249 Mao, D. Y. *et al.* Analysis of Myc bound loci identified by CpG island arrays shows that Max is essential for Myc-dependent repression. *Curr Biol* **13**, 882-886 (2003). https://doi.org/10.1016/s0960-9822(03)00297-5

250 Kim, J., Chu, J., Shen, X., Wang, J. & Orkin, S. H. An extended transcriptional network for pluripotency of embryonic stem cells. *Cell* **132**, 1049-1061 (2008). https://doi.org/10.1016/j.cell.2008.02.039

251 Soufi, A., Donahue, G. & Zaret, K. S. Facilitators and impediments of the pluripotency reprogramming factors' initial engagement with the genome. *Cell* **151**, 994-1004 (2012). https://doi.org/10.1016/j.cell.2012.09.045

252 Takahashi, K. & Yamanaka, S. Induction of pluripotent stem cells from mouse embryonic and adult fibroblast cultures by defined factors. *Cell* **126**, 663-676 (2006). https://doi.org/10.1016/j.cell.2006.07.024

253 Martinato, F., Cesaroni, M., Amati, B. & Guccione, E. Analysis of Myc-induced histone modifications on target chromatin. *PLoS One* **3**, e3650 (2008). https://doi.org/10.1371/journal.pone.0003650

254 Kenneth, N. S. *et al.* TRRAP and GCN5 are used by c-Myc to activate RNA polymerase III transcription. *Proc Natl Acad Sci U S A* **104**, 14917-14922 (2007). https://doi.org/10.1073/pnas.0702909104

255 Amati, B., Frank, S. R., Donjerkovic, D. & Taubert, S. Function of the c-Myc oncoprotein in chromatin remodeling and transcription. *Biochim Biophys Acta* **1471**, M135-145 (2001). https://doi.org/10.1016/s0304-419x(01)00020-8

256 Frank, S. R. *et al.* MYC recruits the TIP60 histone acetyltransferase complex to chromatin. *EMBO Rep* **4**, 575-580 (2003). https://doi.org/10.1038/sj.embor.embor861

257 McMahon, S. B., Van Buskirk, H. A., Dugan, K. A., Copeland, T. D. & Cole, M. D. The novel ATM-related protein TRRAP is an essential cofactor for the c-Myc and E2F oncoproteins. *Cell* **94**, 363-374 (1998). https://doi.org/10.1016/s0092-8674(00)81479-8

258 Cheng, S. W. *et al.* c-MYC interacts with INI1/hSNF5 and requires the SWI/SNF complex for transactivation function. *Nat Genet* **22**, 102-105 (1999). https://doi.org/10.1038/8811

259 Stojanova, A. *et al.* MYC interaction with the tumor suppressive SWI/SNF complex member INI1 regulates transcription and cellular transformation. *Cell Cycle* **15**, 1693-1705 (2016). https://doi.org/10.1080/15384101.2016.1146836

260 Devaiah, B. N. *et al.* MYC protein stability is negatively regulated by BRD4. *Proc Natl Acad Sci U S A* **117**, 13457-13467 (2020). https://doi.org/10.1073/pnas.1919507117

261 Kotekar, A., Singh, A. K. & Devaiah, B. N. BRD4 and MYC: power couple in transcription and disease. *FEBS J* (2022). https://doi.org/10.1111/febs.16580

262 Devaiah, B. N. *et al.* BRD4 is a histone acetyltransferase that evicts nucleosomes from chromatin. *Nat Struct Mol Biol* **23**, 540-548 (2016). https://doi.org/10.1038/nsmb.3228

263 Chapuy, B. *et al.* Discovery and characterization of super-enhancer-associated dependencies in diffuse large B cell lymphoma. *Cancer Cell* **24**, 777-790 (2013). https://doi.org/10.1016/j.ccr.2013.11.003

264 Loven, J. *et al.* Selective inhibition of tumor oncogenes by disruption of super-enhancers. *Cell* **153**, 320-334 (2013). https://doi.org/10.1016/j.cell.2013.03.036

265 Tu, W. B. *et al.* MYC Interacts with the G9a Histone Methyltransferase to Drive Transcriptional Repression and Tumorigenesis. *Cancer Cell* **34**, 579-595 e578 (2018). https://doi.org/10.1016/j.ccell.2018.09.001

266 Knoepfler, P. S. *et al.* Myc influences global chromatin structure. *EMBO J* **25**, 2723-2734 (2006). https://doi.org/10.1038/sj.emboj.7601152

267 Kurland, J. F. & Tansey, W. P. Myc-mediated transcriptional repression by recruitment of histone deacetylase. *Cancer Res* **68**, 3624-3629 (2008). https://doi.org/10.1158/0008-5472.CAN-07-6552

268 Wang, J. *et al.* The interplay between histone deacetylases and c-Myc in the transcriptional suppression of HPP1 in colon cancer. *Cancer Biol Ther* **15**, 1198-1207 (2014). https://doi.org/10.4161/cbt.29500

269 Zhu, P. *et al.* Induction of HDAC2 expression upon loss of APC in colorectal tumorigenesis. *Cancer Cell* **5**, 455-463 (2004). https://doi.org/10.1016/s1535-6108(04)00114-x

270 Marshall, G. M. *et al.* Transcriptional upregulation of histone deacetylase 2 promotes Myc-induced oncogenic effects. *Oncogene* **29**, 5957-5968 (2010). https://doi.org/10.1038/onc.2010.332
271 Poole, C. J. & van Riggelen, J. MYC-Master Regulator of the Cancer Epigenome and Transcriptome. *Genes (Basel)* **8** (2017). https://doi.org/10.3390/genes8050142
272 Cotterman, R. *et al.* N-Myc regulates a widespread euchromatic program in the human genome partially independent of its role as a classical transcription factor. *Cancer Res* **68**, 9654-9662 (2008). https://doi.org/10.1158/0008-5472.CAN-08-1961
273 Frank, S. R., Schroeder, M., Fernandez, P., Taubert, S. & Amati, B. Binding of c-Myc to chromatin mediates mitogen-induced acetylation of histone H4 and gene activation. *Genes Dev* **15**, 2069-2082 (2001). https://doi.org/10.1101/gad.906601
274 Kim, T. H. *et al.* A high-resolution map of active promoters in the human genome. *Nature* **436**, 876-880 (2005). https://doi.org/10.1038/nature03877
275 Grandori, C., Cowley, S. M., James, L. P. & Eisenman, R. N. The Myc/Max/Mad network and the transcriptional control of cell behavior. *Annu Rev Cell Dev Biol* **16**, 653-699 (2000). https://doi.org/10.1146/annurev.cellbio.16.1.653
276 Heidemann, M., Hintermair, C., Voss, K. & Eick, D. Dynamic phosphorylation patterns of RNA polymerase II CTD during transcription. *Biochim Biophys Acta* **1829**, 55-62 (2013). https://doi.org/10.1016/j.bbagrm.2012.08.013
277 Phatnani, H. P. & Greenleaf, A. L. Phosphorylation and functions of the RNA polymerase II CTD. *Genes Dev* **20**, 2922-2936 (2006). https://doi.org/10.1101/gad.1477006
278 Buratowski, S. Progression through the RNA polymerase II CTD cycle. *Mol Cell* **36**, 541-546 (2009). https://doi.org/10.1016/j.molcel.2009.10.019
279 Egloff, S. & Murphy, S. Cracking the RNA polymerase II CTD code. *Trends Genet* **24**, 280-288 (2008). https://doi.org/10.1016/j.tig.2008.03.008
280 Zhou, Q., Li, T. & Price, D. H. RNA polymerase II elongation control. *Annu Rev Biochem* **81**, 119-143 (2012). https://doi.org/10.1146/annurev-biochem-052610-095910
281 Eberhardy, S. R. & Farnham, P. J. c-Myc mediates activation of the cad promoter via a post-RNA polymerase II recruitment mechanism. *J Biol Chem* **276**, 48562-48571 (2001). https://doi.org/10.1074/jbc.M109014200
282 Eberhardy, S. R. & Farnham, P. J. Myc recruits P-TEFb to mediate the final step in the transcriptional activation of the cad promoter. *J Biol Chem* **277**, 40156-40162 (2002). https://doi.org/10.1074/jbc.M207441200
283 Kanazawa, S., Soucek, L., Evan, G., Okamoto, T. & Peterlin, B. M. c-Myc recruits P-TEFb for transcription, cellular proliferation and apoptosis. *Oncogene* **22**, 5707-5711 (2003). https://doi.org/10.1038/sj.onc.1206800
284 Gargano, B., Amente, S., Majello, B. & Lania, L. P-TEFb is a crucial co-factor for Myc transactivation. *Cell Cycle* **6**, 2031-2037 (2007). https://doi.org/10.4161/cc.6.16.4554
285 Rahl, P. B. *et al.* c-Myc regulates transcriptional pause release. *Cell* **141**, 432-445 (2010). https://doi.org/10.1016/j.cell.2010.03.030
286 Baluapuri, A. *et al.* MYC Recruits SPT5 to RNA Polymerase II to Promote Processive Transcription Elongation. *Mol Cell* **74**, 674-687 e611 (2019). https://doi.org/10.1016/j.molcel.2019.02.031
287 Rahl, P. B. & Young, R. A. MYC and transcription elongation. *Cold Spring Harb Perspect Med* **4**, a020990 (2014). https://doi.org/10.1101/cshperspect.a020990
288 Scagnoli, F. *et al.* A new insight into MYC action: control of RNA polymerase II methylation and transcription termination. *bioRxiv*, 2022.2002.2017.480813 (2022). https://doi.org/10.1101/2022.02.17.480813
289 Zhao, D. Y. *et al.* SMN and symmetric arginine dimethylation of RNA polymerase II C-terminal domain control termination. *Nature* **529**, 48-53 (2016). https://doi.org/10.1038/nature16469
290 Schneider, A., Peukert, K., Eilers, M. & Hanel, F. Association of Myc with the zinc-finger protein Miz-1 defines a novel pathway for gene regulation by Myc. *Curr Top Microbiol Immunol* **224**, 137-146 (1997). https://doi.org/10.1007/978-3-642-60801-8_14
291 Wiese, K. E. *et al.* Repression of SRF target genes is critical for Myc-dependent apoptosis of epithelial cells. *EMBO J* **34**, 1554-1571 (2015). https://doi.org/10.15252/embj.201490467
292 Yang, W. *et al.* Repression of transcription of the p27(Kip1) cyclin-dependent kinase inhibitor gene by c-Myc. *Oncogene* **20**, 1688-1702 (2001). https://doi.org/10.1038/sj.onc.1204245
293 Alevizopoulos, K., Vlach, J., Hennecke, S. & Amati, B. Cyclin E and c-Myc promote cell proliferation in the presence of p16INK4a and of hypophosphorylated retinoblastoma family proteins. *EMBO J* **16**, 5322-5333 (1997). https://doi.org/10.1093/emboj/16.17.5322
294 Warner, B. J., Blain, S. W., Seoane, J. & Massague, J. Myc downregulation by transforming growth factor beta required for activation of the p15(Ink4b) G(1) arrest pathway. *Mol Cell Biol* **19**, 5913-5922 (1999). https://doi.org/10.1128/MCB.19.9.5913
295 Shostak, A. *et al.* MYC/MIZ1-dependent gene repression inversely coordinates the circadian clock with cell cycle and proliferation. *Nat Commun* **7**, 11807 (2016). https://doi.org/10.1038/ncomms11807
296 Herkert, B. & Eilers, M. Transcriptional repression: the dark side of myc. *Genes Cancer* **1**, 580-586 (2010). https://doi.org/10.1177/1947601910379012
297 Koh, C. M. *et al.* Myc enforces overexpression of EZH2 in early prostatic neoplasia via transcriptional and post-transcriptional mechanisms. *Oncotarget* **2**, 669-683 (2011). https://doi.org/10.18632/oncotarget.327
298 Sander, S. *et al.* MYC stimulates EZH2 expression by repression of its negative regulator miR-26a. *Blood* **112**, 4202-4212 (2008). https://doi.org/10.1182/blood-2008-03-147645
299 Whitfield, J. R. & Soucek, L. The long journey to bring a Myc inhibitor to the clinic. *J Cell Biol* **220** (2021). https://doi.org/10.1083/jcb.202103090
300 Prochownik, E. V. & Vogt, P. K. Therapeutic Targeting of Myc. *Genes Cancer* **1**, 650-659 (2010). https://doi.org/10.1177/1947601910377494
301 Soucek, L. *et al.* Modelling Myc inhibition as a cancer therapy. *Nature* **455**, 679-683 (2008). https://doi.org/10.1038/nature07260
302 Chen, H., Liu, H. & Qing, G. Targeting oncogenic Myc as a strategy for cancer treatment. *Signal Transduct Target Ther* **3**, 5 (2018). https://doi.org/10.1038/s41392-018-0008-7
303 Whitfield, J. R., Beaulieu, M. E. & Soucek, L. Strategies to Inhibit Myc and Their Clinical Applicability. *Front Cell Dev Biol* **5**, 10 (2017). https://doi.org/10.3389/fcell.2017.00010
304 Chen, B. J., Wu, Y. L., Tanaka, Y. & Zhang, W. Small molecules targeting c-Myc oncogene: promising anti-cancer therapeutics. *Int J Biol Sci* **10**, 1084-1096 (2014). https://doi.org/10.7150/ijbs.10190
305 Neidle, S. Quadruplex Nucleic Acids as Novel Therapeutic Targets. *J Med Chem* **59**, 5987-6011 (2016). https://doi.org/10.1021/acs.jmedchem.5b01835
306 Sklar, M. D. *et al.* Depletion of c-myc with specific antisense sequences reverses the transformed phenotype in ras oncogene-transformed NIH 3T3 cells. *Mol Cell Biol* **11**, 3699-3710 (1991). https://doi.org/10.1128/mcb.11.7.3699-3710.1991
307 Arora, V. *et al.* c-Myc antisense limits rat liver regeneration and indicates role for c-Myc in regulating cytochrome P-450 3A activity. *J Pharmacol Exp Ther* **292**, 921-928 (2000).
308 Dienstmann, R. *et al.* Safety and Activity of the First-in-Class Sym004 Anti-EGFR Antibody Mixture in Patients with Refractory Colorectal Cancer. *Cancer Discov* **5**, 598-609 (2015). https://doi.org/10.1158/2159-8290.CD-14-1432
309 Zhou, Y. *et al.* Targeting Myc Interacting Proteins as a Winding Path in Cancer Therapy. *Front Pharmacol* **12**,

748852 (2021). https://doi.org/10.3389/fphar.2021.748852
310 Mertz, J. A. *et al.* Targeting MYC dependence in cancer by inhibiting BET bromodomains. *Proc Natl Acad Sci U S A* **108**, 16669-16674 (2011). https://doi.org/10.1073/pnas.1108190108
311 Delmore, J. E. *et al.* BET bromodomain inhibition as a therapeutic strategy to target c-Myc. *Cell* **146**, 904-917 (2011). https://doi.org/10.1016/j.cell.2011.08.017
312 Zuber, J. *et al.* RNAi screen identifies Brd4 as a therapeutic target in acute myeloid leukaemia. *Nature* **478**, 524-528 (2011). https://doi.org/10.1038/nature10334
313 Puissant, A. *et al.* Targeting MYCN in neuroblastoma by BET bromodomain inhibition. *Cancer Discov* **3**, 308-323 (2013). https://doi.org/10.1158/2159-8290.CD-12-0418
314 Filippakopoulos, P. & Knapp, S. Targeting bromodomains: epigenetic readers of lysine acetylation. *Nat Rev Drug Discov* **13**, 337-356 (2014). https://doi.org/10.1038/nrd4286
315 Fowler, T. *et al.* Regulation of MYC expression and differential JQ1 sensitivity in cancer cells. *PLoS One* **9**, e87003 (2014). https://doi.org/10.1371/journal.pone.0087003
316 Huang, C. H. *et al.* CDK9-mediated transcription elongation is required for MYC addiction in hepatocellular carcinoma. *Genes Dev* **28**, 1800-1814 (2014). https://doi.org/10.1101/gad.244368.114
317 Gregory, G. P. *et al.* CDK9 inhibition by dinaciclib potently suppresses Mcl-1 to induce durable apoptotic responses in aggressive MYC-driven B-cell lymphoma in vivo. *Leukemia* **29**, 1437-1441 (2015). https://doi.org/10.1038/leu.2015.10
318 Hashiguchi, T. *et al.* Cyclin-Dependent Kinase-9 Is a Therapeutic Target in MYC-Expressing Diffuse Large B-Cell Lymphoma. *Mol Cancer Ther* **18**, 1520-1532 (2019). https://doi.org/10.1158/1535-7163.MCT-18-1023
319 Christensen, C. L. *et al.* Targeting transcriptional addictions in small cell lung cancer with a covalent CDK7 inhibitor. *Cancer Cell* **26**, 909-922 (2014). https://doi.org/10.1016/j.ccell.2014.10.019
320 Chipumuro, E. *et al.* CDK7 inhibition suppresses super-enhancer-linked oncogenic transcription in MYCN-driven cancer. *Cell* **159**, 1126-1139 (2014). https://doi.org/10.1016/j.cell.2014.10.024
321 Wang, C. *et al.* A CRISPR screen identifies CDK7 as a therapeutic target in hepatocellular carcinoma. *Cell Res* **28**, 690-692 (2018). https://doi.org/10.1038/s41422-018-0020-z
322 Zeng, M. *et al.* Targeting MYC dependency in ovarian cancer through inhibition of CDK7 and CDK12/13. *Elife* **7** (2018). https://doi.org/10.7554/eLife.39030
323 Pourdehnad, M. *et al.* Myc and mTOR converge on a common node in protein synthesis control that confers synthetic lethality in Myc-driven cancers. *Proc Natl Acad Sci U S A* **110**, 11988-11993 (2013). https://doi.org/10.1073/pnas.1310230110
324 Sonenberg, N. & Hinnebusch, A. G. Regulation of translation initiation in eukaryotes: mechanisms and biological targets. *Cell* **136**, 731-745 (2009). https://doi.org/10.1016/j.cell.2009.01.042
325 Wiegering, A. *et al.* Targeting Translation Initiation Bypasses Signaling Crosstalk Mechanisms That Maintain High MYC Levels in Colorectal Cancer. *Cancer Discov* **5**, 768-781 (2015). https://doi.org/10.1158/2159-8290.CD-14-1040
326 Berg, T. Small-molecule modulators of c-Myc/Max and Max/Max interactions. *Curr Top Microbiol Immunol* **348**, 139-149 (2011). https://doi.org/10.1007/82_2010_90
327 Fletcher, S. & Prochownik, E. V. Small-molecule inhibitors of the Myc oncoprotein. *Biochim Biophys Acta* **1849**, 525-543 (2015). https://doi.org/10.1016/j.bbagrm.2014.03.005
328 Hart, J. R. *et al.* Inhibitor of MYC identified in a Krohnke pyridine library. *Proc Natl Acad Sci U S A* **111**, 12556-12561 (2014). https://doi.org/10.1073/pnas.1319488111
329 Choi, S. H. *et al.* Targeted Disruption of Myc-Max Oncoprotein Complex by a Small Molecule. *ACS Chem Biol* **12**, 2715-2719 (2017). https://doi.org/10.1021/acschembio.7b00799
330 Castell, A. *et al.* A selective high affinity MYC-binding compound inhibits MYC:MAX interaction and MYC-dependent tumor cell proliferation. *Sci Rep* **8**, 10064 (2018). https://doi.org/10.1038/s41598-018-28107-4
331 Jeong, K. C., Ahn, K. O. & Yang, C. H. Small-molecule inhibitors of c-Myc transcriptional factor suppress proliferation and induce apoptosis of promyelocytic leukemia cell via cell cycle arrest. *Mol Biosyst* **6**, 1503-1509 (2010). https://doi.org/10.1039/c002534h
332 Jeong, K. C. *et al.* Intravesical instillation of c-MYC inhibitor KSI-3716 suppresses orthotopic bladder tumor growth. *J Urol* **191**, 510-518 (2014). https://doi.org/10.1016/j.juro.2013.07.019
333 Soucek, L. *et al.* Design and properties of a Myc derivative that efficiently homodimerizes. *Oncogene* **17**, 2463-2472 (1998). https://doi.org/10.1038/sj.onc.1202199
334 Savino, M. *et al.* The action mechanism of the Myc inhibitor termed Omomyc may give clues on how to target Myc for cancer therapy. *PLoS One* **6**, e22284 (2011). https://doi.org/10.1371/journal.pone.0022284
335 Soucek, L. *et al.* Omomyc, a potential Myc dominant negative, enhances Myc-induced apoptosis. *Cancer Res* **62**, 3507-3510 (2002).
336 Sodir, N. M. *et al.* Endogenous Myc maintains the tumor microenvironment. *Genes Dev* **25**, 907-916 (2011). https://doi.org/10.1101/gad.2038411
337 Annibali, D. *et al.* Myc inhibition is effective against glioma and reveals a role for Myc in proficient mitosis. *Nat Commun* **5**, 4632 (2014). https://doi.org/10.1038/ncomms5632
338 Soucek, L., Nasi, S. & Evan, G. I. Omomyc expression in skin prevents Myc-induced papillomatosis. *Cell Death Differ* **11**, 1038-1045 (2004). https://doi.org/10.1038/sj.cdd.4401443
339 Beaulieu, M. E. *et al.* Intrinsic cell-penetrating activity propels Omomyc from proof of concept to viable anti-MYC therapy. *Sci Transl Med* **11** (2019). https://doi.org/10.1126/scitranslmed.aar5012
340 Dobzhansky, T. Genetics of natural populations; recombination and variability in populations of Drosophila pseudoobscura. *Genetics* **31**, 269-290 (1946). https://doi.org/10.1093/genetics/31.3.269
341 Amati, B., Alevizopoulos, K. & Vlach, J. Myc and the cell cycle. *Front Biosci* **3**, d250-268 (1998). https://doi.org/10.2741/a239
342 Horiuchi, D. *et al.* MYC pathway activation in triple-negative breast cancer is synthetic lethal with CDK inhibition. *J Exp Med* **209**, 679-696 (2012). https://doi.org/10.1084/jem.20111512
343 Campaner, S. *et al.* Cdk2 suppresses cellular senescence induced by the c-myc oncogene. *Nat Cell Biol* **12**, 54-59; sup pp 51-14 (2010). https://doi.org/10.1038/ncb2004
344 MacCallum, D. E. *et al.* Seliciclib (CYC202, R-Roscovitine) induces cell death in multiple myeloma cells by inhibition of RNA polymerase II-dependent transcription and down-regulation of Mcl-1. *Cancer Res* **65**, 5399-5407 (2005). https://doi.org/10.1158/0008-5472.CAN-05-0233
345 Diepstraten, S. T. *et al.* The manipulation of apoptosis for cancer therapy using BH3-mimetic drugs. *Nat Rev Cancer* **22**, 45-64 (2022). https://doi.org/10.1038/s41568-021-00407-4
346 Morschhauser, F. *et al.* A phase 2 study of venetoclax plus R-CHOP as first-line treatment for patients with diffuse large B-cell lymphoma. *Blood* **137**, 600-609 (2021). https://doi.org/10.1182/blood.2020006578
347 Rava, M. *et al.* Therapeutic synergy between tigecycline and venetoclax in a preclinical model of MYC/BCL2 double-hit B cell lymphoma. *Sci Transl Med* **10** (2018). https://doi.org/10.1126/scitranslmed.aan8723
348 Cummin, T. E. C. *et al.* BET inhibitors synergize with venetoclax to induce apoptosis in MYC-driven lymphomas with high BCL-2 expression. *Blood Adv* **4**, 3316-3328 (2020). https://doi.org/10.1182/bloodadvances.2020002231

349 Grabow, S. *et al.* Critical B-lymphoid cell intrinsic role of endogenous MCL-1 in c-MYC-induced lymphomagenesis. *Cell Death Dis* **7**, e2132 (2016). https://doi.org/10.1038/cddis.2016.43

350 Thomas, L. R. *et al.* Interaction of the oncoprotein transcription factor MYC with its chromatin cofactor WDR5 is essential for tumor maintenance. *Proc Natl Acad Sci U S A* **116**, 25260-25268 (2019). https://doi.org/10.1073/pnas.1910391116

351 Thomas, L. R. *et al.* Interaction with WDR5 promotes target gene recognition and tumorigenesis by MYC. *Mol Cell* **58**, 440-452 (2015). https://doi.org/10.1016/j.molcel.2015.02.028

352 Sun, Y. *et al.* WDR5 Supports an N-Myc Transcriptional Complex That Drives a Protumorigenic Gene Expression Signature in Neuroblastoma. *Cancer Res* **75**, 5143-5154 (2015). https://doi.org/10.1158/0008-5472.CAN-15-0423

353 Garcia-Carpizo, V. *et al.* CREBBP/EP300 bromodomains are critical to sustain the GATA1/MYC regulatory axis in proliferation. *Epigenetics Chromatin* **11**, 30 (2018). https://doi.org/10.1186/s13072-018-0197-x

354 Mustachio, L. M., Roszik, J., Farria, A. T., Guerra, K. & Dent, S. Y. Repression of GCN5 expression or activity attenuates c-MYC expression in non-small cell lung cancer. *Am J Cancer Res* **9**, 1830-1845 (2019).

355 Farria, A. T., Mustachio, L. M., Akdemir, Z. H. C. & Dent, S. Y. R. GCN5 HAT inhibition reduces human Burkitt lymphoma cell survival through reduction of MYC target gene expression and impeding BCR signaling pathways. *Oncotarget* **10**, 5847-5858 (2019). https://doi.org/10.18632/oncotarget.27226

356 Kretzner, L. *et al.* Combining histone deacetylase inhibitor vorinostat with aurora kinase inhibitors enhances lymphoma cell killing with repression of c-Myc, hTERT, and microRNA levels. *Cancer Res* **71**, 3912-3920 (2011). https://doi.org/10.1158/0008-5472.CAN-10-2259

357 Pei, Y. *et al.* HDAC and PI3K Antagonists Cooperate to Inhibit Growth of MYC-Driven Medulloblastoma. *Cancer Cell* **29**, 311-323 (2016). https://doi.org/10.1016/j.ccell.2016.02.011

358 Lernoux, M. *et al.* Novel HDAC inhibitor MAKV-8 and imatinib synergistically kill chronic myeloid leukemia cells via inhibition of BCR-ABL/MYC-signaling: effect on imatinib resistance and stem cells. *Clin Epigenetics* **12**, 69 (2020). https://doi.org/10.1186/s13148-020-00839-z

359 D'Andrea, A. *et al.* The mitochondrial translation machinery as a therapeutic target in Myc-driven lymphomas. *Oncotarget* **7**, 72415-72430 (2016). https://doi.org/10.18632/oncotarget.11719

360 Donati, G. *et al.* Targeting mitochondrial respiration and the BCL2 family in high-grade MYC-associated B-cell lymphoma. *Mol Oncol* **16**, 1132-1152 (2022). https://doi.org/10.1002/1878-0261.13115

361 Oran, A. R. *et al.* Multi-focal control of mitochondrial gene expression by oncogenic MYC provides potential therapeutic targets in cancer. *Oncotarget* **7**, 72395-72414 (2016). https://doi.org/10.18632/oncotarget.11718

362 Mattioni, T., Louvion, J. F. & Picard, D. Regulation of protein activities by fusion to steroid binding domains. *Methods Cell Biol* **43 Pt A**, 335-352 (1994). https://doi.org/10.1016/s0091-679x(08)60611-1

363 Eilers, M., Picard, D., Yamamoto, K. R. & Bishop, J. M. Chimaeras of myc oncoprotein and steroid receptors cause hormone-dependent transformation of cells. *Nature* **340**, 66-68 (1989). https://doi.org/10.1038/340066a0

364 Eilers, M., Schirm, S. & Bishop, J. M. The MYC protein activates transcription of the alpha-prothymosin gene. *EMBO J* **10**, 133-141 (1991). https://doi.org/10.1002/j.1460-2075.1991.tb07929.x

365 Whitfield, J., Littlewood, T., Evan, G. I. & Soucek, L. The estrogen receptor fusion system in mouse models: a reversible switch. *Cold Spring Harb Protoc* **2015**, 227-234 (2015). https://doi.org/10.1101/pdb.top069815

366 Littlewood, T. D., Hancock, D. C., Danielian, P. S., Parker, M. G. & Evan, G. I. A modified oestrogen receptor ligand-binding domain as an improved switch for the regulation of heterologous proteins. *Nucleic Acids Res* **23**, 1686-1690 (1995). https://doi.org/10.1093/nar/23.10.1686

367 Fang, C. M., Shi, C. & Xu, Y. H. Deregulated c-myc expression in quiescent CHO cells induces target gene transcription and subsequent apoptotic phenotype. *Cell Res* **9**, 305-314 (1999). https://doi.org/10.1038/sj.cr.7290029

368 Holzel, M. *et al.* Myc/Max/Mad regulate the frequency but not the duration of productive cell cycles. *EMBO Rep* **2**, 1125-1132 (2001). https://doi.org/10.1093/embo-reports/kve251

369 Bernardin, F., Yang, Y., Civin, C. I. & Friedman, A. D. c-Myc overcomes cell cycle inhibition by CBFbeta-SMMHC, a myeloid leukemia oncoprotein. *Cancer Biol Ther* **1**, 492-496 (2002). https://doi.org/10.4161/cbt.1.5.163

370 Fan, Y., Dickman, K. G. & Zong, W. X. Akt and c-Myc differentially activate cellular metabolic programs and prime cells to bioenergetic inhibition. *J Biol Chem* **285**, 7324-7333 (2010). https://doi.org/10.1074/jbc.M109.035584

371 Wilson, A. *et al.* c-Myc controls the balance between hematopoietic stem cell self-renewal and differentiation. *Genes Dev* **18**, 2747-2763 (2004). https://doi.org/10.1101/gad.313104

372 Bettess, M. D. *et al.* c-Myc is required for the formation of intestinal crypts but dispensable for homeostasis of the adult intestinal epithelium. *Mol Cell Biol* **25**, 7868-7878 (2005). https://doi.org/10.1128/MCB.25.17.7868-7878.2005

373 Oskarsson, T. *et al.* Skin epidermis lacking the c-Myc gene is resistant to Ras-driven tumorigenesis but can reacquire sensitivity upon additional loss of the p21Cip1 gene. *Genes Dev* **20**, 2024-2029 (2006). https://doi.org/10.1101/gad.381206

374 Pajic, A. *et al.* Cell cycle activation by c-myc in a burkitt lymphoma model cell line. *Int J Cancer* **87**, 787-793 (2000). https://doi.org/10.1002/1097-0215(20000915)87:6<787::aid-ijc4>3.0.co;2-6

375 Kress, T. R. *et al.* Identification of MYC-Dependent Transcriptional Programs in Oncogene-Addicted Liver Tumors. *Cancer Res* **76**, 3463-3472 (2016). https://doi.org/10.1158/0008-5472.CAN-16-0316

376 Yustein, J. T. *et al.* Induction of ectopic Myc target gene JAG2 augments hypoxic growth and tumorigenesis in a human B-cell model. *Proc Natl Acad Sci U S A* **107**, 3534-3539 (2010). https://doi.org/10.1073/pnas.0901230107

377 Singh, K. *et al.* c-MYC regulates mRNA translation efficiency and start-site selection in lymphoma. *J Exp Med* **216**, 1509-1524 (2019). https://doi.org/10.1084/jem.20181726

378 Nishimura, K., Fukagawa, T., Takisawa, H., Kakimoto, T. & Kanemaki, M. An auxin-based degron system for the rapid depletion of proteins in nonplant cells. *Nat Methods* **6**, 917-922 (2009). https://doi.org/10.1038/nmeth.1401

379 Yesbolatova, A. *et al.* The auxin-inducible degron 2 technology provides sharp degradation control in yeast, mammalian cells, and mice. *Nat Commun* **11**, 5701 (2020). https://doi.org/10.1038/s41467-020-19532-z

380 Sakaue-Sawano, A. *et al.* Genetically Encoded Tools for Optical Dissection of the Mammalian Cell Cycle. *Mol Cell* **68**, 626-640 e625 (2017). https://doi.org/10.1016/j.molcel.2017.10.001

381 Gandin, V. *et al.* Eukaryotic initiation factor 6 is rate-limiting in translation, growth and transformation. *Nature* **455**, 684-688 (2008). https://doi.org/10.1038/nature07267

382 Kim, D. *et al.* TopHat2: accurate alignment of transcriptomes in the presence of insertions, deletions and gene fusions. *Genome Biol* **14**, R36 (2013). https://doi.org/10.1186/gb-2013-14-4-r36

383 Liao, Y., Smyth, G. K. & Shi, W. featureCounts: an efficient general purpose program for assigning sequence reads to genomic features. *Bioinformatics* **30**, 923-930 (2014). https://doi.org/10.1093/bioinformatics/btt656

384 Love, M. I., Huber, W. & Anders, S. Moderated estimation of fold change and dispersion for RNA-seq data with

DESeq2. *Genome Biol* **15**, 550 (2014). https://doi.org/10.1186/s13059-014-0550-8
385 Dobin, A. *et al.* STAR: ultrafast universal RNA-seq aligner. *Bioinformatics* **29**, 15-21 (2013). https://doi.org/10.1093/bioinformatics/bts635
386 Bianchi, V. *et al.* Integrated Systems for NGS Data Management and Analysis: Open Issues and Available Solutions. *Front Genet* **7**, 75 (2016). https://doi.org/10.3389/fgene.2016.00075
387 Zhang, Y. *et al.* Model-based analysis of ChIP-Seq (MACS). *Genome Biol* **9**, R137 (2008). https://doi.org/10.1186/gb-2008-9-9-r137
388 Gentleman, R. C. *et al.* Bioconductor: open software development for computational biology and bioinformatics. *Genome Biol* **5**, R80 (2004). https://doi.org/10.1186/gb-2004-5-10-r80
389 Kishore, K. *et al.* methylPipe and compEpiTools: a suite of R packages for the integrative analysis of epigenomics data. *BMC Bioinformatics* **16**, 313 (2015). https://doi.org/10.1186/s12859-015-0742-6
390 Subramanian, A. *et al.* Gene set enrichment analysis: a knowledge-based approach for interpreting genome-wide expression profiles. *Proc Natl Acad Sci U S A* **102**, 15545-15550 (2005). https://doi.org/10.1073/pnas.0506580102
391 Mootha, V. K. *et al.* PGC-1alpha-responsive genes involved in oxidative phosphorylation are coordinately downregulated in human diabetes. *Nat Genet* **34**, 267-273 (2003). https://doi.org/10.1038/ng1180
392 Liberzon, A. *et al.* The Molecular Signatures Database (MSigDB) hallmark gene set collection. *Cell Syst* **1**, 417-425 (2015). https://doi.org/10.1016/j.cels.2015.12.004
393 Liberzon, A. *et al.* Molecular signatures database (MSigDB) 3.0. *Bioinformatics* **27**, 1739-1740 (2011). https://doi.org/10.1093/bioinformatics/btr260
394 Wu, T. *et al.* clusterProfiler 4.0: A universal enrichment tool for interpreting omics data. *Innovation (Camb)* **2**, 100141 (2021). https://doi.org/10.1016/j.xinn.2021.100141
395 Yu, G., Wang, L. G., Han, Y. & He, Q. Y. clusterProfiler: an R package for comparing biological themes among gene clusters. *OMICS* **16**, 284-287 (2012). https://doi.org/10.1089/omi.2011.0118
396 Schmidt, E. V. The role of c-myc in cellular growth control. *Oncogene* **18**, 2988-2996 (1999). https://doi.org/10.1038/sj.onc.1202751
397 Melnik, S. *et al.* Impact of c-MYC expression on proliferation, differentiation, and risk of neoplastic transformation of human mesenchymal stromal cells. *Stem Cell Res Ther* **10**, 73 (2019). https://doi.org/10.1186/s13287-019-1187-z
398 Wang, H. *et al.* c-Myc depletion inhibits proliferation of human tumor cells at various stages of the cell cycle. *Oncogene* **27**, 1905-1915 (2008). https://doi.org/10.1038/sj.onc.1210823
399 Horton, M. B. *et al.* Multiplexed Division Tracking Dyes for Proliferation-Based Clonal Lineage Tracing. *J Immunol* **201**, 1097-1103 (2018). https://doi.org/10.4049/jimmunol.1800481
400 Podhorecka, M., Skladanowski, A. & Bozko, P. H2AX Phosphorylation: Its Role in DNA Damage Response and Cancer Therapy. *J Nucleic Acids* **2010** (2010). https://doi.org/10.4061/2010/920161
401 Nakayama, K. I. & Nakayama, K. Ubiquitin ligases: cell-cycle control and cancer. *Nat Rev Cancer* **6**, 369-381 (2006). https://doi.org/10.1038/nrc1881
402 Sakaue-Sawano, A. *et al.* Visualizing spatiotemporal dynamics of multicellular cell-cycle progression. *Cell* **132**, 487-498 (2008). https://doi.org/10.1016/j.cell.2007.12.033
403 Nishitani, H., Lygerou, Z., Nishimoto, T. & Nurse, P. The Cdt1 protein is required to license DNA for replication in fission yeast. *Nature* **404**, 625-628 (2000). https://doi.org/10.1038/35007110
404 Vodermaier, H. C. APC/C and SCF: controlling each other and the cell cycle. *Curr Biol* **14**, R787-796 (2004). https://doi.org/10.1016/j.cub.2004.09.020
405 Wei, W. *et al.* Degradation of the SCF component Skp2 in cell-cycle phase G1 by the anaphase-promoting complex. *Nature* **428**, 194-198 (2004). https://doi.org/10.1038/nature02381
406 Benmaamar, R. & Pagano, M. Involvement of the SCF complex in the control of Cdh1 degradation in S-phase. *Cell Cycle* **4**, 1230-1232 (2005). https://doi.org/10.4161/cc.4.9.2048
407 Gressel, S. *et al.* CDK9-dependent RNA polymerase II pausing controls transcription initiation. *Elife* **6** (2017). https://doi.org/10.7554/eLife.29736
408 Cowling, V. H. & Cole, M. D. Myc Regulation of mRNA Cap Methylation. *Genes Cancer* **1**, 576-579 (2010). https://doi.org/10.1177/1947601910378025
409 Lorenzin, F. *et al.* Different promoter affinities account for specificity in MYC-dependent gene regulation. *Elife* **5** (2016). https://doi.org/10.7554/eLife.15161
410 Marks, H. *et al.* The transcriptional and epigenomic foundations of ground state pluripotency. *Cell* **149**, 590-604 (2012). https://doi.org/10.1016/j.cell.2012.03.026
411 Spicuglia, S. & Vanhille, L. Chromatin signatures of active enhancers. *Nucleus* **3**, 126-131 (2012). https://doi.org/10.4161/nucl.19232
412 Calo, E. & Wysocka, J. Modification of enhancer chromatin: what, how, and why? *Mol Cell* **49**, 825-837 (2013). https://doi.org/10.1016/j.molcel.2013.01.038
413 Zeid, R. *et al.* Enhancer invasion shapes MYCN-dependent transcriptional amplification in neuroblastoma. *Nat Genet* **50**, 515-523 (2018). https://doi.org/10.1038/s41588-018-0044-9
414 Jakobsen, S. T. *et al.* MYC enhancer invasion promotes prognostic cancer type-specific gene programs through an epigenetic switch. *bioRxiv* (2023). https://doi.org/https://doi.org/10.1101/2023.01.06.522970
415 Harlen, K. M. & Churchman, L. S. The code and beyond: transcription regulation by the RNA polymerase II carboxy-terminal domain. *Nat Rev Mol Cell Biol* **18**, 263-273 (2017). https://doi.org/10.1038/nrm.2017.10
416 Herzel, L., Ottoz, D. S. M., Alpert, T. & Neugebauer, K. M. Splicing and transcription touch base: co-transcriptional spliceosome assembly and function. *Nat Rev Mol Cell Biol* **18**, 637-650 (2017). https://doi.org/10.1038/nrm.2017.63
417 Cowling, V. H. & Cole, M. D. The Myc transactivation domain promotes global phosphorylation of the RNA polymerase II carboxy-terminal domain independently of direct DNA binding. *Mol Cell Biol* **27**, 2059-2073 (2007). https://doi.org/10.1128/MCB.01828-06
418 Posternak, V., Ung, M. H., Cheng, C. & Cole, M. D. MYC Mediates mRNA Cap Methylation of Canonical Wnt/beta-Catenin Signaling Transcripts By Recruiting CDK7 and RNA Methyltransferase. *Mol Cancer Res* **15**, 213-224 (2017). https://doi.org/10.1158/1541-7786.MCR-16-0247
419 Lombardi, O., Varshney, D., Phillips, N. M. & Cowling, V. H. c-Myc deregulation induces mRNA capping enzyme dependency. *Oncotarget* **7**, 82273-82288 (2016). https://doi.org/10.18632/oncotarget.12701
420 Arava, Y. *et al.* Genome-wide analysis of mRNA translation profiles in Saccharomyces cerevisiae. *Proc Natl Acad Sci U S A* **100**, 3889-3894 (2003). https://doi.org/10.1073/pnas.0635171100
421 Vecchio, E. *et al.* Insights about MYC and Apoptosis in B-Lymphomagenesis: An Update from Murine Models. *Int J Mol Sci* **21** (2020). https://doi.org/10.3390/ijms21124265
422 Singh, R., Letai, A. & Sarosiek, K. Regulation of apoptosis in health and disease: the balancing act of BCL-2 family proteins. *Nat Rev Mol Cell Biol* **20**, 175-193 (2019). https://doi.org/10.1038/s41580-018-0089-8
423 Vaux, D. L., Cory, S. & Adams, J. M. Bcl-2 gene promotes haemopoietic cell survival and cooperates with c-myc to immortalize pre-B cells. *Nature* **335**, 440-442 (1988). https://doi.org/10.1038/335440a0
424 Xu, Z., Yan, Y., Li, Z., Qian, L. & Gong, Z. The Antibiotic Drug Tigecycline: A Focus on its Promising Anticancer Properties.

Front Pharmacol **7**, 473 (2016). https://doi.org/10.3389/fphar.2016.00473
425 Vangapandu, H. V. *et al.* Biological and metabolic effects of IACS-010759, an OxPhos inhibitor, on chronic lymphocytic leukemia cells. *Oncotarget* **9**, 24980-24991 (2018). https://doi.org/10.18632/oncotarget.25166
426 Johnson-Farley, N., Veliz, J., Bhagavathi, S. & Bertino, J. R. ABT-199, a BH3 mimetic that specifically targets Bcl-2, enhances the antitumor activity of chemotherapy, bortezomib and JQ1 in "double hit" lymphoma cells. *Leuk Lymphoma* **56**, 2146-2152 (2015). https://doi.org/10.3109/10428194.2014.981172
427 Stolz, C. *et al.* Targeting Bcl-2 family proteins modulates the sensitivity of B-cell lymphoma to rituximab-induced apoptosis. *Blood* **112**, 3312-3321 (2008). https://doi.org/10.1182/blood-2007-11-124487
428 Klanova, M. *et al.* Targeting of BCL2 Family Proteins with ABT-199 and Homoharringtonine Reveals BCL2- and MCL1-Dependent Subgroups of Diffuse Large B-Cell Lymphoma. *Clin Cancer Res* **22**, 1138-1149 (2016). https://doi.org/10.1158/1078-0432.CCR-15-1191
429 Dang, C. V. *et al.* The c-Myc target gene network. *Semin Cancer Biol* **16**, 253-264 (2006). https://doi.org/10.1016/j.semcancer.2006.07.014
430 Wang, C. *et al.* Alternative approaches to target Myc for cancer treatment. *Signal Transduct Target Ther* **6**, 117 (2021). https://doi.org/10.1038/s41392-021-00500-y
431 Duffy, M. J., O'Grady, S., Tang, M. & Crown, J. MYC as a target for cancer treatment. *Cancer Treat Rev* **94**, 102154 (2021). https://doi.org/10.1016/j.ctrv.2021.102154
432 Holland, A. J., Fachinetti, D., Han, J. S. & Cleveland, D. W. Inducible, reversible system for the rapid and complete degradation of proteins in mammalian cells. *Proc Natl Acad Sci U S A* **109**, E3350-3357 (2012). https://doi.org/10.1073/pnas.1216880109
433 Negishi, T. *et al.* The auxin-inducible degron 2 (AID2) system enables controlled protein knockdown during embryogenesis and development in Caenorhabditis elegans. *Genetics* **220** (2022). https://doi.org/10.1093/genetics/iyab218
434 Heinzel, S. *et al.* A Myc-dependent division timer complements a cell-death timer to regulate T cell and B cell responses. *Nat Immunol* **18**, 96-103 (2017). https://doi.org/10.1038/ni.3598
435 Nguyen, L., Papenhausen, P. & Shao, H. The Role of c-MYC in B-Cell Lymphomas: Diagnostic and Molecular Aspects. *Genes (Basel)* **8** (2017). https://doi.org/10.3390/genes8040116
436 Das, G., Shravage, B. V. & Baehrecke, E. H. Regulation and function of autophagy during cell survival and cell death. *Cold Spring Harb Perspect Biol* **4** (2012). https://doi.org/10.1101/cshperspect.a008813
437 Kimura, S., Fujita, N., Noda, T. & Yoshimori, T. Monitoring autophagy in mammalian cultured cells through the dynamics of LC3. *Methods Enzymol* **452**, 1-12 (2009). https://doi.org/10.1016/S0076-6879(08)03601-X
438 Sears, R., Ohtani, K. & Nevins, J. R. Identification of positively and negatively acting elements regulating expression of the E2F2 gene in response to cell growth signals. *Mol Cell Biol* **17**, 5227-5235 (1997). https://doi.org/10.1128/MCB.17.9.5227
439 Leone, G., DeGregori, J., Sears, R., Jakoi, L. & Nevins, J. R. Myc and Ras collaborate in inducing accumulation of active cyclin E/Cdk2 and E2F. *Nature* **387**, 422-426 (1997). https://doi.org/10.1038/387422a0
440 Adams, M. R., Sears, R., Nuckolls, F., Leone, G. & Nevins, J. R. Complex transcriptional regulatory mechanisms control expression of the E2F3 locus. *Mol Cell Biol* **20**, 3633-3639 (2000). https://doi.org/10.1128/MCB.20.10.3633-3639.2000
441 Wall, M. *et al.* Translational control of c-MYC by rapamycin promotes terminal myeloid differentiation. *Blood* **112**, 2305-2317 (2008). https://doi.org/10.1182/blood-2007-09-111856
442 Elkon, R. *et al.* Myc coordinates transcription and translation to enhance transformation and suppress invasiveness. *EMBO Rep* **16**, 1723-1736 (2015). https://doi.org/10.15252/embr.201540717
443 Xu, Y. *et al.* Translation control of the immune checkpoint in cancer and its therapeutic targeting. *Nat Med* **25**, 301-311 (2019). https://doi.org/10.1038/s41591-018-0321-2
444 Wolf E., E. M. Targeting MYC Proteins for Tumor Therapy. *Annual Review of Cancer Biology* **4** (2020).
445 Das, S. K. *et al.* MYC assembles and stimulates topoisomerases 1 and 2 in a "topoisome". *Mol Cell* **82**, 140-158 e112 (2022). https://doi.org/10.1016/j.molcel.2021.11.016

6. SUPPLEMENTARY FIGURES

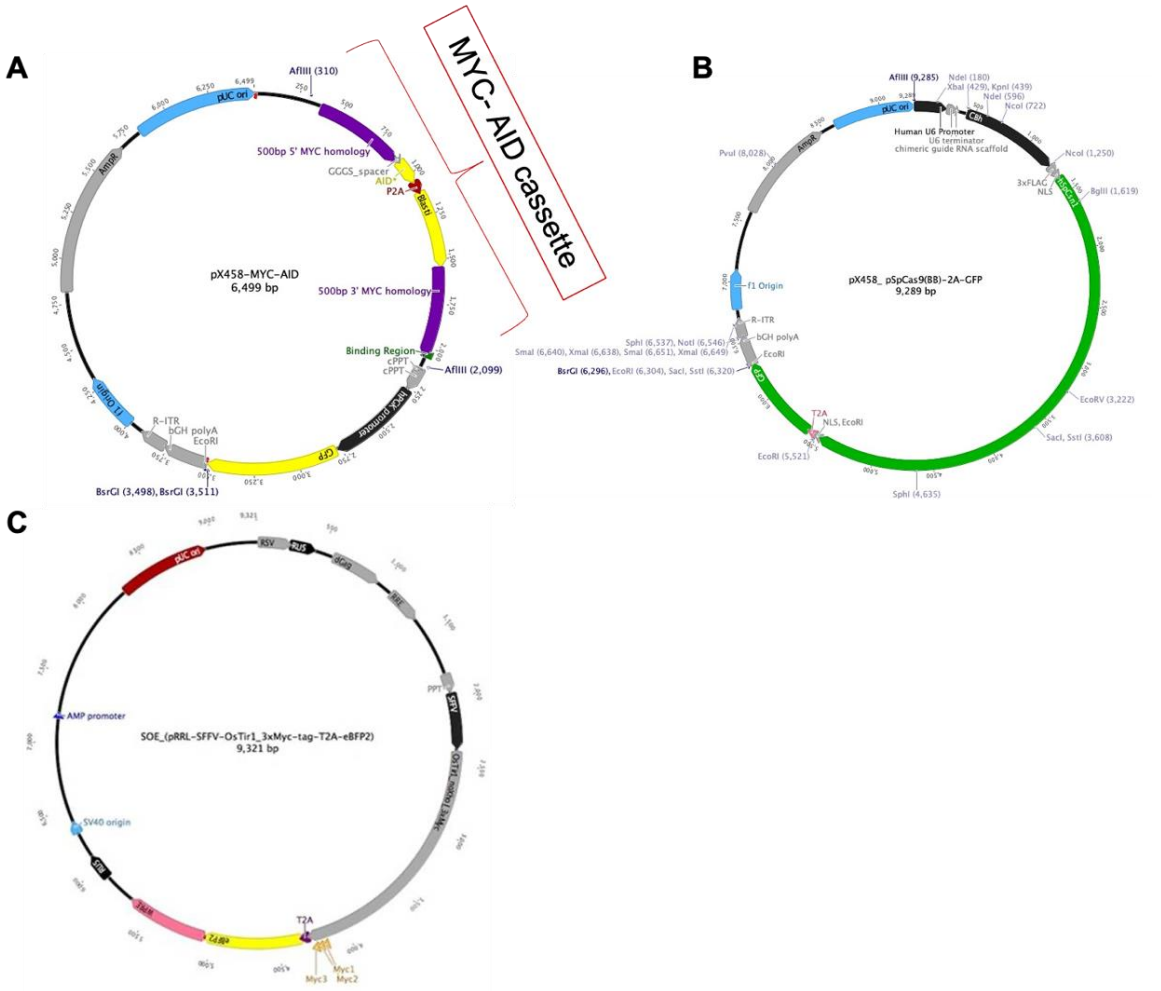

Figure S1: Plasmid vectors used for constructing MYC-AID cell lines.
The plasmids were previously described[235] and were a gift from J. Zuber. **(A)** Vector bearing blasticidin resistance and the AID open-reading frame flanked by the MYC-homology arms. **(B)** Vector expressing specifically designed sgRNAs directing the Cas nuclease to our region of interest. **(C)** Vector expressing the Tir1 auxin binding receptor, with BFP as a marker.

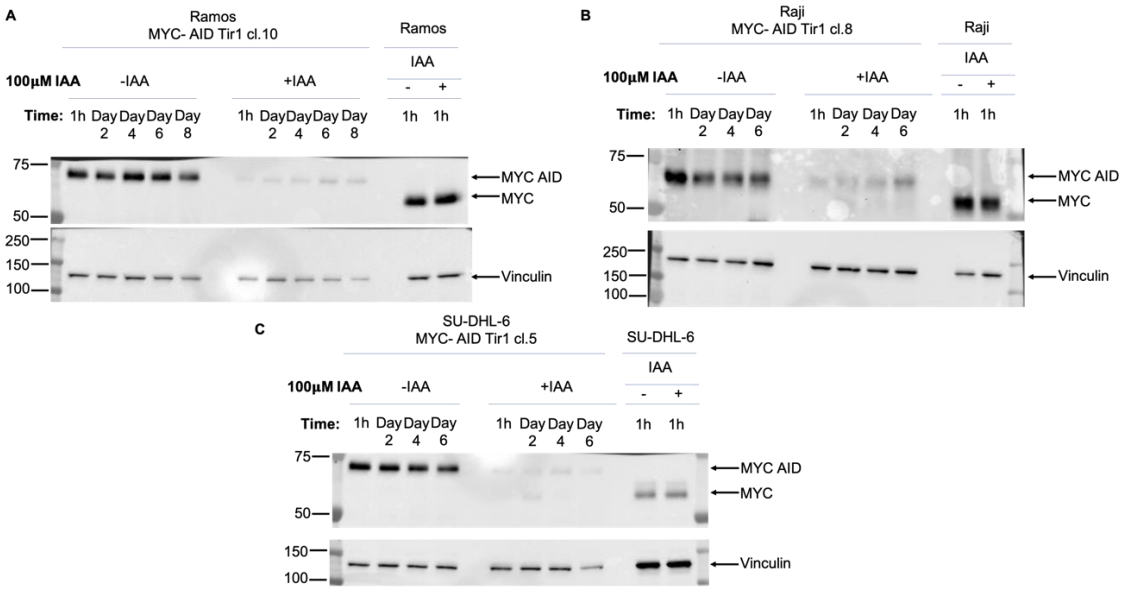

Figure S2: MYC-AID and MYC protein levels.
Assessed by immunoblotting of the indicated MYC-AID and parental cell lines **(A)** Ramos, **(B)** Raji and **(C)** SU-DHL-6 at the indicated time-points. Vinculin was used as loading control.

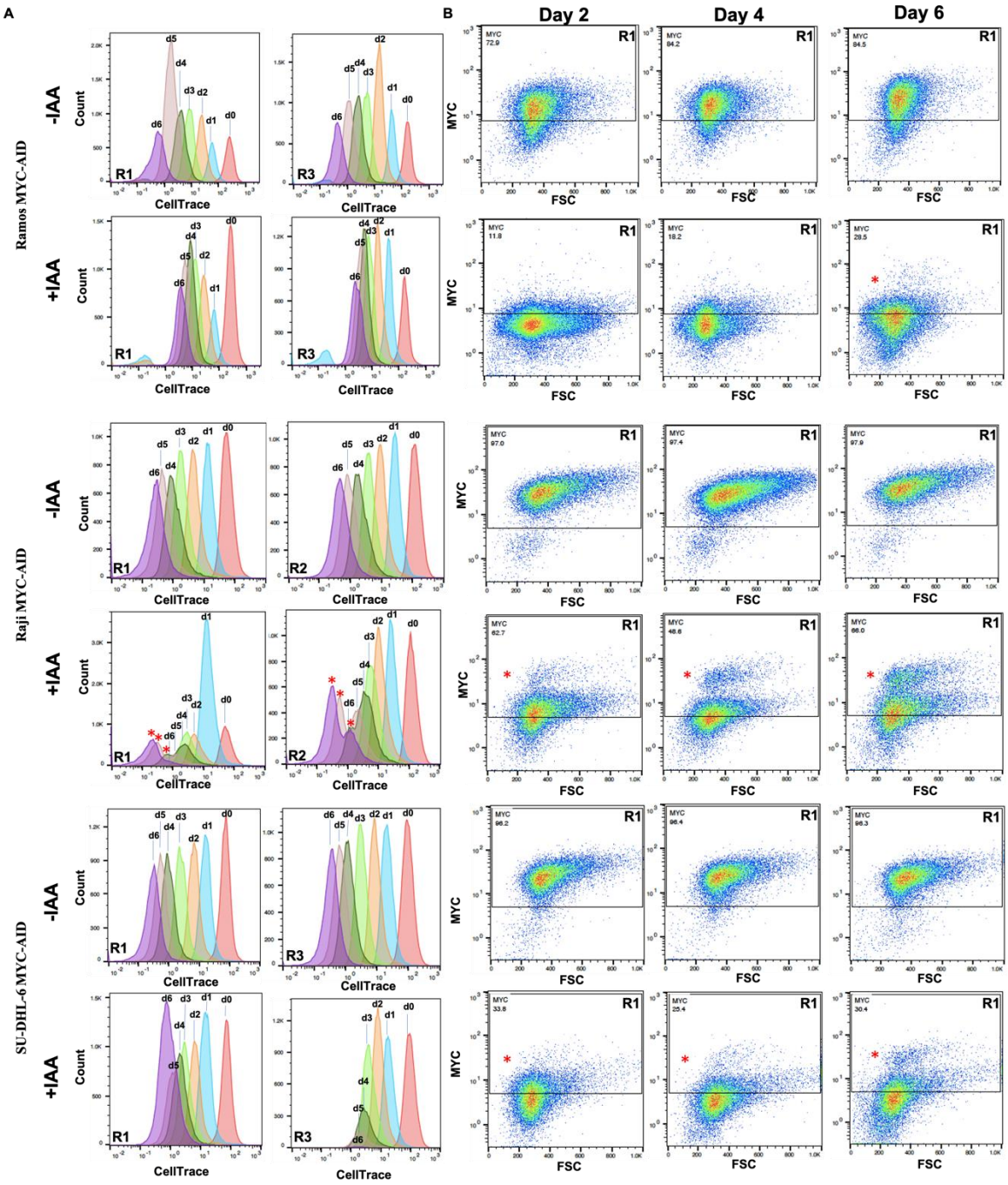

Figure S3: Profiling escapers of MYC-AID degradation.
(A) Same as **Fig. 13A**: Cell Trace profiles of the other two out of 3 biological replicates per cell line, from the experiment shown in **Fig. 13**. In Raji (middle), a second population starts emerging around day 4 in all replicates, while Ramos and SU-DHL-6 do not exhibit such behaviour. **(B)** Raw data of **Fig. 11C** MYC staining for a representative replicate per cell line along a time-course of 6 days. While the panels (A) and (B) do not originate from the same cultures, Raji MYC profiles (panel B, middle) clearly follow the trend of Cell Trace profiles in panel (A). The red asterisks point to the escaping subpopulations and the respective replicate is indicated on the graph.

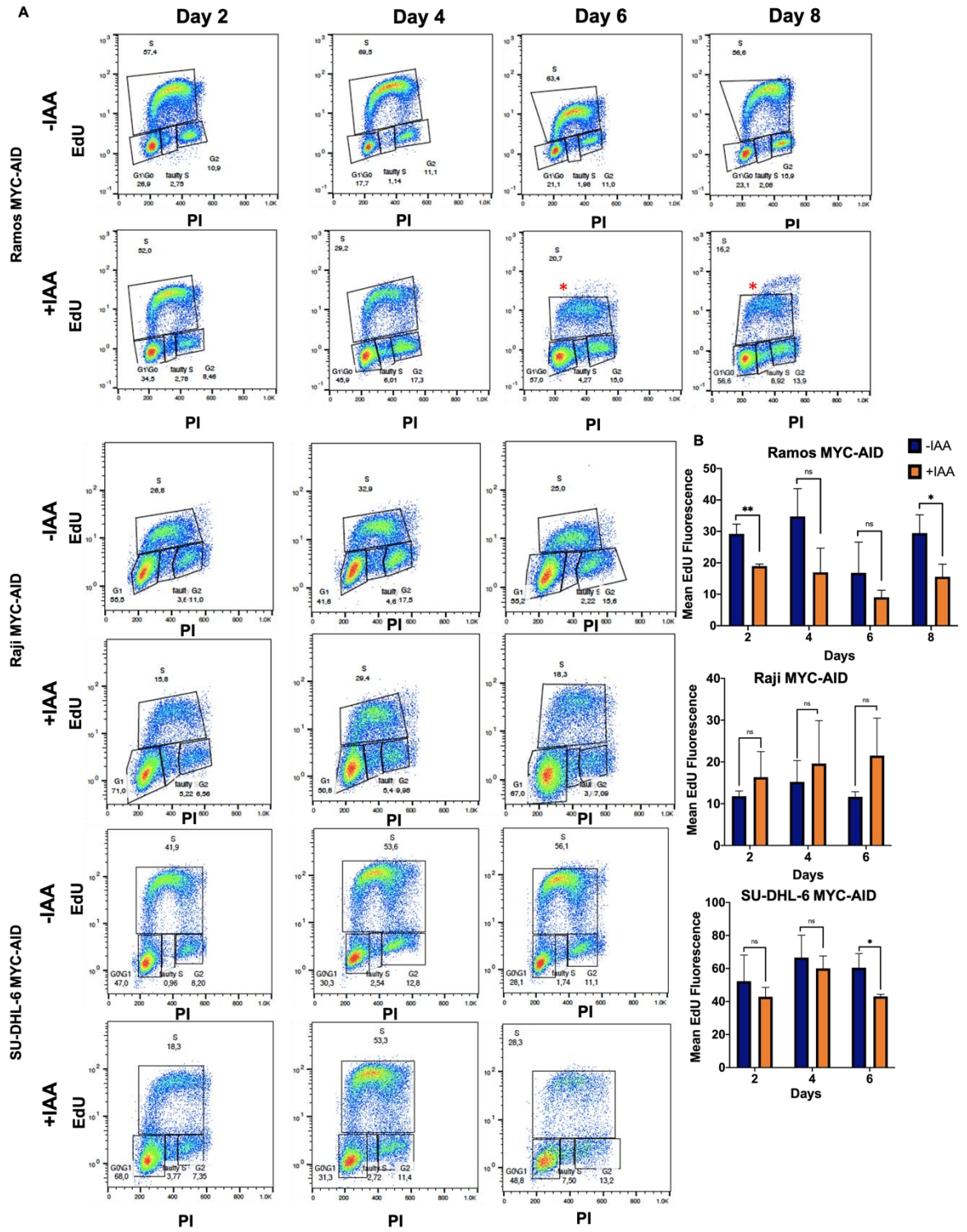

Figure S4: Cell cycle monitoring with EdU/PI staining.
Parallel cultures of the indicated cell lines were passaged with Auxin (+IAA: 100 µM) or without it (-IAA). At the indicated time-points (Days), cells were subject to a 20-minute pulse of EdU incorpotation (10 µM) and processed for 2D-Flow cytometric analysis with EdU and PI staining. The results of this experiment are plotted in **Fig. 15** and **Fig. 12B**. **(A)** Representative profiles from one replicate per cell line. The red asterisks in Ramos point to the small, rising populations of "high EdU incorporating" cells. The "faulty" S-phase indicated Edu-negative cells with intermerdiate DNA content. **(B)** Mean EdU fluorescence, as calculated in the S-phase cells, on the three cell lines as indicated. All data represent the means and SD (T test) from 3 biological replicates; *P≤0.05, **P≤0.01, *** P≤0.001, **** P≤0.0001.

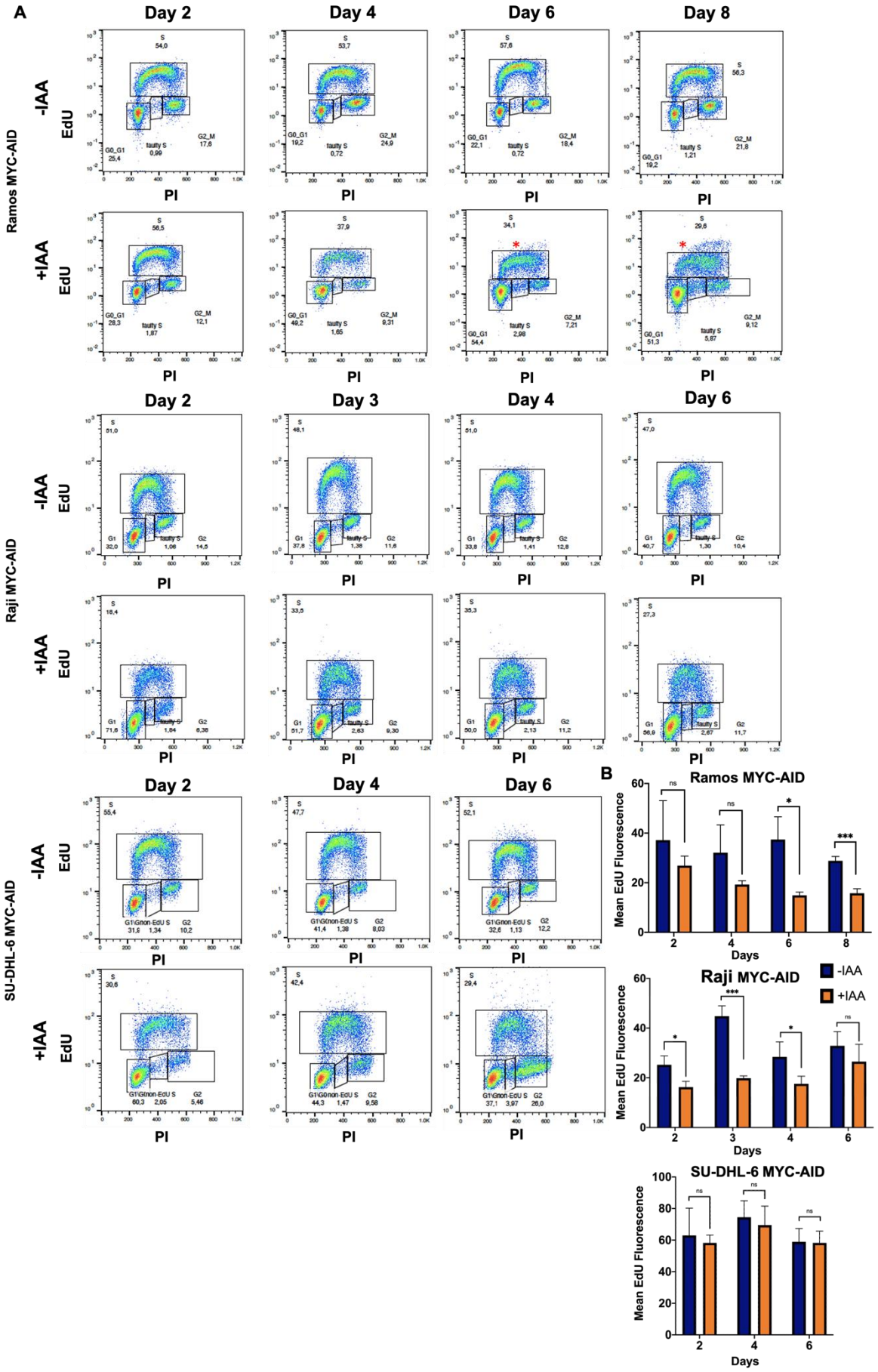

Figure S5: Cell cycle monitoring with EdU/PI staining (data from EdU/γ-H2ax double staining).
Same as Fig. S4 from a separate experiment, also used for γ-H2ax staining. The results of this experiment are plotted in **Fig. 16**. and the γ-H2ax data shown in **Fig. 17**.

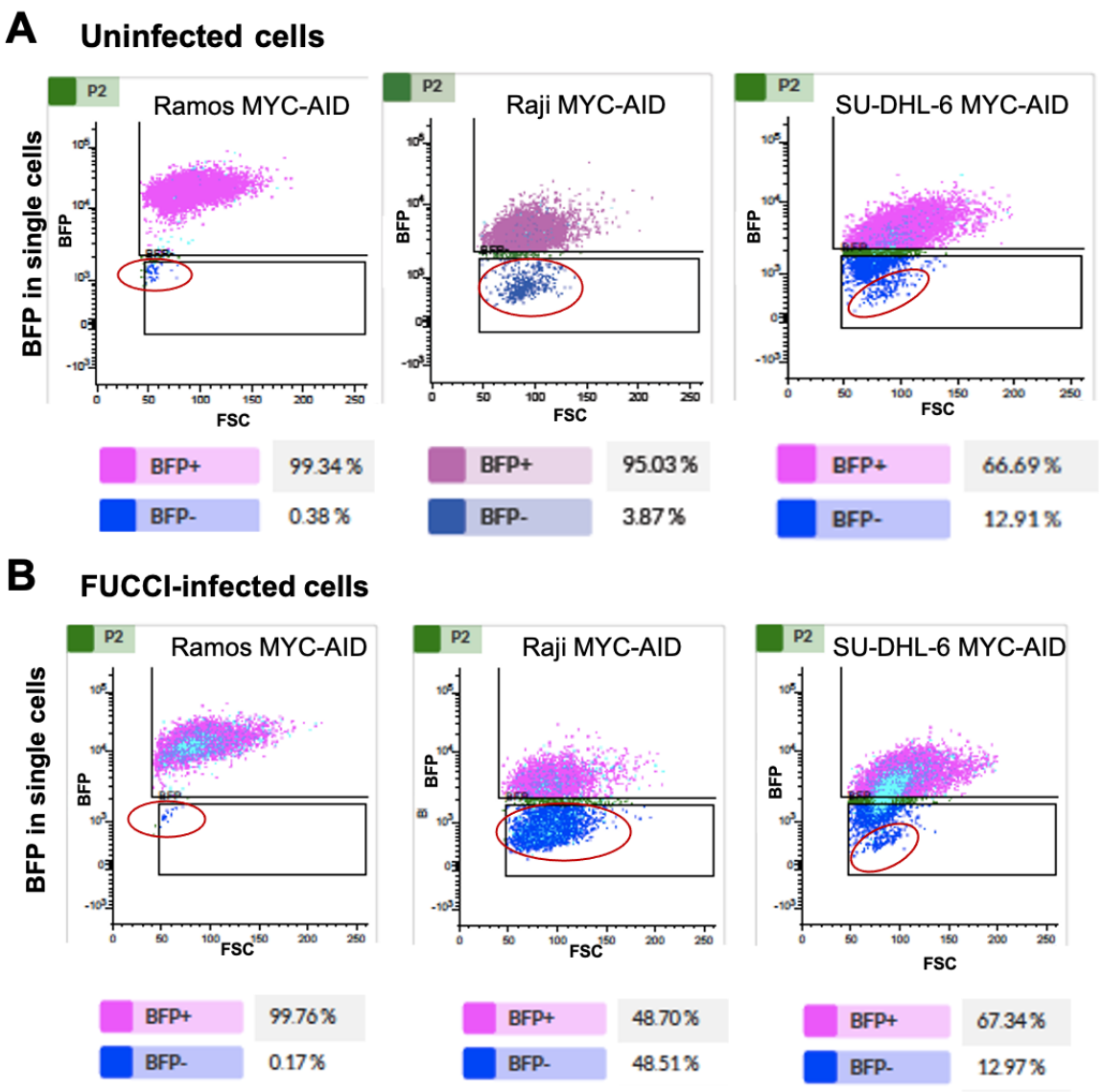

Figure S6: BFP/Tir1 positivity in MYC-AID cell lines before and after infection with the FUCCI vector.
Ramos, Raji and SU-DHL-6 MYC-AID cells (expressing Tir1 with a BFP marker) were infected with the FUCCI(CA)2 vector[380], expressing hCdt1-mCherry and hGem-mVenus probes. Following infection, cells were subjected to a cell sorting procedure for FUCCI positivity (mCherry and mVenus), using the parental cell lines as controls (no fluorescence, data not shown). The plots report BFP and FSC profiles on **(A)** uninfected cells and **(B)** FUCCI-infected populations (analysed before sorting) with their respective BFP+/- percentages, as gated by the black rectangles, mentioned below each plot. Note that SU-DHL-6 MYC-AID BFP+ cells have a low BFP brightness in general; hence, not all the cells coloured in blue are BFP- and the 12,91-12,97% values of BFP- cells represent gross overestimates. The actual BFP- populations in all the cultures are circled in red.

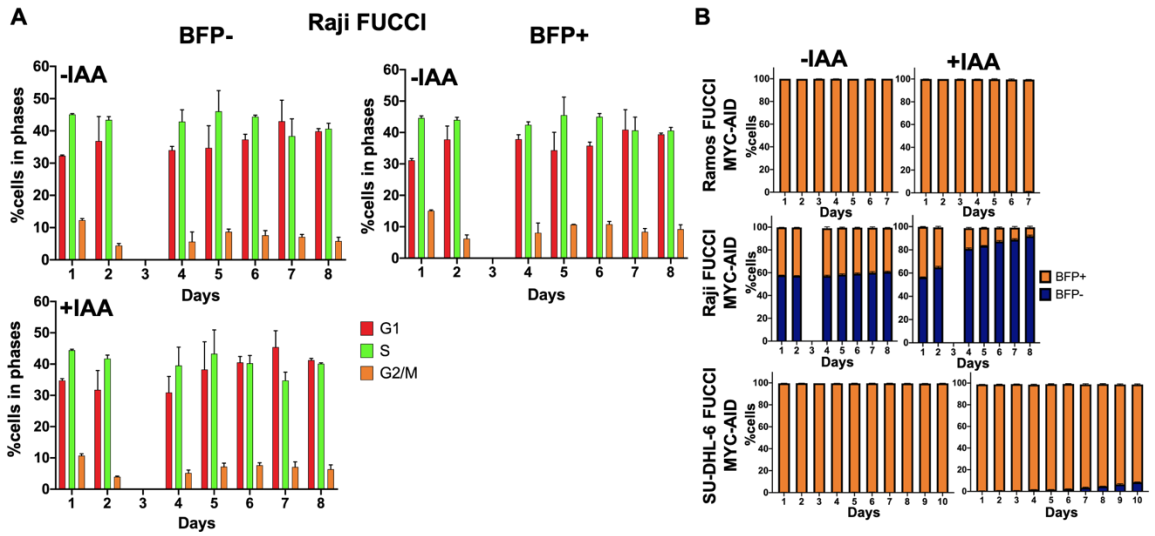

Figure S7: FUCCI system and escapers.

A) Comparison of sorted Raji FUCCI MYC-AID cells between BFP negative (w/wo IAA) with their respective untreated BFP positive cells. Data originating from the experiment shown in **Fig. 18**. **B)** BFP state of the FUCCI cells +/- IAA throughout the time course of the experiment in **Fig. 18**. The data represent the means and SD (T test) from 3 biological replicates.

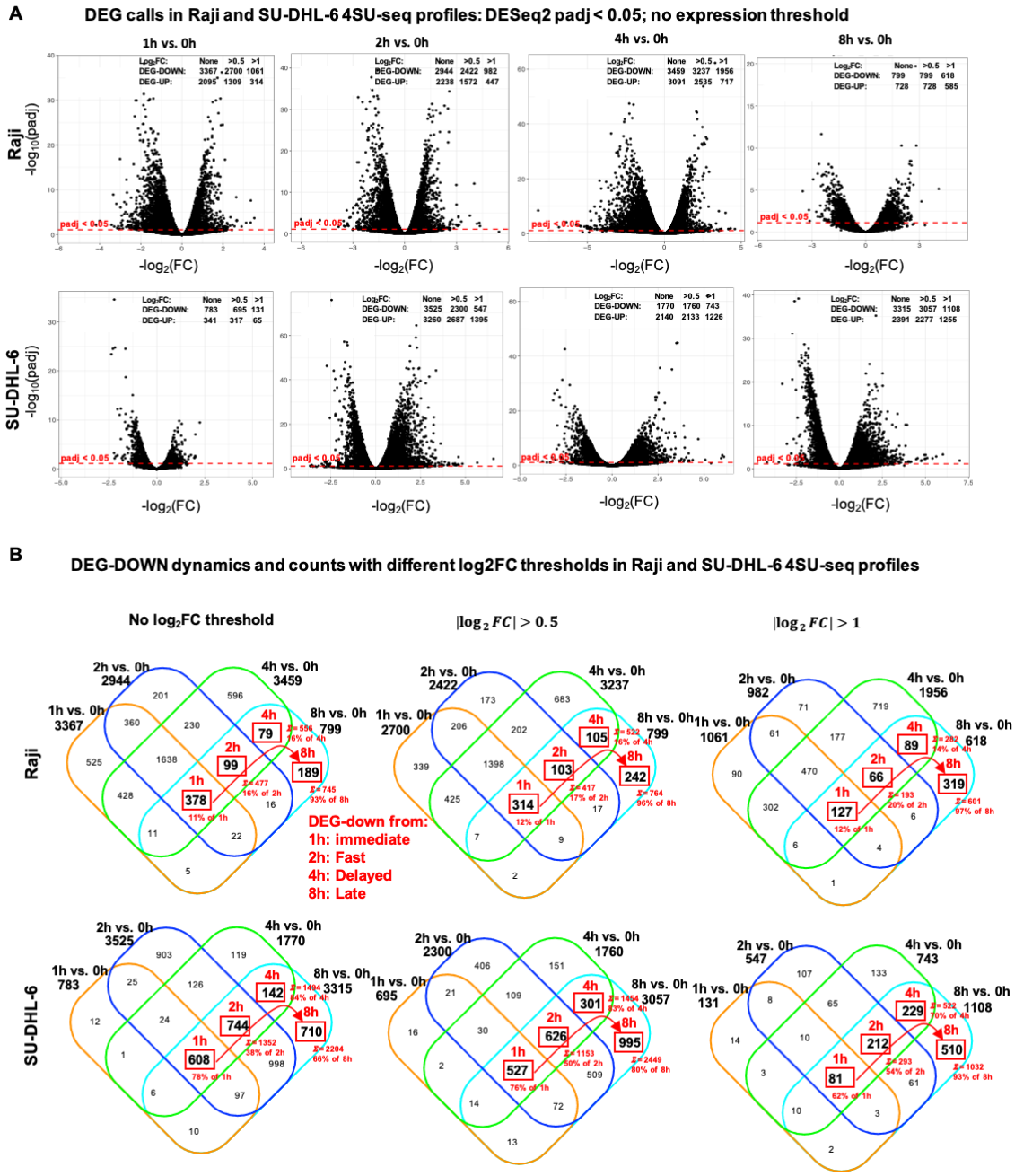

Figure S8: Temporal dynamics of IAA-induced transcriptional changes in Raji and SU-DHL-6 MYC-AID cells.
The data shown here for Raji and SU-DHL-6 lines are the same as for Ramos in **Fig. 20A, B**.

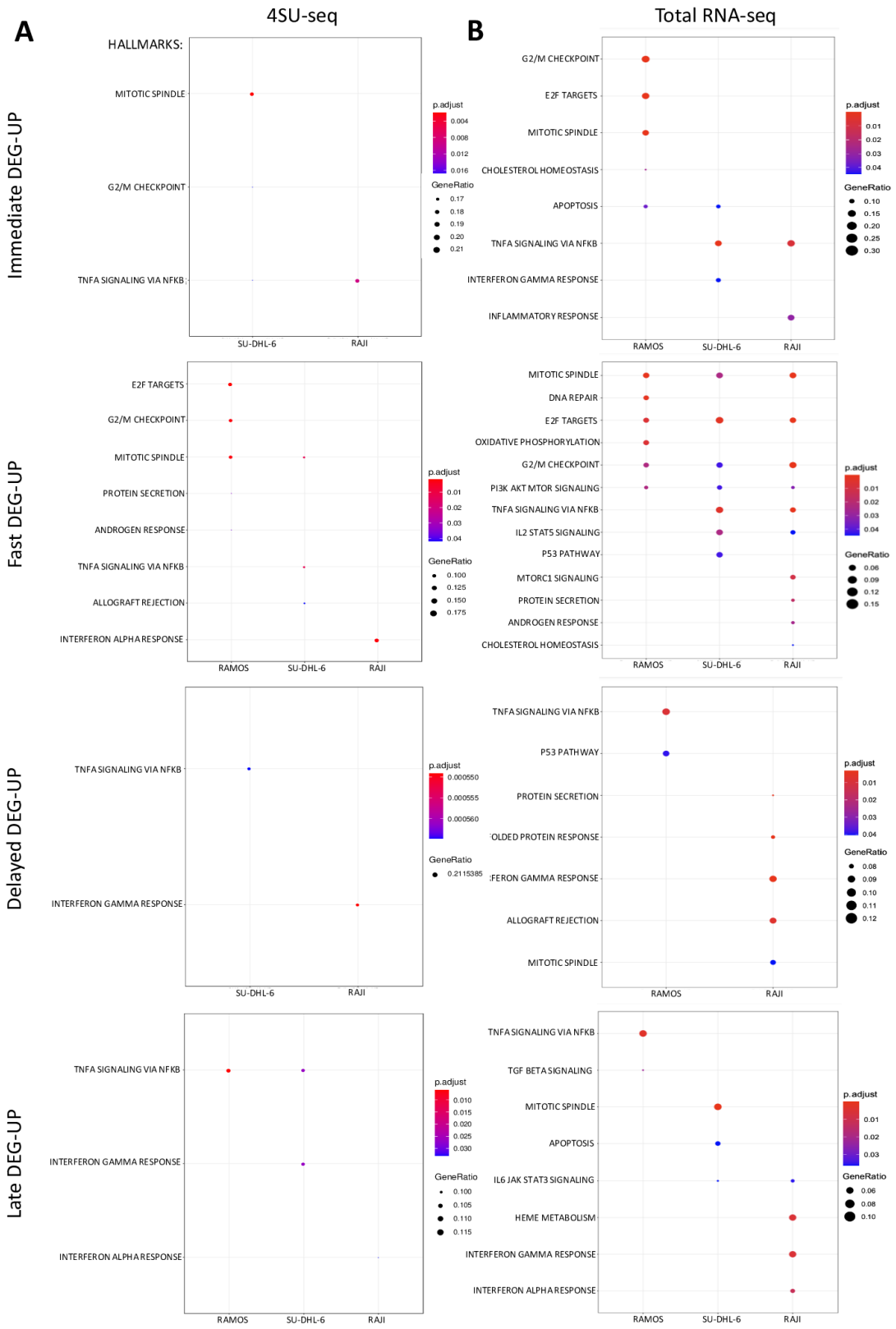

Figure S9: Gene Ontology Analysis on DEG-UP genes from 4SU- and Total RNA-seq for the three cell lines.
Same as **Fig. 23**, but using the temporally defined gene lists for DEG-UP.

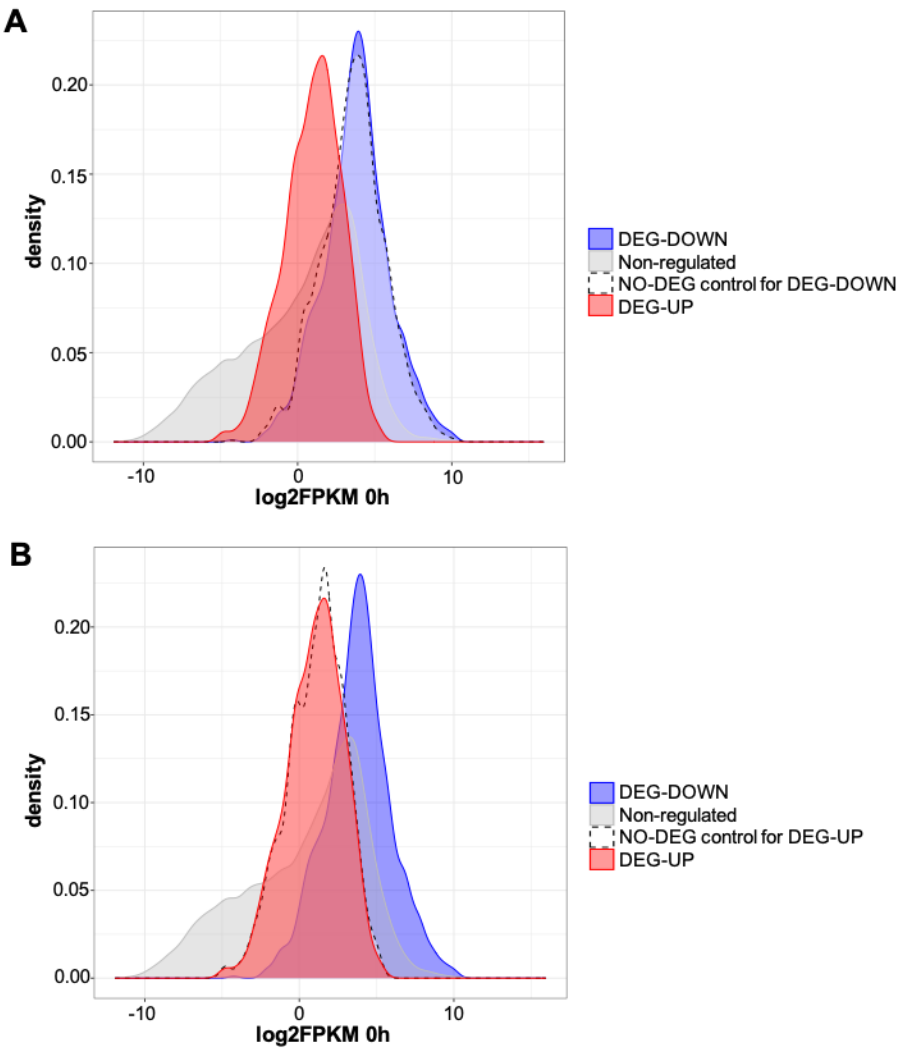

Figure S10: Remodeling Non-regulated control groups according to expression.
Density plot showing the mRNA expression distribution of 4SU-labeled RNA for untreated Ramos cells. The curve represents the estimated probability density function, while each color represents a different expression group: blue for down-regulated, grey for non-regulated and red for up-regulated. The population shown with a dashed line curve is built from non-regulated genes to match the expression distribution of either the **(A)** DEG DOWN or **(B)** DEG UP and functions as a non-regulated control sample (NO-DEG) for the aforementioned groups respectively.

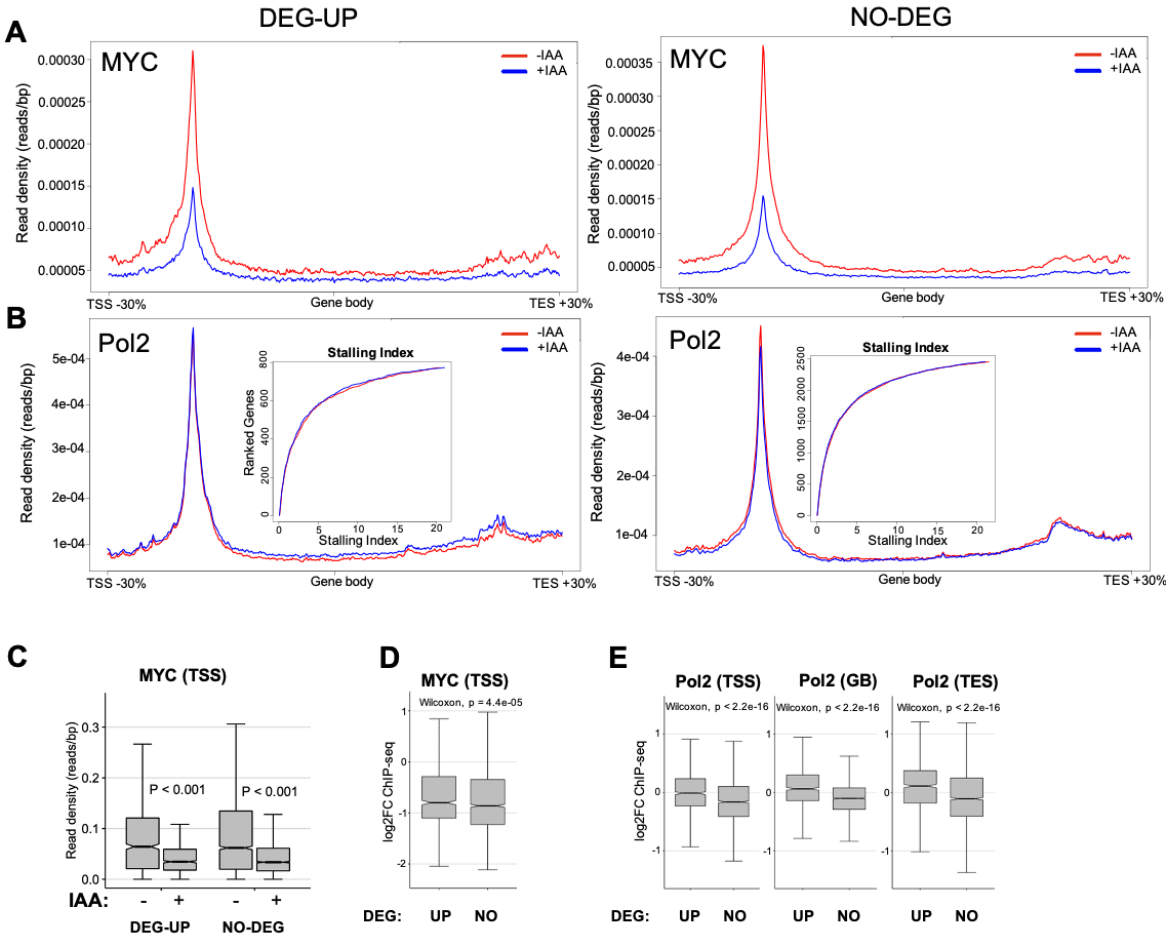

Figure S11: Impact of IAA treatment on MYC-PolII dynamics.
Same as **Fig. 26**, but describing the respective data for DEG-UP.

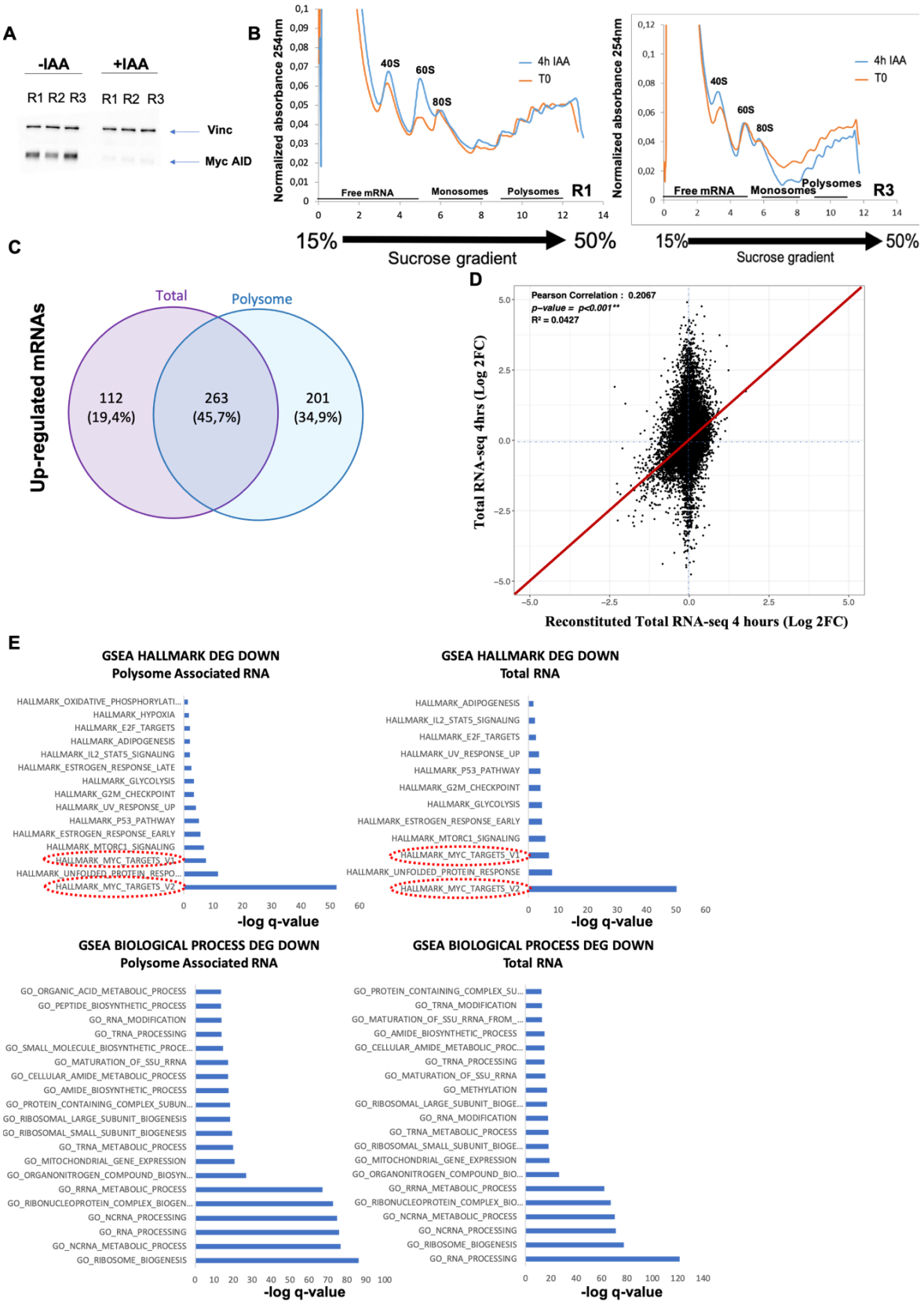

Figure S12: Polysome profiling in Ramos MYC-AID +/- 4hrs IAA.
(A) Immunoblotting of the Ramos triplicate samples from **Fig. 28A-C**, to monitor MYC-AID protein levels after 4h +/-IAA before the polysome profiling and sequencing (n=3 biological replicates). **(B)** Replicates of Ramos Polysome profiles as in **Fig. 28A**. **(C)** Overlap between the RNA populations called as DEG-UP in the total and polysome-associated profiles. **(D)** Comparison of the fold-changes (log2FC) of each mRNA in the total RNA pool reconstituted following polysome fractionation (X-axis) and from our total RNA-seq of the same cell line at the same time-point (Y-axis). The red line indicates the diagonal. **(E)** Gene Set Enrichment Analysis for the MSigDB[390,392,393] Hallmark (top) and Biological Process (bottom) gene sets, in the two RNA groups as indicated. MYC Hallmark target gene sets are circled in red.

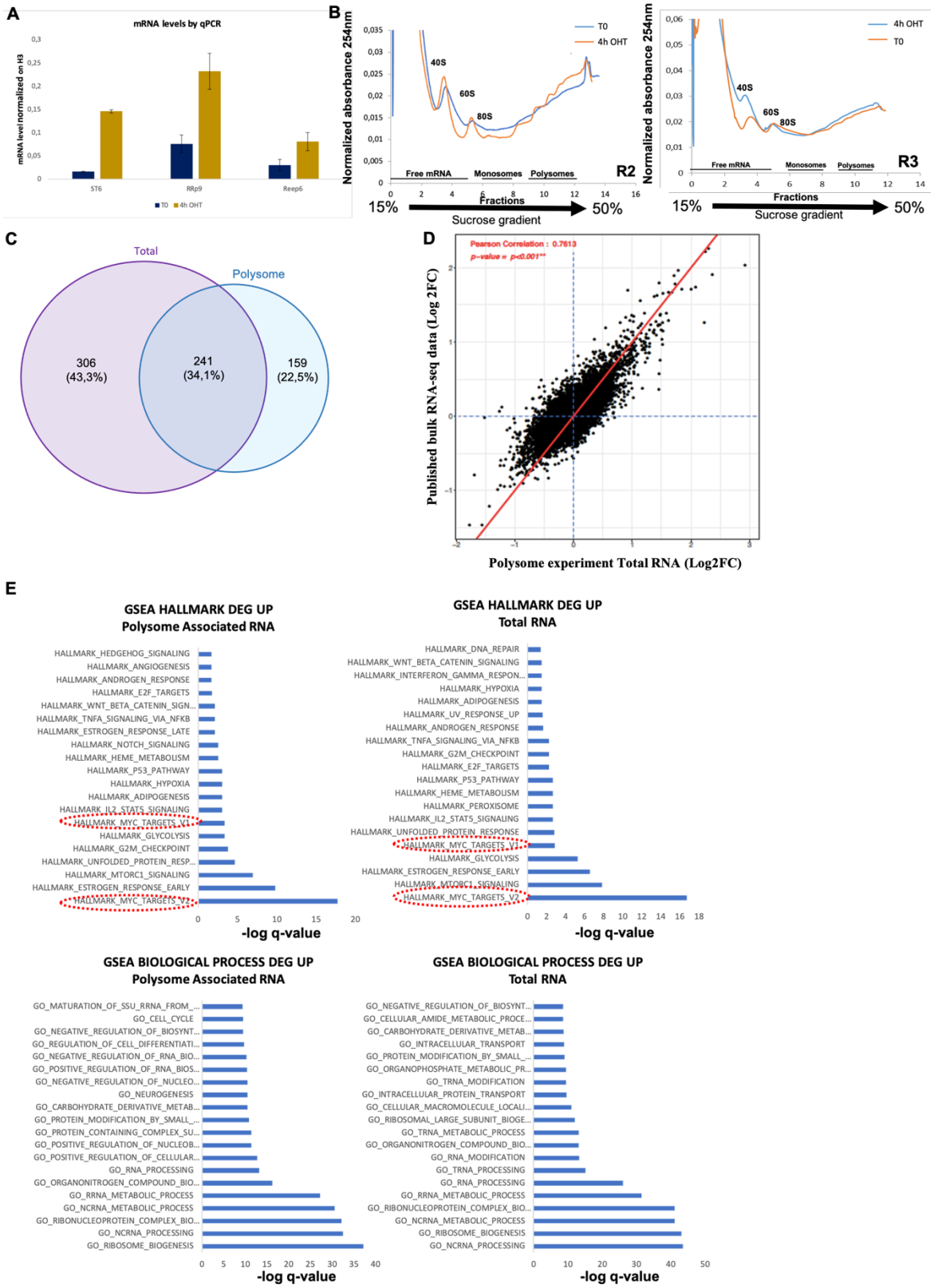

Figure S13: Polysome profiling in 3T9 MycER fibroblasts +/- 4hrs OHT.
(A) Monitoring mRNA levels of known MYC target genes by RT-qPCR in 3T9 MycER +/- 400 nM OHT 4 hours; (n=3 biological replicates from **Fig. 28D-F**). **(B)** Replicates of 3T9 MycER Polysome profiles, as in **Fig. 28D**. **(C)** Overlap between the RNA populations called as DEG-DOWN in the total and polysome-associated profiles. **(D)** Comparison of the fold-changes (log2 FC) of each mRNA in the total RNA pool reconstituted following polysome fractionation (X-axis) and our previously published RNA-seq profile (Y-axis)[85]. The red line indicates the diagonal. **(E)** Gene Set Enrichment Analysis for the MSigDB[390,392,393] Hallmark (top) and Biological Process (bottom) gene sets, in the two RNA groups as indicated. MYC Hallmark target gene sets are circled in red.